CHARACTERISING MACROEVOLUTIONARY PATTERNS WITHIN CROCODYLOMORPHA

by

PEDRO LORENA GODOY

A thesis submitted to the University of Birmingham for the degree of DOCTOR OF PHILOSOPHY

School of Geography, Earth and Environmental Sciences

College of Life and Environmental Sciences

University of Birmingham

September 2018

Abstract

Crocodylians today comprise only 24 recognised species, and are often regarded as morphologically conservative. However, the fossil record of crocodylomorphs, which includes the extinct relatives of crocodylians, is much richer and extends over the last ~220 million years. This great biodiversity is reflected in their morphological disparity, with crocodylomorph species occupying a much wider range of ecological niches. Research effort has concentrated mostly on the description of new taxa and on placing them within the crocodylomorph evolutionary tree, and has greatly contributed to our understanding of crocodylomorph phylogeny and diversity. Nevertheless, another fundamental aspect of crocodylomorph macroevolution, morphological disparity, has only recently been the subject of quantitative scrutiny, with the focus often limited to specific subgroups rather than the entire clade. In this thesis, crocodylomorph morphological disparity is quantitatively assessed using distinct types of data. Body size patterns, characterised via a model-fitting approach, provide new insights into the adaptive landscape of crocodylomorphs. Patterns of cranial shape variation suggest an important link between ecological diversification and morphological disparity. Finally, the action of heterochrony, underlying remarkable cranial modifications in the crocodylomorph clade Notosuchia, is tested using geometric morphometrics. Together, these results represent a significant contribution to better understanding crocodylomorph phenotypic evolution.

Aos meus pais.

Acknowledgements

I am deeply grateful to my supervisor Richard Butler, who offered me the opportunity to develop a project on the research field I always dreamed of, and was a constant source of support, advice and insights throughout my entire PhD. Richard will certainly be my inspiration if I am to become a supervisor in the future. I also thank my internal co-supervisors, Ivan Sansom and James Bendle, and especially my external co-supervisor, Roger Benson, for their ideas, discussions and comments on parts of this thesis.

I am thankful to CAPES (Coordenação de Aperfeiçoamento de Pessoal em Nível Superior) and the University of Birmingham for jointly funding my PhD project. I also thank the financial support from Universitas 21, the Palaeontological Association, and the "Doris O. and Samuel P. Welles Research Fund", from the University of California's Museum of Paleontology.

I acknowledge the access to fossil specimens provided by Lorna Steel (NHMUK, London, UK), Zoltán Szentesi (MTM, Budapest, Hungary), Attila Ősi (MTM), Eliza Howlett (OUMNH, Oxford, UK), Matthew Riley (CAMSM, Cambridge, UK), Ronan Allain (MNHN, Paris, France), Rainer Schoch (SMNS, Stuttgart, Germany), Erin Maxwell (SMNS), Marisa Blume (HLMD, Darmstadt, Germany), Eberhard Frey (SMNK, Karlsruhe, Germany), Oliver Rauhut (BSPG, Munich, Germany), Max Langer (LPRP/USP, Ribeirão Preto, Brazil), Sandra Tavares (MPMA, Monte Alto, Brazil), Fabiano Iori (MPMA), Thiago Marinho (CPP, Peirópolis, Brazil), Jaime Powel (PVL, San Miguel de Tucumán, Argentina), Rodrigo Gonzáles (PVL), Martín Ezcurra (MACN, Buenos Aires, Argentina), Stella Alvarez (MACN), Alejandro Kramarz (MACN), Patricia Holroyd (UCMP, Berkeley, USA), Kevin Padian (UCMP), William Simpson (FMNH, Chicago, USA), Akiko Shinya (FMNH), Paul Sereno

(UCRC, Chicago, USA), Tayler Keillor (UCRC), Mark Norell (AMNH, New York, USA), Carl Mehling (AMNH), Judy Galkin (AMNH), Alan Turner (SUNY, Stony Brook, USA), Liu Jun (IVPP, Beijing, China), Corwin Sullivan (IVPP), Zheng Fang (IVPP), Amanda Millhouse (USNM, Washington, D. C., USA).

I thank all my colleagues from the Paleobiology research theme of the University of Birmingham, specially Dan Cashmore, Emma Dunne, Andy Jones and Juan Benito Moreno, for their help, assistance, and friendship. Further thanks to my Brazilian palaeontologist colleagues Julio Marsola, Gabriel Ferreira, Mario Bronzati, Felipe Montefeltro, Bruno Vila Nova, and Max Langer, who not only have been friends for many years, but also contributed to parts of this thesis. I also thank Trina Du, Louise Meunier and Hans Larsson, who provided me with an enjoyable and fruitful period at the Redpath Museum (McGill University).

I express special appreciation to the many Brazilian friends that lived or are still living in Birmingham, including Carlos, Carol, Lais, Tupá, Julio, Dalila, Camila, Douglas, Jamila, José Carlos, Pedro, Tati, Mario, Mari, Samara, Vítor, Elis, Valter, Giana, Ravenna, David, Renata, Willians, Emily, Serginho, Paula, Walter, Rubens, and Glauco, as well as those living in London (Giu, Tarso and Victor) and Sheffield (Ligia and Matheus). Special thanks to my dearest friend Matheus, for his incredible companionship over more than 10 years.

Finally, my sincere and immense gratitude to my family, Solange, João and Lucas, whose unconditional love and support were surely crucial for my engagement in research and ultimately led me to finish this thesis. And I extend my gratitude to Mariana, the most recent member of the family, for her affection and (intense) support, particularly during the last months before handing the thesis. Thank you, my love.

Table of Contents

Chapter 1: Introduction 1

1.1. Taxonomic diversity versus morphological disparity in macroevolutionary studies 2

1.2. The study group: Crocodylomorpha 4

1.3. Objectives 8

Chapter 2: Crocodylomorph body size evolution 9

2.1. Background 9

2.2. Material and Methods 14

2.2.1. Proxy for body size 14

2.2.2. Phylogenetic framework 17

2.2.3. Time-calibration 21

2.2.4. Macroevolutionary analyses 23

2.2.5. Correlation with abiotic factors 29

2.3. Results 31

2.3.1. Comparative model-fitting analyses 31

2.3.2. Appraising the SURFACE model fits 33

2.3.3. Describing the body size macroevolutionary patterns in Crocodylomorpha 39

2.3.4. Investigating the modes of body size evolution within Notosuchia and Crocodylia 48

2.3.5. The influence of palaeolatitude and palaeotemperature 51

2.4. Discussion 56

2.4.1. The adaptive landscape of crocodylomorph body size evolution 56

2.4.2. Ecological diversification and its implications for crocodylomorph body size distribution 61

2.4.3. Cope's rule cannot explain the evolution of larger sizes in Crocodylomorpha 65

2.4.4. Correlation of crocodylian body size with global cooling ____ 68

2.4.5. Body size selectivity and diversification across Mesozoic boundaries ____ 69

2.5. Conclusions ____ 73

Chapter 3: Crocodylomorph cranial shape disparity ____ 75

3.1. Background ____ 75

3.2. Material and Methods ____ 78

3.2.1. Sampling and data collection ____ 78

3.2.2. Phylogenetic framework ____ 80

3.2.3. Geometric morphometric analyses ____ 82

3.2.4. Estimating disparity ____ 88

3.3. Results ____ 91

3.3.1. Geometric morphometric analyses ____ 91

3.3.2. Disparity through time and between groups ____ 105

3.4. Discussion ____ 113

3.4.1. Assessing the different methods to minimise the effects of interobserver error ____ 113

3.4.2. Crocodylomorph cranial shape variation ____ 115

3.4.3. Crocodylomorph cranial shape disparity ____ 117

3.4.4. Ecological diversity and crocodylomorph skull shape ____ 121

3.5. Conclusions ____ 123

Chapter 4: Heterochrony in the cranial evolution of notosuchians ____ 125

4.1. Background ____ 125

4.1.1. Heterochrony terminology ____ 128

4.2. Material and Methods ____ 131

4.2.1. Systematic Palaeontology ____ 131

4.2.2. Sampling and data collection ____ 133

4.2.3. Phylogenetic framework 135

4.2.4. Geometric morphometric analyses 137

4.3. Results 141

4.4. Discussion 147

4.4.1. Peramorphosis in Baurusuchidae 147

4.4.2. Acceleration, predisplacement or hypermorphosis 150

4.4.3. Heterochrony explains hypercarnivory 153

4.5. Conclusions 154

Chapter 5: Summary and perspectives 156

5.1. General conclusions 156

5.2. Prospects and future work 158

Appendices 160

Appendix A: Supplementary information for Chapter 2 160

Appendix B: List of specimens sampled for the geometric morphometric analyses of Chapter 3 161

Appendix C: Example R script of the geometric morphometric analyses performed in Chapter 3 171

Appendix D: Supplementary results of the disparity-through-time analyses of Chapter 3 176

Appendix E: Supplementary information for Chapter 4 194

References 195

List of Abbreviations

Institutional abbreviations

ACAP, Association Culturelle, Archéologique et Paléontologique de l'Ouest Biterrois, Cruzy, Hérault, France. **AMNH,** American Museum of Natural History, New York, United States of America. **CAS,** Sirindhorn Museum, Kalasin Province, Sahatsakhan, Thailand. **CNM,** Chongqing Natural Museum, Sichuan, China. **BHI,** Black Hills Institute, Hill City, United States of America. **BHN2R,** Muséum d'Histoire Naturelle de Boulogne-sur-Mer, France. **BP,** Bernard Price Institute for Palaeontological Research, Johannesburg, South Africa. **BRLSI,** Bath Royal Literary and Scientific Institute, Bath, United Kingdom. **BSPG,** Bayerische Staatssammlung für Paläontologie und Geologie, Munich, Germany. **BYU,** Brigham Young University, Provo, United States of America. **ChM,** Charleston Museum, Charleston, United States of America. **CM,** Carnegie Museum of Natural History, Pittsburgh, United States of America. **CPP,** Centro de Pesquisas Paleontológicas Llewellyn Ivor Price, Peirópolis, Brazil. **DFMMh,** Dinosaurier-Freilichtmuseum Münchehagen, Münchehagen, Germany. **DG-CTG-UFPE,** Centro de Tecnologia e Geociências, Universidade Federal de Pernambuco, Recife, Brazil. **DGM,** Museu de Ciências da Terra, Departamento Nacional de Produção Mineral (DNPM), Rio de Janeiro, Brazil. **DORCM,** Dorset County Museum, Dorchester, United Kingdom. **DM,** Darwin Museum, Keelung, Taipei. **FMNH,** Field Museum of Natural History, Chicago, United States of America. **GM,** Geiseltalmuseum, Martin Luther Universitat Halle, Halle, Germany. **HLMD,** Hessisches Landesmuseum Darmstadt, Darmstadt, Germany. **HUE,** Lo Hueco Collection, Museo de las Ciencias de Castilla-La Mancha, Cuenca, Spain. **IGM,** Mongolian Institute of Geology, Ulaan Bataar, Mongolia. **IGV,** Geological Institute of the Chinese Academy of Geological Sciences, Beijing, China.

IRSNB, Institut Royal des Sciences Naturelles de Bruxelles, Belgium. **IVPP,** Institute of Vertebrate Paleontology and Paleoanthropology, Beijing, China. **KM,** Krahuletz Museum, Eggenburg, Austria. **KNM,** Kenya National Museums, Nairobi, Kenya. **LACM,** Los Angeles County Museum of Natural History, Los Angeles, United States of America. **LO,** Lund University, Lund, Sweden. **LPRP/USP,** Laboratório de Paleontologia, Universidade de São Paulo, Ribeirão Preto, Brazil. **MACN,** Museo Argentino de Ciencias Naturales "Bernardino Rivadavia", Buenos Aires, Argentina. **Mal,** Malawi Department of Antiquities, Malawi. **MBLUZ,** Museo de Biologia de la Universidad del Zulia, Maracaibo, Venezuela. **MCNC,** Museo de Ciencias Naturales de Caracas, Venezuela. **MCSNT,** Museo Civico di Storia Naturale di Trieste, Italy. **MGHF,** Museo Geológico H. Fuenzalida, Universidad Católica del Norte, Antofagasta, Chile. **MHNH,** Muséum d'Histoire Naturelle du Havre, Havre, France. **MJCM,** Museo de Ciencias Naturales y Antropológicas 'Juan Cornelio Moyano', Mendoza, Argentina. **MLP,** Museo de La Plata, La Plata, Argentina. **MNHN,** Museum National d'Histoire Naturelle, Paris, France. **MNK,** Museo Noel Kempff Mercado, Santa Cruz de la Sierra, Bolivia. **MNN,** Musée National du Niger, Niamey, Republic of Niger. **MOR,** Museum of the Rockies, Bozeman, United States of America. **MOU,** Museum of Osaka University, Japan. **MOZ,** Museo Provincial de Ciencias Naturales "Profesor Dr. Juan A. Olsacher", Zapala, Neuquén, Argentina. **MPMA,** Museu de Paleontologia de Monte Alto, Monte Alto, Brazil. **MPZ,** Museo Paleontológico de la Universidad de Zaragoza, Spain. **MSU,** Dunn-Seiler Museum, Mississippi State University, Starkville, United States of America. **MTM,** Hungarian Natural History Museum, Budapest, Hungary. **MZSP,** Museu de Zoologia da Universidade de São Paulo, São Paulo, Brazil. **NHM,** Natural History Museum, London, United Kingdom. **NMC,** Canadian Museum of Nature, Ottawa, Ontario, Canada. **OMNH,** Oxford University Museum of Natural History, Oxford, United Kingdom. **PC,** Museo di

Paleontologia del Centro Museale dell'Università di Napoli Federico II University, Naples, Italy. **PETMG,** Peterborough Museum, Peterborough, United Kingdom. **PIN,** Paleontological Institute Moscow, Russia. **PVL,** Museo de Ciencias Naturales, Fundación Miguel Lillo, San Miguel de Tucumán, Argentina. **QM,** Queensland Museum, Brisbane, Australia. **ROM,** Royal Ontario Museum, Toronto, Canada. **RMBR,** Raffles Museum of Biodiversity Research, Singapore. **RRBP,** Rukwa Rift Basin Project (Tanzanian Antiquities Unit), Tanzania. **RTMP,** Royal Tyrrell Museum of Palaeontology, Drumheller, Canada. **SAM,** Iziko South African Museum, Cape Town, South Africa. **SMM,** Science Museum of Minnesota, St. Paul, United States of America. **SMNK,** Staatliches Museum für Naturkunde, Karlsruhe, Germany. **SMNS,** Staatliches Museum für Naturkunde, Stuttgart, Germany. **TMM,** Texas Memorial Museum, The University of Texas, Austin, United States of America. **UA,** UA, Université d'Antananarivo, Antananarivo, Madagascar. **UCMP,** University of California Museum of Paleontology, Berkeley, United States of America. **UF,** University of Florida, Gainesville, United States of America. **UFAC,** Universidade Federal do Acre, Rio Branco, Brazil. **UFRJ,** Coleção de Paleontologia de Vertebrados da Universidade Federal do Rio de Janeiro, Rio de Janeiro, Brazil. **UNC,** Department of Geological Sciences, University of North Carolina at Chapel Hill, United States of America. **UNEFM,** Universidad Nacional Experimental Francisco de Miranda, Coro, Venezuela. **USNM,** Smithsonian National Museum of Natural History, Washington , United States of America. **YPM,** Yale Peabody Museum of Natural History, New Haven, United States of America. **ZDM,** Zigong Dinosaur Museum, Zigong, Sichuan, China.

Measurements

DCL, dorsal cranial length.

ODCL, orbito-cranial length.

TL, total length.

Evolutionary models

BM, Brownian motion.

EB, Early burst model.

OU, Ornstein-Uhlenbeck.

BMS, multi-regime BM model that allows parameter σ2 to vary.

OUMV, multi-regime OU model that allows θ and σ2 to vary.

OUMA, multi-regime OU model in which θ and α can vary.

OUMVA, OU model in which all three parameters (θ, α and σ2) can vary.

Model parameters

θ, trait optimum of OU-based models.

α, attraction parameter of OU-based models.

σ2, Brownian variance or rate parameter of BM or OU-based models.

μ, evolutionary trend parameter of BM-based models.

Z_0, estimated trait value at the root of the tree of OU-based models.

Optimality criteria

AIC, Akaike's information criterion.

AICc, Akaike's information criterion for finite sample sizes.

BIC, Bayesian information criterion.

pBIC, Phylogenetic Bayesian information criterion.

Geometric morphometric methods

GPA, Generalised Procrustes analysis.

RWA, Relative Warp analysis.

SS, sum of squares

PC, Principal components.

PCA, Principal components analysis.

Other methodological implementations

OLS, Ordinary least squares.

GLS, Generalised least squares.

PGLS, Phylogenetic generalised least squares.

ANOVA, Analysis of variance.

PhyloANOVA, Phylogenetic Analysis of variance.

MANOVA, Multivariate analysis of variance.

npMANOVA, Non-parametric multivariate analysis of variance.

Chapter 1: Introduction

The main goal of palaeontology is to understand the history of life on Earth, which is documented by fossils of organisms that have been inhabiting the planet for at least 3.7 billion years (Awramik 1992; Bell *et al.* 2015; Dodd *et al*. 2017). The attempt to comprehend the past is driven not only by curiosity in uncovering the mysteries of ancient life, but also by the possibility of predicting the future transformations of the planet. In studying past animals, plants and environments we provide ourselves with crucial tools that help us to identify patterns and trends of changes that happened repeatedly in the past and that may be mirrored today (Benton and Harper 2013; Cowen 2013).

As opposed to experimental sciences, hypotheses formulated within the scope of historical sciences, such as palaeontology, cannot usually be tested via laboratory experiments (which does not make historical science epistemologically inferior to experimental science Cleland 2001; 2002). Within experimental sciences, the "traditional" approach of the scientific method seeks to explore the causal relationship between present and future events, which is ultimately assessed by testing hypotheses in controlled laboratory settings. Alternatively, historical scientists use a parallel route of evidential reasoning, looking for correlations between present and past events, which creates a time asymmetry between historical and experimental research. In other words, historical hypotheses are formulated to explain effects of long-past events, and multiple hypotheses can be tested by evidence that unambiguously discriminates one hypothesis from a set of other available ones (Cleland 2002). Accordingly, better hypotheses emerge and evolve from the accumulation of more and more diverse evidence (including those arising from Kuhnian paradigm shifts; Cleland 2002; Benton and Harper 2013). Numerous examples illustrate this pattern of evidential reasoning,

from Wegener's hypothesis of continental drift (Cleland 2002) to the extinction of the dinosaurs as the result of an asteroid impact (Brusatte *et al*. 2015).

Recent advances in many methodological techniques have provided palaeontologists with tools to more quantitatively assess the evidence yielded by the fossil record, allowing palaeontological research to flourish (Benton and Harper 2013). Although the basis of palaeontology remains the discovery and description of new specimens or species, additional steps and approaches to better understand the history of life are now common in palaeontological studies, such as investigating how closely related those species are (with systematic phylogenetic analyses) or if there were periods in geological time with greater or lower biodiversity (by estimating diversity in statistically appropriate ways). This "new era" of palaeobiology (the subfield of palaeontology created in the first half of the 20th century to better integrate the emerging concepts of evolutionary biology; Sepkoski 2012), driven by abundant data derived from quantitative approaches, has permitted more frequent and comprehensive investigations of macroevolutionary patterns (i.e., evolutionary changes that occurred over long geological time scales, usually above the species level).

1.1. Taxonomic diversity versus morphological disparity in macroevolutionary studies

During the modern synthesis, the concepts introduced by G. G. Simpson's *Tempo and Mode in Evolution* (1944), such as that of adaptive radiation, were key for the consolidation of macroevolutionary studies and the marriage between palaeontological evidence and that from other subfields of evolutionary biology (e.g., molecular data) (Benton 2015). Since Simpson's days, palaeontologists have engaged in the characterisation of macroevolutionary temporal patterns from different types of data. Perhaps the most classical way of recognising macroevolutionary patterns is by estimating taxonomic diversity. Although species richness in

the past has long been the subject of studies by naturalists (Mayr 1982), the modern concept of diversity estimation was arguably founded by the prominent work of Raup and Sepkoski (e.g., Raup 1972; Sepkoski 1978; 1979; 1981; Sepkoski *et al*. 1981; Raup and Sepkoski 1982; Sepkoski 1984), which has been subsequently improved by statistical approaches that more adequately account for biases in the fossil record (e.g., Alroy 2010).

However, another important branch of macroevolutionary studies focuses on the long-term variation of organisms' morphologies, rather than changes in taxic biodiversity (Gould 1991). The distinction between morphological disparity (i.e., the amount of morphological variation among species) and taxonomic diversity was greatly clarified by the work of Foote (e.g., Foote 1993; 1997), which showed that the signals from these two distinct types of data are not always consistent, as changes in the number of species do not necessarily translate into changes in the morphological differences among them (Foote 1993; Hopkins and Gerber 2017). For instance, many studies have indicated that even though morphological variation patterns seem to track those of biodiversity curves during the early evolution of clades (e.g., Foote 1993; Hughes *et al*. 2013), subsequent discordant signals are frequently observed.

There are different approaches for quantifying morphological variation, also known as phenotypic variation, which usually include data from continuous characters (using traditional or geometric morphometrics) or discrete (i.e., cladistic) characters (Benton 2015; Hopkins and Gerber 2017). Continuous characters require measurements of specimens and are often associated with more restricted morphologies (e.g. a specific part of the skeleton). The use of discrete characters potentially allows the examination of many aspects of morphology simultaneously, but with the drawback that realistic descriptions of the morphologies are usually lost (i.e., it is more difficult to objectively visualise which parts of morphology are varying) (Hopkins and Gerber 2017). Furthermore, some linear measurements, such as those

used as proxies for body size, can summarise successfully information from complex traits, and modern geometric morphometric techniques (e.g., using three-dimensional data) can detect extremely nuanced morphological variation.

1.2. The study group: Crocodylomorpha

Crocodylomorpha, the group that includes extant crocodylians and their extinct relatives, represents an excellent system for studying phenotypic macroevolutionary patterns. In particular, crocodylomorphs are one of two archosaur lineages that, together with birds, survived until the present day. Living representatives are important as they serve as analogues for inferring many biological features (such as physiology and behaviour). Additionally, the more than 200-million-year-old evolutionary history of the group has a rich fossil record, with more than 500 species described, which exhibit remarkable morphological variation (Fig. 1.1).

Another crucial characteristic of Crocodylomorpha, which helps make the group a useful model for studying macroevolution, is the ongoing effort to establish clearer phylogenetic relationships between its members. A plethora of phylogenetic studies on crocodylomorphs have been published over the last three decades, from the pioneering work of Benton and Clark (1988), which introduced the classification of crocodylians and their fossil relatives within a cladistic framework, to more recent studies that aimed at reconciling phylogenetic signals from both molecular and morphological data (e.g., Lee and Yates 2018). This allows the employment of phylogenetic comparative methods (i.e., the use of information from phylogenies to test evolutionary hypotheses; Harvey and Pagel 1991; Martins and Hansen 1997), essential for more accurately characterising macroevolutionary patterns.

Figure 1.1. Skulls of some crocodylomorph representatives in dorsal view, illustrating the morphological and size variation exhibited by the group. **A,** *Sarcosuchus imperator* (MNHN.F 1973-9 GDF 662), Early Cretaceous. **B,** *Steneosaurus bollensis* (SMNS 54063), Early Jurassic. **C,** *Voay robustus* (NHMUK R 36685), Pleistocene. **D,** *Ikanogavialis gameroi* (MCNC unnumbered), Miocene. **E,** *Dibothrosuchus elpahros* (IVPP V7907), Early Jurassic. **F,** *Simosuchus clarki* (cast of UA8679 housed at Stony Brook University, USA), Late Cretaceous. **G,** *Purussaurus neivensis* (UCMP 39704), Miocene. Scale bar = 15 cm.

Although some major uncertainties remain, recent discoveries and phylogenetic works have successfully established a near consensus on the "backbone" of the crocodylomorph tree, and most major subgroups are currently supported by phylogenetic definitions (Table 1.1). The most prominent of these studies include Andrade *et al*. (2010; 2011), Brochu (1997; 1999; 2003; 2006; 2010; 2011; 2012), Brochu and Storrs (2012), Brochu *et al*. (2012), Bronzati *et al*. (2012), Buckley and Brochu (1999), Buckley *et al*. (2000), Buscalioni (2017), Buscalioni *et al*. (2001; 2011), Carvalho *et al*. (2004), Clark (2011), Clark and Sues (2002), Clark *et al*. (2000; 2004), Delfino *et al*. (2005; 2008*a*, *b*), Fiorelli and Calvo (2007; 2008), Fiorelli *et al*. (2016), Foffa and Young (2014), Foffa *et al*. (2018), Fortier and Schultz (2009), Fortier *et al*. (2011; 2014), Gasparini *et al*. (2006), Hastings *et al*. (2010; 2011; 2013; 2015), Herrera *et al*. (2013; 2015), Hua and Jouve (2004), Hua *et al*. (2007), Irmis *et al*. (2013), Jouve (2005; 2009; 2016), Jouve *et al*. (2005; 2006; 2008; 2015), Larsson and Sues (2007), Martin (2007; 2010); Martin and de Lapparent de Broin (2016), Martin *et al*. (2013; 2016), Montefeltro *et al*. (2011; 2013), Narváez *et al*. (2015; 2016), Novas *et al*. (2009), O'Connor *et al*. (2010), Ortega *et al*. (2000), Ősi *et al*. (2007), Piras *et al*. (2007; 2010), Pol (2003; 2005) Pol and Gasparini (2009), Pol and Norell (2004) Pol *et al*. (2004; 2009; 2012; 2013; 2014), Salas-Gismondi *et al*. (2015), Salisbury *et al*. (2006), Scheyer *et al*. (2013), Sereno and Larsson (2009), Sereno *et al*. (2001; 2003), Tennant *et al*. (2016*a*); Turner (2006; 2015), Turner and Buckley (2008), Turner and Sertich (2010), Tykoski *et al*. (2002), Wilberg (2015), Young (2014), Young and Andrade (2009), and Young *et al*. (2012; 2013; 2014).

Table 1.1. Phylogenetic definitions of major crocodylomorph subclades, which are frequently referred to in this thesis.

Clade	Definition	Source
Archosauria	The least inclusive clade containing *Crocodylus niloticus* and *Passer domesticus*.	Sereno (2005)
Crocodylomorpha	The most inclusive clade containing *Crocodylus niloticus*, but not *Rauisuchus tiradentes*, *Poposaurus gracilis*, *Gracilisuchus stipanicicorum*, *Prestosuchus chiniquensis*, or *Aetosaurus ferratus*.	Nesbitt (2011)
Crocodyliformes	Last common ancestor of *Protosuchus richardsoni*, *Crocodylus niloticus* and all of its descendants.	Sereno *et al*. (2001)
Mesoeucrocodylia	All crocodyliforms more closely related to *Crocodylus niloticus* than to *Protosuchus richardsoni*.	Sereno *et al*. (2001)
Notosuchia	All crocodyliforms more closely related to *Notosuchus terrestris* than to *Crocodylus niloticus*.	Sereno *et al*. (2001)
Neosuchia	All crocodyliforms more closely related to *Crocodylus niloticus* than to *Notosuchus terrestris*.	Sereno *et al*. (2001)
Thalattosuchia	The most inclusive clade consisting of *Teleosaurus cadomensis* and *Metriorhynchus geoffroyii*, but not *Pholidosaurus schaumburgensis*, *Goniopholis crassidens*, or *Dyrosaurus phosphaticus*.	Young and Andrade (2009)
Tethysuchia	Last common ancestor of *Pholidosaurus purbeckensis* and *Dyrosaurus phosphaticus* and all of its descendants.	Andrade *et al*. (2011)
Eusuchia	Last common ancestor of *Hylaeochampsa vectiana*, *Crocodylus niloticus*, *Gavialis gangeticus*, and *Alligator mississippiensis* and all of its descendants.	Brochu (2003)
Crocodylia	Last common ancestor of *Gavialis gangeticus*, *Alligator mississippiensis*, and *Crocodylus niloticus* and all of its descendants.	Brochu (2003)
Gavialoidea	*Gavialis gangeticus* and all crocodylians closer to it than to *Alligator mississippiensis* or *Crocodylus niloticus*.	Brochu (2003)
Alligatoroidea	*Alligator mississippiensis* and all crocodylians closer to it than to *Crocodylus niloticus* or *Gavialis gangeticus*.	Brochu (2003)
Crocodyloidea	*Crocodylus niloticus* and all crocodylians closer to it than to *Alligator mississippiensis* or *Gavialis gangeticus*.	Brochu (2003)

1.3. Objectives

The main goal of this thesis is to quantitatively assess morphological variation within Crocodylomorpha, characterising phenotypic macroevolutionary patterns using different sources of information.

Chapter 2 investigates body size evolution across the entire crocodylomorph tree. A model-fitting approach is applied to explore the modes of evolution that underlie observed body size patterns. Furthermore, possible evolutionary drivers are assessed by testing for correlations with biotic and abiotic factors.

Chapter 3 explores crocodylomorph cranial shape variation using a taxonomically comprehensive approach. Landmark-based geometric morphometrics is used to assess the morphospace occupation of different crocodylomorph subgroups, as well as to estimate morphological disparity (through-time and between groups).

Finally, Chapter 4 focuses on Notosuchia, an extremely disparate group of crocodylomorphs, and tests the hypothesis that heterochronic processes underpin cranial shape modifications seen in the hypercarnivorous baurusuchids. Geometric morphometric techniques are once more employed to quantify notosuchian cranial shape variation, and allometric and ontogenetic changes are assessed using specific protocols.

Chapter 2: Crocodylomorph body size evolution

This chapter is a modified version of a manuscript submitted for publication in *BMC Evolutionary Biology*, which is currently under review. Additionally, the same manuscript was submitted as a preprint to *bioRxiv*, and can be found online as:

GODOY, P. L., BENSON, R. B. J., BRONZATI, M. and BUTLER, R. J. 2018*a*. The multi-peak adaptive landscape of crocodylomorph body size evolution. *bioRxiv*, 405621, https://doi.org/10.1101/405621

My contribution to this manuscript involved conducting all parts of the research, including co-co-designing the project, collecting the data, analysing it and interpreting the results, as well as writing the manuscript. My colleagues collaborated by co-designing parts of the research project and providing crucial feedback on interpretation of results and drafts of the manuscript.

2.1. Background

Body size influences many aspects of ecology, physiology and evolutionary history (Hutchinson and MacArthur 1959; Peters 1983; Calder 1984; Schmidt-Nielsen 1984; McKinney 1990*a*; McClain and Boyer 2009), and patterns of animal body size evolution are a long-standing subject of macroevolutionary investigation (e.g., Cope 1887; 1896; Depéret 1909; Newell 1949; Stanley 1973). As a major focus of natural selection, it is expected that significant variation should occur in the body size of animals, although confined within biological constraints, such as skeletal structure, thermoregulation and resource availability (Schmidt-Nielsen 1984; McKinney 1990*a*; Price and Hopkins 2015). Furthermore, body size

can often be easily measured or estimated from both fossil and modern specimens, and has therefore been widely used in phenotypic macroevolutionary studies (Cope 1887; 1896; Depéret 1909; Stanley 1973; Raup 1988; McKinney 1990*a*; Alroy 1998; Smith *et al*. 2010; Venditti *et al*. 2011; Heim *et al*. 2015).

With few exceptions (e.g., Laurin 2004; Benson *et al*. 2014*a*), previous studies of tetrapod body size evolution have focused on mammals (e.g., Alberdi *et al*. 1995; Alroy 1998; Smith *et al*. 2010; Smith and Lyons 2011; Venditti *et al*. 2011; Saarinen *et al*. 2014; Churchill *et al*. 2015; Gearty *et al*. 2018) and dinosaurs or birds (e.g., Burness *et al.* 2001; Hone *et al*. 2005; Carrano 2006; Turner *et al*. 2007; Butler and Goswami 2008; Lee *et al*. 2014; Benson *et al.* 2014*b*; Carballido *et al*. 2017; Benson *et al.* 2018). Little is known, however, about other diverse and morphologically disparate clades. Among those, Crocodylomorpha represents an excellent group for studying large-scale evolutionary patterns, with a rich and well-studied fossil record covering more than 200 million years, as well as living representatives (Bronzati *et al*. 2012; 2015; Mannion *et al*. 2015). Previous work has investigated multiple aspects of crocodylomorph macroevolution, including spatial and temporal patterns of diversity (Markwick 1998*a*; Bronzati *et al*. 2015; Mannion *et al*. 2015), as well as morphological variation, disparity, and evolution, with a particular focus on the skull (Langston 1973; Brochu 2001; Sadleir and Makovicky 2008; Stubbs *et al*. 2013; Toljagić and Butler 2013; Wilberg 2017; Chapter 4).

Nevertheless, studies quantitatively investigating macroevolutionary patterns of body size in crocodylomorphs have been restricted to particular time periods (e.g., Triassic-Jurassic body size disparity; Turner and Nesbitt 2013) or clades (e.g., metriorhynchids; Young *et al*. 2011), limiting broader interpretations. For instance, the influence of environmental temperature on the growth and adult body size of animals has long been acknowledged as an

important phenomenon (Schmidt-Nielsen 1984), and has been considered of significant influence on the physiology and distribution of crocodylians (Allsteadt and Lang 1995; Markwick 1998*b*). There is also strong evidence for climate-driven biodiversity patterns in the group (e.g., Markwick 1998*a*; Mannion *et al*. 2015). Nevertheless, it remains unclear whether extrinsic factors, such as temperature and geographic distribution, have impacted long-term patterns of crocodylomorph body size evolution (Delfino and de Vos 2014).

Most of the earliest crocodylomorphs, such as *Litargosuchus* and *Hesperosuchus*, were small-bodied animals (with estimated total lengths of less than 1 metre; Clark *et al*. 2000; Clark and Sues 2002), contrasting with some giant forms that appeared later, such as *Sarcosuchus* and *Deinosuchus* (possibly more than 10 metres long; Erickson and Brochu 1999; Sereno *et al*. 2001), as well as with the intermediate to large sizes of extant crocodylians (1.5–7 m; Ross 1998; Grigg *et al*. 2001). The absence of small-bodied forms among extant species indicates a long-term pattern of body size increase in crocodylomorphs. Directional trends of increasing body size through time (see McShea 1994), differential extinction of small bodied taxa, or other factors, such as climate-driven evolutionary change could explain this observation. However, because patterns of body size evolution along phylogenetic lineages of crocodylomorphs have not been characterised, its causes are unaddressed.

Since the end of the last century, palaeontologists have more frequently used quantitative comparative methods to investigate the tempo and mode of evolution along phylogenetic lineages (Felsenstein 1985; Hansen 1997; Pennell and Harmon 2013), including studies of body size evolution (MacFadden 1986; McKinney 1990*a*; Alroy 1998; Carrano 2006; Butler and Goswami 2008; Smith *et al*. 2010). More recently, numerous studies have employed a phylogeny-based model-fitting approach, using maximum likelihood or Bayesian

framework to identify the best-fitting statistical macroevolutionary model for a given phylogenetic comparative (Butler and King 2004; Hunt and Carrano 2010; Hunt 2012; Slater 2013; Benson *et al*. 2014*a*, *b*; Slater 2015; Benson *et al*. 2018).

Many of these works have tested the fit of a uniform macroevolutionary model, with a single set of parameters applied across all branches of a phylogeny (e.g., Cooper and Purvis 2010; Young *et al*. 2011; Sookias *et al*. 2012*a*; Slater 2013). This approach can be problematic as the dynamics of evolutionary trends vary through time, space and among clades (Hunt 2008*a*, *b*; Mahler and Ingram 2014; Hunt *et al*. 2015; Khabbazian *et al*. 2016). Therefore, uniform models are incompatible with the complexity of the natural world. In the present Chapter, this is approached in the context of the Simpsonian Adaptive Landscape (Simpson 1944; 1953), which have proved to be a fruitful conceptual framework for characterizing macroevolutionary changes, encompassing ideas such as adaptive zone invasion and quantum evolution (Hansen 2012; Arnold 2014; Mahler and Ingram 2014). Macroevolutionary landscapes provide a conceptual bridge for dialogues between studies of micro- and macroevolution, and have benefitted from the subsequent advancements of molecular biology and genetics (Arnold *et al*. 2001). Within this paradigm, uniform models primarily represent static macroevolutionary landscapes, with unchanged peaks (or maximum adaptive zones; Stanley 1973) persisting through long time intervals and across the phylogeny (Simpson 1953; Hansen 2012; Mahler and Ingram 2014).

Incorporating biological realism into statistical models of evolution is challenging (Uyeda and Harmon 2014). Many existing models are based on a Brownian motion (BM) process resulting from random walks of trait values along phylogenetic lineages (Felsenstein 1985; Hansen and Martins 1996; Hansen 2012). Uniform Brownian motion has many interpretations. For example, it can be used as a model of drift, or of adaptive evolution

towards lineage-specific selective optima that undergo random walks through time, and seems reasonable for describing undirected stochastic change (Felsenstein 1985). Elaborations of BM models were subsequently proposed. Among these, the BM model with a tendency for directional evolution was formulated by adding a parameter μ (Pagel 2002), similar to the slope of trait values through time. "Trend-shift" models have also been proposed, in which the trend parameter (μ) undergoes clade-specific or time-specific shifts (Benson *et al.* 2018).

Several evolutionary models also describe trait evolution under an Ornstein–Uhlenbeck (OU) process (Felsenstein 1988; Hansen 1997; Butler and King 2004; Beaulieu *et al*. 2012; Slater 2013), which describes the evolution of a trait towards or around a stationary peak or optimum value, at a given evolutionary rate. Thus, multi-regime OU models can account for the existence of multiple macroevolutionary regimes (or adaptive zones, in the Simpsonian Adaptive Landscape paradigm). Even though many OU-based models typically require *a priori* adaptive hypotheses for inferring the trait optima of regimes (Butler King 2004), more recent methods attempt to solve this problem by estimating location, values and magnitudes of regime shifts without *a priori* designation of selective regimes (Ingram and Mahler 2013; Mahler and Ingram 2014; Uyeda and Harmon 2014). In particular, the SURFACE method (Ingram and Mahler 2013) aims to identify convergent adaptive zones by allowing regime shifts to occur and identifying convergent regimes using AICc (Akaike's information criterion for finite sample sizes; Akaike 1974). Originally designated to identify convergent trait evolution across phylogenetic lineages, the SURFACE algorithm makes use of a multi-peak OU-model and can be a tool to determine heterogeneity of macroevolutionary landscapes (Mahler *et al*. 2013; Davis *et al*. 2014; Benson *et al.* 2018). In this Chapter, a model-fitting approach is employed to characterize the adaptive landscape of body size

evolution in Crocodylomorpha. This represents the first comprehensive investigation of major body size evolutionary patterns across the entire evolutionary history of crocodylomorphs.

2.2. Material and Methods

2.2.1. Proxy for body size

Extinct Crocodylomorpha are morphologically diverse, and frequently known from incomplete remains. Therefore, precise estimation of their body sizes, and those of comparable fossil groups, can be challenging (see Brocklehurst [2016] and Young *et al*. [2016*a*] for related considerations). There are many methods and equations for estimating crocodylomorph body size (either body mass or length) available in the literature. The most frequently used equations are derived from linear regressions based on specimens of modern species, using both cranial (Webb and Messel 1978; Hall and Portier 1994; Sereno *et al.* 2001; Hurlburt *et al*. 2003; Platt *et al*. 2009; 2011) and postcranial (Bustard and Singh 1977; Farlow *et al*. 2005) measurements as proxies. Although some of these approaches have been claimed to work well when applied to extinct taxa (e.g., Farlow *et al*. 2005), they are expected to be less accurate for extinct species that have different body proportions to those of extant species (Young *et al*. 2011; Pol *et al*. 2012; Godoy *et al*. 2016; Young *et al*. 2016*a*). An alternative approach that has been suggested is to use clade-specific equations that are derived from regressions using fossil specimens with complete skeletons preserved, such as the recently proposed equations for estimating body length in the highly specialised marine clade Thalattosuchia (Young *et al*. 2011; 2016*a*). Nevertheless, using this approach for the entire Crocodylomorpha would require numerous different equations and, consequently, complete specimens for all desired subclades.

Campione and Evans (2012) demonstrated a universal scaling relationship between proximal (stylopodial) limb bone circumferences and the body masses of terrestrial tetrapods. For instance, their equations, using both femur and humerus circumference, have been applied to estimate body mass of fossil dinosaurs (e.g., Campione and Evans 2012; Campione *et al*. 2014; Benson *et al*. 2014*b*; Carballido *et al*. 2017; Benson *et al*. 2018). However, due to a historical neglect of crocodylomorph postcranial anatomy, especially for Mesozoic taxa (Godoy *et al*. 2016), relatively less information is available on this part of the skeleton. Based on data collected for the present study, total or partial skull lengths (i.e., complete skulls or lacking only the snouts) can be measured in fossil specimens of approximately 50% of crocodylomorph species, whereas femoral and humeral shaft circumferences or lengths can only be measured in 35% of species. This greatly reduces the number of taxa that can be sampled and limits the utility of using postcranial elements as a proxy for body size. Similar problems exist for other methods, such as the "Orthometric Linear Unit" proposed by Romer and Price (1940) that uses dorsal centrum cross section (Currie 1978), as well as volumetric reconstructions (e.g., Colbert 1962; Hurlburt 1999; Motani 2001; Bates *et al*. 2009; Sellers *et al*. 2012), since relatively complete postcranial specimens are required.

For studying body size across all crocodylomorph evolutionary history, it was necessary to find an appropriate body size proxy, allowing the sampling to be as comprehensive as possible. Thus, two cranial measurements were used as proxies for total body length: total dorsal cranial length (DCL) and dorsal orbito-cranial length (ODCL), which is measured from the anterior margin of the orbit to the posterior margin of the skull. Ultimately, using cranial measurements results in a study of the patterns of cranial size evolution in crocodylomorphs (instead of patterns of body size evolution). Nevertheless, by doing this, the addition of potential errors to the model-fitting analyses is avoided, since

previous works have reported problems when estimating total body length from cranial measurements, particularly skull length (Fig. 2.1), as the equations were formulated using modern species and different crocodylomorph clades are likely to have body proportions distinct from those of living taxa (e.g., Young *et al*. 2011; Godoy *et al*. 2016; Young *et al*. 2016*a*). Furthermore, the range of body sizes among living and extinct crocodylomorphs is considerably greater than variation among size estimates for single species. Therefore, it is expected that the analyses will recover the most important macroevolutionary body size changes even when using only cranial measurements. The use of ODCL, in addition to DCL, is justified as it allows to examine the sensitivity of the results to changes in proportional snout length, as a major aspect of length change in crocodylomorph skulls results from proportional elongation or shortening of the snout (Clark 1994; Pol and Gasparini 2009; Wilberg 2015). Also, more taxa could be included in the analyses when doing so, because ODCL can be measured from some incomplete skulls.

The DCL dataset includes 219 specimens (representing 178 taxa), whereas the ODCL dataset includes 240 specimens (195 taxa). In total, measurements from 118 specimens (83 taxa) were collected via first-hand examination from specimens, using callipers and measuring tape. The remaining information was collected from the literature (98 specimens) or photographs (21 specimens) supplied by other researchers, and measurements were estimated using the software ImageJ (for the complete list of sampled specimens see information in Appendix A). Mean values were used in those cases where cranial measurements were collected for multiple specimens of the same taxon. For both the model-fitting and correlation tests, skull measurements (in millimetres) were log-transformed prior to the analyses. However, to help with the further interpretation and discussion of the results,

total body length was subsequently estimated using the equations presented by Hurlburt *et al.* (2003).

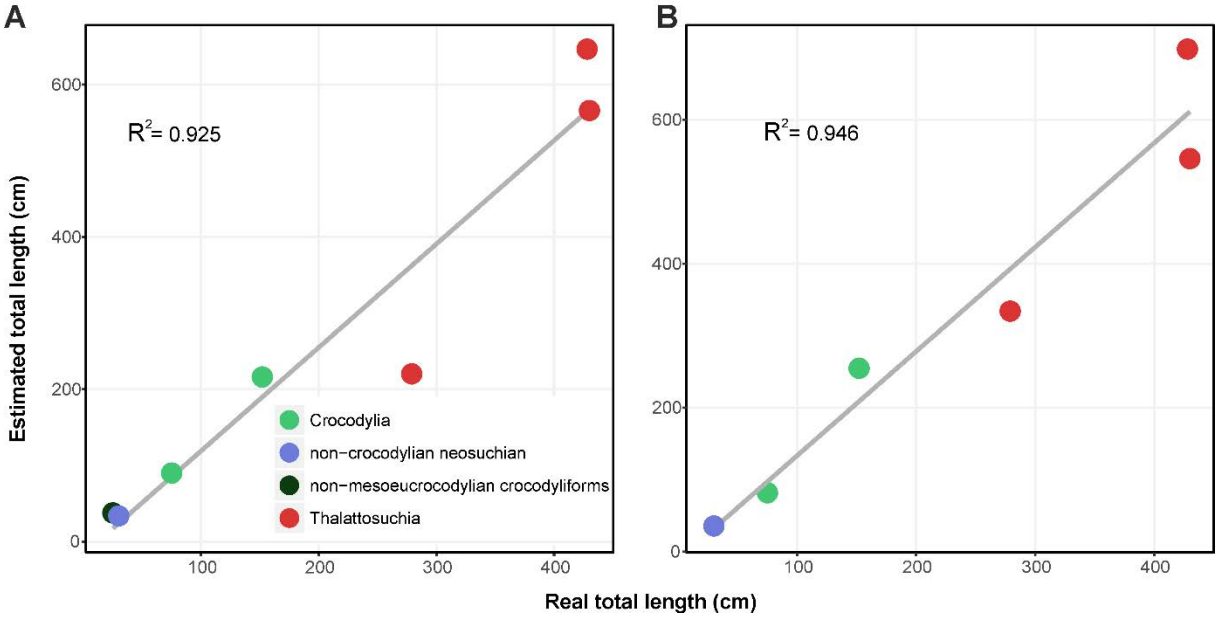

Figure 2.1. Real total body length (measured from some complete fossil crocodylomorph specimens) plotted against total length estimated from the cranial measurements DCL (**A**) and ODCL (**B**) (equations from Hurlburt *et al.* [2003]), exemplifying the amount of error expected when using the two measurements to estimate total body length of crocodylomorphs. R^2 value illustrates the strength of the correlation between real and estimated total lengths. Colours represent different mono- or paraphyletic crocodylomorph groups. See Appendix A for information on the specimens used to construct these plots.

2.2.2. Phylogenetic framework

For the phylogenetic framework of Crocodylomorpha, the aim was to maximise taxon inclusion and to use a phylogenetic hypothesis that best represents the current consensus. Thus, an updated version of the supertree presented by Bronzati *et al.* (2015) was primarily used. This supertree, which originally contained 245 taxa, was manually modified ("informal approach") using the software Mesquite version 3.51 (Maddison and Maddison 2018). Apart from modifications seeking to maximise congruence of the tree with the current understanding of the phylogeny of the group, some recently published species were also

added, and taxa that have not yet received a formal description and designation were removed. Species not previously included in phylogenetic studies but for which body size data was available were also added to the supertree.

The supertree presented by Bronzati *et al.* (2015) is restricted to Crocodyliformes, which is less inclusive than Crocodylomorpha. Thus, non-crocodyliform crocodylomorphs taxa were added, following the phylogenetic hypotheses presented by Pol *et al.* (2013) and Leardi *et al*. (2017). Within Crocodyliformes, as in Bronzati *et al.* (2015) and other recent studies (e.g., Andrade *et al.* 2011; Montefeltro *et al.* 2013; Pol *et al.* 2014; Turner and Pritchard 2015; Buscalioni 2017), taxa classically associated to "Protosuchia" are paraphyletically arranged in relation to Mesoeucrocodylia, with less inclusive subgroups displayed following Bronzati *et al*. (2015). Accordingly, *Hsisosuchus* is the sister-group of Mesoeucrocodylia (as in Clark 2011; Pol *et al.* 2014; Buscalioni 2017) and the following groups represent taxa successively more distant from Mesoeucrocodylia: Shartegosuchidae (Clark 2011); an unnamed clade composed by taxa such as *Sichuanosuchus* and *Shantungosuchus;* an unnamed clade composed by *Zaraasuchus* and *Gobiosuchus* (Pol *et al.* 2014); Protosuchidae (Clark 2011; Pol *et al.* 2014; Turner and Pritchard 2015).

Within Mesoeucrocodylia, Notosuchia corresponds to the sister group of all the other mesoeucrocodylians (= Neosuchia in our topology), similar to what is presented by Andrade *et al.* (2011), Pol *et al.* (2014), and Turner and Pritchard (2015). Yet, Notosuchia comprises forms such as baurusuchids, sebecosuchians, peirosaurids, sphagesaurids, uruguaysuchids, and *Araripesuchus.* The relationships among taxa within Notosuchia follow the general arrangement presented by Pol *et al.* (2014).

One of the branches at the basal split of Neosuchia leads to a clade composed by longirostrine forms, which includes Thalattosuchia and Tethysuchia (i.e., Dyrosauridae and

"pholidosaurids"). The sister-group relationship between Thalattosuchia and Tethysuchia follows what was recovered in the supertree of Bronzati *et al.* (2015). Within Tethysuchia, "pholidosaurids" are paraphyletic in relation to Dyrosauridae (also found in Pol *et al.* 2014; Meunier and Larsson 2017; Young *et al.* 2017). Relationships among Dyrosauridae follow Hastings *et al.* (2015). Relationships among thalattosuchians follow Young (2014) and Herrera *et al*. (2015).

The sister-group of the longirostrine clade mentioned above contains Eusuchia and its closest relatives such as Atoposauridae and Goniopholididae. The latter is depicted as the sister group of Eusuchia, whereas the former corresponds to the sister group of Eusuchia + Goniopholididae. This arrangement follows that recovered in Pol *et al.* (2014) and Bronzati *et al.* (2015). Regarding the internal relationships of Goniopholididae, the hypotheses of Martin *et al.* (2016) and Ristevski *et al*. (2018) were followed. For Atoposauridae, the arrangements presented by Tennant *et al*. (2016*a*) and Schwarz *et al*. (2017) were followed. For Paralligatoridae and Susisuchidae, the phylogenetic hypotheses of Turner (2015) and Turner and Pritchard (2015) were followed.

In relation to non-crocodylian eusuchians, the topology of Bronzati *et al*. (2015) was primarily followed, with modifications to accommodate the arrangements proposed by Turner (2015) and Turner and Pritchard (2015) within Paralligatoridae and Susisuchidae. The topology of Narváez *et al.* (2015) was followed regarding the interrelationships of the crown-group, as well as the position of Hylaeochampsidae + Allodaposuchidae as the sister group of Crocodylia. For the relationships within the crown-group, Brochu (2012), Brochu *et al*. (2012), Scheyer *et al*. (2013), and Narváez *et al*. (2015) were followed.

The final updated version of this supertree contains 296 crocodylomorph species, as well as nine closely related taxa used as outgroups for time-scaling the trees (see below).

Additionally, to accommodate major uncertainties in the crocodylomorph phylogeny, two other supertrees were constructed, with alternative positions of Thalattosuchia. Thalattosuchians are Jurassic–Early Cretaceous aquatic crocodylomorphs, some of which were probably fully marine (Herrera *et al*. 2017). They have classically been placed within Neosuchia, as the sister taxon of Tethysuchia (Pol and Gasparini 2009). Nevertheless, some authors have argued that this close relationship may result from the convergent acquisition of longirostrine snouts in both groups (Clark 1994; Jouve *et al*. 2006), and some recent works have suggested alternative positions for Thalattosuchia, within or as the sister group of Crocodyliformes (i.e., only distantly related to Neosuchia; Young and Andrade 2009; Montefeltro *et al*. 2013; Turner 2015; Wilberg 2015).

Accordingly, to test the influence of uncertainty over the phylogenetic position of Thalattosuchia, the macroevolutionary analyses were performed using three distinct topologies of Crocodylomorpha (Fig. 2.2). In the first topology, the more classic position of Thalattosuchia was maintained (Thalattosuchia as the sister taxon of Tethysuchia and within Neosuchia; as in the original supertrees of Bronzati *et al*. (2012; 2015). In the two alternative topologies, Thalattosuchia was placed as the sister group of either Crocodyliformes (as non-crocodyliform crocodylomorphs), following the position proposed by Wilberg (2015), or Mesoeucrocodylia, following Larsson and Sues (2007) and Montefeltro *et al*. (2013). It is worth stressing that discrepancies among competing phylogenetic hypotheses do not concern only the "longirostrine problem" described above. However, the decision to further investigate only the impact of the different positions of Thalattosuchia is based on its high taxic diversity and the impact that its phylogenetic position has on branch lengths across multiple parts of the tree, factors that can substantially alter macroevolutionary patterns detected by the analyses.

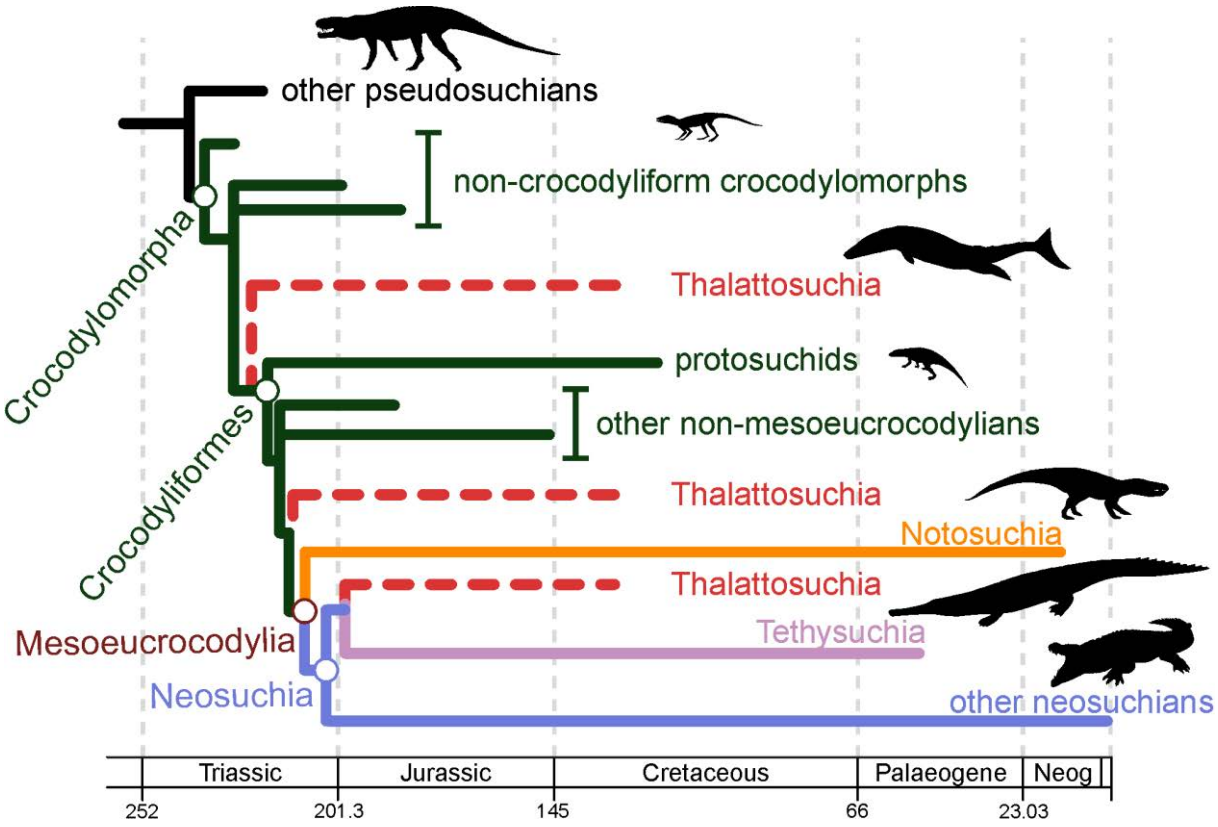

Figure 2.2. Simplified cladogram showing the phylogenetic relationships among crocodylomorphs and the alternative positions of Thalattosuchia (dashed red lines), following Larsson and Sues (2007), Bronzati *et al*. (2012; 2015), Montefeltro *et al*. (2013), and Wilberg (2015). Silhouettes of crocodylomorph representatives in figures are from illustrations by Dmitry Bogdanov, Smokeybjb, and Nobumichi Tamura, hosted at Phylopic (http://phylopic.org), where license information is available.

2.2.3. Time-calibration

To perform the macroevolutionary analyses, it was necessary to time-calibrate the phylogenies, assigning ages to both terminal taxa and nodes (Bapst 2014*a*). This is a crucial step in comparative analyses of trait evolution, as the use of different methods may impact upon the inference of evolutionary models and the interpretation of results (Bapst 2013; 2014*b*). As such, three different time-scaling methods were used, each one with benefits and drawbacks. For these methods, ages (first and last occurrence dates) were initially obtained

from the Paleobiology Database (PBDB), but were then checked using primary sources in the literature. To accommodate uncertainties related to the ages of terminal taxa (i.e., most taxon ages are based on single occurrences, known only within rather imprecise bounds), first and last occurrence dates were treated as maximum and minimum possible ages and drew terminal dates for time-calibration from a uniform distribution between these.

The first time-scaling method used was the minimum branch length method (*mbl*; Laurin 2004), in which a minimum branch duration is set *a priori*, to avoid the presence of undesirable and unrealistic zero-length branches (Bapst 2014*a*, *b*). For the analyses within this Chapter, the minimum of 1 Myr was set. Additionally, two recently introduced probabilistic time-scaling methods were also used. The *cal3* is a stochastic calibration method that requires estimates of sampling and diversification (branching and extinction) rates to draw likely divergence dates under a birth–death-sampling model (Bapst 2013; Lloyd *et al*. 2016). The fact that most crocodylomorph taxa are singletons (i.e., very few genera or species have multiple occurrences in different time intervals) prevented the direct calculation of speciation, extinction and sampling rates needed as inputs to the *cal3* method. Thus, when using this time-scaling method for the analyses within this Chapter, the same rates estimated for dinosaurs in Lloyd *et al*. (2016) were adopted (i.e., extinction and speciation rates = 0.935; sampling rate = 0.018), which used the apparent range-frequency distribution of dinosaurs in the PBDB for these estimates. Although essentially different from that of dinosaurs, the crocodylomorph fossil record is arguably comparable enough to result in similar rates, and *a posteriori* comparison to other time-scaling methods demonstrated that results were reasonable. The last time-scaling method used was the extended *Hedman* method, proposed by Lloyd *et al*. (2016), which is an expansion of the Bayesian approach presented by Hedman (2010), that uses the ages of successive outgroup taxa relative to the age of the node of

interest to date this node by sampling from uniform distributions (Lloyd *et al*. 2016; Brocklehurst 2017).

Since the input phylogenies were not completely resolved (i.e., the three alternative topologies of the supertree), the polytomies were randomly resolved, generating 20 completely resolved trees for each alternative phylogenetic scenario (i.e., with different positions of Thalattosuchia). These trees were then time-scaled using the three time-calibration methods. Time-scaling with the *mbl* and *cal3* methods were performed using the package *paleotree* (Bapst 2012) in R version 3.5.1 (R Core Team 2018), whilst the *Hedman* method was implemented also in R, using the protocol published by Lloyd *et al*. (2016).

2.2.4. Macroevolutionary analyses

A model-fitting approach was applied to characterize patterns of body size evolution in Crocodylomorpha, with an emphasis on evolutionary models based on the Ornstein-Uhlenbeck (OU) process (Hansen 1997; Butler and King 2004; Ingram and Mahler 2013; Slater 2013; Benson *et al.* 2018). The first formulation of an OU-based model was proposed by Hansen (1997), to incorporate Felsenstein's (1988) suggestion of using the Ornstein-Uhlenbeck (OU) process as a basis for comparative studies (Butler and King 2004; Beaulieu *et al*. 2012). OU-based models (also known as "Hansen" models) express the dynamics of a quantitative trait evolving along the branches of a phylogeny as the result of stochastic variation around a trait "optimum" (expressed as theta: θ), towards which trait values are deterministically attracted (the strength of attraction is given by alpha: α). The constant σ^2, describes the stochastic spread of the trait values over time (i.e., under a Brownian motion process). Accordingly, the OU model can be formulated as:

$$dX(t) = \alpha\,[\theta - X(t)]\,dt + \sigma dB(t)$$

This equation expresses the amount of change in trait X during the infinitesimal time interval from t to $t + dt$. As expressed above, the formulation includes a term describing trait attraction towards θ, which is the product of α and the difference between $X(t)$ and θ. The term $\sigma dB(t)$ describes stochastic evolution in the form of Brownian motion (BM), with random variables of mean zero and variance of dt (thus, σ^2 is the rate of stochastic evolution). In this sense, if α is zero, the attraction term becomes zero, and the result is evolution by BM as a special case of OU (Butler and King 2004; Slater 2013; Benson *et al*. 2018). The OU model can also simulate trait evolution patterns similar to that observed under other evolutionary models, such as BM with a trend incorporated, and "white noise" or stasis (Hansen 1997; Slater 2013; Benson *et al*. 2018). Thus, the parameters of the OU model are crucial for interpreting the mode of evolution (Hansen 1997; Butler and King 2004). For example, the estimated ancestral trait value (i.e., the value of θ at the root of the tree) is given by the parameter Z_0. Also, the time taken for a new macroevolutionary regime to become more influential than the ancestral regime (i.e., how long it takes to θ to be more influential than Z_0) can be obtained by calculating $\ln(2)/\alpha$. This parameter is often called the phylogenetic half-life (or $t_{0.5}$).

Among the methods that attempt to model adaptive evolution under the framework of an Ornstein-Uhlenbeck process (e.g., Harmon *et al*. 2008; Beaulieu *et al*. 2012; Uyeda and Harmon 2014), the SURFACE algorithm (Ingram and Mahler 2013) estimates the fit of a non-uniform OU-based model by allowing shifts in trait optima (θ) among macroevolutionary regimes. SURFACE locates regime shifts using stepwise AICc (Akaike's information criterion for finite sample sizes; Akaike 1974; Sugiura 1978; Burnham and Anderson 2003),

with a forward phase (that searches for all regime shifts in the phylogeny) and a backward phase (in which improvements of AICc scores merge similar regimes, detecting convergent evolution). Although it allows θ to vary among regimes, SURFACE assumes fixed whole-tree values of σ^2 and α (Ingram and Mahler 2013).

The performance of two different OU-based models was compared, one with a single trait optimum or a single macroevolutionary regime ("OU model") and another non-uniform model with multiple regimes ("SURFACE model"). To test if other macroevolutionary models could provide a better description of the observed patterns of crocodylomorph body size evolution, these OU-based models were also compared to other BM-based models. First, the diffusion by Brownian motion (BM model), which assumes evolution via random walks, with a constant normally distributed deviation from the observed morphology, resulting in no directional trend in trait mean, but with increasing trait variance through time (Felsenstein 1985; Hunt and Carrano 2010; Hunt 2012; Slater 2013). Second, the "early burst" (EB model; also known as "ACDC model"; Blomberg *et al*. 2003), in which the lineages experience an initial maximum in evolutionary rate of change, that decreases exponentially through time according to the parameter *r* (Harmon *et al.* 2010). This results in a rapid increase of trait variance in the early evolution of the lineages, followed by a deceleration (Blomberg *et al*. 2003; Harmon *et al*. 2010).

Finally, a set of uniform and non-uniform trend-like models were also fitted to the data. In the uniform "trend" model (i.e., with a single regime), the parameter μ is incorporated into the BM model to describe directional multi-lineage increase or decrease in trait values through time, in the entire clade (Pagel 2002; Hunt and Carrano 2010; Hunt 2012). Non-uniform "trend" models allow for shifts in the parameter μ, which can be explored in two different ways according to the formulations of non-uniform trend models formulated by G.

Hunt and presented in Benson *et al*. (2018): temporal shifts in μ ("time-shift trend models") or shifts in μ at specific nodes of the tree ("node-shift trend models"). In time-shift trend models, evolutionary dynamics are uniform across all branches alive during each interval. Shifts to a new value of μ occurs at time-horizons and are applied to all lineages alive at that time. In node-shift trend models, values of μ can vary among lineages. In a similar approach to the forward phase of SURFACE, the shifts in these non-uniform trend-like models are detected via stepwise AICc. In both time-shift and node-shift models, the Brownian variance (σ^2) is constant across all regimes (Benson *et al*. 2018). For the macroevolutionary analyses with the entire crocodylomorph phylogeny, trend-like models allowing up to three time-shifts and ten node-shifts to occur were fitted.

Then, a set of exploratory analyses were performed to test which of these evolutionary models (SURFACE, OU, BM, EB and trend-like models) offered the best fit to the data, using the different time-scaling methods (*mbl*, *cal3* and *Hedman* methods) and both log-transformed cranial measurements (DCL and ODCL). To reduce the computational demands, only 20 randomly resolved trees of the original supertree topology were used (with Thalattosuchia positioned traditionally within Neosuchia). The aim was to compare the performance of the OU-based models, particularly the SURFACE model, against the other evolutionary models, but also to evaluate possible influences of the different time-scaling methods and body size proxies. Maximum-likelihood was employed to fit these models to body size data and the phylogeny of Crocodylomorpha, and AICc scores were used to compare the performance of each model.

Previous works suggested caution when fitting OU models in comparative analyses (e.g., Ho and Ané 2014; Cooper *et al*. 2016). The issue of "large p small n" when using multi-regime OU models, demonstrated by Ho and Ané (2014), can result in false positives and

spurious support to more complex models (Khabbazian *et al*. 2016; Benson *et al*. 2018). This issue may be reduced when using non-ultrametric trees (as done here), as this improves identifiability of the parameters of OU models (Slater 2013; Ho and Ané 2014). Another approach would be using the phylogenetic Bayesian information criterion ("pBIC"), proposed by Khabbazian *et al*. (2016), as an alternative to using AICc for selecting the best fit. Ho and Ané (2014) demonstrated that AICc is biased towards model overfit and suggested using pBIC, a modified Bayesian information criterion (mBIC; Zhang and Siegmund 2007), which is more conservative and has low rates of false positive identification of OU model regime shifts (Khabbazian *et al*. 2016; Benson *et al.* 2018). The pBIC criterion is still not implemented for all evolutionary models used in this Chapter, which prevents its usage for the comparative model-fitting analyses. However, pBIC was used during the backward phases of SURFACE model searches, to ensure that artefactually complex models were not returned.

Following these exploratory analyses, the analyses focused on the SURFACE model, as the AICc scores indicated that this evolutionary model outperforms the others (see the "Results" section of this Chapter). This second phase of analyses made use of all three alternative phylogenetic scenarios (varying the position of Thalattosuchia) to test the influence of phylogeny in interpretations of evolutionary regimes for body size in Crocodylomorpha. SURFACE models were fitted to 20 randomly resolved trees from each of these alternative topologies, using three different time-scaling methods (*mbl*, *cal3* and *Hedman* methods) and two log-transformed cranial measurements (DCL and ODCL). As before, a conservative backward-phase of SURFACE was implemented, with pBIC searches instead of AICc.

Two well-recognized crocodylomorph subclades, Notosuchia and Crocodylia, returned a high frequency of macroevolutionary regime shifts, representing an apparently complex

evolutionary history under the SURFACE paradigm. However, SURFACE fits a single value of α to all regimes, and therefore could overestimate the strength of evolutionary constraint within regimes, and consequently miscalculate the number of distinct regimes within clades showing more relaxed patterns of trait evolution. This possibility was investigated by fitting the initial set of evolutionary models (SURFACE, OU, BM, EB and trend-like models) to the phylogenies of these two subclades (using 100 randomly resolved trees of each group, time-scaled with the *mbl* method) and their body size data (using only the ODCL dataset, since it includes more species). Differently from what was done for the entire crocodylomorph phylogeny, trend-like models fitted to Notosuchia allowed up to 2 time-shifts and 5 node-shifts to occur, whereas for Crocodylia 3 time-shifts and 7 node-shifts were allowed to occur (given that these two clades include fewer species and fewer shifts are expected, and that models with an exceeding number of shifts usually receive weaker support). In addition, for these same clades, the OUwie model-fitting algorithm was also employed (Beaulieu *et al.* 2012), fitting different BM and OU-based models which allow all key parameters to vary freely (since SURFACE allows only θ to vary, whereas it assumes fixed values of σ^2 and α for the entire tree). However, differently from SURFACE, OUwie needs *a priori* information on the location of regime shifts in order to be implemented. Thus, the same regime shifts identified by SURFACE were incorporated into the data (phylogenetic and body size data) to fit four additional evolutionary models using the OUwie algorithm: BMS, which is a multi-regime BM model that allows the rate parameter σ^2 to vary; OUMV, a multi-regime OU-based model that allows σ^2 and the trait optimum θ to vary; OUMA, also a multi-regime OU model, in which θ and the constraint parameter α can vary; and OUMVA, in which all three parameters (θ, α and σ^2) can vary. Since computing all these parameters estimates can be an intensively demanding task (Beaulieu *et al.* 2012), some of the model fits returned

nonsensical values and were, therefore, discarded. Nonsensical values were identified by searching for extremely disparate parameter estimates, among all 100 model fits (e.g., some model fits found σ2 values higher than 100,000,000 and α lower than 0.00000001).

All macroevolutionary analyses were performed in R version 3.5.1 (R Core Team 2018). Macroevolutionary models BM, trend, EB, and OU with a single regime were fitted using the R package *geiger* (Harmon *et al*. 2008). The SURFACE model fits were performed with package *surface* (Ingram and Mahler 2013). Implementation of pBIC functions in the backward-phase of SURFACE model fits, as well as the functions for fitting non-uniform trend-like models, were possible with scripts presented by Benson *et al*. (2018). The additional model-fitting analyses, using the OUwie algorithm, were implemented with the package *OUwie* (Beaulieu and O'Meara 2016).

2.2.5. Correlation with abiotic factors

To test whether abiotic environmental factors could be driving the evolution and distribution of body sizes in crocodylomorphs, environmental information was extracted from the literature. As a proxy for palaeotemperature, $\delta^{18}O$ data from two different sources was used. The dataset from Zachos *et al*. (2008) assembles benthic foraminifera isotopic values from the Late Cretaceous (Maastrichtian) to the Recent. The work of Prokoph *et al*. (2008) compiled sea surface isotopic values from a range of marine organisms. Their dataset is divided into subsets representing palaeolatitudinal bands. For the analyses in this Chapter, two subsets were used: the temperate palaeolatitudinal subset, which extends from the Jurassic to the Recent, as well as the tropical palaeolatitudinal subset, which extends back to the Cambrian. For the correlation analyses, 10 Myr time bins were used (see Appendix A for information about the time bins), by taking the time-weighted mean $\delta^{18}O$ for data points that fall within

each time bin. For the body size data used in the correlation tests, maximum and mean size values were calculated for each time bin, using both DCL and ODCL datasets. Correlations between the body size data and the proxies for palaeotemperature were first assessed using ordinary least squares (OLS) regressions. Then, to avoid potential inflation of correlation coefficients created by temporal autocorrelation (the correlation of a variable with itself through successive data points), a first-order autoregressive model was incorporated to generalised least squares (GLS) regressions (see e.g., Hunt *et al.* 2005; Marx and Uhen 2010; Benson and Butler 2011; Mannion *et al.* 2015). Furthermore, to test the possible differential influence of temperature on marine versus continental (terrestrial and freshwater) animals, two additional body size data subsets were created, one with only marine and another with only non-marine crocodylomorphs.

Additionally, palaeolatitudinal data was collected, from the PBDB and the literature, for every specimen in the datasets (DCL and ODCL datasets). The correlation between this palaeolatitudinal data and the body size data was first tested by applying OLS regressions to untransformed data. Then, to deal with possible biases generated by phylogenetic dependency, phylogenetic generalized least squares regressions (PGLS; Martins and Hansen 1997) were used. For this, branch length transformations were optimised between bounds with maximum likelihood using Pagel's λ (Pagel 1999), by setting the argument λ = "ML" within in the function *pgls()* of the R package *caper* (Orme *et al.* 2018). As for the correlation analyses between body size data and palaeotemperature, the datasets were also divided into two subsets each (only marine and only non-marine taxa).

Finally, to explore the effects of these two abiotic factors on the distribution of body sizes at more restricted levels (temporal and phylogenetic), all these regression analyses were repeated using subsets including only species of Crocodylia, Notosuchia, Thalattosuchia, and

Tethysuchia. For crocodylians, correlations with paleotemperature were restricted to the Maastrichtian until the Recent (i.e., data from Zachos *et al*. 2008). All correlation analyses used log-transformed cranial measurements (DCL and ODCL) in millimetres and were performed in R version 3.5.1 (R Core Team 2018). GLS regressions with an autoregressive model were carried out using the package *nlme* (Pinheiro *et al*. 2017), whereas PGLS regressions used the package *caper* (Orme *et al.* 2018).

2.3. Results

2.3.1. Comparative model-fitting analyses

Comparisons between the AICc scores for all the evolutionary models fitted to the crocodylomorph body size data (Fig. 2.3) show extremely strong support for the SURFACE model (note that lower AICc values indicate higher support). This is observed for all time-scaling methods (*mbl*, *cal3* and *Hedman* methods) and both body size proxies (DCL and ODCL). All uniform models exhibit relatively similar AICc scores, including the OU model with a single macroevolutionary regime, and all of these have poor support compared to the SURFACE model. Node-shift trend models received higher support than both uniform and time-shift trend models for most phylogenies, but have AICc values that are more similar to the set of uniform models than to the SURFACE models. Single-regime OU models only have better AICc scores than multi-trend models when trees are time-scaled with the *mbl* method. Even the best trend-like model (usually the models with six or seven node-shifts) have significantly weaker support than SURFACE, regardless of the time-calibration method (see Appendix A for a complete list of AICc scores, including for all trend-like models). Based on the extremely strong support found for the SURFACE model, as well as on the capability of the SURFACE algorithm to locate the regime shifts across the phylogeny

(Ingram and Mahler 2013), the subsequent analyses focused on the SURFACE model fits, to characterize in more detail the patterns of crocodylomorph body size macroevolution.

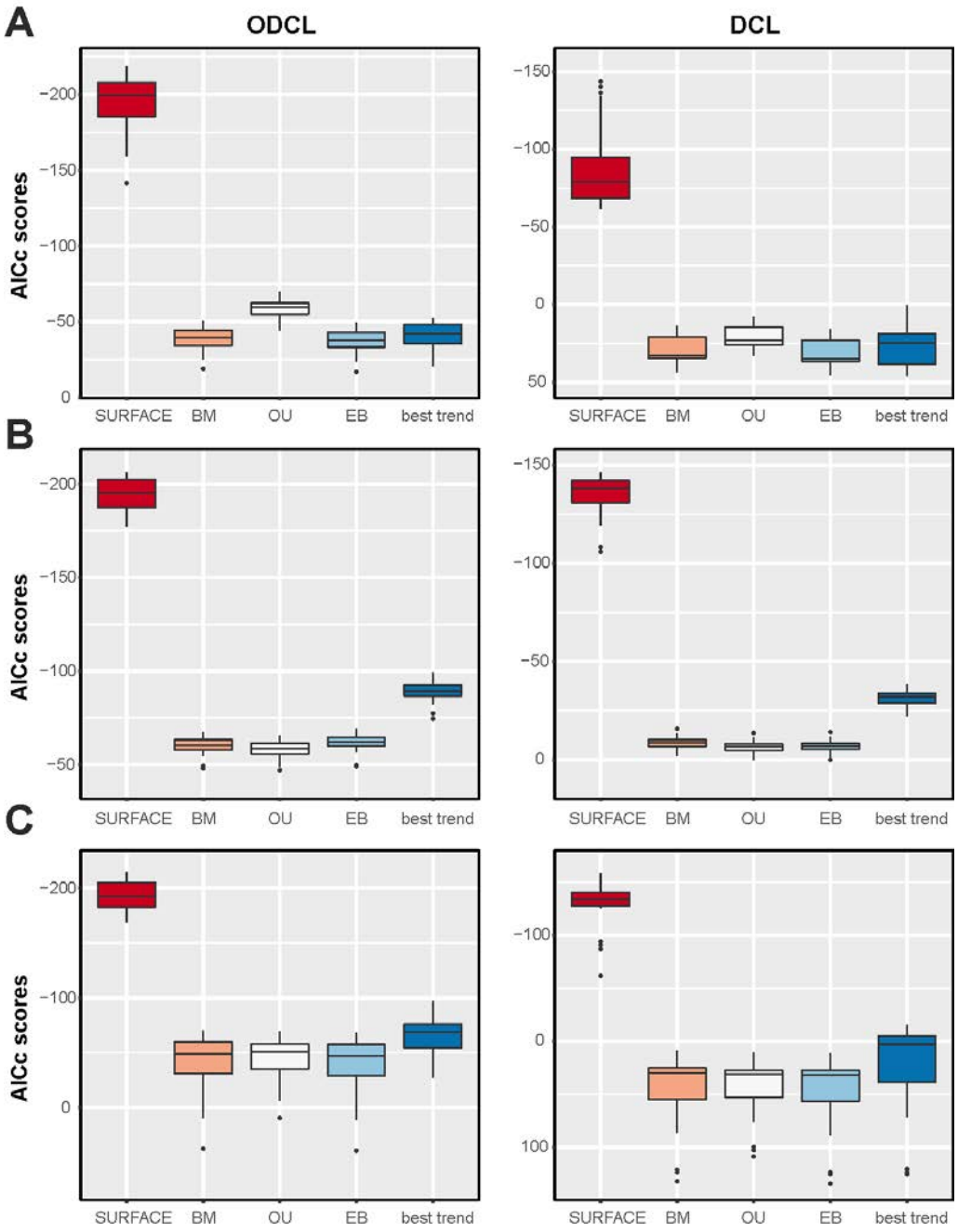

Figure 2.3. AICc scores of the evolutionary models fitted to crocodylomorph phylogeny and body size data. Results shown for two cranial measurement datasets (ODCL in the left column and DCL in the right one), as well as using three different methods to time-calibrate 20 randomly resolved phylogenies of Crocodylomorpha: **(A)** *mbl*, **(B)** Hedman, and **(C)** cal3 methods. For the trend-like models, only the AICc of the best model ("best trend") is shown.

2.3.2. Appraising the SURFACE model fits

Aiming to minimise the problem of biased AICc support for more complex models (see Ho and Ané 2014; Khabbazian *et al*. 2016), two rounds of SURFACE model fits were implemented: one using the original algorithm (Ingram and Mahler 2013), with stepwise AICc searches in the two phases of SURFACE; and another using a modified version of the SURFACE algorithm presented by Benson *et al*. (2018), which uses pBIC searches in the backward-phase. This latter approach is more conservative and potentially should be able to indicate when overly complex models are being inappropriately supported, since the input trees used for this alternative implementation of SURFACE were the same as those used for the model fits with the original algorithm (i.e., with AICc searches only). Comparisons between the SURFACE results using pBIC and only AICc show that, in almost all cases, identical model fits are found for the same trees, with the same parameter estimates (Table 2.1). For the very few trees in which this is not true, the models are still very similar, with only minimal differences in the parameter values, mainly in θ values. This pattern was maintained when using any time-scaling method, cranial measurement or tree topology, indicating that the SURFACE model fits are not erroneously complex.

Table 2.1. Parameter estimates from some of the SURFACE model fits, using both stepwise search algorithms: full-AICc searches and backward-phase of SURFACE with pBIC searches. Model fits of the first ten trees (using the ODCL dataset, the *mbl* time-scaling method and with Thalattosuchia within Neosuchia). Z_0 values in $\log_{10}$ millimetres. "Number of regimes" represents the number of main ("convergent") regimes for each model fit. See Appendix A for plots of all SURFACE model fits, containing information about parameter estimates.

Tree number	**Parameter estimates**							
	full-AICc searches				**pBIC in the backward-phase**			
	α	**σ^2**	**Z_0**	**Number of regimes**	**α**	**σ^2**	**Z_0**	**Number of regimes**
1	0.217	0.005	1.642	10	0.217	0.005	1.642	10
2	16.06	0.418	1.648	8	16.06	0.418	1.648	8
3	0.162	0.004	1.647	10	0.162	0.004	1.647	10
4	0.148	0.004	1.653	10	0.148	0.004	1.653	10
5	0.128	0.003	1.639	10	0.128	0.003	1.639	10
6	0.055	0.002	1.696	9	0.055	0.002	1.696	9
7	0.058	0.002	1.704	10	0.058	0.002	1.704	10
8	0.08	0.003	1.657	9	0.08	0.003	1.657	9
9	0.148	0.003	1.641	9	0.148	0.003	1.641	9
10	0.523	0.012	1.648	8	0.523	0.012	1.648	8

The SURFACE model fits exhibit a strong correlation between AICc/pBIC scores and the number of macroevolutionary regime shifts (Fig. 2.4; see Appendix A for plots of all SURFACE model fits). In general, model fits with lower (i.e., better) AICc/pBIC values tend to have more regime shifts. In other words, more complex models seem to be favoured by better AICc/pBIC values. Additionally, apart from higher (i.e., worse) AICc/pBIC values, simpler SURFACE model fits also tend to exhibit lower α values. Thus, simpler model fits are

characterised by high-AICc/pBIC scores and low values of α. Because the same randomly resolved tree topologies were used for each of the time-scaling methods (*mbl*, *cal3* and *Hedman*), it was possible to compare the SURFACE model fits of these same trees obtained across different branch-length calibration methods, by calculating pBIC scores (e.g., calculating the pBIC score the regime configuration obtained from analysis of the *cal3*-calibrated tree on the *mbl*-calibrated tree; see Appendix A for all cross plotting of SURFACE model fits on trees using different time-scaling methods). This shows that many of the simplest SURFACE model fits are suboptimal (i.e., received worse pBIC scores) compared to more complex regime configurations obtained during searches on trees with different branch-lengths (Table 2.2). The simple models returned by some searches therefore represent failure of the stepwise-AICc search to find the best regime configuration and are consequently not considered when the macroevolutionary patterns of body size in crocodylomorphs are described. Suboptimal model fits were more frequent on topologies with Thalattosuchia placed as the sister group of Crocodyliformes, particularly when time-scaled using *mbl* and *cal3* methods. Although a full explanation cannot be provided for why the frequency of suboptimal model fits varied among topologies with alternative positions of Thalattosuchia, it is expected that AIC procedures face difficulties when finding the best fits for complex datasets (Burnham *et al*. 2011), even when using pBIC. However, the SURFACE model fits represent a useful simplification of major patterns of body size evolution in a group, and particularly the shifts of average body sizes among clades on the phylogeny. In this respect, they provide an overview of crocodylomorph body size evolution that is otherwise lacking from current literature.

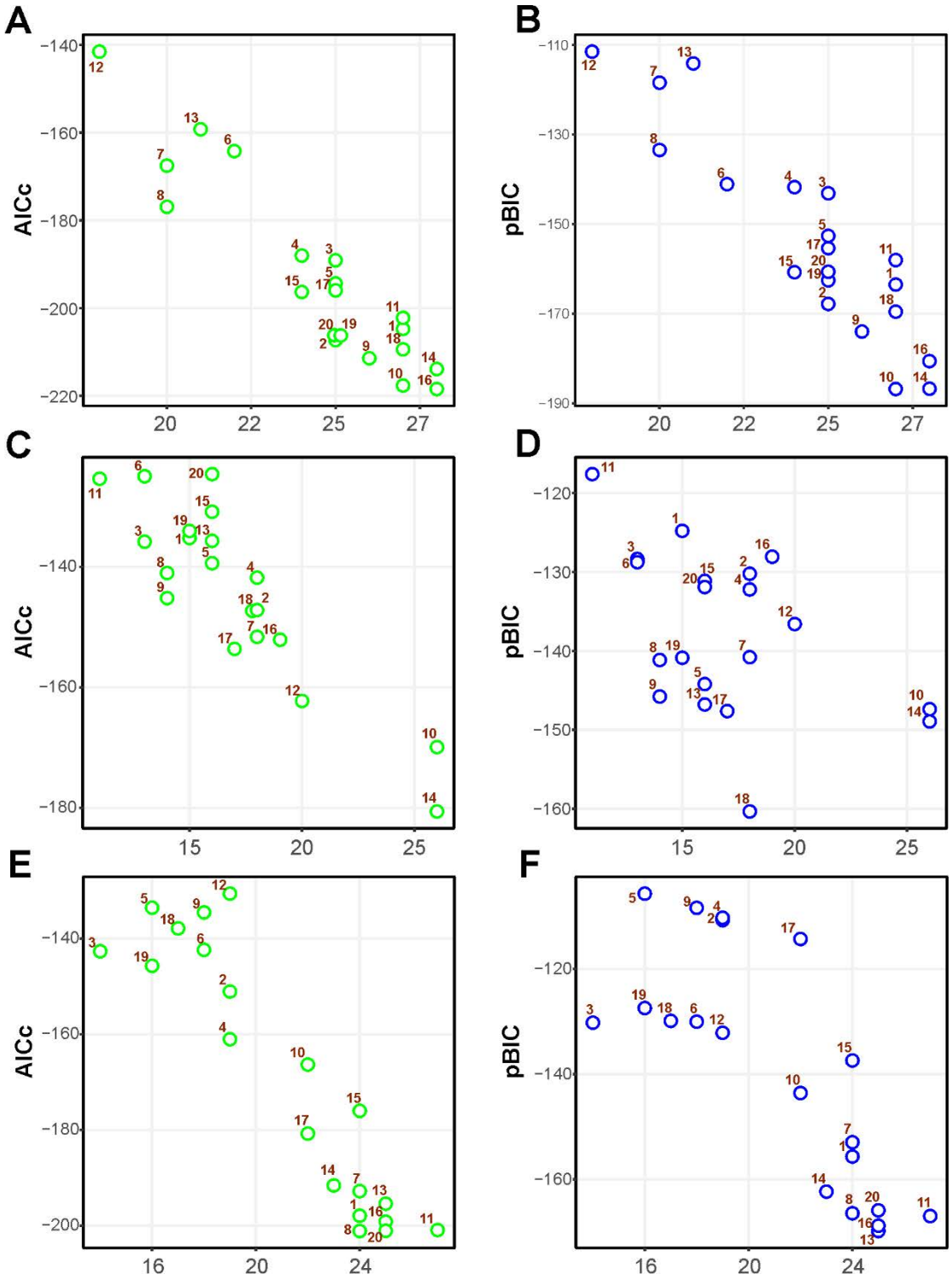

Figure 2.4. AICc (left) and pBIC (right) plotted against the number of regime shifts of SURFACE model fits, using crocodylomorph topologies with alternative positions of Thalattosuchia: **A** and **B,** Thalattosuchia within Neosuchia; **C** and **D,** Thalattosuchia as the sister group of Crocodyliformes; **E** and **F,** Thalattosuchia as the sister group of Mesoeucrocodylia. Numbers represent the 20 randomly resolved trees (time-calibrated using the *mbl* method) used for each model fit. Body size data from the ODCL dataset only.

Table 2.2. Examples of comparisons between simpler and more complex SURFACE model fits for the same trees. pBIC scores were obtained for regime configuration mapped onto trees with the same topology but using different time-calibration methods. By doing this, it was possible to compare the pBIC scores between simpler and more complex SURFACE model fits. Model fits shown are for trees with Thalattosuchia as the sister group of Crocodyliformes and using body size data from the ODCL dataset only. See Appendix A for all cross plotting of regime configurations.

Tree number and original time-scaling method	**pBIC scores**	
	Simple model	**Complex model**
Tree 3 (*mbl*-calibrated)	**mbl fit on mbl tree** -130.2	**Hedman fit on mbl tree** -158.9*
Tree 3 (*cal3*-calibrated)	**cal3 fit on cal3 tree** -139.1	**Hedman fit on cal3 tree** -157*
Tree 4 (*cal3*-calibrated)	**cal3 fit on cal3 tree** -132.6	**Hedman fit on cal3 tree** -133.8*
Tree 5 (*mbl*-calibrated)	**mbl fit on mbl tree** -105.7	**cal3 fit on mbl tree** -133.5*
Tree 6 (*mbl*-calibrated)	**mbl fit on mbl tree** -130.1	**Hedman fit on mbl tree** -160.4*
Tree 7 (*Hedman*-calibrated)	**Hedman fit on Hedman tree** −164.9*	**mbl fit on Hedman tree** -152.8

The SURFACE analyses using different body size proxies (DCL and ODCL) and time-scaling methods (*mbl*, *cal3* and *Hedman* methods) enabled the assessment of the influence of these factors on the SURFACE results. First, in general, alternative time-scaling methods did not cause substantial modifications to the SURFACE model fits in terms of

numbers of regimes or parameter values. However, as these methods generate different divergence times, branch lengths and ages estimated for the origin of subclades are expected to be distinct. Comparatively, while the *Hedman* method tended to estimate arguably too old ages for the origins of some clades (estimating, for example, the origin of the crown-group to be as old as the Late Jurassic compared to the Late Cretaceous ages of the oldest known unequivocal crocodylians), trees that used the *cal3* method often included branches with lengths very close to zero. Furthermore, trees that were time-scaled using *cal3* recovered comparatively more suboptimal SURFACE model fits than those that used the other two methods. Thus, the SURFACE model fits with trees calibrated using the *mbl* method were favoured when describing and discussing the SURFACE results (even though those model fits generated using the other two methods were not completely discarded).

Second, comparable results are found across model fits with different cranial measurements (DCL and ODCL) when using the same time-scaling methods and tree topologies. Although there are slightly more suboptimal model fits when using the DCL dataset, there is not enough evidence to support the idea that the use of a different cranial measurement is causing this pattern, as due to taxon sampling the phylogenetic trees used for fitting models using DCL and ODCL are different. However, in order to minimise the number of model fits used to characterise crocodylomorph body size evolution, the results obtained from the ODCL dataset were favoured for the description of the macroevolutionary patterns, as this dataset includes more species than the DCL, and it usually provides more realistic estimated body size values (for θ and Z_0) when using the equations presented by Hurlburt *et al.* (2003).

The position of Thalattosuchia had an influence on the range of the attraction parameter (α), which is a whole-tree, fixed parameter in the SURFACE model fits. When

Thalattosuchia is placed as the sister taxon of Crocodyliformes, the lowest values of α were obtained (ranging from 0.0072 to 0.1399), perhaps reflecting the more frequent suboptimal model fits for this scenario, and consequently the highest phylogenetic half-lives ($t_{0.5}$ = 4.95 to 95.99 Myr). In the other two alternative scenarios (i.e., Thalattosuchia either within Neosuchia or as the sister group of Mesoeucrocodylia), comparable values of α were found, ranging from 0.0136 to 0.6595, with considerably shorter phylogenetic half-lives ($t_{0.5}$ = 1.05 to 50.89 Myr).

2.3.3. Describing the body size macroevolutionary patterns in Crocodylomorpha

The SURFACE model fits were used to describe patterns of crocodylomorph body size evolution, focusing on the best model fits from the analyses implemented with pBIC searches (i.e., the low-pBIC/high-α model class), using body size data from the ODCL dataset and trees time-calibrated mainly (but not only) with the *mbl* method (see Appendix A for plots of all SURFACE model fits). Most SURFACE model fits identified more than four main macroevolutionary regimes (with different θ values). These are distributed along crocodylomorph phylogeny by means of numerous regime shifts, usually more than 15, independently of the position of Thalattosuchia. Trait optima values for these regimes varied significantly among different crocodylomorph subclades and are described in detail below. Overall, regime shifts are frequently detected at the bases of well-recognised clades, such as Thalattosuchia, Notosuchia and Crocodylia. Nevertheless, shifts to new regimes are not restricted to the origins of these diverse clades, since many other regime shifts are observed across crocodylomorph phylogeny, including regimes containing only a single species.

The SURFACE results indicate an ancestral regime of small body sizes for Crocodylomorpha, regardless of the topology or time-scaling method used (Figs. 2.5, 2.6, and

2.7). This is consistent with the small body sizes of most non-crocodyliform crocodylomorphs such as *Litargosuchus leptorhynchus* and *Hesperosuchus agilis* (Clark *et al*. 2000; Clark and Sues 2002). Trait optima for this initial regime (Z_0) ranged from 66 to 100 cm (total body length was estimated only after the SURFACE model fits, based on the equation from Hurlburt *et al*. [2003]; see the "Material and Methods" section of this Chapter). Very few or no regime shifts are observed among non-crocodyliform crocodylomorphs (Figs. 2.5, 2.6 and 2.7B), except for when Thalattosuchia is placed outside Crocodyliformes (Fig. 2.7A). But even in this latter case, shifts are seen only within or at the base of Thalattosuchia. For example, some trees time-scaled with *mbl* (tree number 11; Fig. 2.7B) and *cal3* (trees number 13 and 15) methods show a Late Triassic regime shift towards much larger body lengths (θ = 560–880 cm) at the base of Thalattosuchia, but many model fits that used these methods also exhibit much simpler models, with very few regime shifts. When using the *Hedman* method, however, a shift at the base of Thalattosuchia is more frequently observed, in many cases representing the oldest regime shift in the evolutionary history of Crocodylomorpha, and the only one to occur before the Triassic-Jurassic boundary (although the oldest thalattosuchian fossils only occur in the Early Jurassic). Regardless of the position of Thalattosuchia, the ancestral regime of all crocodylomorphs (Z_0) was inherited by protosuchids (such as *Protosuchus*, *Orthosuchus*, and *Edentosuchus*) and some other non-mesoeucrocodylian crocodyliforms (e.g., *Shantungosuchus*, *Fruitachampsa*, *Sichuanosuchus* and *Gobiosuchus*).

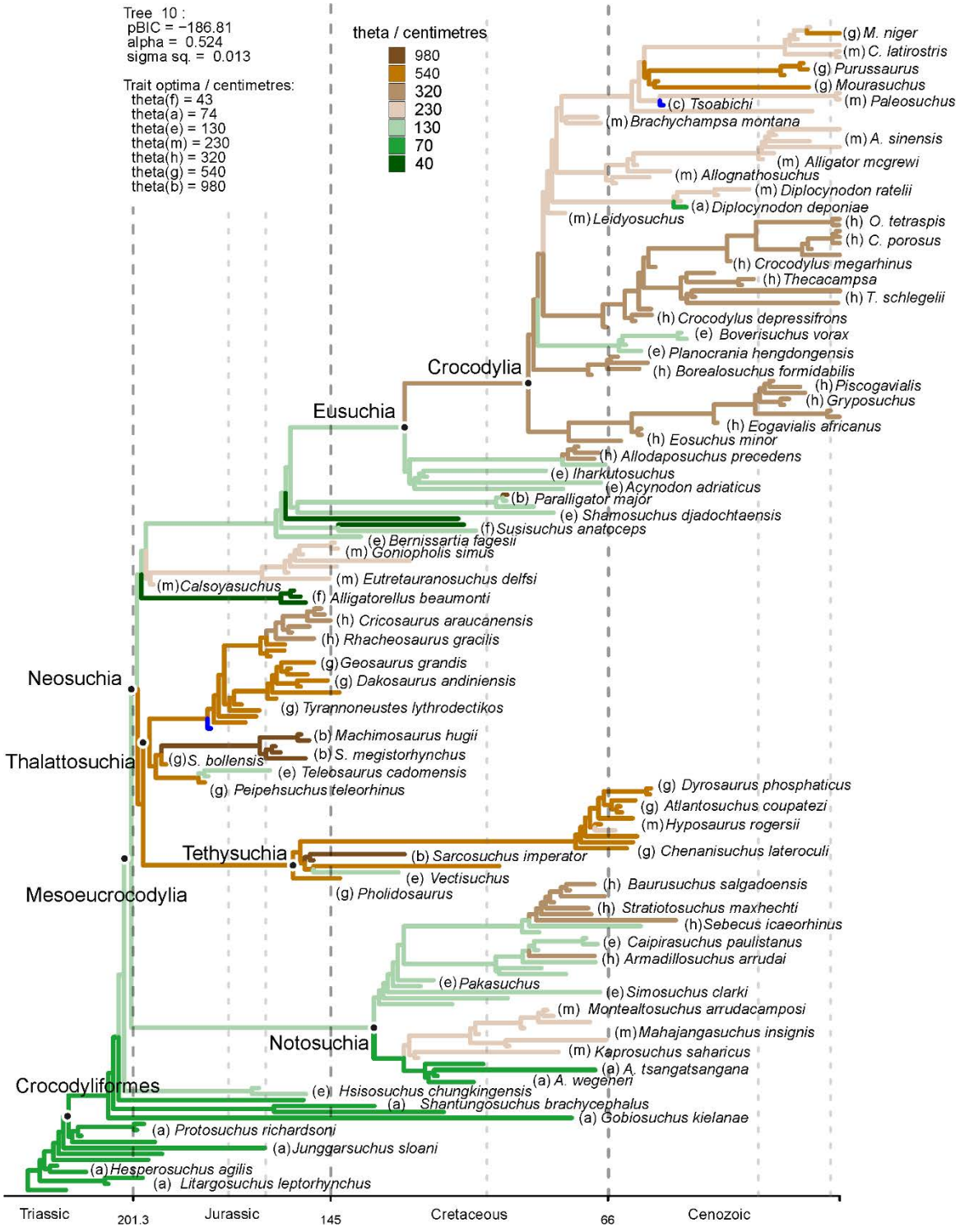

Figure 2.5. SURFACE model fit (using pBIC searches in the backward-phase) of tree number 10 among crocodylomorph topologies with Thalattosuchia placed within Neosuchia, using the ODCL dataset and time-calibrated with the *mbl* method. Attraction to unrealized low or high trait optima are highlighted in blue and red, respectively. Model fits of trees sharing the same position of Thalattosuchia show very similar regime configurations, regardless of the dataset used (ODCL or DCL) and the time-calibration method (see Appendix A for all SURFACE plots).

Patterns of body size evolution at the base of Mesoeucrocodylia are influenced by the position of Thalattosuchia. In nearly all model fits with Thalattosuchia within Neosuchia (Figs. 2.5 and 2.6), a regime of smaller body sizes (θ = 130–230 cm) is observed at the base of the branch leading to Mesoeucrocodylia, with the same regime frequently inherited by the branches leading to both Notosuchia and Neosuchia. When thalattosuchians are placed as the sister group of Crocodyliformes, a similar pattern is observed in most trees time-scaled with the *Hedman* method, but also in trees number 13 and 15 with the *cal3* method, and number 11 (Fig. 2.7A) with the *mbl* method. With Thalattosuchia as the sister group of all the other mesoeucrocodylians (i.e., Notosuchia + Neosuchia), most trees exhibit a change to a regime of larger sizes (θ = 210–490 cm) occurring at the branch leading to Mesoeucrocodylia (Fig. 2.7B), although some model fits (e.g., trees number 5, 8, 10, and 16 using all time-scaling methods) show no shift at the base Mesoeucrocodylia (i.e., inheriting the same regime as non-mesoeucrocodylian crocodyliforms). When a change at the base of Mesoeucrocodylia is observed, this same regime is usually inherited by Neosuchia, and shifts to regimes of smaller sizes (θ = 66–140 cm) are subsequently seen either at the base of or within Notosuchia.

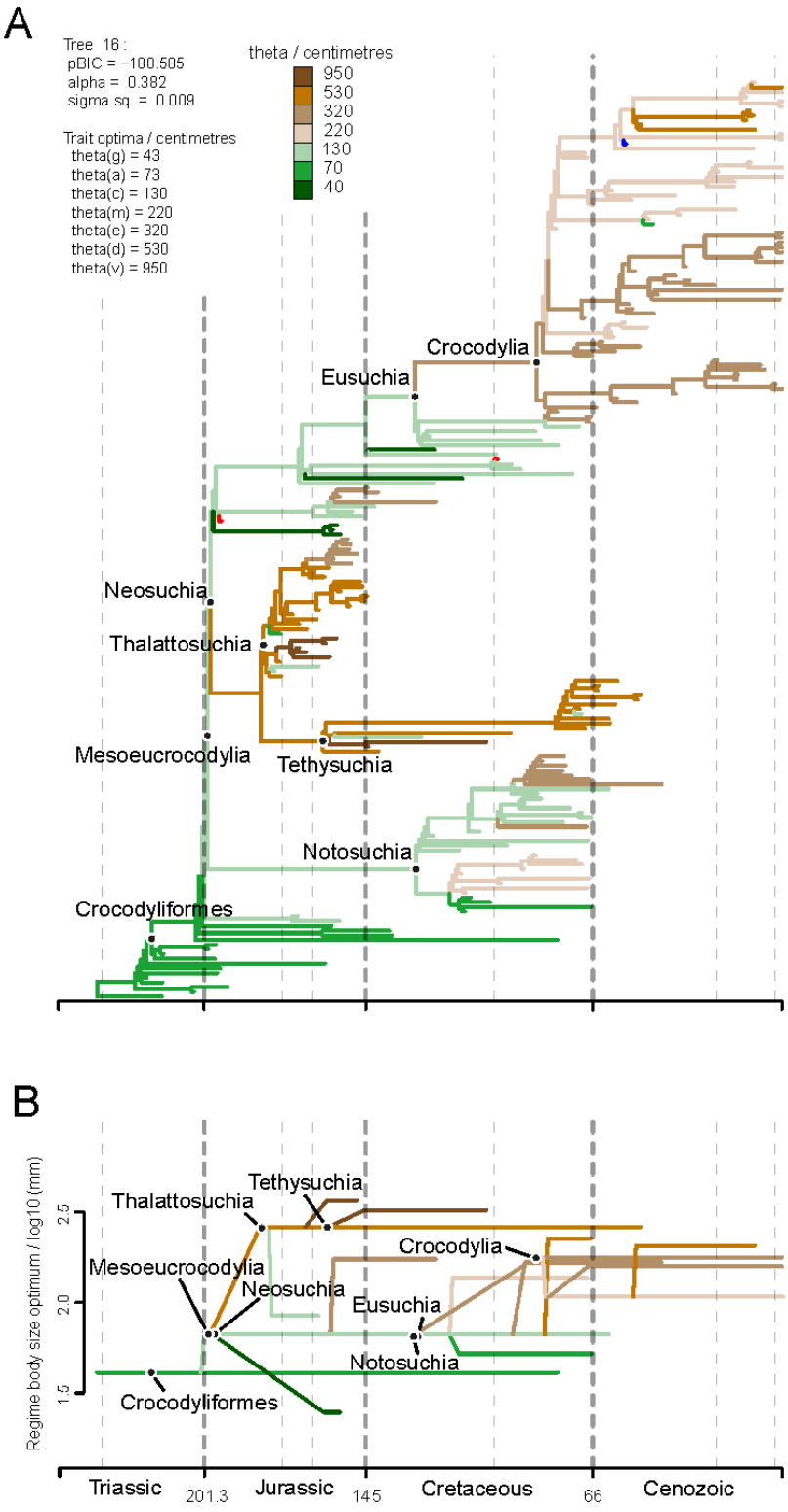

Figure 2.6. A, SURFACE model fit (using pBIC searches in the backward-phase) of tree number 16 among crocodylomorph topologies with Thalattosuchia placed within Neosuchia, using the ODCL dataset and time-calibrated with the *mbl* method. Attraction to unrealized low or high trait optima are highlighted in blue and red, respectively. **B,** Simplified version of (**A**) with independent multi-taxon regimes collapsed to single branches.

The position of Thalattosuchia also has an impact on the configuration of regime shifts among non-eusuchian neosuchians. The regime of relatively smaller sizes at the base of Mesoeucrocodylia is maintained at the base of Neosuchia in most model fits of trees with Thalattosuchia within Neosuchia (Fig. 2.5 and 2.6). Subsequently, regime shifts towards larger sizes (θ = 210–500 cm) are seen among some taxa such as goniopholidids, *Agaresuchus* and *Allodaposuchus*, whereas shifts to regimes of smaller θ values (41–140 cm) are also detected in branches associated with small taxa (e.g., atoposaurids, susisuchids and *Pietraroiasuchus*). More complex models of trees with Thalattosuchia placed as the sister group of Crocodyliformes (e.g., tree 11, using the *mbl* method; Fig. 2.7A) show the same pattern. Comparatively, when Thalattosuchia is placed as the sister taxon of Mesoeucrocodylia (Fig. 2.7B), the regime of larger sizes seen at the base of Neosuchia is frequently inherited by most non-eusuchian neosuchians (except for some of the smallest taxa, such as atoposaurids and susisuchids), resulting in fewer regime shifts amongst non-eusuchian neosuchians than in the other two alternative scenarios.

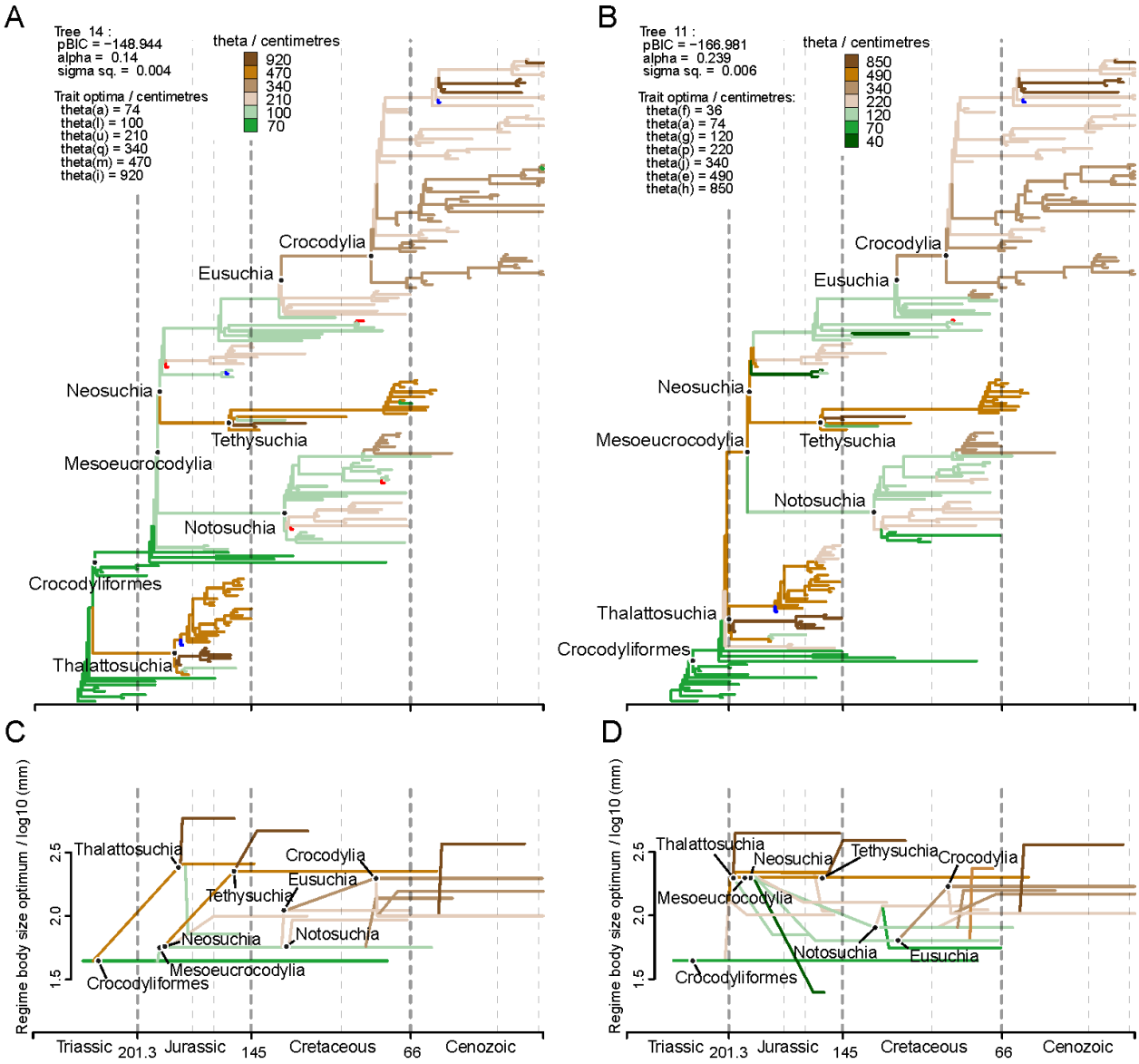

Figure 2.7. SURFACE model fits of trees time-calibrated with the mbl method, using the ODCL dataset. **A,** Model fit of tree number 14 with Thalattosuchia as the sister group of Crocodyliformes. However, many model fits of trees sharing this same position of Thalattosuchia show simpler model configurations, with significantly fewer regimes (see text for details). **B,** Model fit of tree number 11 with Thalattosuchia as the sister group of Mesoeucrocodylia. A few model fits of other trees with Thalattosuchia in the same position are simpler, particularly when using the cal3 time-scaling method (see Appendix A for all SURFACE plots). **C** and **D** are simplified versions of (**A**) and (**B**), respectively, with independent multi-taxon regimes collapsed to single branches.

Within Notosuchia, most model fits show many taxa inheriting the same regime of smaller sizes present at the base of the clade (θ = 66–140 cm), regardless of the position of Thalattosuchia and the time-scaling method used. Nevertheless, the group is also characterised by many additional regimes, with considerably variable trait optima, usually ranging from 66 to 460 cm. Shifts to regimes of smaller sizes are often seen in uruguaysuchids, *Anatosuchus*, *Pakasuchus* and *Malawisuchus*, with θ values very similar to or the same as the ancestral crocodylomorph regime (Z_0). Furthermore, shifts towards larger sizes are seen among peirosaurids (θ = 210–250 cm), and, more dramatically, in sebecosuchids and in the armoured sphagesaurid *Armadillosuchus arrudai* (θ = 320–850 cm).

Tethysuchia and Thalattosuchia are characterised by a dominance of macroevolutionary regimes of large body sizes (θ = 320–980 cm), usually with lower body size disparity than Notosuchia. When Thalattosuchia is placed as sister taxa of either Tethysuchia, within Neosuchia (Figs. 2.5 and 2.6), or Mesoeucrocodylia (Fig. 2.7B), both Tethysuchia and Thalattosuchia share the same regime of large sizes (θ = 460–610 cm), which is subsequently inherited by many of their members. In the first scenario, the shift to this regime takes place during the Early Jurassic, in the neosuchian branch that leads to the dichotomy Thalattosuchia + Tethysuchia. In the second case, most model fits show the shift regime occurring earlier in time, during the Late Triassic, at the base of Mesoeucrocodylia or among non-mesoeucrocodylian crocodyliforms. In the last alternative phylogenetic scenario, when Thalattosuchia is placed as the sister taxon of Crocodyliformes (Fig. 2.7A), even though Tethysuchia and Thalattosuchia do not share the same inherited regime, the model fits indicate that independent regime shifts to larger sizes occur at the bases of both clades, usually with very similar (or the same) trait optima values (also around 500 cm).

Within Tethysuchia, many trees exhibit a regime shift towards even larger sizes in a clade formed by the giant forms *Sarcosuchus imperator* and *Chalawan thailandicus* (θ = 840–980 cm). Among thalattosuchians, a shift to a regime with the same trait optimum (i.e., convergent) as that of the largest tethysuchians is usually observed in the teleosaurid clade formed by *Machimosaurus* and *Steneosaurus*. Despite the dominance of regimes of larger sizes, there are regimes of smaller sizes within Tethysuchia and Thalattosuchia, exemplified by some trees with isolated shifts in *Pelagosaurus typus*, *Teleosaurus cadomensis* and *Platysuchus multiscrobiculatus*, in Thalattosuchia, and *Vectisuchus leptognathus* and *Hyposaurus rogersii*, in Tethysuchia.

Crocodylia is also characterized by a dominance of macroevolutionary regimes of relatively large sizes, as in Thalattosuchia and Tethysuchia. Indeed, regimes towards larges sizes are frequently associated with clades of predominantly aquatic or semi-aquatic forms, although not strictly restricted to them. Regarding Crocodylia, a Cretaceous regime shift is usually detected at the base of the clade (Figs. 2.5, 2.6, and 2.7), changing from the macroevolutionary regime of smaller sizes (θ = 110–210 cm) found for non-crocodylian eusuchians (such as hylaeochampsids and some allodaposuchids) to a regime of larger trait optima (θ = 320–340 cm). This same ancestral regime for all crocodylians is inherited by many members of the clade, particularly within Crocodyloidea and Gavialoidea. Although some model fits show Crocodylia inheriting the same regime as closely related non-crocodylian eusuchians, these trees are less common in general. In these trees, shifts towards larger body sizes are seen in members of Crocodyloidea and Gavialoidea, but they only occur later in time and arise independently. In comparison to the other two main lineages of Crocodylia, Alligatoroidea is characterized by a regime of lower trait optima values (θ = 210–230 cm), which frequently occurs as a Late Cretaceous shift at the base of the clade. But

Alligatoroidea is also distinct from the other two clades by exhibiting more regime shifts, reflecting its great ecological diversity and body size disparity (ranging from very small taxa, such as the caimanine *Tsoabichi greenriverensis*, to the huge *Purussaurus* and *Mourasuchus*).

2.3.4. Investigating the modes of body size evolution within Notosuchia and Crocodylia

The significant number of regime shifts that occur within both Notosuchia and Crocodylia led to deeper scrutiny of the modes of body size evolution in these two clades. For that, another round of model-fitting analyses was conducted, initially fitting the same evolutionary models (SURFACE, OU, BM, EB and trend-like models) to subtrees representing both groups. In addition, the same regime shifts identified by the SURFACE algorithm were used to fit four additional models using the OUwie algorithm (BMS, OUMV, OUMA and OUMVA), which allow more parameters to vary, but need regime shifts to be set *a priori*.

The results of these analyses indicate different modes of body size evolution during the evolutionary histories of these two groups. In Crocodylia (Fig. 2.8A; see Appendix A for a complete list of AICc scores), AICc scores indicate a clear preference for OU-based models, with highest support found for the SURFACE model, but also strong support for the uniform OU model, as well as OUMA and OUMVA models. The SURFACE algorithm frequently identified three main macroevolutionary regimes for crocodylians (with θ values around 200, 350 and 750 cm, respectively), with α ranging from 0.053 to 0.247 and σ^2 between 0.0014 and 0.0054. When allowed to vary among regimes (i.e., in models OUMA and OUMVA), ranges of both parameters increase significantly, with some model fits displaying extremely unrealistic parameter values, which might explain the stronger support found for SURFACE compared to these latter models. Among the BM-based models, even the best trend-like

model (usually the one with the best AICc scores among BM-based models) received consistently worse support than any of these four OU-based models.

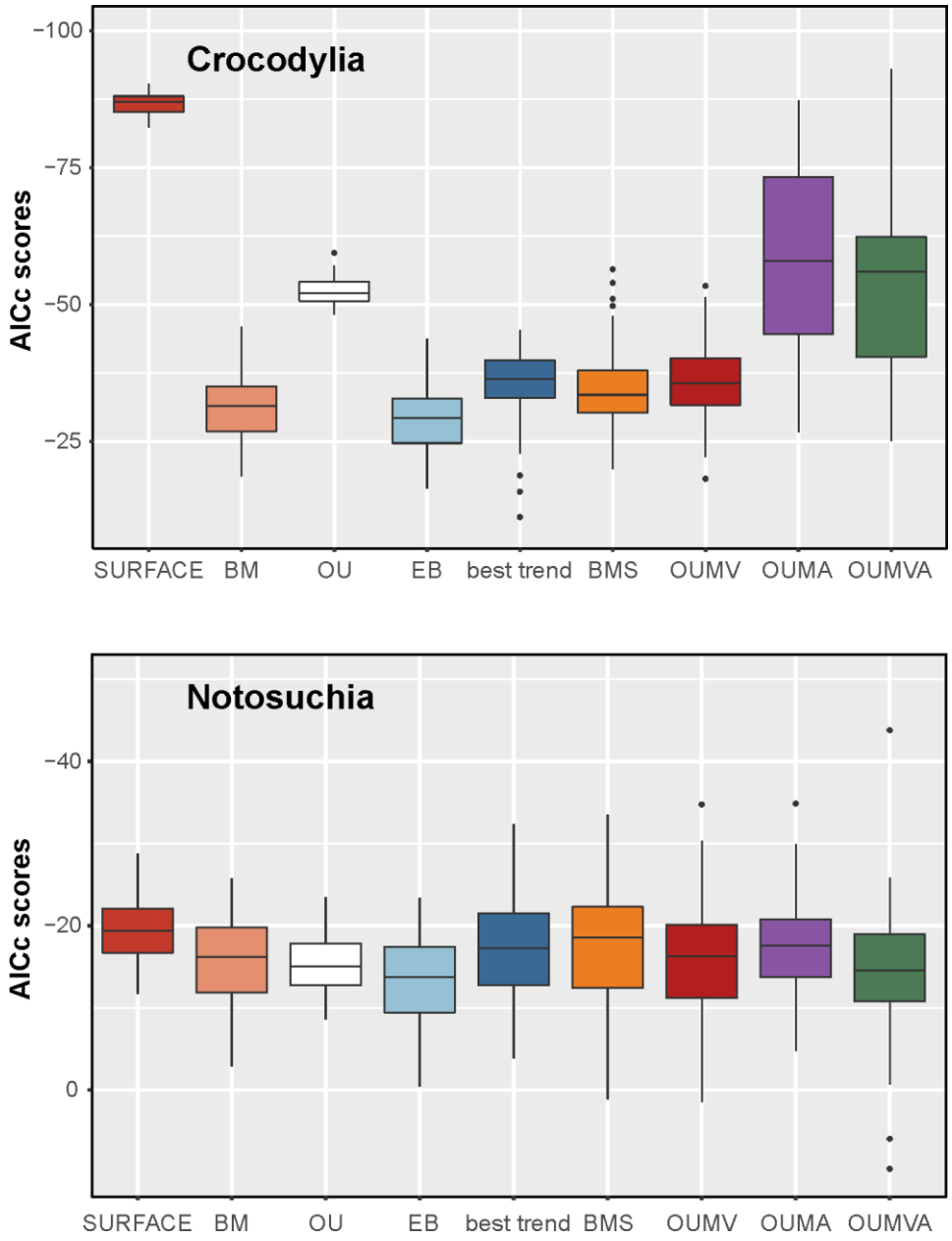

Figure 2.8. AICc scores of all evolutionary models fitted to the phylogenies and body size data of Crocodylia and Notosuchia. For the trend-like models, only the AICc of the best model ("best trend") is shown.

The results show a different scenario for Notosuchia, for which comparable support was found for all evolutionary models analysed (Fig. 2.8B). Among OU-based models, slightly better AICc scores were found for the SURFACE model. However, this model received virtually the same support as the BMS model, the best of the BM-based models. BMS is a multi-regime BM model that allows the rate parameter (σ^2) to vary, and, as α is effectively set to zero, represents diffusive model of evolution. The support found for this model might suggest a more relaxed mode of body size evolution in notosuchians, which is consistent with the wide range of body sizes observed in the group, even among closely-related taxa. Indeed, even though the sample includes twice as many crocodylians (n = 70) as notosuchians (n = 34), many SURFACE model fits found three main macroevolutionary regimes for notosuchians, similar to what was found for Crocodylia (although model fits with less regimes were more frequent for Notosuchia than in Crocodylia). For these, θ values were usually around 80, 150 and 280 cm, with α usually ranging from 0.0124 to 0.6213 and σ^2 between 0.0011 and 0.0201. When the same regimes detected by the SURFACE algorithm were used by the OUwie algorithm to fit the BMS model, values of σ^2 rarely varied significantly from the range of whole-tree σ^2 estimated for the SURFACE model fits. The few exceptions were usually related to regimes with unrealised θ values, as in the case of *Armadillosuchus arrudai* (probably with more than 2 metres in total length, whereas other sampled sphagesaurids reach no more than 1.2 m; Marinho and Carvalho 2009), and sebecosuchians (top predators of usually more than 2.5 metres; Godoy *et al*. 2016), even though these values might still be realistic when simulating trend-like dynamics (i.e., in a single lineage with extremely disparate trait values; Hansen 1997; Benson *et al*. 2014*a*).

2.3.5. The influence of palaeolatitude and palaeotemperature

Most of the correlation analyses between the body size data and the different datasets of the abiotic factors palaeotemperature and palaeolatitude yielded very weak or non-significant correlations (see Appendix A for all regression results). The phylogenetic regressions of body size and palaeolatitudinal data found some significant correlations. However, in all cases the coefficient of determination (R^2) was very low (always smaller than 0.1), indicating that the correlation is very weak and only a small proportion (less than 10%) of the body size variation observed can be explained by the palaeolatitudinal data (Fig. 2.9).

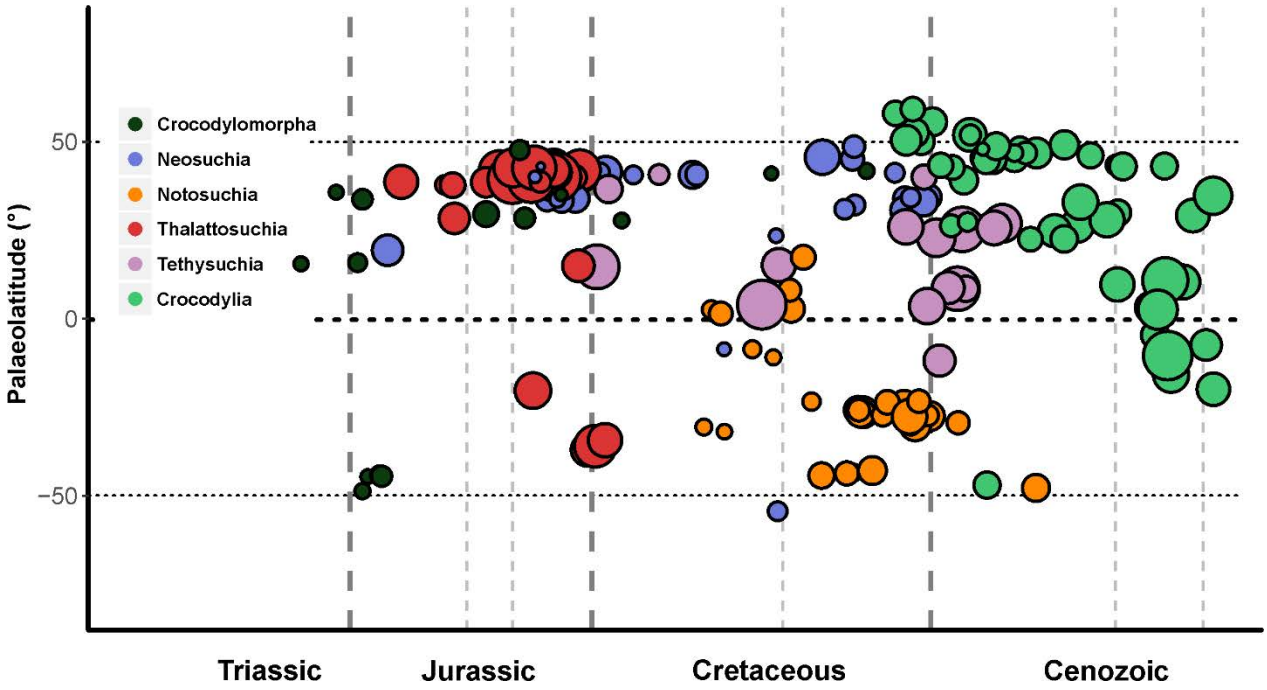

Figure 2.9. Palaeolatitudinal distribution of extinct crocodylomorphs through time, incorporating body size information (circle sizes), with colours representing different mono- or paraphyletic (i.e., Crocodylomorph = non-mesoeucrocodylian crocodylomorphs, excluding Thalattosuchia; Neosuchia = non-crocodylian neosuchians) crocodylomorph groups. Body sizes are $\log_{10}$ values of orbito-cranial dorsal length (ODCL), in millimetres.

The situation was similar regarding temporal patterns of body size compared to global palaeotemperature, with most analyses revealing very weak or non-significant correlations.

Significant correlations were found in some cases, but they were frequently inconsistent (i.e., correlations did not persist in both ODCL and DCL datasets or were absent when accounting for serial autocorrelation using GLS). The lack of strong correlations between environmental variables and body size is consistent with the results from the macroevolutionary (model-fitting) analyses, which found strong support for a multi-regime OU model (SURFACE). This suggests that shifts between adaptive zones are more important in determining large-scale macroevolutionary patterns of crocodylomorph body size evolution than abiotic factors, at least when analysed separately.

However, one important exception was found between mean body size values and palaeotemperatures from the Late Cretaceous (Maastrichtian) to the Recent (data from Zachos *et al*. [2008]). Moderate to strong correlations were found when using either all taxa in the datasets or only non-marine species (R^2 ranging from 0.376 to 0.635), with higher mean body size values found in time intervals with lower temperatures (i.e., positive slopes, given that the $\delta^{18}O$ proxy is inversely proportional to temperature). The correlation was present even when applying GLS regressions with an autoregressive model (Table 2.3), which returned very low to low autocorrelation coefficients (Phi = 0.01–0.15). This suggests that temperature might have had an influence in determining the body size distribution of crocodylomorphs at smaller temporal and phylogenetic scales (Fig. 2.10A). For this reason, further analyses scrutinised the relationships between the distribution of body sizes and these abiotic factors at these smaller scales, by repeating the regression analyses using only data for Crocodylia, Notosuchia, Thalattosuchia, and Tethysuchia (see the "Material and Methods" section of this Chapter).

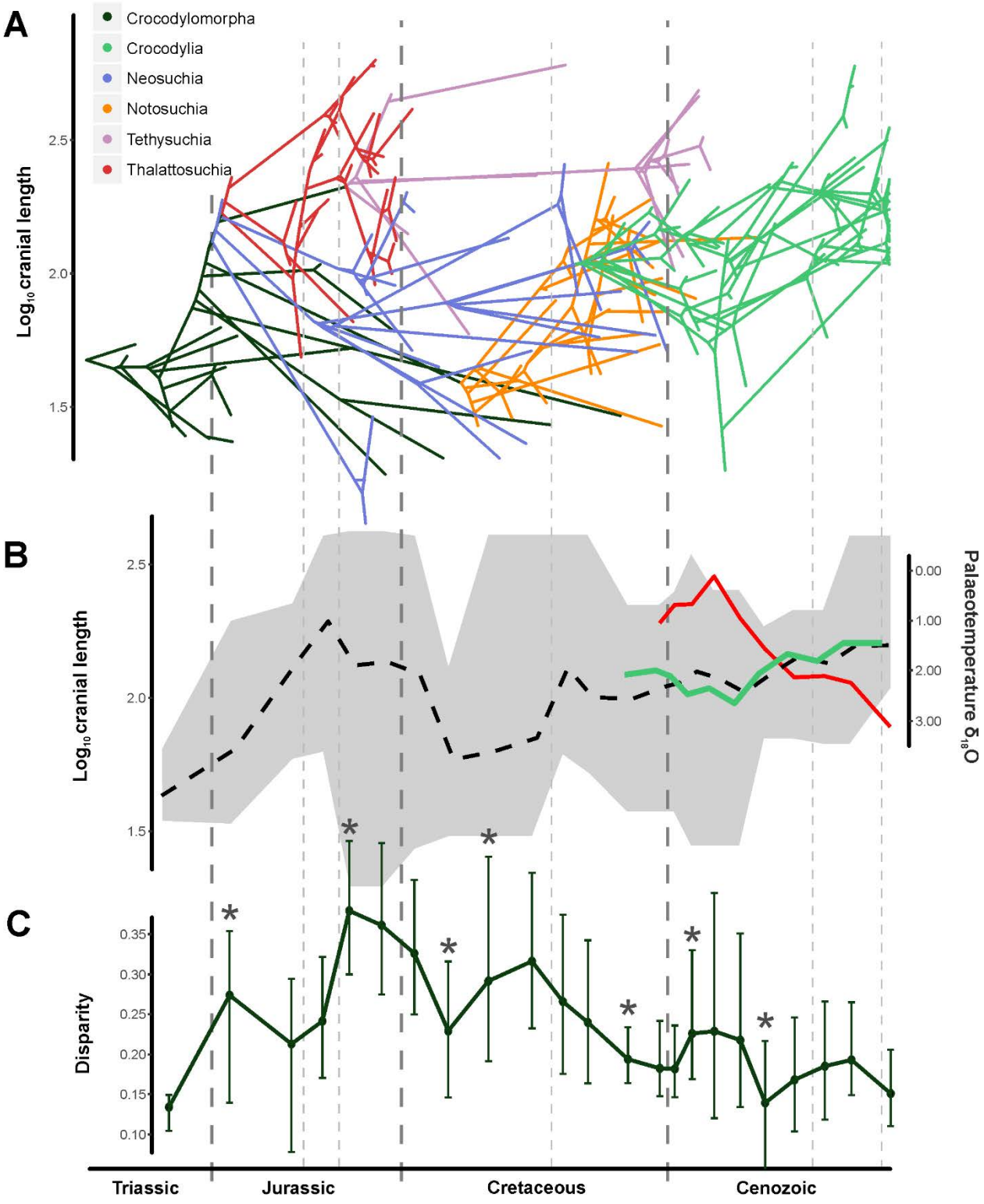

Figure 2.10. *Caption on next page.*

Figure 2.10. A, Phenogram with body size (log_{10} ODCL) incorporated into crocodylomorph phylogeny, with colours representing different crocodylomorph groups. **B,** Crocodylomorph body size and palaeotemperature through time. Mean log_{10} ODCL represented by dashed black line, shaded polygon shows maximum and minimum values for each time bin. Continuous light green displays mean log_{10} ODCL values only for Crocodylia. Palaeotemperature ($\delta^{18}O$) data from Zachos *et al*. (2008). **C,** Body size disparity through time. Disparity is represented by the standard deviation of log10 ODCL values for each time bin (only time bins with more than 3 taxa were used for calculating disparity). Error bars are accelerated bias-corrected percentile limits (BCa) of disparity from 1,000 bootstrapping replicates. Asterisks mark the events of largest interval-to-interval changes in disparity.

Table 2.3. Regression results of mean body size values (from both DCL and ODCL datasets) on palaeotemperature. Results of GLS (with an autoregressive model) and OLS (untransformed data) regressions. Mean body size values represented by log-transformed cranial, in millimetres. Data from both datasets was divided into subsets with all crocodylomorphs or only non-marine species. 10 time bins were analysed in all four subsets (n =10). Palaeotemperature data from Zachos *et al*. (2008), represented by $\delta^{18}O$ data from the Late Cretaceous to Recent. Only significant correlations ($p < 0.05$) are shown.

Dataset	**GLS**				**OLS (untransformed)**			
ODCL (all taxa)	**Phi**	**Intercept**	**Slope**	**AIC**	**R^2**	**Intercept**	**Slope**	**AIC**
	-0.046	2.022	0.055 (0.002)	-31.576	0.635	2.023	0.054 (0.003)	-33.557
DCL (all taxa)	**Phi**	**Intercept**	**Slope**	**AIC**	**R^2**	**Intercept**	**Slope**	**AIC**
	0.014	2.433	0.081 (0.011)	-19.577	0.527	2.433	0.081 (0.01)	-21.575
ODCL (non-marine)	**Phi**	**Intercept**	**Slope**	**AIC**	**R^2**	**Intercept**	**Slope**	**AIC**
	-0.157	1.964	0.06 (0.007)	-24.96	0.502	1.965	0.06 (0.013)	-26.706
DCL (non-marine)	**Phi**	**Intercept**	**Slope**	**AIC**	**R^2**	**Intercept**	**Slope**	**AIC**
	-0.089	2.345	0.07 (0.027)	-16.045	0.376	2.346	0.07 (0.034)	-18.272

These additional regressions corroborate the hypothesis that at least some crocodylomorph subclades show a correspondence between body size and global

palaeotemperature. Although most of the regressions provided non-significant or weak/very weak correlations (see Appendix A for all regression results), including all regressions of body size on palaeolatitudinal data, both maximum and mean body size values of Crocodylia are strongly correlated to palaeotemperature through time (Table 2.4). The positive slopes and coefficients of determination (R^2 = 0.632 and 0.647) indicate that the lowest temperatures are associated with the highest body size values in the crown-group. However, correlations with data from other subclades (Notosuchia, Thalattosuchia and Tethysuchia) were mostly non-significant, suggesting that this relationship between body size and temperature was not a widespread pattern among all groups.

Table 2.4. Regression results of maximum and mean body size values (from both DCL and ODCL datasets) on palaeotemperature. Results of GLS (with an autoregressive model) and OLS (untransformed data) regressions. Mean body size values represented by log-transformed cranial, in millimetres. Data from both datasets was divided into subsets with all crocodylomorphs or only non-marine species. 10 time bins were analysed in all four subsets (n =10). Palaeotemperature data from Zachos *et al*. (2008), represented by $\delta^{18}O$ data from the Late Cretaceous to Recent. Only significant correlations ($p < 0.05$) are shown.

Dataset	**GLS**				**OLS (untransformed)**			
ODCL maximum size	**Phi**	**Interc.**	**Slope**	**AIC**	**R^2**	**Interc.**	**Slope**	**AIC**
	0.19	2.133	0.121 (0.017)	-11.989	0.554	2.124	0.127 (0.008)	-13.662
ODCL mean size	**Phi**	**Interc.**	**Slope**	**AIC**	**R^2**	**Interc.**	**Slope**	**AIC**
	-0.297	1.98	0.075 (0.0003)	-29.953	0.698	1.987	0.07 (0.001)	-31.137
DCL maximum size	**Phi**	**Interc.**	**Slope**	**AIC**	**R^2**	**Interc.**	**Slope**	**AIC**
	-0.215	2.618	0.165 (0.001)	-10.724	0.632	2.627	0.157 (0.003)	-12.355
DCL mean size	**Phi**	**Interc.**	**Slope**	**AIC**	**R^2**	**Interc.**	**Slope**	**AIC**
	-0.235	2.386	0.105 (0.0007)	-20.748	0.647	2.395	0.098 (0.003)	-22.325

2.4. Discussion

2.4.1. The adaptive landscape of crocodylomorph body size evolution

Crocodylomorph body size disparity increased rapidly during the early evolution of the group, from the Late Triassic to the Early Jurassic (Hettangian–Sinemurian), which is mostly a result of the appearance of the large-bodied thalattosuchians (Fig. 2.10C). After a decline in the Middle Jurassic, body size disparity reaches its maximum peak in the Late Jurassic, with the appearance of atoposaurids, some of the smallest crocodylomorphs, as well as large teleosaurids (such as *Machimosaurus*). This increase in disparity may have occurred earlier than the results suggest, given that Middle Jurassic records of atoposaurids (Young *et al*. 2016*b*) could not be included in the analyses due to their highly incomplete preservation.

Since this peak in the Middle/Late Jurassic, crocodylomorphs underwent an essentially continuous decline in body size disparity, with some short-term fluctuations related to the extinction or diversification of particular lineages. The Early Cretaceous witnessed the extinction of thalattosuchians, and a sharp decrease in disparity is seen from the Berriasian to the Barremian (although this time interval is also relatively poorly sampled in the dataset). A subsequent increase in disparity is seen in the Aptian, probably reflecting the appearance of small-bodied crocodylomorphs (such as susisuchid eusuchians). Nevertheless, this is followed by a continuing decline for the remainder of the Cretaceous (in spite of the occurrence of highly disparate notosuchians). The Cenozoic is also characterised by an overall decrease in disparity, even though some short-term increases in disparity do occur, mostly related to the presence of smaller-bodied crocodylians in the Palaeogene (such as *Tsoabichi*).

The macroevolutionary patterns that gave rise to these patterns of body size disparity through time were characterised by performing comparative model-fitting analyses. The results indicate a strong support found for a multi-peak OU model (i.e., the SURFACE model;

Fig. 2.3). Within the concept of adaptive landscape (Simpson 1944; 1953; Hansen 2012), the SURFACE regimes, with different trait optima, can be interpreted as shifts to new macroevolutionary adaptive zones (Van Valen 1971; Stanley 1973). Thus, the support found for the SURFACE model indicates that lineage-specific innovations and/or adaptations in body size play an important role in determining the patterns of crocodylomorph body size evolution. The comparative model-fitting analyses also indicate that uniform or BM-based models provide poor explanations for the overall patterns of crocodylomorph body size evolution. Thus, the hypothesis of long-term, multi-lineage trends during the evolution of crocodylomorph body size is rejected. This is true even for Crocodylia, which shows increases in maximum, minimum and mean body sizes during the past 70 million years (Fig. 2.10C), a pattern that is classically taken as evidence for trend-like dynamics (McShea 1994). In fact, explicitly phylogenetic models of the dynamics along evolving lineages reject this.

Likewise, diffusive Brownian-motion like dynamics can also be rejected for most of Crocodylomorpha, although Notosuchia might be characterised by relatively unconstrained dynamics (Fig. 2.8). Single-regime (i.e., uniform) models received poor support in general, which might be expected for long-lived and disparate clades such as Crocodylomorpha, that show complex and non-uniform patterns of body size evolution (see Stanley 1973, McKinney 1990; Hansen 1997; Butler and King 2004). Although multi-regime trend-like models received stronger support than uniform models for most phylogenies (Fig. 2.3), multi-peak OU models (SURFACE) received overwhelmingly still greater support. This suggests that the macroevolutionary landscape of crocodylomorph body size evolution is best described by shifts between phylogenetically defined regimes that experience constrained evolution around distinct trait optima (Butler and King 2004; Hansen 2012; Ingram and Mahler 2013; Mahler and Ingram 2014).

The success of a multi-peak OU model indicates that, in general, a significant amount of crocodylomorph body size variance emerged through pulses of body size variation, and not from a gradual, BM-based dispersal of lineages through trait (body size) space. These pulses, represented by regime shifts, indicate that lineage-specific innovations (such as ecological diversification; see below) and adaptations are important for the large-scale patterns of crocodylomorph body size evolution.

This can also explain the weak support for the early burst ("EB") model found in the analyses. This model was proposed as an attempt to simulate Simpson's (1944) idea of diversification through "invasion" of new adaptive zones (niche-filling). However, it only focuses on a particular pattern of the idea, more specifically on the more widespread concept of adaptive radiation, in which evolutionary rates of changes are higher in the early evolution of a clade and decelerate through time (Harmon *et al*. 2010). In this sense, the EB model does represent the complete idea of "quantum evolution" proposed by Simpson (1953) (i.e., abrupt phenotypic shifts along evolving lineages resulting from the distribution of opportunities or "unfilled niches"). This might explain why Harmon *et al*. (2010), in the study that formally proposed the EB model, found that early bursts receive little support from phylogenetic comparative data, even though some studies have found otherwise for some specific clades (e.g., in the body size evolution of some dinosaur subgroups; Benson *et al*. 2014).

Accordingly, the weak support for the EB model in this Chapter does not reject Simpson's hypothesis "quantum evolution" or adaptive zone invasion. Furthermore, the pattern of crocodylomorph body size evolution could still be explained by niche-filling if niche availability was distributed through time rather than being concentrated early in the evolution of the clade. This is one possible explanation of the pattern of regime shifts returned by the SURFACE analyses, and might be particularly relevant for clades with long

evolutionary histories spanning many geological intervals and many episodes of possible radiation.

Bronzati *et al*. (2015) examined variation in rates of species diversification among clades using methods based on tree asymmetry. They found that most of crocodyliform diversity was achieved by a small number of significant diversification events that were mostly linked to the origin of some subclades, rather than via a continuous process through time. Some of the diversification shifts from Bronzati *et al*. (2015) coincide with body size regime shifts found in many of the SURFACE model fits (as at the base of Notosuchia, Eusuchia and Alligatoroidea; Fig. 2.11). However, many of the shifts in body size regimes detected by the analyses are found in less-inclusive groups (as in the case of "singleton" regimes, that contain only a single taxon).

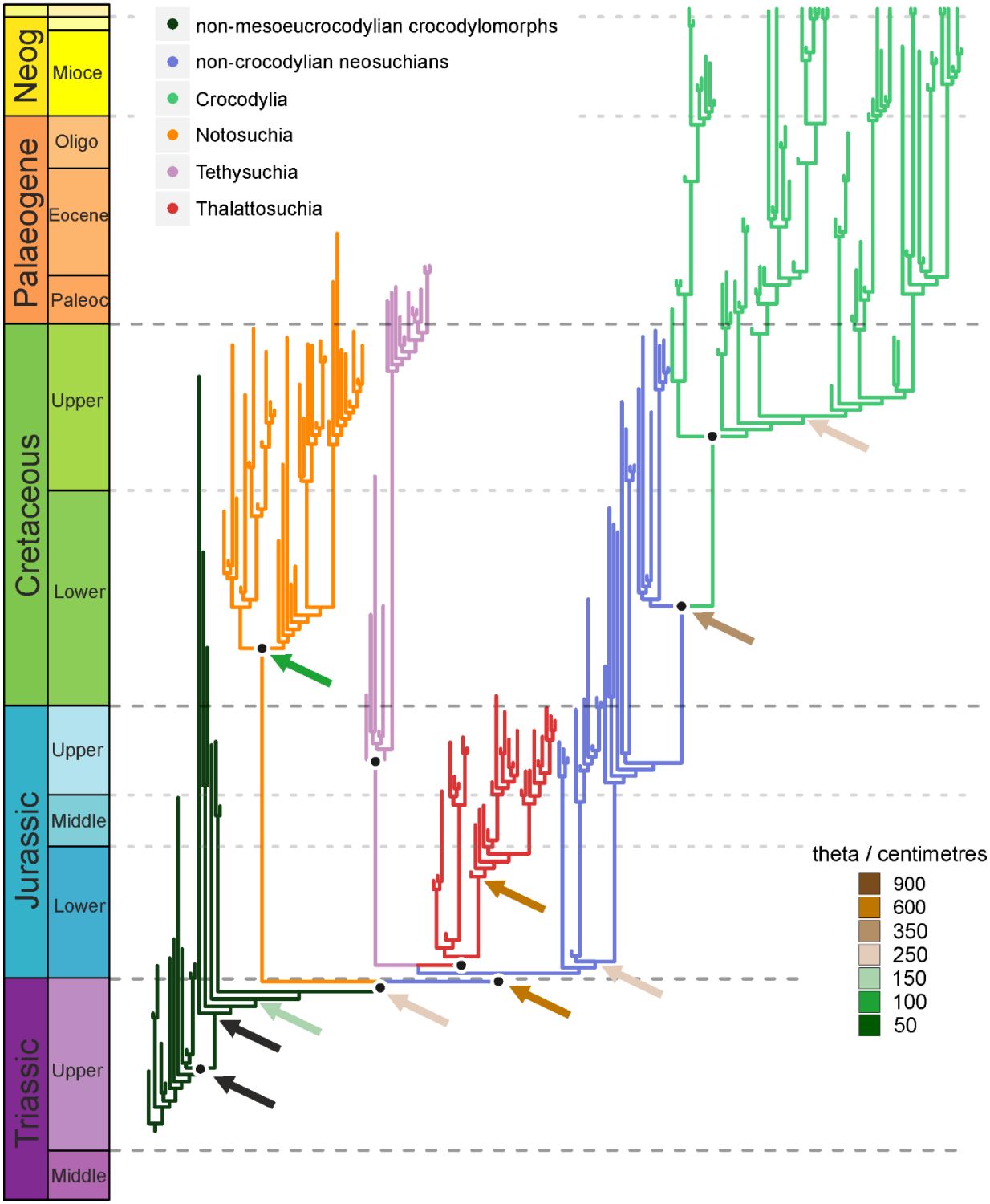

Figure 2.11. Summary of the SURFACE results combined with the crocodylomorph diversification shifts found by Bronzati *et al*. (2015). Nodes with diversification shifts are indicated by arrows, the colours of which represent distinct trait optima values (total body length in centimetres, after applying formula from Hurlburt *et al*. [2003]), of different body size regimes. Black arrows indicate nodes for which diversification shifts were identified, but no body size regime shift was found by SURFACE.

2.4.2. Ecological diversification and its implications for crocodylomorph body size distribution

Ecological factors seem to be important for the large-scale patterns of body size in crocodylomorphs. Many of the regime shifts to larger sizes detected by the SURFACE analyses occur at the base of predominantly aquatic or semi-aquatic clades, such as Thalattosuchia, Tethysuchia and Crocodylia (Figs. 2.5, 2.6 and 2.7), although there are also small-bodied aquatic and semi-aquatic clades, such as Atoposauridae. Some terrestrial clades also display relatively large sizes (such as sebecosuchians and peirosaurids, within Notosuchia). However, most terrestrial species are small-bodied (Fig. 2.12), including many of the earliest crocodylomorphs (such as *Litargosuchus leptorhynchus* and *Hesperosuchus agilis*; Clark *et al*. 2000; Clark and Sues 2002; Fig. 2.12A), and are within body size regimes of lower values of θ (< 150 cm; Figs. 2.5, 2.6 and 2.7). In contrast, the regimes with the highest values of θ (> 800 cm) are almost always associated with aquatic or semi-aquatic crocodylomorphs (e.g., the tethysuchians *Sarcosuchus imperator* and *Chalawan thailandicus*, the thalattosuchians *Machimosaurus* and *Steneosaurus*, and the crocodylians *Purussaurus* and *Mourasuchus*).

To further investigate this, the body size data was subdivided into three discrete categories to represent different generalised lifestyles: terrestrial, semi-aquatic/freshwater, and aquatic/marine. Initially, a relationship was found between the lifestyle and body size using analysis of variance (ANOVA), showing that terrestrial, freshwater and marine species had significantly different body sizes (Fig. 2.12B; Table 2.5). Next, to account for phylogenetic dependency, a phylogenetic ANOVA (Garland *et al*. 1993; Revell 2012) was performed. This asks specifically whether evolutionary habitat transitions are consistently associated with particular body size shifts as optimised on the phylogeny and returned non-significant results. This indicates that, although crocodylomorphs with more aquatic lifestyles (particularly

marine species) tend to be large-bodied, the evolutionary transitions between these lifestyle categories were probably not accompanied by immediate non-random size changes. Furthermore, the smaller bodies of some lineages (e.g., atoposaurids, *Tsoabichi* and *Pelagosaurus*) show that adaptive peaks of smaller sizes are also viable among aquatic/semi-aquatic species. This suggests that, even though there seem to be an ecological advantage for larger-sized freshwater/marine crocodylomorphs, the body size lower limit (i.e., minimum body sizes achieved) of these aquatic species might have been comparable to that of terrestrial ones.

Table 2.5. Pairwise comparison between body size of crocodylomorphs subdivided into three lifestyle categories. Body size data from the ODCL dataset (log-transformed cranial measurement, in millimetres). Number of species in each category: 45 (terrestrial), 100 (semi-aquatic/freshwater), and 50 (aquatic/marine). Results of one-way analysis of variance (ANOVA), without accounting for phylogenetic dependency, and phylogenetic ANOVA (Garland *et al*. 1993; Revell 2012). *Bonferroni-corrected p-values (q-values) significant at alpha = 0.05

Category	**Mean**	**Std. Deviation**	**Std. Error**	**Pairwise comparisons**	**t-value**	**ANOVA q-value**	**Phylo ANOVA q-value**
Terrestrial	1.854	0.223	0.0333	**Terrestrial – Freshwater**	4.196	< 0.001*	1
Semi-aquatic/ freshwater	2.026	0.249	0.0249	**Terrestrial – Marine**	8.721	< 0.001*	0.138
Aquatic/ marine	2.263	0.185	0.0261	**Freshwater – Marine**	5.997	< 0.001*	0.537

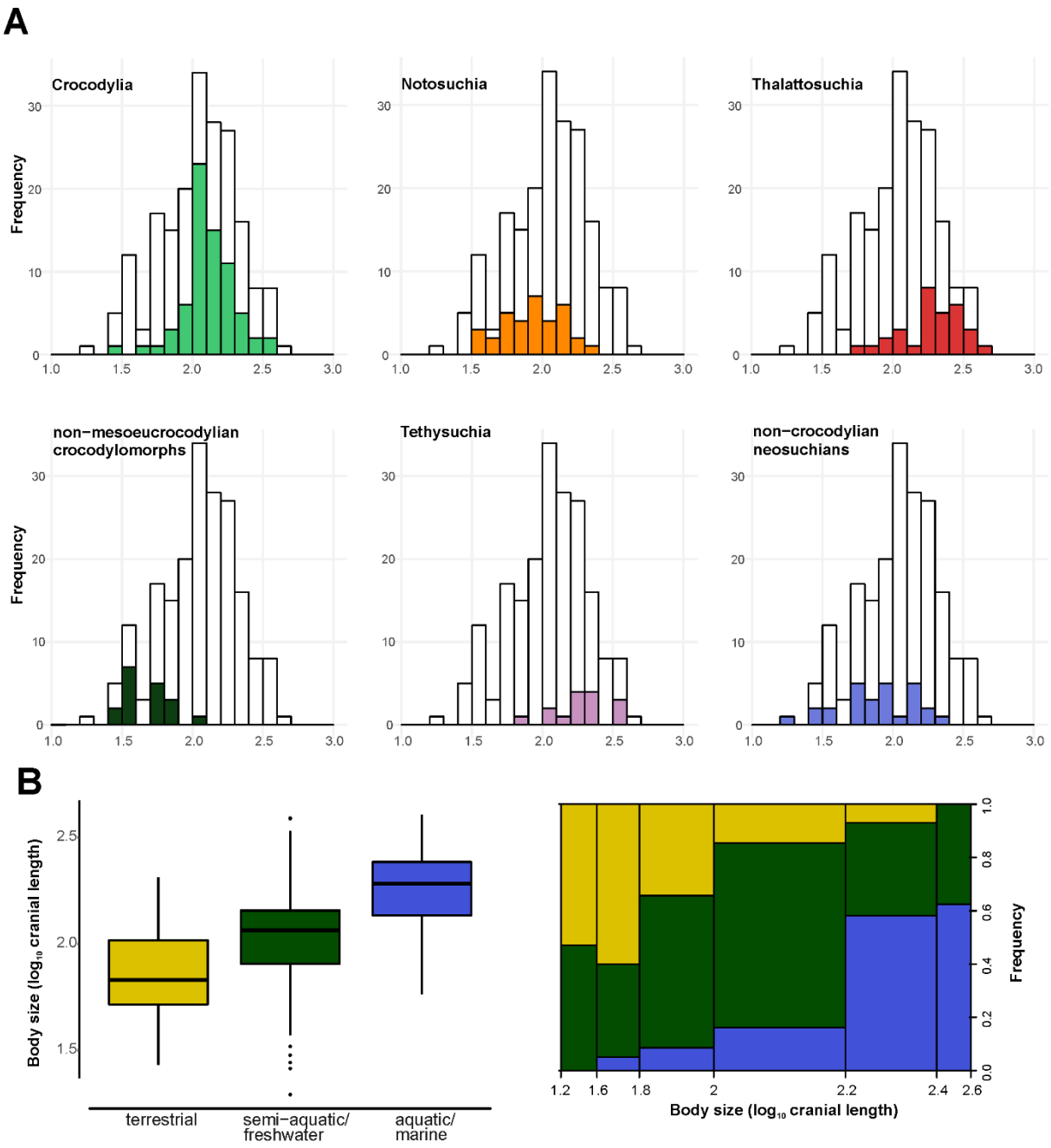

Figure 2.12. A, Body size frequency distributions of different crocodylomorph groups, constructed using the full set of 240 specimens in the ODCL dataset. Underlying unfilled bars represent values for all crocodylomorphs. Filled bars represent values for Crocodylia, Notosuchia, Thalattosuchia, non-mesoeucrocodylian crocodylomorphs (excluding thalattosuchians), Tethysuchia and non-crocodylian neosuchians (excluding tethysuchians and thalattosuchians). **B,** Body size distributions of different crocodylomorph lifestyles, shown with box-and-whisker plots (on the left) and a mosaic plot (on the right). The 195 species from the ODCL dataset were subdivided into terrestrial, semi-aquatic/freshwater and aquatic/marine categories (n = 45, 100 and 50, respectively) based on the literature.

Previous studies have investigated a possible link between an aquatic/marine lifestyle and larger body sizes in other animals, particularly in mammals (e.g., Smith and Lyons 2011; Heim *et al*. 2015; Gearty *et al*. 2018). For instance, it has been previously shown that aquatic life in mammals imposes a limit on minimum body size (Downhower and Bulmer 1988; Gearty *et al*. 2018) and relaxes constraints on maximum size (Williams 1999). Therefore, aquatic mammals (especially marine ones) have larger body sizes than their terrestrial relatives (Smith and Lyons, 2011; Vermeij 2016). Here, a similar pattern is documented in crocodylomorphs, although the phylogenetic ANOVA results (Table 2.5) revealed that changes in size are not abrupt after environmental invasions (as also suggested by the diminutive size of some semiaquatic lineages, such as atoposaurids and some crocodylians). As animals lose heat faster in water than in air (given the different rates of convective heat loss in these two environments), it has demonstrated that thermoregulation plays an important role in determining the larger sizes of aquatic mammals (Downhower and Bulmer 1988; Ahlborn and Blake 1999; Gearty *et al*. 2018). Although mammals have distinct thermal physiology to crocodylomorphs (which are ectothermic poikilotherms), it has been reported that American alligators (*Alligator mississippiensis*) heat up more rapidly than cool down, and that larger individuals are able to maintain their inner temperature for longer than smaller ones (Smith 1976). Thus, given that both heating and cooling rates are higher in water than in air (Smith 1976), larger aquatic/semi-aquatic animals could have advantages in terms of physiological thermoregulation. If extinct crocodylomorphs had similar physiologies, this could provide a plausible explanation for the larger sizes of non-terrestrial species.

2.4.3. Cope's rule cannot explain the evolution of larger sizes in Crocodylomorpha

Previous interpretations of the fossil record suggest a dominance of small sizes during the early evolution of crocodylomorphs (Irmis *et al*. 2013; Turner and Nesbitt 2013), inferred from the small body sizes of most early crocodylomorphs. Consistent with this, the SURFACE results revealed a small-bodied ancestral regime for Crocodylomorpha (Z_0 between 66 and 100 cm), which was inherited virtually by all non-crocodyliform crocodylomorphs. Larger non-crocodyliform crocodylomorphs have also been reported for the Late Triassic (e.g., *Carnufex carolinensis* and *Redondavenator quayensis*, with estimated body lengths of approximately 3 metres; Zanno *et al*. 2015), but the fragmentary nature of the specimens prevented their inclusion in the macroevolutionary analysis. Nevertheless, given the larger numbers of small-bodied early crocodylomorphs, taxa like *Carnufex* and *Redondavenator* probably represent derived origins of large body size and their inclusion would likely result in similar values of ancestral trait optima ($=Z_0$).

The small ancestral body size inferred for crocodylomorphs, combined with the much larger sizes seen in most extant crocodylians and in some other crocodylomorph subclades (such as thalattosuchians and tethysuchians), suggests a pattern of increasing average body size during crocodylomorph evolutionary history. The idea is reinforced by the overall increase in crocodylomorph mean body size through time, particularly after the Early Cretaceous (Fig. 2.10B). The same pattern also occurs within Crocodylia during the past 70 million years (Fig. 2.10B), as some of the earliest taxa (such as *Tsoabichi*, *Wannaganosuchus* and *Diplocynodon deponiae*) were smaller-bodied (< 2m) than more recent species, such as most extant crocodylians (usually > 3m). Cope's rule is most frequently conceived as the occurrence of multi-lineage trends of directional evolution towards larger body sizes (Cope

1887; 1896; Stanley 1973), and this can be evaluated using BM-based models that incorporate a directional trend (parameter μ; see e.g., Hunt and Carrano, 2010; Benson *et al*. 2018).

Little support was found for trend-like models as a description of crocodylomorph or crocodylian body size evolution. Therefore, the applicability of Cope's rule to crocodylomorph evolution is rejected. This reinforces previous works suggesting that multi-lineage trends of directional body-size evolution are rare over macroevolutionary time scales (Sookias *et al*. 2012*a*, *b*; Huttenlocker 2014; Benson *et al*. 2018; but see Benson *et al*., 2014*a*). Furthermore, the SURFACE model fits indicate that regime shifts towards smaller-bodied descendent regimes occurred approximately as frequently (9–13 times) as shifts to regimes of larger body sizes (13–16 times; Fig. 2.13). Together, these results indicate that long-term increases in the average body size of crocodylomorphs also cannot be explained either by multi-lineage trends of directional evolution towards larger size, or by a biased frequency of transitions to large-bodied descendent regimes.

Instead, the apparent trend towards larger body sizes can be explained by extinctions among small-bodied regimes. Crocodylomorph body size disparity decreased gradually through the Cretaceous (Fig. 2.10B). This occurred due to the decreasing abundance of small-bodied species. Despite this, the SURFACE model fits mostly indicate the survival of clades exhibiting small-bodied regimes ($\theta < 200$ cm) until approximately the end of the Mesozoic, (e.g., gobiosuchids, uruguaysuchids, sphagesaurids, hylaeochampsids and some allodaposuchids; Figs. 2.5, 2.6, and 2.7). Many of these small-bodied clades became extinct at least by the Cretaceous/Palaeogene (K/Pg) boundary, resulting in a substantial reduction of small-bodied species. Further reductions among the crown-group (Crocodylia) occurred by the Neogene, from which small-bodied species are absent altogether (Figs. 2.5, 2.6, and 2.7).

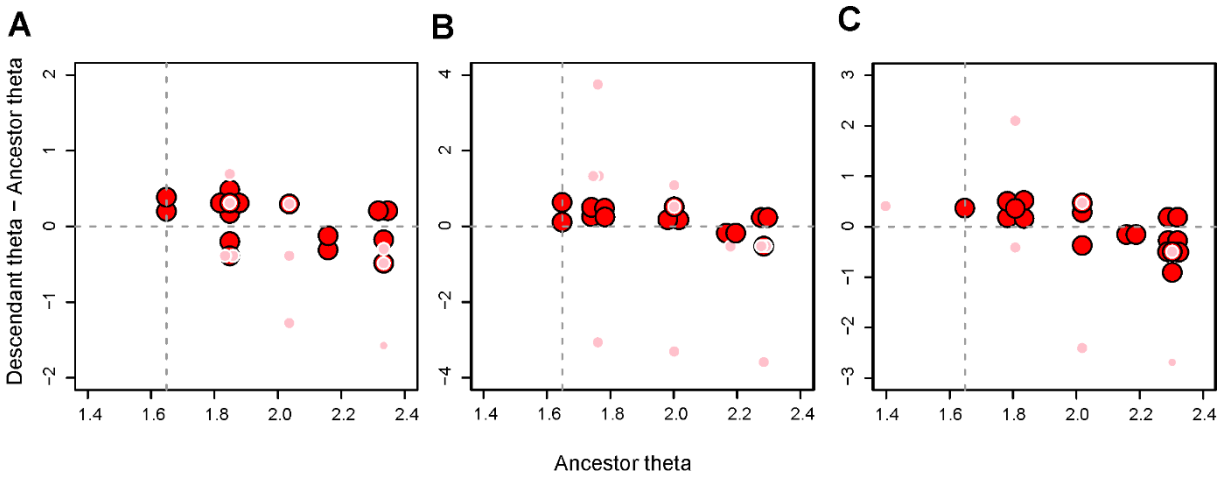

Figure 2.13. Distribution of regime shifts represented by the difference between descendant and ancestral regimes trait optima values (θ) plotted against the θ of the ancestral regime. Large red circles represent shifts that led to clades containing multiple taxa, while smaller pink circles represent "singleton" regimes, containing only single taxa. Vertical dashed line indicates the ancestral regime for all crocodylomorphs (Z_0), while horizontal dashed line can be used as a reference to identify regime shifts giving rise to larger (circles above the line) or smaller-bodied (circles below the line) descendants. Circles at the exact same position (i.e., shifts with the same θ values for both ancestral and descendant regimes) were slightly displaced in relation to one another to enable visualization. This plot was constructed using the θ values from trees with different positions of Thalattosuchia: **A,** Tree number 10, with Thalattosuchia within Neosuchia; **B,** Tree number 14, with Thalattosuchia as the sister group of Crocodyliformes; **C,** Tree number 11, with Thalattosuchia as the sister group of Mesoeucrocodylia. θ values in $\log_{10}$ mm, relative to the cranial measurement ODCL (orbito-cranial dorsal length).

This predominance of regimes of large sizes today is also linked to the occurrence of large body sizes in Crocodylia. The SURFACE analyses focusing on Crocodylia, indicate ancestral body size regimes with relatively high values of θ (Z_0 between 220 and 350 cm). The shift to a larger-sized regime (when compared to smaller-bodied eusuchian regimes) probably occurred at the Late Cretaceous (Figs. 2.5, 2.6, and 2.7), and this same regime was inherited by many members of the clade (predominantly semi-aquatic species). During the Palaeogene, however, shifts to regimes of smaller sizes also happen (such as in *Tsoabichi*

greenriverensis, *Diplocynodon deponiae* and planocraniids), increasing body size disparity (Fig. 2.10C). The crocodylian body size distribution shifts upwards mainly during the latter part of the Cenozoic (from the Miocene; Fig. 2.10B), when even larger-bodied animals occur (e.g., *Purussaurus* and *Mourasuchus*), combined with the disappearance of lineages of smallest species.

2.4.4. Correlation of crocodylian body size with global cooling

The time-series regressions demonstrate a moderate to strong correlation between crocodylian size and palaeotemperature (Table 2.4). This results from the upward-shift of the crocodylian body size distribution, coinciding with cooling global climates in the second half of the Cenozoic (Zachos *et al*. 2008; Linnert *et al*. 2014). Even though this is an apparently counter-intuitive relationship, it is not interpreted here as a result of direct causation. Previous studies have shown that crocodylian species richness decreased with declining global temperatures of the Cenozoic (Markwick 1998*a*; Mannion *et al*. 2015). Furthermore, the palaeolatitudinal ranges of both marine and continental crocodylomorphs have contracted as temperatures decreased (Fig. 2.9; see also Markwick 1998*a*; Mannion *et al*. 2015). Therefore, the temperatures experienced by evolving lineages of crocodylians are not equivalent to global average temperatures. It is proposed here that the association between global cooling and increasing crocodylian body size results from a systematic reduction of available habits/niches (due to a more restricted geographical distribution), with differential extinction of smaller-bodied species. The hypothesis of selective extinction is also consistent with the decreasing disparity of body size disparity of crocodylians during the Cenozoic (Fig. 2.10B).

2.4.5. Body size selectivity and diversification across Mesozoic boundaries

Numerous comparative studies have investigated a possible link between extinction risk and animal body size (e.g., Alroy 2001; Johnson 2002; Fisher and Owens 2004; Cardillo *et al*. 2005; Clauset and Erwin 2008). For example, larger body sizes, in association with dietary specializations, might increase susceptibility to extinction in some animal groups, such as hypercarnivorous canids (Purvis *et al*. 2000; Van Valkenburgh *et al*. 2004). On the other hand, the recovery of some animal clades after extinction events can also be associated with a subsequent increase in diversity and morphological disparity (e.g., Palaeogene mammals; Alroy 1998), potentially leading to the exploration of new regions of body size space (i.e., invasions of new body size adaptive zones). Thus, although for some groups (and for some extinctions) body size might play an important role, this is evidently not a generalised pattern across all animals.

For crocodylomorphs, little is known about possible influence of body size on differential extinction. In one of the few studies to quantitatively investigate this, Turner and Nesbitt (2013), using femoral length as a proxy for total body size, recognized a drop in mean body size of crocodylomorphs across the Triassic-Jurassic (T–J) boundary. The SURFACE results, however, indicate otherwise, as all Triassic crocodylomorphs are within a macroevolutionary regime of smaller sizes ($\theta < 100$ cm) when Thalattosuchia is placed within Neosuchia (Figs. 2.5 and 2.6). In the other two phylogenetic scenarios, the origin of thalattosuchians (which are predominantly large-bodied animals) is placed either at the middle of the Late Triassic or closer to the T–J boundary (Fig. 2.7). However, as the first records of thalattosuchians only occur in the Early Jurassic, mean body size increases immediately after the boundary (Fig. 2.10A). The differences between the results obtained in this Chapter and those found by Turner and Nesbitt (2013) might be related to the distinct body size proxies

used, or to sampling, as those authors also included non-crocodylomorph taxa in the pseudosuchian lineage. In this context, it is acknowledged that the inclusion of larger non-crocodyliform crocodylomorphs, such as *Carnufex carolinensis* (~3 metres; Zanno *et al*. 2015), in the analyses of this Chapter might change the results. Thus, at the moment the is no empirical or statistical evidence to demonstrate selectivity of body sizes in crocodylomorphs during the end-Triassic extinction.

The Early Jurassic was characterized by key events of crocodylomorph diversification (Bronzati *et al*. 2015) and an increase in morphological disparity (Toljagić and Butler 2013), following the end-Triassic extinction. Similarly, the body size data collected for this Chapter suggests an increase in body size disparity after the T–J boundary (Fig. 2.10B). Although a decrease in disparity is observed subsequently, this is probably due to the relatively few crocodylomorphs known for the latest Early Jurassic and the Middle Jurassic (Sinemurian–Aalenian; Mannion *et al*. 2015). Subsequently, the diversification of thalattosuchians during the Late Jurassic, together with the occurrence of smaller- to intermediate-bodied neosuchians (such as atoposaurids and goniopholidids), created the greatest observed disparity of crocodylomorph body sizes during their evolutionary history (Fig. 2.10C).

Recent studies (Tennant *et al*. 2016*b*, *c*; 2017) suggested that a combination of environmental perturbations occurred during the Jurassic-Cretaceous (J/K) transition, which might have led to the extinction of some tetrapod lineages. For crocodylomorphs the boundary is characterised by a decrease in marine diversity (Mannion *et al*. 2015; Tennant *et al*. 2016*b*, *c*), highlighted by declines in thalattosuchian diversity, especially among teleosaurids, which suffered widespread extinction (except, apparently, at lower palaeolatitudes; Fanti *et al*. 2016). Nevertheless, Wilberg (2017) did not find evidence for a substantial decrease in crocodylomorph cranial disparity across the J/K boundary (neither did

the analyses performed in Chapter 3 of this thesis). Similarly, the SURFACE results do not suggest dramatic changes in body size space exploration immediately before or after the J/K boundary (Figs. 2.5, 2.6 and 2.7), and there seems to be no defined body size selectivity across this boundary, as the multiple survivor crocodylomorph lineages were within regimes of very disparate optima values. Furthermore, the decrease in disparity observed in the middle of the Early Cretaceous (i.e., Valanginian–Barremian) is likely due to poor sampling (Butler *et al*. 2012; Benson *et al*. 2013), resulting in the scarcity of more completely preserved crocodylomorphs during these stages.

The Late Cretaceous is marked by a remarkable fossil richness of notosuchians, in Gondwana (Carvalho *et al*. 2010; Pol and Leardi 2015), and the diversification of eusuchian crocodylians (Brochu 2003). Notosuchia exhibits a wide range of body sizes (Fig. 2.12A), to some extent reflecting its remarkable diversity (Mannion *et al*. 2015; Pol and Leardi 2015) and morphological disparity (Wilberg 2017; see Chapters 3 and 4 of this thesis for further examples). The model-fitting analyses performed using only notosuchian data suggest more relaxed modes of body size evolution (Fig. 2.9), which is consistent with their species richness and morphological disparity. This could be explained by a combination of intrinsic (i.e., innovations and/or adaptations, such as a highly modified feeding apparatus; Ősi 2014; Pol *et al*. 2014) and extrinsic factors (i.e., specific environmental conditions, such as the predominantly hot and arid climate of the Gondwanan landmasses occupied by notosuchians; Carvalho *et al*., 2010; Marsola *et al*., 2016).

Even though the body size data of this Chapter show no specific pattern at the K/Pg boundary, a decline in body size disparity is present through the Late Cretaceous, combined with an increase in mean body size (Fig. 2.10), a pattern that generally continued through the Cenozoic (although with some short-term fluctuations). This supports the hypothesis that the

K/Pg extinction had only minor impacts on crocodylomorphs (Russell and Wu 1997; Markwick 1998*a*; Bronzati *et al*. 2015; Mannion *et al*. 2015). Although subsampled data suggests a decline in terrestrial diversity during the Late Cretaceous, it occurred prior to the boundary, from the Campanian into the Maastrichtian, in both Europe and North America (Mannion *et al*. 2015). Indeed, different crocodylomorph subclades lost several species prior to the end of the Cretaceous (in particular notosuchians and non-crocodylian eusuchians; Bronzati *et al*. 2015; Mannion *et al*. 2015; Figs. 2.5, 2.6, and 2.7), and multiple lineages within other groups, such as dyrosaurid tethysuchians and crocodylians, crossed the boundary with little change (Russell and Wu 1997; Markwick 1998*a*; Jouve *et al*. 2008; Figs. 2.5, 2.6, and 2.7). The results of this Chapter suggest a long-term pattern of extinctions among small-bodied taxa, starting from the Late Cretaceous and continuing to the Recent. This may have resulted from a longstanding trend of global cooling (Zachos *et al*. 2008; Linnert *et al*. 2014), resulting in more restricted geographical distributions, and reducing niche availability for crocodylomorphs. This is consistent with the SURFACE results (Figs. 2.5, 2.6, and 2.7), that show very few smaller-bodied regimes ($\theta < 150$ cm) during the Palaeogene and a complete absence after the Neogene. This pattern strikingly contrasts with that proposed for mammals, which may have experienced selectivity against larger bodied taxa across the boundary (Wilson 2013), although an increase in body size is observed subsequently during the Palaeogene (Alroy 1998; Smith *et al*. 2010). It also differs from that suggested for squamates (lizards and snakes), for which survival was possibly associated with small body sizes (Longrich *et al*. 2012).

2.5. Conclusions

After an early increase (with the highest peak in the Late Jurassic), crocodylomorph body size disparity experienced sustained decline during virtually its entire evolutionary history. This disparity decrease is combined with an increase of average body size through time, with highest peaks in the Middle Jurassic and today. In particular, the increase in mean body size seen during the Cenozoic (mostly related to crocodylians) is linked to an overall decrease in global temperatures.

Comparative model-fitting analyses were used to further characterise these body size macroevolutionary patterns in crocodylomorphs. The results show extremely strong support for a multi-peak Ornstein-Uhlenbeck model (SURFACE), rejecting the hypothesis of evolution based on Brownian motion dynamics (including those representing the concept of Cope's rule). This suggests that crocodylomorph body size evolution can be described within the concept of a macroevolutionary adaptive landscape, with a significant amount of crocodylomorph body size variance evolving from pulses of body size changes, represented by shifts between macroevolutionary regimes (or adaptive zones). This is reflected in the regime shifts frequently detected at the base of well-recognised and diverse crocodylomorph subclades, such as Notosuchia, Thalattosuchia, and Crocodylia.

At large temporal and phylogenetic scales, no strong correlation was found between the body size data and abiotic factors, indicating that shifts between macroevolutionary regimes are more important for determining long-term patterns of crocodylomorph body size than isolated climatic factors. However, at more refined scales, body size variation may track changes in climate. In the case of Crocodylia, a global cooling event might explain the long-term increases in body size, as a result of systematic reduction of available habitats/niches

(due to a more latitudinally-restricted geographical distribution during cooler global climates), with differential extinction of smaller-bodied species.

Shifts towards larger sizes are often associated with aquatic/marine or semi-aquatic subclades, indicating that ecological diversification may also be relevant, and suggesting a possible link between aquatic adaptations and larger body sizes in crocodylomorphs. These shifts to larger sizes, occurred throughout crocodylomorph evolutionary history, combined with the extinction of smaller-sized regimes, particularly during the Late Cretaceous and Cenozoic, explain the overall increase in mean body size, as well as the large-bodied distribution of extant crocodylians compared to earlier taxa.

Chapter 3: Crocodylomorph cranial shape disparity

3.1. Background

Transformations in the shape of living organisms have historically been the subject of scientific investigations (e.g., Russell 1916; Thompson 1917; Huxley 1932), as the study of shape provides crucial morphological information, which is fundamental for understanding the evolution of life on Earth (Darwin 1859). Morphometrics (namely the "measurement of shape") is the systematic study of shape of organisms using multivariate statistical methods, and is usually subdivided into "traditional morphometrics" (which involves linear measurements, angles and ratios; Marcus 1990) and the more recent "geometric morphometrics", in which two- or three-dimensional landmark-based data is used to capture the geometry of the structure being studied (Bookstein 1991; Rohlf and Marcus 1993; Adams *et al*. 2004; Mitteroecker and Gunz 2009; Cooke and Terhune 2015).

Although there are other methods available for quantifying shape changes (e.g. Euclidian distance matrix analysis; Lele and Richtsmeier [1991; 2001]; and elliptic Fourier analysis; Lestrel [1982]; Haines and Crampton [2000]), the use of landmark-based geometric morphometrics has become increasingly more frequent in ecological and evolutionary studies (Adams *et al*. 2004; Zelditch *et al*. 2012). However, the long recognised and often tight relationship between form and function (Cuvier 1817; Russell 1916; Gould 1977; Lauder 1981) potentially increases the frequency of convergent evolution, which challenges the accurate characterisation of macroevolutionary patterns (Harvey and Pagel 1991; Martins and Hansen 1997; Banavar *et al*. 2014; Cooke and Terhune 2015). This makes imperative the incorporation of phylogenetic information for assessing shape variation in an evolutionary

framework, paving the way for the use of phylogenetic comparative methods in geometric morphometric studies (Rohlf 2001; Monteiro 2013; Zelditch *et al*. 2012).

In this context, data collected from fossil organisms can yield essential information for a better comprehension of evolutionary shape changes. Among tetrapods, crocodylomorphs represent a good system for studying large-scale phenotypic evolution, given their long and rich fossil record (Bronzati *et al*. 2015; Mannion *et al*. 2015), as well as extensive recent effort to resolve major phylogenetic uncertainties (e.g., Jouve *et al*. 2006; Larsson and Sues 2007; Andrade *et al*. 2011; Clark 2011; Brochu 2011; 2012; Bronzati *et al*. 2012; Pol *et al*. 2013; Montefeltro *et al*. 2013; Pol *et al*. 2014; Young 2014; Herrera *et al*. 2015; Turner 2015; Wilberg 2015). Historically, the crocodylomorph skull has received substantial attention in anatomical studies, (Iordansky 1973), which might explain the preference for this part of the skeleton as the source of morphological information in most works quantitatively investigating phenotypic evolution in the group. Important exceptions include: Stubbs *et al*. (2013) and Walmsley *et al*. (2013), which assessed mandibular morphology; Bonnan *et al*. (2008) and Chamero *et al*. (2013), which used postcranial shape data; Gold *et al*. (2014), which assessed braincase shape variation; and Toljagić and Butler (2013), which used discrete characters to investigate morphological variation in the entire skeleton.

Previous work on crocodylomorph cranial shape variation have mostly focused on specific subgroups, especially crocodylians (Monteiro *et al*. 1997; Pierce *et al*. 2008; Sadleir and Makovicky 2008; Piras *et al*. 2009; 2010; 2014; Watanabe and Slice 2014; Clarac *et al*. 2016; Iijima 2017; McCurry *et al*. 2017*a*; Foth et al. 2017*a*; Bona *et al*. 2018), but also thalattosuchians (Pierce *et al*. 2009*a*; Young *et al*. 2010) and notosuchians (Chapter 4). One exception, however, is the recent work of Wilberg (2017), which assessed cranial shape variation for Crocodyliformes as a whole, sampling a large number of species (n = 131).

Nevertheless, although larger than anything previously compiled, the landmark dataset presented by Wilberg (2017) did not include numerous crocodylomorphs (e.g., non-crocodyliform crocodylomorphs), and morphospace occupation was only compared between members of the crown-group (i.e., crocodylians) and non-crown crocodylomorphs. Therefore, the sample size of Wilberg (2017) could be significantly increased, potentially permitting the assessment of morphospace occupation among a larger number of crocodylomorph subgroups (e.g., notosuchians and thalattosuchians).

Furthermore, Wilberg (2017) used cranial shape data to estimate morphological disparity in crocodylomorphs through time, a practice also implemented previously by several other crocodylomorph studies (e.g., Pierce *et al*. 2008; Young *et al*. 2010; Stubbs *et al*. 2013) and very frequently in studies of other tetrapod groups (e.g., in dinosaurs [Benton *et al*. 2014; Brusatte *et al*. 2008*a*, *b*], turtles [Foth and Joyce 2016; Foth *et al*. 2017*b*], pterosaurs [Butler *et al*. 2012; Foth *et al*. 2012], and early archosaurs [Foth *et al*. 2016*a*]). Wilberg (2017) compared disparity estimation using distinct disparity metrics (i.e., range- and variance-based metrics; Foote 1993; Wills *et al*. 1994; Foote 1997), as well as using different numbers of time bins (i.e., time bins based on chronostratigraphic divisions and equal-length time bins). However, a recent study (Guillerme and Cooper, 2018) suggests that alternative time sub-sampling methods can impact significantly on disparity-through-time analyses, given the uneven nature of the fossil record and that distinct methodologies have different assumptions for sampling taxa in each time interval. Additionally, Wilberg (2017) did not investigate cranial shape disparity among different crocodylomorph subgroups or ecologies (e.g., aquatic, semi-aquatic or terrestrial lifestyles).

In this Chapter, I use geometric morphometric techniques to comprehensively quantify crocodylomorph cranial shape variation, by combining a previously available landmark

dataset (from Wilberg [2017]) with newly digitised specimens. I also quantify cranial shape disparity between distinct crocodylomorph subgroups, and estimate disparity through time across the entire evolutionary history of the group using a variety of alternative methods. Accordingly, this Chapter aims to assess the impact on both shape variation and disparity estimates of significantly increasing taxon sample size, as well as the possible drivers of the observed variation. Additionally, I aim to investigate the impacts of different methods used to estimate disparity over time.

3.2. Material and Methods

3.2.1. Sampling and data collection

I used two-dimensional landmark-based geometric morphometric analyses to quantify cranial shape variation among crocodylomorphs. Ideally, skull shape would be fully assessed in a three-dimensional approach, using landmarks on 3D surfaces. However, most crocodylomorph crania are taphonomically deformed, usually by dorsoventral compression, which prevents a comprehensive study using 3D data. Thus, I initially used the data published by Wilberg (2017), as this was the most phylogenetically comprehensive 2D landmark dataset available for the group. This dataset comprised 131 crocodylomorph specimens, most of which were identified to species level, and used only dorsal views of skulls, as this view is less susceptible to compression and taphonomic distortion across different crocodylomorph groups. Wilberg (2017) digitised four landmarks on the right side of the skulls of individual specimens (reflecting the left side of the skull when only this was available or it was better preserved or more complete than the right side): “Landmark 1” at the caudalmost point of the skull at the midline (excluding the occipital condyle), “Landmark 2” at the rostralmost point of the snout, “Landmark 3” at the rostralmost point of the orbit margin, and “Landmark 4” at

the caudalmost point of the quadrate or quadratojugal (when visible) or the caudolateralmost point of the skull. Apart from these four landmarks, the outlines of skulls were digitised by Wilberg (2017) using sliding semilandmarks (Bookstein 1996; 1997; Adams *et al*. 2004). As described by Wilberg (2017), the outline is traced as a curve extending from "Landmark 1" to "Landmark 2", on the right side of the skull, and subsequently resampled to contain 60 equidistant semilandmarks (Fig. 3.1).

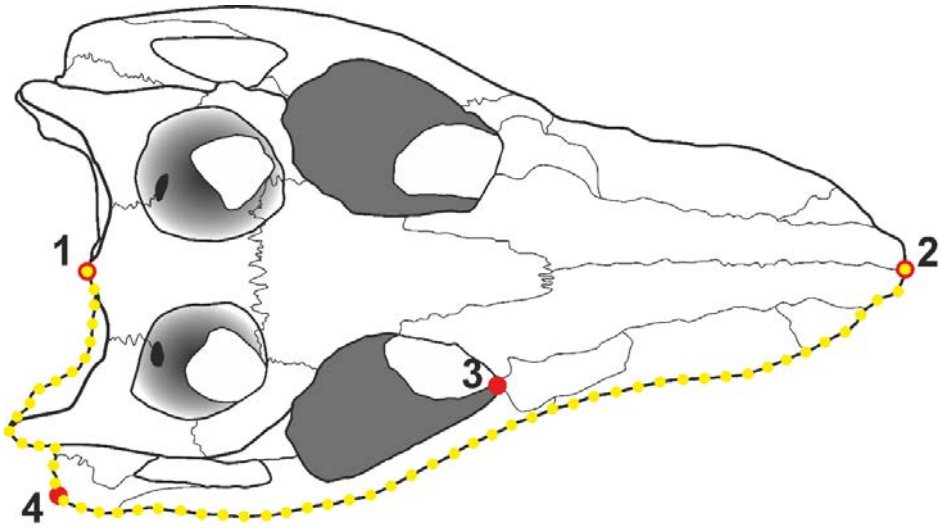

Figure 3.1. Example, using one specimen (*Araripesuchus wegeneri*, MNN GAD19), of the position of the four landmarks (in red) and the 60 equidistant semilandmarks curve (in yellow) used in this Chapter.

To expand this dataset, I digitised landmarks for 86 new specimens, representing an increase of nearly 65% over the dataset of Wilberg (2017). Non-mesoeucrocodylian crocodylomorphs were particularly underrepresented in Wilberg (2017), with only three taxa present in the original dataset, but 18 in my expanded dataset. However, in general it was possible to expand the taxonomic sample of all crocodylomorph subgroups. From the 131 specimens included in the original dataset, five were removed, including three unnamed specimens ("*Borealosuchus* Tullock specimen", "*Mecistops* Lothagam specimen", and

"*Prodiplocynodon* Utah specimen"), as well as *Stomatosuchus* (because the fossil material was lost during World War II [Sereno and Larsson 2009], preventing the inclusion of the taxon in more recent phylogenetic analyses), and *Hamadasuchus* sp. (because first-hand observation allowed me to instead use the holotype specimen of this genus). Following Wilberg (2017), I did not include specimens identified by previous workers as juvenile or sub-adult in the expanded dataset, in order to reduce the effect of ontogeny on cranial shape variation. Furthermore, I also updated the taxonomy, permitting me to identify all specimens at least to species level and to incorporate more recent taxonomic opinions. Thus, some of the specimens treated by Wilberg (2017) as different species were merged (this was mostly the case among thalattosuchians following recent taxonomic work: e.g., Parrilla-Bel *et al*. [2013], Herrera *et al*. [2015], and Foffa *et al*. [2018]). In the cases where multiple specimens are present for a species, averaged values were obtained before the Procrustes alignment. The final expanded dataset includes 212 specimens, representing 209 species (see Appendix B for the complete list of specimens). For landmark data collection, I followed the procedure described in Wilberg (2017), using tpsUTIL version 1.76 (Rohlf 2015) for compiling the images into a single .tps file, then digitising the landmarks and semilandmarks in tpsDIG2 version 2.30 (Rohlf 2015).

3.2.2. Phylogenetic framework

For the phylogenetic framework, I used a modified version of the crocodylomorph supertree constructed for Chapter 2, which is itself a newer version of the supertrees previously constructed by Bronzati *et al*. (2012; 2015). As in Chapter 2, I used three alternative positions for the clade Thalattosuchia, as this represents one of the major uncertainties in crocodylomorph phylogeny (see "Material and Methods" section of Chapter 2 for details). I

then used an informal approach (by manually modifying the tree using the software Mesquite version 3.51; Maddison and Maddison 2018) to add species for which I had landmark data, but which were not previously included in the supertree. The final version of the supertree includes 325 species (316 crocodylomorphs and nine non-crocodylomorph species, as outgroups), representing an increase of 20 taxa in comparison to the supertree used in Chapter 2. For the phylogenetic positions of the additional taxa included, I followed recently proposed phylogenetic hypotheses. These included Brochu (2006) for gavialoids, Jouve *et al*. (2015) for tomistomines, Meunier and Larsson (2017) for tethysuchians, and Parrilla-Bel *et al*. (2013), Herrera *et al*. (2015), Fanti *et al*. (2016), Foffa *et al*. (2018), and Ősi *et al*. (2018) for thalattosuchians. Additionally, I followed the phylogenetic hypothesis presented in Wilberg (2017) for some extant crocodylians included in his original landmark dataset.

For performing disparity analyses, it was necessary to time-calibrate the trees (Bapst 2014*a*). I used the *mbl* method (Laurin 2004), which uses a minimum branch duration (in this case set as 1 Myr) that is defined before time-scaling the phylogenies, in order to avoid zero-length branches. Only one time-calibration method was used, although several alternative approaches are available (see "Material and Methods" section of Chapter 2 for details), since the aim here was to assess the impact of other factors on the analyses (such as different topologies and distinct disparity metrics). For time-calibration, crocodylomorph age data (first and last occurrence dates) were initially obtained from the Paleobiology Database (PBDB), but were subsequently checked using the literature. To accommodate uncertainties related to both debatable phylogenetic positions (reflected as polytomies in the supertree) and ages of terminal taxa (i.e., ages based on single imprecise bounds, such as entire periods or ages/stages), I generated 10 randomly resolved trees, each one of which was time-calibrated with first and last occurrences dates treated as maximum and minimum possible ages,

drawing terminal dates (for the *mbl* method) from a uniform distribution between these. Time-scaling was performed using the package *paleotree* (Bapst 2012) in R version 3.5.1 (R Core Team 2018).

3.2.3. Geometric morphometric analyses

Prior to all geometric morphometric analyses, the crocodylomorph landmark data was subjected to a generalised Procrustes analysis (GPA), using the package *geomorph* (Adams and Otárola-Castillo 2013) in R version 3.5.1 (R Core Team 2018). GPA (also known as Procrustes superimposition, Procrustes fit or GPA-alignment) is performed for obtaining shape variables from landmark data after translating, rescaling and rotating the specimens, resulting in aligned Procrustes coordinates for each specimen (Gower 1975; Rohlf and Slice 1990). Semilandmarks were defined using function *define.sliders()* in the same package, and the location of sliding semilandmarks during GPA-alignment was optimised by minimizing the bending energy between the reference and target specimen (i.e., argument ProcD=FALSE within in the function *gpagen()*, also in *geomoph*; see Bookstein 1997). Subsequently, the Procrustes coordinates of specimens were used as the input data for an ordination method, to investigate which aspects of cranial shape varied the most among the sampled crocodylomorph taxa. For that, I used principal component analysis (PCA; Hotelling 1933), which was also performed in *geomorph*.

It is worth mentioning that these initial procedures (i.e., GPA followed by PCA) are, to some extent, different from those applied by Wilberg (2017). The first difference was that during Procrustes alignment, Wilberg (2017) allowed up to three iterations to occur (with semilandmarks allowed to slide differently in each iteration). As I did not set a maximum number of iterations, this resulted in up to six iterations in my analyses. Furthermore, Wilberg

(2017) also used a different software for performing GPA and ordination (tpsRELW; Rohlf 2015). Instead of PCA, Wilberg used Relative Warp Analysis (RWA) as the ordination method, which should produce equivalent results to PCA, as he did not weight the variation by bending energy (i.e., $\alpha = 0$; Zelditch *et al*. 2012; Rohlf 2015). However, as a sensitivity analysis, I submitted the original landmark data from Wilberg (2017) to the same procedure used for the expanded dataset, in order to estimate the impact of these alternative procedures on the results (i.e., morphospace occupation and PC scores [eigenvalues of each principal component or eigenvector from the PCA]).

As the landmark data used in this Chapter derives from two distinct sources (i.e., the dataset provided by Wilberg [2017] and the data collected for the present study), particular attention was paid to the potential impact of interobserver error on the cranial shape data (i.e., measurement error caused by different observers/operators during the digitisation of landmarks). This issue has received increased attention recently, given that sharing of geometric morphometric datasets among scientists has become more frequent, and that a significant amount of data (particularly three-dimensional data) have been collected from multiple instruments (e.g., Fruciano 2016; Fruciano *et al*. 2017; Robinson and Tefhune 2017; Shearer *et al*. 2017; Daboul *et al*. 2018). To assess whether interobserver error could be influencing the morphospace occupation within my sample of crocodylomorphs, I initially examined the scatterplot of scores along the first two principal components, dividing the specimens into two groups: those originally included in the dataset of Wilberg (2017) and those newly included in this Chapter. Additionally, to more quantitatively approach this issue, I used Procrustes ANOVA (i.e., linear models) in *geomorph* (Goodall 1991; Klingenberg and McIntyre 1998; Anderson 2001) to compute the amount of variation caused by interobserver error. The Procrustes coordinates of all taxa were used as the response variable in the

Procrustes ANOVA formula, and the independent (grouping) variable was a discrete vector indicating whether the landmark data was originally collected by Wilberg (2017) or by me. As recommended by Collyer *et al*. (2015), I used a residual randomization permutation procedure with 10,000 permutations to test the model significance. The percentage of variation driven by interobserver error was then calculated by dividing the sum of squares (SS; see Goodall 1991) for the term (grouping variable) by the total sum of squares of the model. The same procedure was employed for examining the amount of variation originating from measurement error in the first principal components (i.e., computing the percentage of variation caused by interobserver error for each of these PCs).

Two procedures were then followed to attempt to minimise the effects of interobserver error on the shape data. First, I applied Burnaby's (1966) procedure of statistical correction (also known as Burnaby back-projection or Burnaby's projection), used for removing the effect of extraneous variables from morphometric data (Rohlf and Bookstein 1987; Adams 1999). Burnaby's method was originally designed as a size correction procedure, but it can be used for removing the effects of other undesirable variables (vectors), by projecting the original shape data into a subspace orthogonal to these vectors (Adams 1999; Fruciano 2016). Apart from being frequently applied as a size correction in both traditional and geometric morphometrics (Jungers *et al*. 1995; Klingenberg 1996; 2016; McCoy *et al*. 2006), this method has proved itself useful for eliminating or reducing the artefactual variation caused by other factors, particularly the body arching in fish (e.g., Valentin *et al*. 2008; Fruciano *et al*. 2011; Ingram 2015). The subspace (**L**) orthogonal to an extraneous variable ($\mathbf{f_1}$) is obtained with matrix algebra, using the formula:

$$\mathbf{L} = \mathbf{I}_q - \mathbf{f_1}(\mathbf{f'_1}\,\mathbf{f_1})^{-1}\mathbf{f'_1}$$

For *N* specimens, $\mathbf{f_1}$ is a *q* x 1 column vector, where *q* is the number of variables. **I** is the identity matrix of *q* x *q* dimensions, whereas **L** is an idempotent symmetric matrix of rank *q* – 1 (Rohlf and Bookstein 1987; Adams 1999). By multiplying the original data matrix by **L**, the dataset of "adjusted specimens" (i.e., specimens with variation projected only to the hyperplane orthogonal to the vector $\mathbf{f_1}$) is obtained (in this case, landmark coordinates without the effect of an undesirable factor). For the purpose of this Chapter, $\mathbf{f_1}$ should be a vector that best represents the shape variation caused by interobserver error. Accordingly, I used the sum of squares from Procrustes ANOVA models to identify the principal component with the highest percentage of variation explained by interobserver error, and subsequently used the specimens' PC scores for that principal component to represent $\mathbf{f_1}$. The matrix algebra for the procedure described above was performed in R, adapting the script from Claude (2008). The resulting adjusted landmarks were subjected to GPA and PCA, and the scatterplot of the first two principal components was used to inspect the results (once again dividing the specimens into two groups).

The second procedure used for reducing the effect of interobserver error focused on the landmark digitisation protocol. As specified above, I followed the digitising protocol defined by Wilberg (2017). For assessing the accuracy of this protocol, I opened the .tps file (i.e., the "raw" landmark coordinates of each specimen) made available by Wilberg (2017) in the software tpsDIG2 version 2.30. As I did not have access to the source images of specimens originally used for digitising the landmarks, I modified the .tps file to use a blank image, which allowed me to visualise the landmarks of all specimens. I then compared the landmarks digitised by Wilberg (2017) and by me, searching for possible differences that

could generate biases during the digitisation process. I then attempted to minimise possible differences by re-digitising the landmarks, following a standardised protocol.

Following these two procedures, landmark data were subjected to GPA and PCA, and the results were then inspected using a plot of PC scores from the first two principal components (with specimens divided into the same two groups), as well as by using Procrustes ANOVA to calculate the percentage of variation caused by interobserver error. To better visualise the morphospace occupation of different crocodylomorph subgroups (in PC1 versus PC2 scatterplots), I used distinct colours and convex hulls (i.e., the area inside the minimum convex polygon; Cornwell *et al*. 2006) for six groups: Crocodylia, Tethysuchia, Thalattosuchia, Notosuchia and two paraphyletic groupings of non-crocodylian neosuchians (excluding tethysuchians and thalattosuchians) and non-mesoeucrocodylian crocodylomorphs (excluding thalattosuchians). To statistically assesses the differences in the morphospace occupied by these groups, I used non-parametric multivariate analysis of variance (npMANOVA). In contrast to a parametric MANOVA, npMANOVA does not require the data to be normally distributed, and tests for significant differences on the basis of permutations (Anderson 2001). Pairwise comparisons between groups were performed, with PC scores of taxa within each group transformed into a Euclidean distance matrix and permuted 10,000 times. I then obtained adjusted p-values, to reduce the likelihood of type 1 statistical errors, using the Bonferroni correction (Rice 1989). It is worth mentioning that, as the Bonferroni correction is considered very conservative, other methods for dealing with multiple comparisons were also applied (such as the “Holm” and the “BH” methods; Holm [1979]; Benjamini and Hochberg [1995]), as a sensitive test. Nevertheless, when different methods provided similar results, only the Bonferroni-corrected p-values were reported.

I used phylomorphospaces to visually examine the influence of phylogeny on the shape variation described by the first two principal components, by projecting phylogenetic hypotheses onto the morphospace of PC1 against PC2. For that, the ancestral states were estimated (i.e., landmark coordinates of hypothetical ancestors) using the R package *geomorph*, which in turn uses function *fastAnc()* from package *phytools* (Revell 2012). This function uses the "re-rooting method" (i.e., re-rooting the tree at every internal node; Yang *et al*. 1996; Garland and Ives 2000) for estimating ancestral states with maximum likelihood and assumes Brownian motion as the model of evolutionary change. Additionally, I more quantitatively assessed the phylogenetic signal present in the shape data using a multivariate generalisation of the K statistic of Bloomberg *et al*. (2003), which is a distance-based approach described by Adams (2014). Using the function *physignal()* present in R package *geomorph*, I obtained Adams' K_{mult}, which provides a statistical measure of phylogenetic signal based on Brownian motion dynamics (i.e., the expected value of K_{mult} under Brownian motion is 1). The input data for this function is the entire dataset of aligned landmarks (Procrustes coordinates of all specimens), which means that all aspects of shape variation are being analysed (not only PC1 and PC2). For that, I used all 10 trees of each alternative phylogenetic scenario (i.e., with different positions of Thalattosuchia), and calculated K_{mult} for each tree performing 1000 iterations.

Furthermore, I also divided crocodylomorph species into three categories representing distinct ecological habits (or lifestyles): marine/aquatic, freshwater/semi-aquatic and terrestrial species. For dividing taxa into these subsets, I used information available in the literature (mostly the information available in Mannion *et al*. 2015), as well as in the PBDB (see Appendix B for a list of the lifestyles of all taxa). I then visually assessed the differences in morphospace occupation using colours and convex hulls, and statistically scrutinised these

differences using npMANOVA (using the same parameters as for the taxonomic groups). For analyses with taxonomic groups and ecological categories, pairwise npMANOVA tests were performed using package *RVAideMemoire* (Hervé 2018), in R version 3.5.1 (R Core Team 2018).

3.2.4. Estimating disparity

Following the above procedures that accounted for measurement error, I performed analyses to calculate the cranial shape disparity of the sampled crocodylomorphs. There are numerous different methods for quantifying morphological disparity, which for geometric morphometric data correspond to alternative proxies for space occupation (commonly known as disparity metrics or indices; Foote 1993; Wills *et al*. 1994; Foote 1997; Wills 2001; Zelditch *et al*. 2012; Hopkins and Gerber 2017). Among these, the most frequently used in palaeontological studies are the sums and products of ranges and variances (Wills *et al*. 1994; Guillerme and Cooper 2018), which usually provide somewhat different results, and have their own limitations (e.g., range metrics are more susceptible to problems arising from uneven sampling, and variance metrics can introduce co-variance between not measured dimensions; Butler *et al*. 2012; Guillerme and Cooper 2018). For the analyses within this Chapter, I selected the sum of variances as the disparity metric, as it seems to be more robust for measuring disparity through time (see Wills *et al*. 1994; Guillerme and Cooper 2018), and also because it allows comparisons with the results from Wilberg (2017) as well as other studies (e.g., Stubbs *et al*. 2003; Toljagić and Butler 2013). Thus, herein, disparity is defined as the sum of variances expressed for all dimensions (eigenvectors), using PC scores of specimens from all non-null principal components.

For disparity-through-time analyses, I included the estimated ancestral states, using all 10 time-calibrated trees for each of the three alternative phylogenetic scenarios. Subsequently, two sub-sampling procedures were used for assessing crocodylomorph disparity through time: time binning and time-slicing. As detailed by Guillerme and Cooper (2018), different methods for sub-sampling taxa through time can have important impacts on the results of disparity-through-time studies. For example, using stratigraphic intervals such as stages (a widely employed approach; e.g., Prentice *et al*. 2011; Foth *et al*. 2012; Hughes *et al*. 2013; Stubbs *et al*. 2013; Benton *et al*. 2014; Wilberg 2017) usually introduces sampling biases, since some short time bins can include very few taxa, leading to large confidence intervals (Guillerme and Cooper 2018). Alternatively, time bins can be arbitrarily set to represent equal length intervals (e.g., Butler *et al*. 2012; Foth and Joyce 2016; Foth *et al*. 2016*a*; 2017*b*; Wilberg 2017), which might diminish the issues of uneven sampling. However, as this approach only allows comparisons of changes in disparity that occur between intervals, it potentially assumes a punctuated model of evolution (i.e., "punctuated equilibrium", *sensu* Gould and Eldredge 1977), and prevents the assessment of variation within intervals as a result of gradual evolution (Guillerme and Cooper 2018). As an alternative to this time binning method, Guillerme and Cooper (2018) recently proposed the "time-slicing" method, which is a phylogeny-based method (i.e., using data from terminal taxa, nodes and branches) and takes into consideration those taxa contemporaneous at specific equidistant points in time (instead of taxa that were present between two points in time), resulting in even sampling. Furthermore, this method allows *a priori* definition of the evolutionary model underlying the changes in disparity.

Therefore, to more rigorously assess the patterns of crocodylomorph cranial shape disparity through time, I used both time sub-sampling methods, with time sub-samples (either

time bins or time slices) defined by the number of intervals (i.e., using the same number of time intervals for both methods). In this case, I used 10 and 20 time intervals (i.e., equal-length time bins, in the time binning method, and equally distant specific points in time, in the time-slicing method), to assess the impact of the number of time intervals. In both methods, I used landmark data for both terminal taxa and hypothetical ancestors, and I also allowed taxa to occur in multiple time intervals, by using taxon first and last occurrence dates. PC scores of taxa in each time bin were subjected to bootstrapping (1,000 iterations) to calculate confidence intervals. Finally, for the time-slicing method, I calculated disparity assuming gradual and punctuated models of evolution. For punctuated evolution, selection of values of ancestors or descendants was based on the position of the time slice along the branch, using the score of the ancestor if it is located in the first half of the branch, and the score of the descendant if it is in the second half (i.e., "proximity"; Guillerme and Cooper 2018). For gradual evolution, a probability function of the distance between the nodes/tip at the ends of the branch and the slice was used for selecting the values (i.e., "gradual splits"; Guillerme and Cooper 2018).

I further inspected disparity among different crocodylomorph subgroups by dividing the PC scores for each species into distinct subsets. First, I assessed disparity using six subsets: Crocodylia, Tethysuchia, Thalattosuchia, Notosuchia, non-crocodylian neosuchians and non-mesoeucrocodylian crocodylomorphs. Second, to investigate if the inclusion of crocodylians and tethysuchians within Neosuchia could significantly change the results, I divided the species into four subsets (Notosuchia, Thalattosuchia, Neosuchia and non-mesoeucrocodylian crocodylomorphs). PC scores were subsequently bootstrapped 100 times and, during each bootstrap replication, the number of elements (taxa) drawn was standardised in all groups, by rarefying the data to 18 elements (the minimum number of species in a group

[in this case, non-mesoeucrocodylian crocodylomorphs]). As for disparity-through-time analyses, the metric used was the sum of variances (i.e., "disparity" is the median of the sum of variances in each group). Significant differences in bootstrapped median values were statistically assessed using npMANOVA with 10,000 permutations, followed by a Bonferroni correction for adjusted p-values (Rice 1989, Anderson 2001). Finally, in addition to these analyses investigating disparity among different taxonomic groups, I also calculated disparity for crocodylomorphs divided into three ecological categories. As for the taxonomic groups, PC scores were bootstrapped (100 times) and rarefied (to 45 elements, as this is the minimum number of taxa within any of the ecological categories), and I subsequently used npMANOVA to test for statistically significant differences. All disparity analyses (through-time and between groups) were performed using the R package *dispRity* (Guillerme 2018). An example R script of the morphometric geometric and disparity analyses can be found in Appendix C.

3.3. Results

3.3.1. Geometric morphometric analyses

The results obtained after subjecting the landmark dataset made available by Wilberg (2017) to Procrustes alignment (GPA) and ordination (PCA) were very similar to those originally presented by Wilberg (2017). The minor differences are possibly due to slightly different methodological settings between the two software packages (tpsRELW and the R package *geomorph*; as detailed in the "Material and Methods" section of this Chapter). However, the first two principal components represent very similar percentages of total shape variation (i.e., PC1 = 70.76% in this work and 73.55% in Wilberg [2017], PC2 = 9.58% in this work and 10.81% in Wilberg [2017]) and describe almost identical aspects of morphological changes

(PC1 mainly represents snout length, whereas PC2 shows variation in snout width, position of the orbit and quadrate condyle width). A morphospace scatterplot of PC1 against PC2 (Fig. 3.2) also shows taxa in similar positions in the morphospace to that presented in Wilberg (2017; figure 4), and convex hulls of crocodylians and non-crocodylian crocodylomorphs illustrate comparable morphospace occupations. These results indicate that any dissimilarities found after expanding the landmark dataset would not be the result of differences in the alignment and ordination procedures.

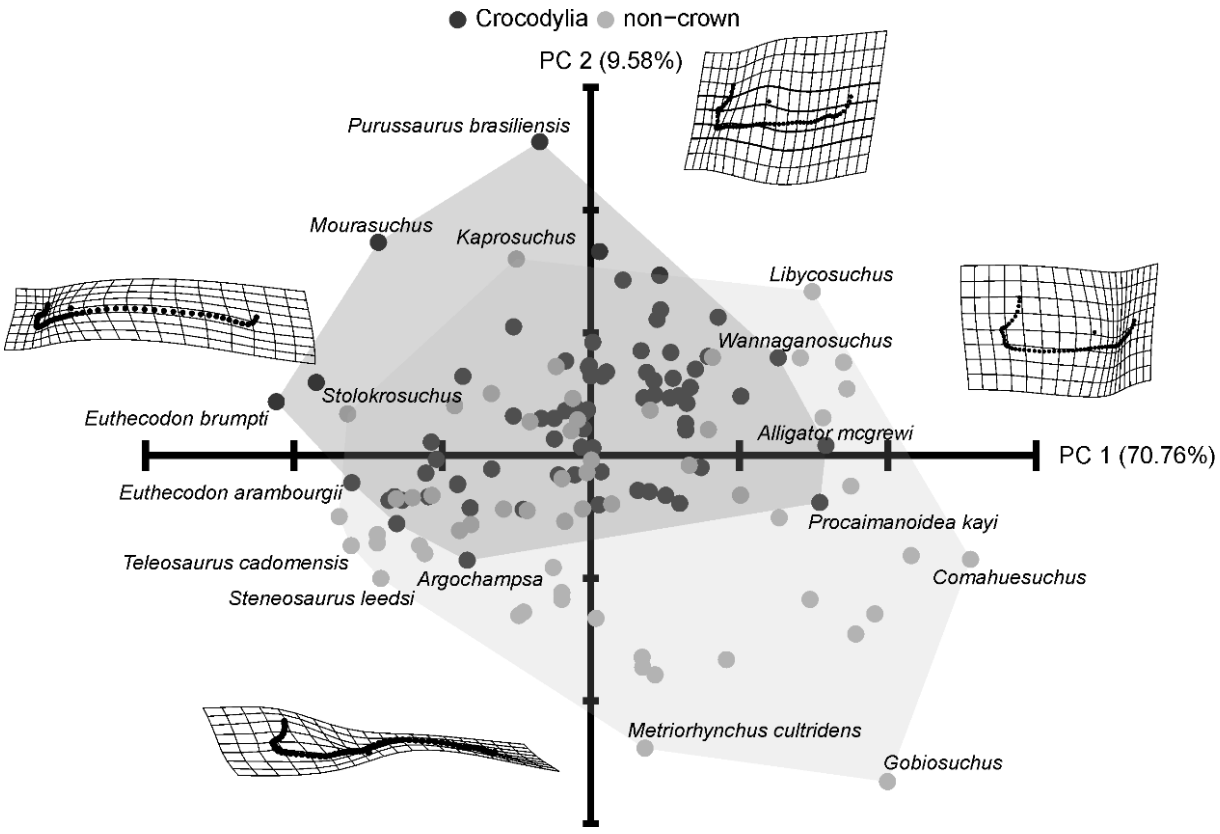

Figure 3.2. Morphospace scatterplot of the first two principal components using only specimens included in the original dataset of Wilberg (2017), with 131 taxa. Comparative morphospace occupation of crocodylians (crown group) and non-crocodylian crocodylomorphs (non-crown) is shown using convex hulls. Deformation grids illustrate the cranial shape at the extremes of each PC.

Following this initial sensitivity analysis, I investigated the cranial shape variation of crocodylomorphs using the expanded dataset of 209 species. Following GPA and PCA, the PC1 versus PC2 morphospace (Fig. 3.3) exhibits a pattern unequivocally caused by interobserver error (i.e., measurement error introduced to data due to different observers/operators during data collection). Taxa originally included in Wilberg's (2017) dataset are clearly separated from those included in the present study, mainly along the PC2 axis. Whereas PC1 (50.89% of the variation) still seems to represent changes in snout length, PC2 accounts for a significant larger amount of the total variation (22.89% of the variation) compared to the sensitivity analysis. Furthermore, apart from changes in the quadrate condyle width, PC2 does not seem to represent variations in other meaningful aspects of cranial morphology, suggesting PC2 might mainly represent interobserver error.

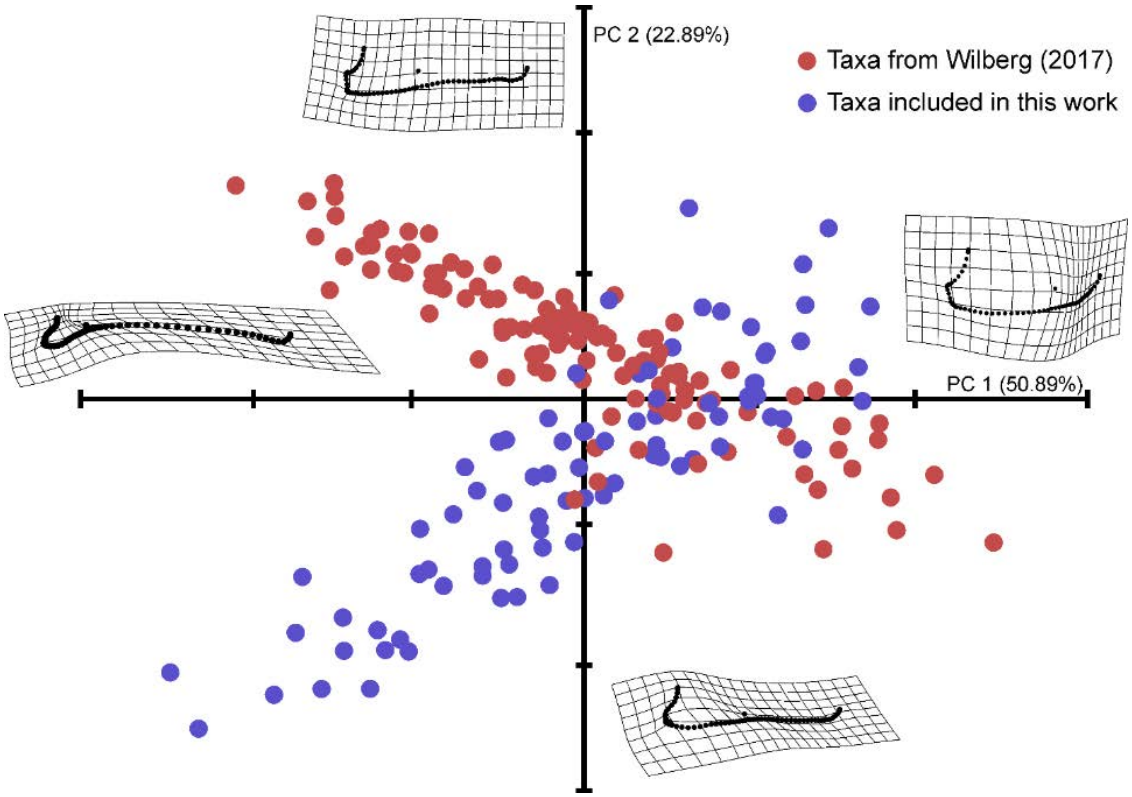

Figure 3.3. Morphospace plot (PC1 versus PC2) using the expanded dataset, with 209 taxa. Different colours were used for taxa originally in the dataset of Wilberg (2017), in red, and those newly included in the present Chapter, in blue. Deformation grids illustrate the cranial shape at the extremes of each PC.

Table 3.1. Procrustes ANOVA results investigating the amount of variation in shape data caused by interobserver error. **SS,** sum of squares after 10,000 permutations; **MS,** mean squares; **% of variation,** obtained by dividing the sum of squares of the independent variable (groups) by the total sum of squares; **F,** F-statistic; **p,** p-value. * Significant at alpha = 0.05.

Total shape variation (all PCs)

Effect	SS	MS	% of variation	F	p
Interobserver error	0.3507	0.35069	7.342348	16.403	0.0001*
Residuals	4.4255	0.02138			
Total	4.7762				

Shape variation represented by PC2

Effect	SS	MS	% of variation	F	p
Interobserver error	0.32754	0.32754	29.96293	88.558	0.0001*
Residuals	0.76562	0.00370			
Total	1.09316				

To quantitatively estimate the amount of measurement error in the shape data, I used Procrustes ANOVA with two distinct groups (taxa originally sampled by Wilberg [2017] and those included in this Chapter) as the independent variable. The results show that interobserver error corresponds to more than 7% of total shape variation, and virtually 30% when assessing only the variation expressed by PC2 (Table 3.1). Among other PCs, interobserver error represents a much smaller, sometimes marginal, percentage of the

variation (e.g., PC1 = 0.01%; PC3 = 2.84%; PC4 = 1.8%). This confirms that, among all principal components, PC2 contains the largest amount of interobserver error, suggesting that it could be used as a proxy vector (i.e., vector $\mathbf{f_1}$) for performing Burnaby's (1966) projection, aiming at removing the effects of an extraneous variable (in this case, interobserver error) from the shape data. Thus, I subsequently employed Burnaby's (1966) method, projecting the landmark data into a subspace orthogonal to scores from PC2.

After GPA and PCA, the amount of variation accounted for interobserver error was evidently reduced (from more than 7% to 1.68% of total shape variation). However, the morphospace of PC1 against PC2 reveals that essential shape information was also eliminated, as the morphological aspects represented by the first principal components are rather unrealistic (Fig. 3.4A). Since this procedure did not produce satisfactory results, I then more rigorously assessed the landmark digitising protocol, by visualising the landmarks from the original dataset on a blank image (see "Material and Methods" section of this Chapter for details). This allowed me to identify an important difference in the protocol. Different to what was described by Wilberg (2017), the curve representing the skull outline did not contain 60 equidistant semilandmarks. Instead, there were two separate but adjoining curves. The first curve, containing 35 semilandmarks, extended from "Landmark 1" to the level of the rostralmost point of the orbit. The other, with 25 semilandmarks, started just after the end of the first curve and extended until "Landmark 2". Even though these curves were merged in the final .tps file made available by Wilberg (2017), they were very likely drawn separately, creating two modules on the outline of the skull (one rostral to and another caudal to the level rostralmost point of the orbit), potentially exacerbating differences between longirostrine and brevirostrine forms. Thus, to reduce the bias caused by differences in the digitising protocol, I used the software tpsDIG2 (Rohlf 2015) to manually modify all specimens in the original

Wilberg's dataset, resampling the outline curves to contain 60 equidistant semilandmarks. I then added the remaining specimens (those included for the first time in the present work) and subjected the landmark data to GPA and PCA.

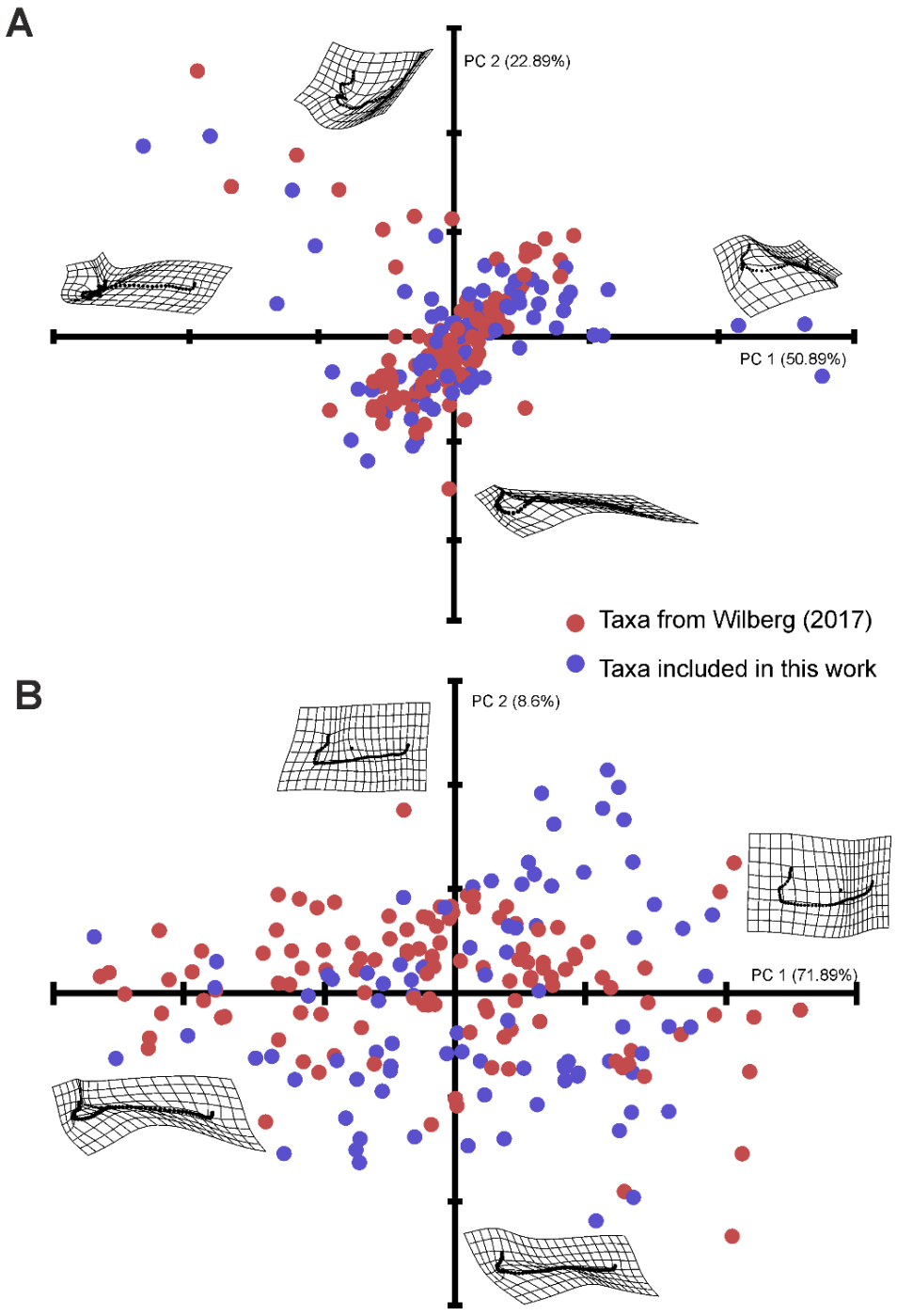

Figure 3.4. Morphospace plot (PC1 versus PC2) using the expanded dataset, after applying two procedures for removing the effect of interobserver error: **A,** Burnaby's (1966) projection method and **B,** standardisation of the landmark digitising protocol. Different colours were used for taxa originally in the dataset of Wilberg (2017), in red, and those included for the first time in the present Chapter, in blue. Deformation grids illustrate the cranial shape at the extremes of each PC.

Procrustes ANOVA results (Table 3.2) show that potential error caused by multiple observers was drastically reduced (i.e., interobserver error accounts for 1.6% of total shape variation), which indicates that biases originating from imprecisions in the digitising protocol generated most of the error. For this reason, I used this modified version of the expanded dataset for all subsequent analyses. The morphospace scatterplot of PC1 versus PC2 provides further evidence that interobserver error has been considerably reduced following the standardisation of the digitising protocol, as specimens are not clearly separated (Fig. 3.4B). The aspects of morphology represented by PC1 and PC2 are equivalent to those found by the original analysis (Wilberg, 2017). PC1 (71.89% of the variation) still describes variation in snout length, but it also expresses changes in the caudolateral region of the skull, maybe reflecting the addition of many metriorhynchoid thalattosuchians (twice as many as in the original dataset) and some gavialoids (such as *Piscogavialis jugaliperforatus* and *Ikanogavialis gameroi*). PC2 (8.6% of the variation) mostly describes changes in the quadrate condyle and the position of the orbit in relation to the lateral outline of the skull. All other principal components summed up represent less than 16% of total shape variation, none of which represents more than 4% (Fig. 3.5).

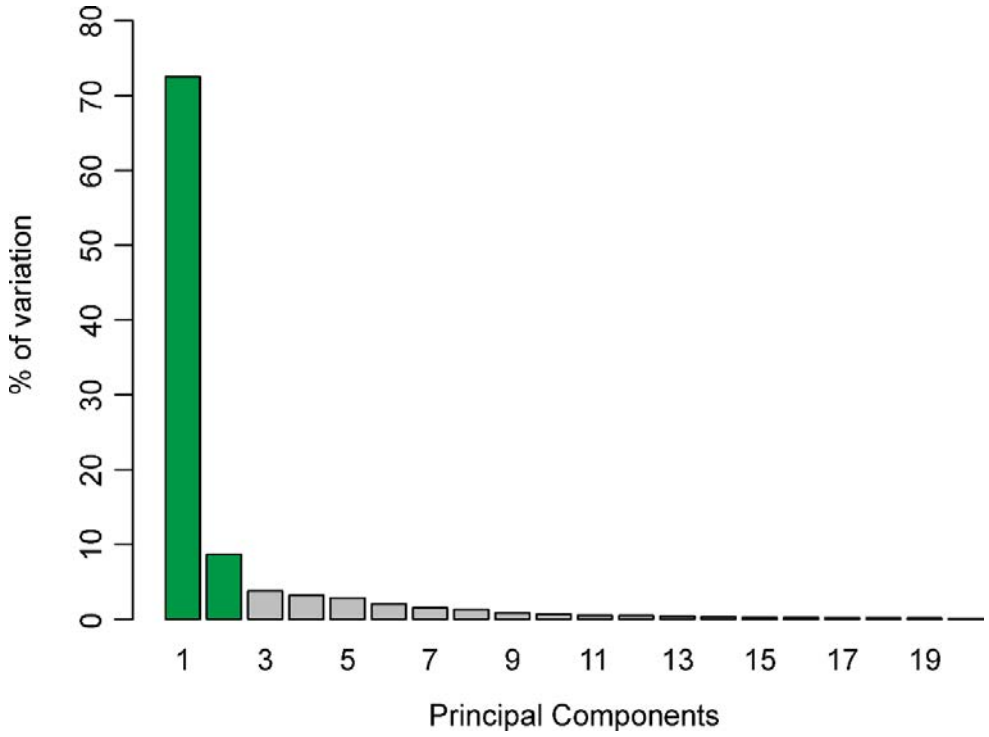

Figure 3.5. Percentage of the cranial shape variation expressed by each of the first 20 principal components, using the modified version of the expanded dataset (after the standardisation of the landmark digitising protocol). Shown in green are the principal components (PC1 and PC2) used for morphospace scatterplots in this Chapter.

Table 3.2. Procrustes ANOVA results investigating the amount of variation in shape data caused by interobserver error after the standardisation of the landmark digitising protocol. **SS,** sum of squares after 10,000 permutations; **MS,** mean squares; **% of variation,** obtained by dividing the sum of squares of the independent variable (groups) by the total sum of squares; **F,** F-statistic; **p,** p-value. * Significant at alpha = 0.05.

Total shape variation (all PCs)

Effect	SS	MS	% of variation	F	p
Interobserver error	0.0870	0.086985	1.606624	3.38	0.038*
Residuals	5.3272	0.025735			
Total	5.4142				

The region around the negative end of the PC1 axis (left side of the plot; Fig. 3.6) shows a concentration of longirostrine species, most of which are gavialoids (such as *Piscogavialis jugaliperforatus* and *Ikanogavialis gameroi*), thalattosuchians (such as *Pelagosaurus typus*, *Steneosaurus bollensis*, and *Teleosaurus cadomensis*), and tethysuchians (such as the "pholidosaurid" *Terminonaris browni* and the dyrosaurid *Rhabdognathus keiniensis*). However, some representatives of other groups are also present in this region, such as the notosuchian *Stolokrosuchus lapparenti* and the crocodyloid *Euthecodon brumpti*. The positive extremity of PC1 (Fig. 3.6) is dominated by forms with very short rostra, such as the notosuchians *Notosuchus terrestris* and *Comahuesuchus brachybuccalis*, the non-crocodylian neosuchians *Iharkutosuchus makadii* and *Acynodon adriaticus*, as well as the non-mesoeucrocodylian crocodyliform *Gobiosuchus kielanae*. The distribution along the PC2 axis is not as extreme as for PC1, but, in general, taxa at the positive end of the axis (at the top of the plot; Fig. 3.6) have broader snouts and wider quadrate condyles. This region is occupied by the caimanine alligatoroid *Purussaurus brasiliensis*, as well as some notosuchians (such as *Lorosuchus nodosus* and *Armadillosuchus arrudai*). Notosuchians (such as C*andidodon itapecuruense*) are also observed in the region of negative PC2 scores (at the bottom of the plot; Fig. 3.6), in addition to many thalattosuchians (such as *Cricosaurus lithographicus*, *Maledictosuchus riclaensis* and *Rhacheosaurus gracilis*).

Comparisons of the morphospace occupied by different crocodylomorph subgroups (Fig. 3.7) reveals a wide distribution of crocodylians and notosuchians. Crocodylian species (Fig. 3.7A) exhibit almost the entire range of morphological variation described by PC1 (i.e., long versus short snouts), whereas most notosuchians (Fig. 3.7B) occupy the region of short rostra (although the presence of *Stolokrosuchus lapparenti* in the analysis expands the morphospace occupation of the group towards the "longirostrine region"). Pairwise statistical

assessment using npMANOVA (Table 3.3) reinforces the apparently disparate cranial morphology of these two groups, as it shows that their morphospaces are significantly different to one another, and also from most of the groups tested.

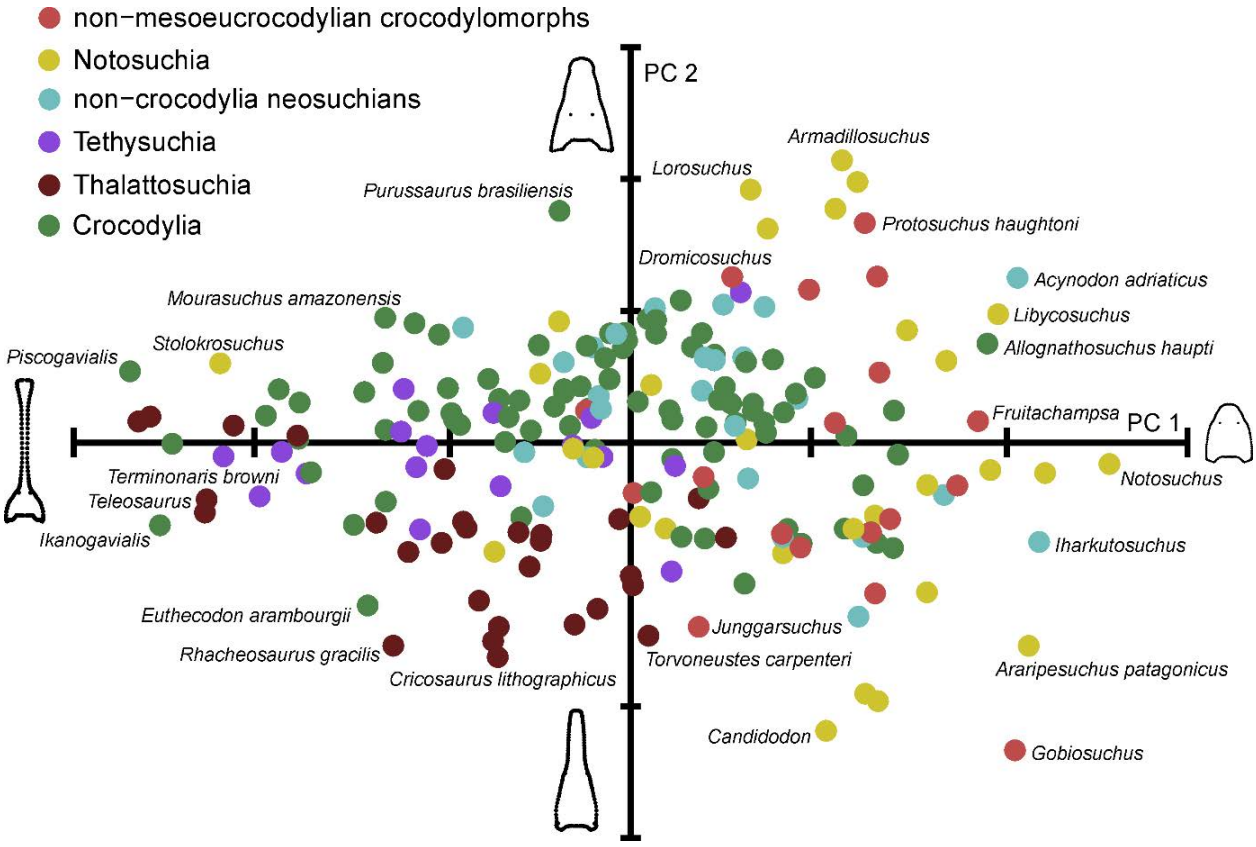

Figure 3.6. Morphospace plot (PC1 versus PC2) of crocodylomorph cranial shape variation, using the expanded dataset, after removing the effect of interobserver error (by standardising the landmark digitising protocol). Different colours represent distinct crocodylomorph subgroups: non-mesoeucrocodylian crocodylomorphs (excluding thalattosuchians), Notosuchia, non-crocodylian neosuchians (excluding tethysuchians and thalattosuchians), Tethysuchia, Thalattosuchia, and Crocodylia.

The morphospaces of thalattosuchians and tethysuchians (Fig. 3.7C, and D) are more restricted to the "longirostrine region" of the scatterplot, and the npMANOVA tests further indicate that their morphospaces do not differ significantly from each other (Table 3.3). The

npMANOVA results also show that the morphospace of non-mesoeucrocodylian crocodylomorphs is not significantly distinct from that of notosuchians, although they exhibit an apparently less disparate morphospace occupation, with nearly all species confined to the region of shorter snouts (Fig. 3.7E). Lastly, even though the morphospace of non-neosuchian crocodylians is, in general, more restricted than that of crocodylians and they do not differ significantly (Fig. 3.7F; Table 3.3), some species explore regions of the morphospace not occupied by members of the crown-group (e.g., those of extremely short snouts, such as *Acynodon* and *Iharkutosuchus*).

Table 3.3. npMANOVA results illustrating differences in the morphospace occupied by distinct crocodylomorph subgroups in a pairwise comparison. *Bonferroni-corrected p-values significant at alpha = 0.05.

Pairwise comparison	**p-values**
Crocodylia – Notosuchia	0.0015*
Crocodylia – Thalattosuchia	0.0015*
Crocodylia – Tethysuchia	0.0585
Crocodylia – Non-crocodylian neosuchians	0.0615
Crocodylia – Non-mesoeucrocodylian crocodylomorphs	0.0015*
Notosuchia – Thalattosuchia	0.0015*
Notosuchia – Tethysuchia	0.0015*
Notosuchia – Non-crocodylian neosuchians	1
Notosuchia – Non-mesoeucrocodylian crocodylomorphs	1
Thalattosuchia – Tethysuchia	1
Thalattosuchia – Non-crocodylian neosuchians	0.0015*
Thalattosuchia – Non-mesoeucrocodylian crocodylomorphs	0.0015*
Tethysuchians – Non-crocodylian neosuchians	0.0015*
Tethysuchians – Non-mesoeucrocodylian crocodylomorphs	0.0015*
Non-neosuchians crocodylians – Non-mesoeucrocodylian crocodylomorphs	0.081

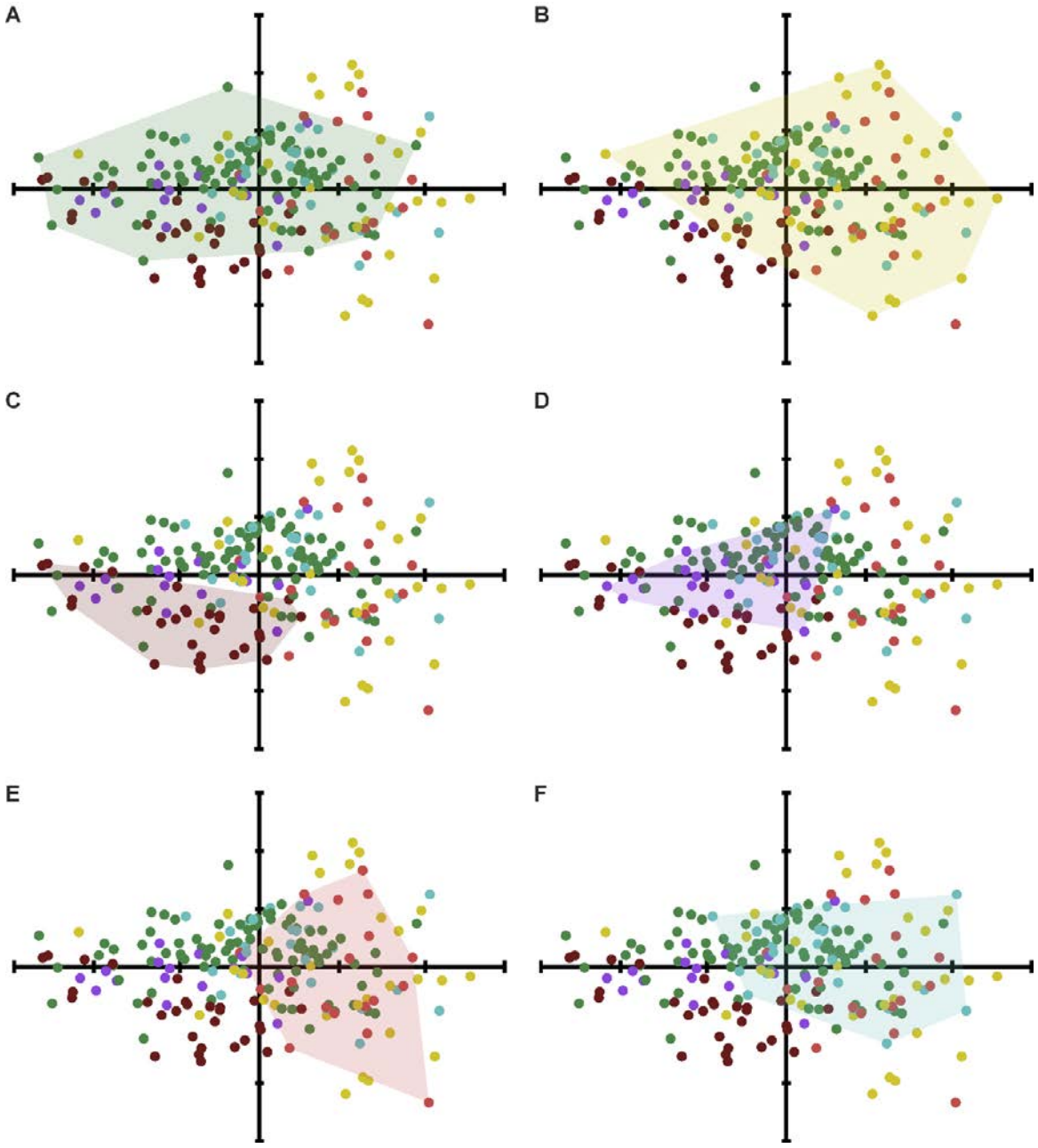

Fig. 3.7. Comparative morphospace occupation (PC1 versus PC2) of different crocodylomorph subgroups using convex hulls (colour-coded as in Fig. 3.6). **A,** Crocodylia (n = 89). **B,** Notosuchia (n = 30). **C,** Thalattosuchia (n = 29). **D,** Tethysuchia (n = 18). **E,** Non-mesoeucrocodylian crocodylomorphs (without thalattosuchians; n = 18). **F,** Non-crocodylian neosuchians (without tethysuchians and thalattosuchians; n = 25).

Even though some crocodylomorph subgroups exhibit morphospaces that are significantly distinct from other groups, no clear signal is recovered when phylogenetic

information is incorporated into tangent space, producing a phylomorphospace plot of PC1 against PC2 (Fig. 3.8). The results were similar across all phylogenetic hypotheses available (i.e., 10 trees for each phylogenetic scenario, with different positions of Thalattosuchia). Indeed, using any of these trees, the phylogenetic signal estimated for the shape data was relatively weak, although significant (K_{mult} values between 0.152 and 0.201, p-values = 0.001), which is consistent with the multiple intersections of branches seen in the phylomorphospace.

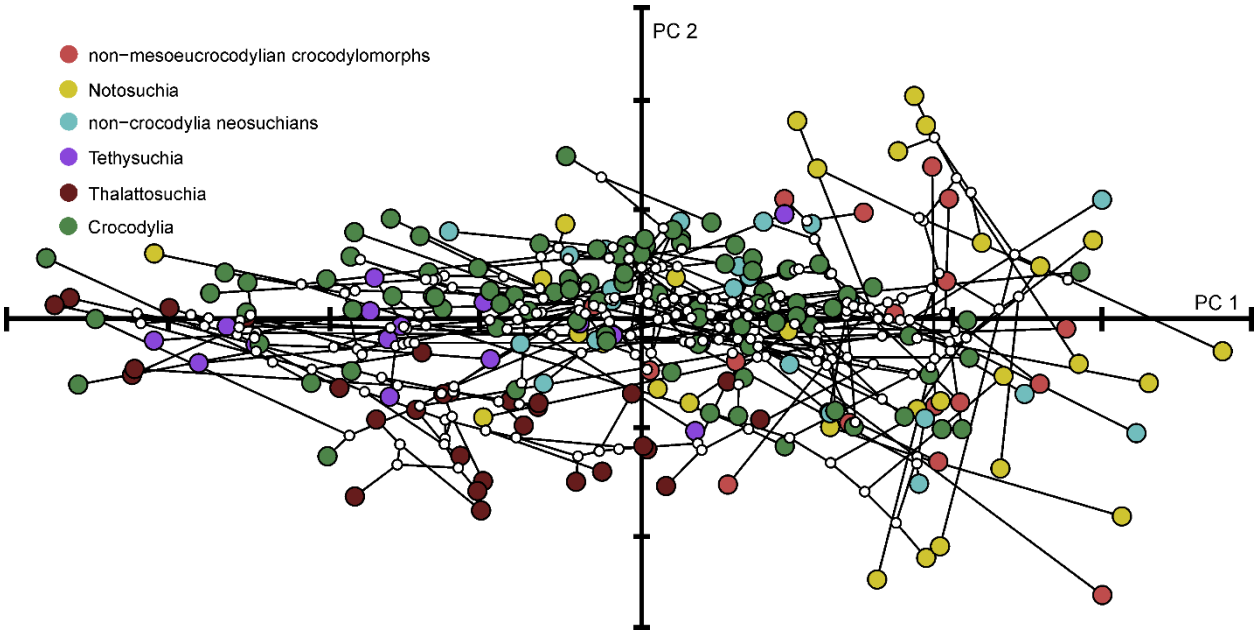

Figure 3.8. Phylomorphospace (i.e., phylogenetic relationships plotted on to PC scores of specimens) of crocodylomorph cranial shape variation (PC1 versus PC2). Circles of different colours represent distinct crocodylomorph subgroups: non-mesoeucrocodylian crocodylomorphs, Notosuchia, non-crocodylian neosuchians, Tethysuchia, Thalattosuchia, and Crocodylia. White circles represent ancestor states (Procrustes coordinates), which were reconstructed using maximum likelihood. Phylogenetic hypothesis from tree number 1, with Thalattosuchia within Neosuchia, but different trees produce very similar results.

I further assessed the morphospace occupation of crocodylomorphs divided into three distinct ecological categories (i.e., aquatic/marine, semi-aquatic/freshwater and terrestrial).

Although most terrestrial taxa are restricted to the region of the morphospace that represents short-snouted skulls (positive end of the PC1 axis in Fig. 3.9), they also range along the entire PC2 axis. Conversely, aquatic crocodylomorphs are more confined to the negative end of the PC1 axis (Fig. 3.9) and are represented by some of the most extreme longirostrine forms (such as *Ikanogavialis gameroi*). Semi-aquatic species are more widespread along the PC1 axis (Fig. 3.9), although their distribution along the PC2 axis seems to be similar to that observed for aquatic forms. These differences between the distinct ecologies are reflected in the npMANOVA results, which indicate that all three categories have significantly different morphospace occupation (p-values < 0.001).

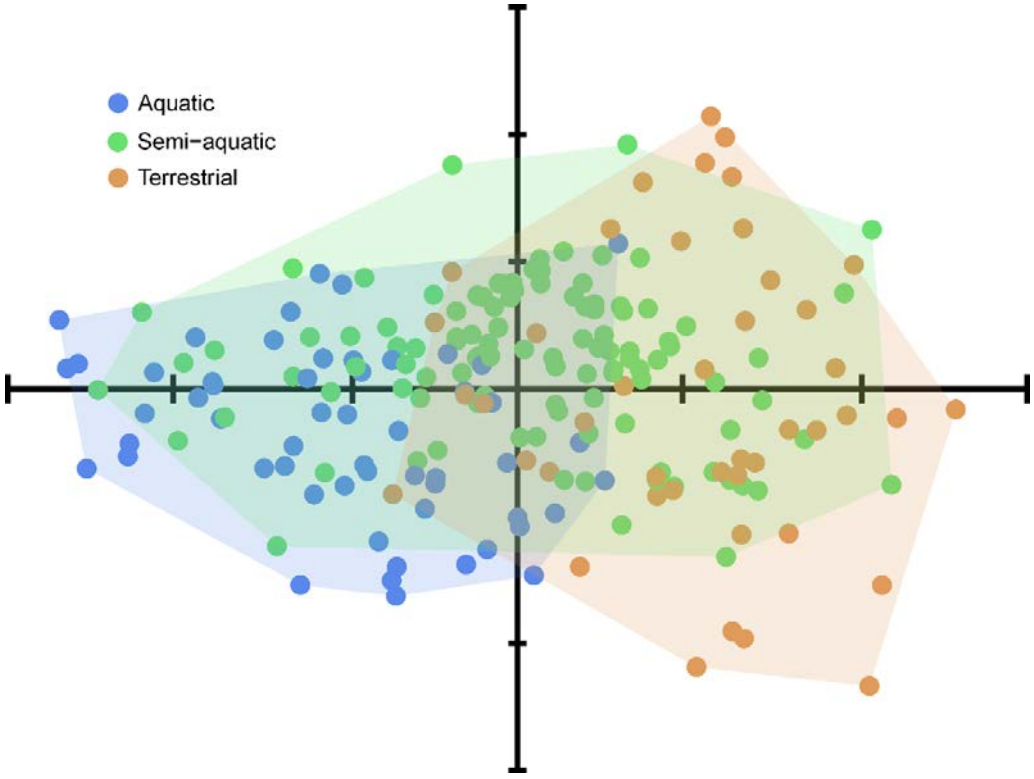

Figure 3.9. Morphospace occupation of crocodylomorphs divided into three ecological categories: aquatic/marine (n = 56), semi-aquatic/freshwater (n = 109) and terrestrial (n = 44).

3.3.2. Disparity through time and between groups

Distinct tree topologies, as well as different time sub-sampling methods, had significant impacts on the disparity-through-time analyses (see Appendix D for plots of all disparity-through-time analyses). For each alternative phylogenetic scenario (i.e., changing the position of Thalattosuchia), 10 distinct randomly resolved trees were time-scaled, generating different branch lengths in each tree. Furthermore, as these trees were used for estimating the ancestral states (i.e., landmark coordinates of hypothetical ancestors), they presumably produce distinct PC scores for ancestors. Comparisons of trees sharing the same position of Thalattosuchia show some dissimilarities in the pattern of disparity through time, and these differences are more marked when a greater number of time intervals are used (using either the time binning or the time-slicing methods). Using trees with Thalattosuchia as the sister group of Crocodyliformes as an example (Fig. 3.10), analyses using distinct randomly resolved and time-scaled trees disagree on the timing and magnitude of a disparity peak during the early evolution of the group. Whereas some trees show this peak beginning prior to the Triassic-Jurassic (T–J) boundary, other trees yield a later start, only after the boundary. Other differences include whether there is an increase or a decrease in disparity from the middle of the Neogene (Eocene) to the Recent, as well as if a peak observed during the Early Cretaceous corresponds to the highest disparity seen in the group's entire evolutionary history (Fig. 3.10). The use of alternative phylogenetic positions of Thalattosuchia did not cause significant changes to the patterns of disparity after the Late Jurassic, having instead the greatest impact on disparity estimation during the Jurassic, since this corresponds to the age range of thalattosuchians.

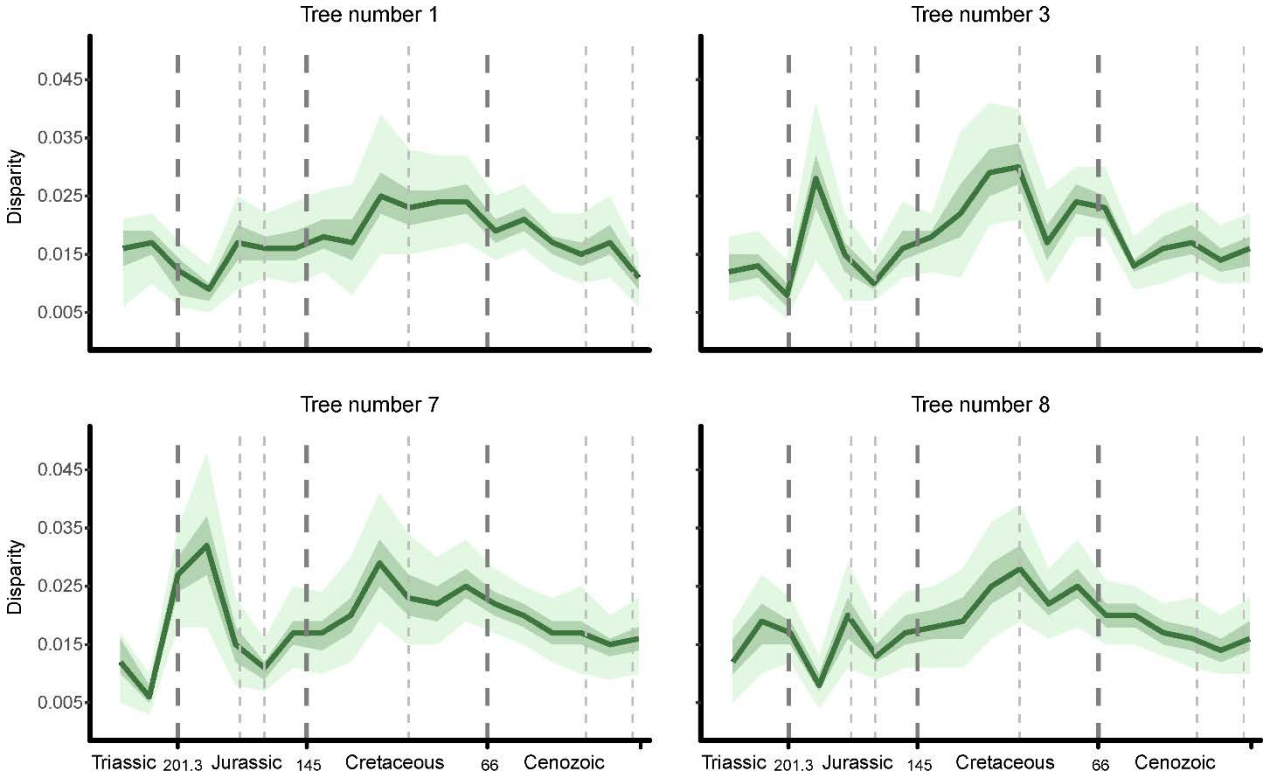

Figure 3.10. Comparison between different randomly resolved and time-scaled trees used for disparity-through-time analyses. All trees share the same phylogenetic position of thalattosuchians (as sister to Crocodyliformes) and the analyses used the same time sub-sampling method (time binning method, with 20 equal-length time bins). The sum of variance is used as the disparity metric. Light and dark green shades represent, respectively, 75% and 97.5% confidence intervals from 1,000 bootstrapping replicates.

In general, disparity-through-time analyses using more time intervals (either time bins or time slices) reconstruct more nuanced changes in disparity, even though they also often have larger confidence intervals (Fig. 3.11). When comparing different time sub-sampling methods, similar differences are observed to those seen when different tree topologies are compared (i.e., variation in the timing and magnitude of disparity peaks). For example, analyses using the time-slicing method more frequently detected an increase in disparity during the Palaeogene (Eocene) than those using the time-binning method. Similarly, the magnitude estimated for the peak seen at the end of the Early Cretaceous (i.e., Aptian–Albian)

was usually greater when using the time-slicing method. Furthermore, comparing analyses using only the time-slicing method, but with different numbers of time slices, analyses with 10 time slices more often failed to detect an early disparity peak (during the Early Jurassic) than those using 20 time slices. By contrast, almost identical results were found when different evolutionary models (i.e., punctuated or gradual model) were assumed for analyses using the time-slicing method (Fig. 3.11).

Despite these dissimilarities arising from different time-scaled trees and time sub-sampling methods, most analyses seem to agree on some overall patterns of crocodylomorph cranial shape disparity through time (Figs. 3.10, 3.11 and Appendix D). An early peak in disparity is frequently observed, most often during the Early Jurassic (although sometimes even prior to the Triassic-Jurassic boundary). Following a sharp decrease during the Middle Jurassic, disparity undergoes a continuous increase until the middle of the Cretaceous (Aptian–Albian), when maximum disparity is reached in most analyses. Subsequently, a near constant decline is observed during the Late Cretaceous and the Palaeocene, with analyses only disagreeing whether it continues until the Recent or ceases during the Eocene. In these latter cases (more frequently seen in analyses using the time-slicing method), the sharp increase in disparity seen in the Eocene is sometimes maintained until the Recent.

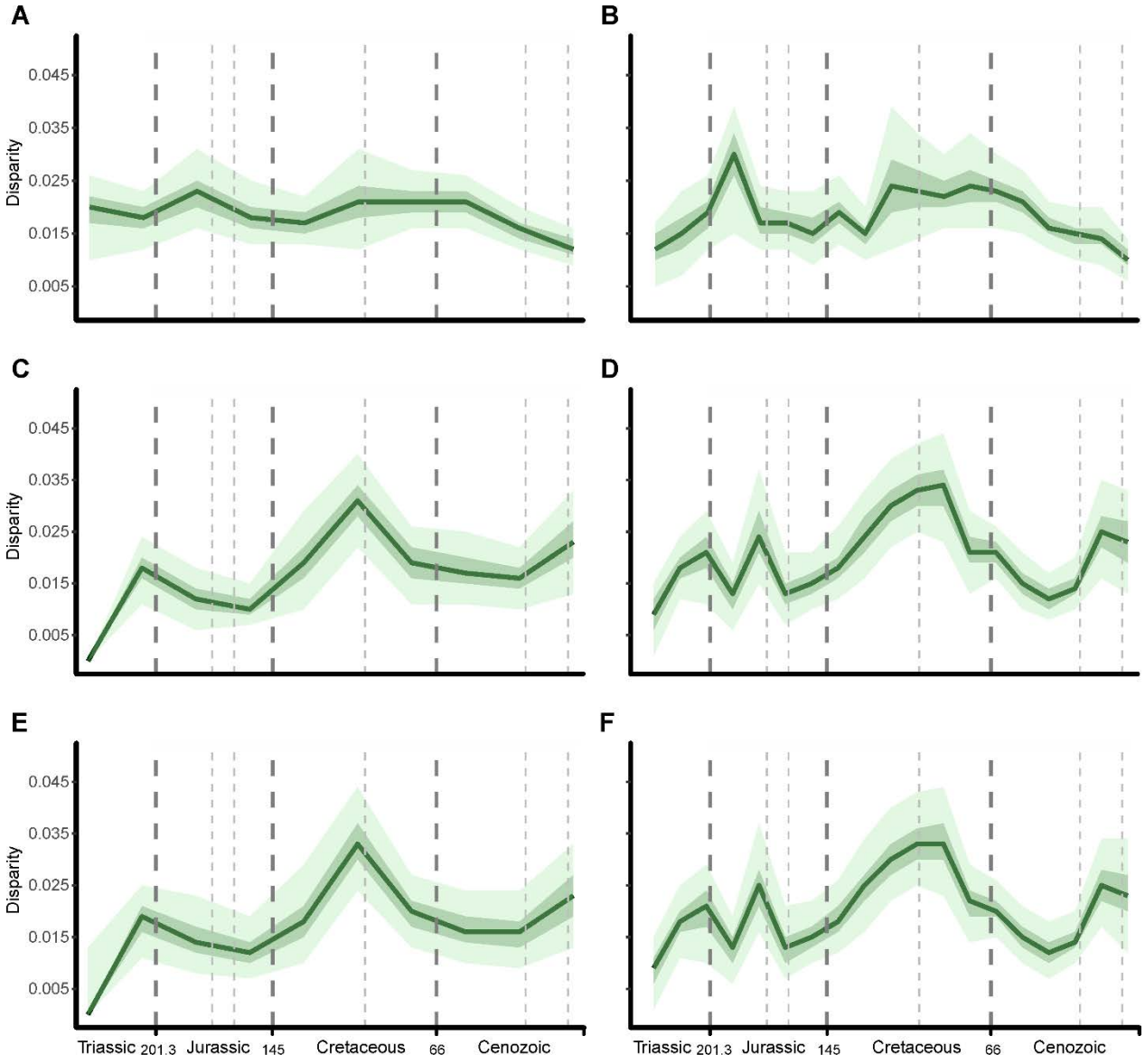

Figure 3.11. Comparison between different time sub-sampling methods used for calculating crocodylomorph disparity through time. All analyses used the same time-scaled tree (tree number 4 with Thalattosuchia within Neosuchia). **A,** Time binning method, with 10 equal-length time bins. **B,** Time binning method, with 20 equal-length time bins. **C,** Time-slicing method, with 10 time slices, assuming punctuated evolution. **D,** Time-slicing method, with 20 time slices, assuming punctuated evolution. **E,** Time-slicing method, with 10 time slices, assuming gradual evolution. **F,** Time-slicing method, with 20 time slices, assuming gradual evolution. The sum of variance is used as the disparity metric. Light and dark green shades represent, respectively, 75% and 97.5% confidence intervals from 1,000 bootstrapping replicates.

Subsequently, I examined cranial shape disparity among different crocodylomorph subgroups. Analyses with six subsets (i.e., Crocodylia, Notosuchia, Thalattosuchia, Tethysuchia, non-crocodylian neosuchians, and non-mesoeucrocodylian crocodylomorphs) revealed that Notosuchia has the highest cranial shape disparity among all groups assessed (Fig. 3.12A). Crocodylia exhibits a smaller disparity, although slightly higher than the other four groups (Tethysuchia, Thalattosuchia, non-crocodylian neosuchians, and non-mesoeucrocodylian crocodylomorphs), which have comparable median values. Pairwise comparisons (Table 3.4) show that disparity in both Notosuchia and Crocodylia is significantly different from that in all other groups analysed, whereas some other groups have statistically equivalent disparities (e.g., thalattosuchians and non-mesoeucrocodylian crocodylomorphs, as well as tethysuchians and non-crocodylian eusuchians). The same results were recovered when fewer subsets of taxa were analysed (i.e., Notosuchia, Thalattosuchia, non-mesoeucrocodylian crocodylomorphs, and Neosuchia), with notosuchian disparity still higher and significantly different from the other groups (Fig. 3.12B; Table 3.5). Finally, I assessed the differences in disparity between the three ecological categories (i.e., aquatic/marine, semi-aquatic/freshwater and terrestrial). Whereas aquatic and semi-aquatic species exhibit similar median disparity (Fig. 3.13), which is supported by the npMANOVA results (Table 3.6), terrestrial crocodylomorphs show significantly higher disparity than the other two categories (Fig. 3.13; Table 3.6).

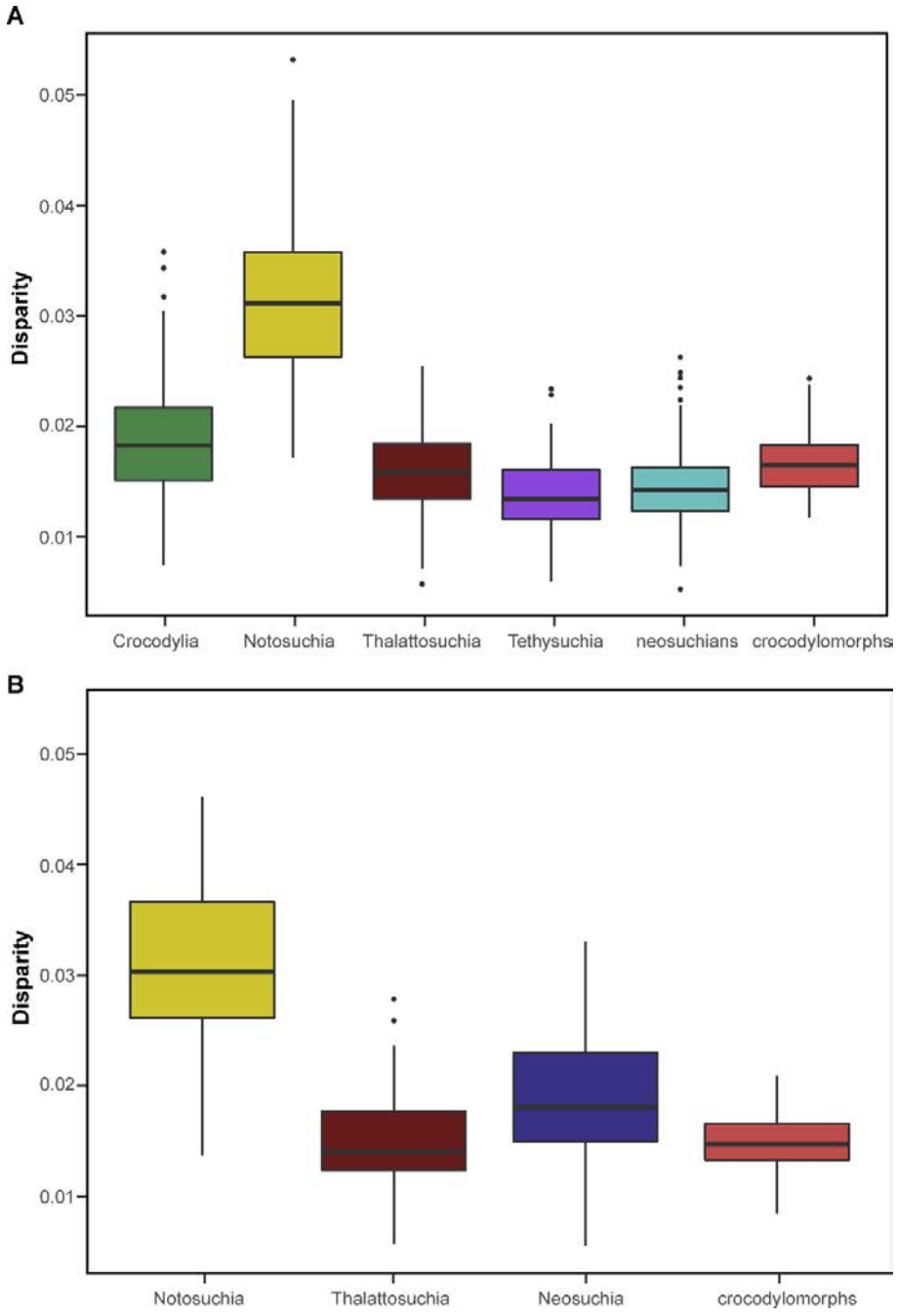

Figure 3.12. Cranial shape disparity (sum of variances) among different crocodylomorph subgroups. **A,** Species divided into six taxonomic subsets ("neosuchians" represent crocodylian neosuchians, without thalattosuchians and tethysuchians; "crocodylomorphs" represent non-mesoeucrocodylian crocodylomorphs, without thalattosuchians). **B,** Species divided into four taxonomic subsets ("Neosuchia" also includes crocodylians and tethysuchians). PC scores of specimens were bootstrapped and rarefied for disparity calculation.

Table 3.4. npMANOVA results for pairwise comparisons of cranial shape disparity (sum of variances) in different crocodylomorph subgroups (divided into six subsets). *Bonferroni-corrected p-values significant at alpha = 0.05.

Pairwise comparison	**p-values**
Crocodylia – Notosuchia	0.0015*
Crocodylia – Thalattosuchia	0.0015*
Crocodylia – Tethysuchia	0.0015*
Crocodylia – Non-crocodylian neosuchians	0.0015*
Crocodylia – Non-mesoeucrocodylian crocodylomorphs	0.0090*
Notosuchia – Thalattosuchia	0.0015*
Notosuchia – Tethysuchia	0.0015*
Notosuchia – Non-crocodylian neosuchians	0.0015*
Notosuchia – Non-mesoeucrocodylian crocodylomorphs	0.0015*
Thalattosuchia – Tethysuchia	0.0090*
Thalattosuchia – Non-crocodylian neosuchians	0.7919
Thalattosuchia – Non-mesoeucrocodylian crocodylomorphs	0.6884
Tethysuchians – Non-crocodylian neosuchians	1
Tethysuchians – Non-mesoeucrocodylian crocodylomorphs	0.0015*
Non-neosuchians crocodylians – Non-mesoeucrocodylian crocodylomorphs	0.0015*

Table 3.5. npMANOVA results for pairwise comparisons of cranial shape disparity (sum of variances) in different crocodylomorph subgroups (divided into four subsets). *Bonferroni-corrected p-values significant at alpha = 0.05.

Pairwise comparison	**p-values**
Notosuchia – Neosuchia	0.0006*
Notosuchia – Thalattosuchia	0.0006*
Notosuchia – Non-mesoeucrocodylian crocodylomorphs	0.0006*
Neosuchia – Thalattosuchia	0.0006*
Neosuchia – Non-mesoeucrocodylian crocodylomorphs	0.0006*
Thalattosuchia – Non-mesoeucrocodylian crocodylomorphs	1

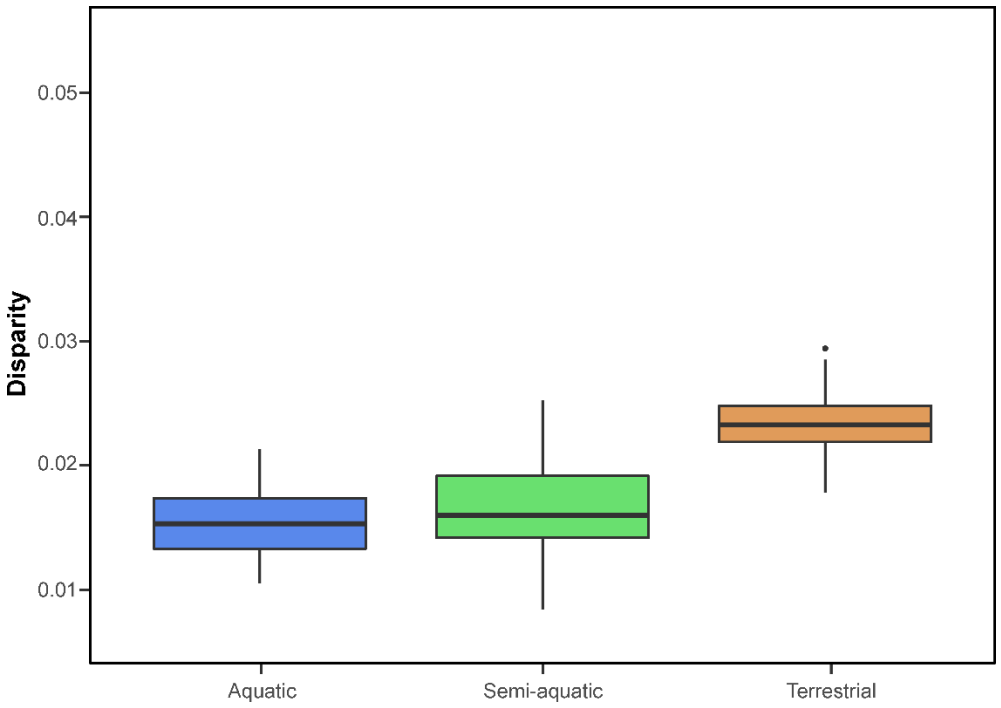

Figure 3.13. Cranial shape disparity (sum of variances) with crocodylomorphs subdivided into three different lifestyle categories: marine/aquatic (n = 56), freshwater/semi-aquatic (n = 109), and terrestrial (n = 44) species. PC scores of specimens were bootstrapped and rarefied for disparity calculation.

Table 3.6. npMANOVA results (pairwise comparisons) of cranial shape disparity (sum of variances) of crocodylomorphs assessed in different lifestyle categories. *Bonferroni-corrected p-values (q-values) significant at alpha = 0.05.

Pairwise comparison	**q-values**
Aquatic – Semi-aquatic	0.096
Aquatic – Terrestrial	0.0003*
Semi-aquatic – Terrestrial	0.0003*

3.4. Discussion

3.4.1. Assessing the different methods to minimise the effects of interobserver error

Among the two methods applied for diminishing the effects of interobserver error, only the standardisation of the landmark digitising protocol proved itself useful in the context of this Chapter. Although other studies previously successfully applied Burnaby's (1966) projection method, most of these were able to create a model to more appropriately represent the extraneous variable, which can be either a size-factor or undesirable morphological features (e.g., Gharaibeh 2005; Valentin *et al*. 2008). For example, Valentin *et al*. (2008) presented a protocol for removing the effects of upward and downward arching in the body of fish due to preservation. For that approach, the authors digitised landmarks from 10 arched specimens (photographed 20 times each) to create a deformation model that represented the arching effect. The landmark data of this model was then subjected to GPA and RWA (equivalent to PCA), and the first eigenvector (i.e., principal component), representing 97.3% of total variation, accurately described the arching effect. Subsequently, Burnaby's (1966) projection method was applied, by projecting the original landmark data to a subspace orthogonal to the first eigenvector of the deformation model. This procedure was further applied in other studies (e.g.; Fruciano *et al*. 2011; 2012; Franchini *et al*. 2014; Ingram 2015; Fruciano *et al*. 2016), for which it also provided satisfactory results.

For the analyses in this Chapter, however, the extraneous variable (i.e., interobserver error) could not be modelled. Thus, the second principal component (PC2) was used as a proxy, since among all PCs, PC2 described the largest amount of interobserver error (~30% of the variation described by this eigenvector). Nevertheless, after applying Burnaby's projection method, other components of morphological variation described by PC2 were also removed, generating in unrealistic result (which could be assessed after performing GPA and PCA; Fig.

3.4A). Similar issues were reported by Berner (2011), which used simulated data to assess the effectiveness of size-correction methods based on principal components, a widely applied approach (Klingenberg 2016). This approach assumes that, in datasets with a substantial amount of variation correlated with size, PC1 should mostly reflect size variation, and could hypothetically be used as a proxy vector for Burnaby's projection method. Nevertheless, Berner (2011) demonstrated that this method produced systematic statistical artefacts, especially when all traits in the dataset were strongly correlated with size, making it inappropriate for size correction. Likewise, similar artefacts are expected in the context of the present Chapter, since the interobserver error is very likely correlated with all aspects of morphological variation (described by the principal components).

By contrast, the second approach used (i.e., looking for differences in the landmark digitising protocol) sensibly reduced the effects of interobserver error (from 7.35% to 1.6% of total shape variation; Tables 3.1 and 3.2). After performing GPA and PCA, it was possible to confirm that the aspects of morphology described by the principal components were realistic and compatible with the variation seen in the actual specimens (Fig. 3.4B). These results demonstrate, in practice, the importance of well-described, standardised digitisation protocols. Similarly, Fruciano *et al.* (2017) suggested that, if more than one observer/operator is required during the digitisation of landmarks, the exclusion of landmarks that are potentially difficult to digitise can robustly reduce interobserver error. Thus, if we are to more frequently use landmark data from different sources in geometric morphometric studies, by either combining published datasets with newly digitised specimens or using more than one operator during the digitisation process, approaches towards best practice should include clearer, simpler and well-described digitisation protocols.

3.4.2. Crocodylomorph cranial shape variation

The geometric morphometric analyses showed that most of the shape variation in crocodylomorph skulls represents changes in the snout, particularly in its length and width (Figs. 3.5 and 3.6). This is consistent with what was found in previous geometric morphometric studies (e.g., Pierce *et al*. 2008; Sadleir and Makovicky 2008; Pierce *et al*. 2009*a*; Piras *et al*. 2009; Young *et al*. 2010; Foth *et al*. 2017*a*; Wilberg 2017; Chapter 4), indicating that this region of the skull has the highest morphological variation. High variability in crocodylomorph snout length has long been acknowledged (Langston 1973; Busbey 1995; Brochu 2001), even leading early taxonomists (e.g., Lydekker 1888) to erroneously classify crocodylomorphs into different groups (Pierce *et al*. 2008). More recently, however, the high plasticity of crocodylomorph snouts has been more frequently recognised, resulting from the strong ecological selective pressures on this region of the skull, such as those arising from feeding behaviour (see McCurry *et al*. [2017*a*] for an exceptional example of convergent evolution in snouts of crocodylians and odontocete cetaceans). Consequently, cladistic studies (e.g., Clark 1994; Jouve *et al*. 2006; Pol and Gasparini 2009; Wilberg 2015) have suggested that convergences in crocodylomorph snouts during their evolutionary history have created the "longirostrine problem", in which clades that are not necessarily closely related tend to be grouped together in phylogenetic analyses. Even though the variation seen within snout lengths may differ between different crocodylomorph groups (for example, in Notosuchia snout length variation seems to represent a less substantial amount of total skull shape variation; Chapter 4), this seems to be a key feature during the group's evolutionary history.

Snout length can provide useful insights into ecological specializations (Taylor 1987; Busbey 1995; Brochu 2001; McHenry *et al*. 2006; Pierce *et al*. 2008; Walmsley *et al*. 2013).

For example, longer snouts are traditionally associated with a piscivorous diet, since the tip of the snout moves faster through water, facilitating the capture of small prey such as fish (Thorbjarnarson 1990; McHenry *et al*. 2006; Walmsley *et al*. 2013; McCurry *et al*. 2017*b*). Similarly, snout width also has important biomechanical implications, such as impacting on hydrodynamic pressure drag (e.g., longirostrine animals compensate the higher pressure from dragging with narrower snouts; McHenry *et al*. 2006; Walmsley *et al*. 2013). Unfortunately, the two-dimensional nature of the geometric morphometric data used in the present study, using skulls only in dorsal view, prevents the assessment of crocodylomorph snout height, which represents a relevant aspect of rostral morphology and has important biomechanical implications (Taylor 1987; Busbey 1995; McHenry *et al*. 2006).

Other regions of the crocodylomorph skull also vary significantly according to the aspects of morphology described by the principal components. Changes in the quadrate condyle width and in the caudolateral region of the skull are described by both PC1 and PC2 (Fig. 3.6). As for the variation seen in among crocodylomorph snouts, modifications in the quadrate condyle, presumably associated with the craniomandibular joint, also have important implications for biomechanics and feeding strategies (Kley *et al*. 2010; Stubbs *et al*. 2013; Ősi 2014).

Some crocodylomorph subgroups occupy regions of the morphospace that are significantly distinct from other groups (Fig. 3.7; Table 3.3), which might indicate that clade-specific innovations led to the exploration of new cranial morphologies. However, the relatively weak phylogenetic signal estimated, independently of the phylogenetic hypothesis used, is consistent with the multiple intersections of branches seen in the phylomorphospace (Fig. 3.8). Indeed, it seems clear that whereas some clades, such as Thalattosuchia, are more confined to a given region of the morphospace, others are more widespread, including

Neosuchia, Crocodylia and Notosuchia. Previous work also found only weak to moderate correlations between phylogeny and morphospace occupation in some crocodylomorph subgroups (such as crocodylians and thalattosuchians; Pierce *et al*. 2008; 2009*a*, *b*), indicating the highly convergent nature of crocodylomorph cranial shape evolution. However, if Thalattosuchia are considered to be within Neosuchia, non-mesoeucrocodylian crocodylomorphs are almost entirely restricted to the brevirostrine region of morphospace. If this "longirostrine region" represents a new adaptive zone (*sensu* Simpson 1953; Hansen 2012), this could be reflecting an episode of adaptive zone invasion (i.e., evolution into a region of the morphospace never explored by non-mesoeucrocodylian crocodylomorphs). If real, the timing of this evolutionary innovation (i.e., mesoeucrocodylians exploring a new region of the morphospace) would be consistent with the shifts in diversity and body size identified at the base of Mesoeucrocodylia (Bronzati *et al*. 2015; Chapter 2).

3.4.3. Crocodylomorph cranial shape disparity

Disparity-through-time results were highly sensitive to changes in the time sub-sampling method and in the phylogenetic hypothesis used (Figs. 3.10 and 3.11). The considerable variation seen in these results has multiple causes. First, distinct time-scaled trees vary in assuming different stratigraphic dates for the occurrences of individual taxa (reflecting the uncertainties in the stratigraphic occurrences of most taxa used in these analyses, with many taxa known from point occurrences but with stratigraphic uncertainty often spanning two or more stages), as well as in different resolutions for polytomies (which were randomly resolved in each tree). For similar reasons, although not tested here, it is very likely that alternative time-scaling methods (e.g., *cal3* and the *extended Hedman* methods; Bapst 2013; Lloyd *et al*. 2016) would also impact on disparity-through-time estimation (see "Material and

Methods" section of Chapter 2, as well as Bapst [2013; 2014*b*] for further discussion). Furthermore, the use of distinct phylogenetic hypotheses, in this case the variable position of Thalattosuchia, results in different ancestral state estimations. Similarly, distinct approaches to estimating ancestral states could also potentially impact on the results (see Ekman *et al*. 2008; Slater *et al*. 2012). Finally, the use of distinct time sub-sampling methods, as well as different numbers of time intervals (either time bins or time slices), results in different taxa being sampled in each time interval, since the rates of sedimentation (and fossilisation) are uneven in space and time (Butler *et al*. 2012; Guillerme and Cooper 2018).

These results shed light on the importance of using multiple time sub-sampling methods and trees for these analyses (as previously highlighted by Guillerme and Cooper 2018), but also multiple phylogenetic hypotheses (for groups with major uncertainties in stratigraphic occurrence dates and phylogenetic relationships). However, many previous studies have ignored this issue, often presenting results based on one time-scaled phylogeny and one time binning approach (e.g., Brusatte *et al*. 2008*a*, *b*; Stubbs *et al*. 2013; Foth and Joyce 2016). Accordingly, rather than using a single analysis, a better way to report the results might be by describing shared patterns among the outputs, as I have done here.

The overall disparity patterns seen in most disparity-through-time analyses resemble those found by Wilberg (2017), in that a clear peak is observed in the Cretaceous, followed by a nearly continuous decline towards the Recent. Some differences, however, are also noted. Since Wilberg (2017) used different disparity metrics in his analyses, my comparisons between my results and his focus on the results of variance-based disparities. The first discrepancy arises from the fact that Wilberg (2017) restricted his study to Crocodyliformes (with the exception of thalattosuchians) and did not include any Late Triassic species, resulting in an absence of information about crocodylomorph disparity prior to the Jurassic.

When using stratigraphic intervals as time bins for his disparity-through-time analyses (resulting in 36 time bins), Wilberg (2017) found two significant disparity peaks during the Jurassic (one in the Pliensbachian and another in the Aalenian–Bajocian), whereas in most of my analyses a single Jurassic peak was estimated, usually occurring from the Sinemurian to the Toarcian (Figs. 3.10 and 3.11). However, similarly to my results, Wilberg's analyses did not detect Jurassic peaks in disparity when using fewer, equal-length time bins (n = 9), at least not with comparable magnitude to the peak in the Cretaceous. The timing of the disparity peak in the Cretaceous is another divergence between the two studies, with the analyses performed by Wilberg (2017) indicating a Late Cretaceous peak (Cenomanian), whereas most of my analyses show a slightly earlier peak (Aptian–Albian). Finally, another difference was found in the pattern of disparity from the Eocene to the Recent. Whereas many of my analyses (particularly when using the time-slicing method) indicate a disparity increase starting in the Eocene, this increase is not identified by the variance-based analyses in Wilberg (2017).

The discrepancies between these two studies can be explained by the increase in the sample size, by the differences in ages assigned to both terminal taxa and lineage divergences, and by methodological differences in time sub-sampling strategies and the consideration of divergent phylogenetic hypotheses. A similar argument may explain differences seen between my results and those presented by Stubbs *et al*. (2013). Stubbs *et al*. (2013) found that mandibular morphological disparity was greater during the Late Cretaceous. Besides using a different proxy for morphological disparity (mandibular shape instead of cranial), Stubbs *et al*. (2013) also sampled 23 non-crocodylomorphs (such as phytosaurs and aetosaurs), as they were interested in pseudosuchian disparity more broadly.

Regarding the disparity patterns that are common to most of my results, the early peak seen during the Jurassic is very likely associated with the origin and diversification of

thalattosuchians, as already pointed out by Wilberg (2017) and Stubbs *et al*. (2013). The subsequent sharp decline, which is detected prior to the Jurassic-Cretaceous boundary in many analyses, is probably related to the extinction of some thalattosuchians (mostly teleosaurids, as suggested by Stubbs *et al*. [2013]). However, it might further indicate that the Early Jurassic peak was also driven by the diversity of non-mesoeucrocodylian crocodylomorphs (such as protosuchids, *Dibothrosuchus*, *Litargosuchus* and *Sphenosuchus*), most of which disappear from the record after the Toarcian. Subsequently, the peak seen in the Cretaceous is presumably related to the diversification of notosuchians, as also noted by Wilberg (2017) and Stubbs *et al*. (2013). Indeed, comparisons of disparity between groups indicate that notosuchians have the highest disparity among the groups assessed (Fig. 3.12). However, other groups also contribute to this Cretaceous increase in disparity, such as the aquatic tethysuchian dyrosaurids.

The subsequent decrease in disparity seen from the Late Cretaceous to Eocene can be explained by the extinction of most notosuchians and dyrosaurids, as well as some non-crocodylian eusuchians. Finally, the peak in the Eocene, identified by some analyses, might reflect the thermal optimum during the epoch (Early Eocene Climatic Optimum; Zachos *et al*. 2008), as also suggested by Wilberg (2017). This event possibly contributed to an expansion of the geographic range of crocodylians, leading to an increase in diversity (Mannion *et al*. 2015). Some analyses using the time-slicing method show disparity subsequently either increasing until the Recent or at least sustained at similar levels to that in the Eocene. Conversely, most analyses using the time binning method did not detect this increase in disparity during the Eocene, suggesting caution is required in interpreting Eocene–Recent patterns.

3.4.4. Ecological diversity and crocodylomorph skull shape

The high variability of the crocodylomorph snout, which associated with ecological specializations (particularly the ones related to feeding; McHenry *et al*. 2006; Walmsley *et al*. 2013), combined with the weak phylogenetic signal found for cranial shape data, suggests that crocodylomorph cranial shape evolution is mostly driven by ecology. I further examined the effect of ecology on shape variation by subdividing the species into three ecological categories (aquatic/marine, semi-aquatic/freshwater and terrestrial), using habitat (i.e., the hypothesised environment in which these species lived in) as a proxy for ecological diversity. The npMANOVA results provide further support for this hypothesis, as they show that all three categories have significantly distinct morphospaces.

Closer inspection of the morphospace reveals that semi-aquatic/freshwater forms are more widespread along the PC1 axis in comparison to terrestrial and aquatic/marine crocodylomorphs (Fig. 3.9), suggesting a higher diversity of feeding strategies in semi-aquatic/freshwater species. However, when cranial shape disparity is quantified, terrestrial forms show higher disparity than both aquatic and semi-aquatic categories (Fig. 3.13). Disparity estimation includes the shape variation described by all principal components, not just that shown in the morphospace scatterplot of PC1 against PC2. Thus, although exhibiting less variability in terms of snout length, skulls of terrestrial species are more disparate in general.

This higher disparity in terrestrial taxa is possibly related to the cranial shape variation of notosuchians, which show greater disparity than any other crocodylomorph subgroup (Fig. 3.12). Notosuchians explored a wide range of cranial morphologies, some of which are unique within crocodylomorph evolutionary history (such as mammal-like adaptations and putative herbivory; Buckley *et al*. 2000; O'Connor *et al*. 2010; Ősi 2014). The remarkable species

diversity and morphological disparity of notosuchians have previously been recognised by other studies (e.g., Stubbs *et al*. 2013; Bronzati *et al*. 2015; Leardi and Pol 2015; Mannion *et al*. 2015; Wilberg; 2017), and could be explained by either extrinsic (e.g., specific environmental conditions; Carvalho *et al*. 2010) or intrinsic factors, including adaptations and biological innovations (such as their unique feeding apparatus; Ősi 2014; Pol *et al*. 2014) potentially driven by modes of evolution distinct from that of other crocodylomorphs (as suggested by the body size analyses in Chapter 2).

Apart from notosuchians, other crocodylomorph subgroups contribute to the higher disparity of terrestrial forms, mainly non-mesoeucrocodylian crocodylomorphs (such as protosuchids, gobiosuchids and shartegosuchoids; Pol and Norell 2004; Clark 2011; Irmis *et al*. 2013; Buscalioni 2017; Dollman *et al*. 2018), for which a series of cranial specialisations have been previously reported (Buscalioni 2017; Dollman *et al*. 2018). Among these, modifications related to brachycephaly (e.g., snout length reduction, rounded neurocranial shape, dorsal rotation of the mandibles, mandibular asymmetry, and tooth loss and/or orientation change; Buscalioni 2017) are possibly associated with feeding behaviour and might represent the result of ecological selective pressures.

Finally, the lower disparity of aquatic/marine taxa, together with the more restricted morphospace occupation along both PC1 and PC2 axes, suggests that marine taxa are more morphologically constrained, at least regarding some aspects of cranial shape variation. This would be consistent with other phenotypic constraints possibly associated with an aquatic lifestyle in crocodylomorphs, such as body size limits, as indicated by the shifts towards larger body sizes that is more frequently detected at the bases of marine clades (Chapter 2).

3.5. Conclusions

In this Chapter, I assessed crocodylomorph cranial shape variation with 2D landmark-based geometric morphometrics, using the most phylogenetically comprehensive dataset to date, including 209 species. To do that, I combined a previously published dataset with newly digitised specimens. After manually assessing the differences in the landmarks digitised by multiple observers/operators, which could be causing a significant amount of interobserver error, I was able to substantially reduce the error (from ~30% to ~1.5%), demonstrating the importance of a standardised digitisation protocol.

Most of cranial shape variation of crocodylomorphs is related to changes in the snout, in terms of both length and width. This is consistent with previous work and provides additional evidence of a strong link between ecology and crocodylomorph cranial morphology, since changes in snout length are likely related to feeding behaviour. Indeed, the weak phylogenetic signal in the shape data, as well as the significantly different morphospace occupied by distinct ecological categories (i.e., aquatic/marine, semi-aquatic/freshwater and terrestrial groupings), further supports the hypothesis that ecological selective pressures could be driving crocodylomorph cranial shape variation.

Disparity quantified between different crocodylomorph subgroups shows that the species-rich and ecologically diverse clade Notosuchia exhibits the highest disparity, which is also probably the greatest contributor to the peak in disparity seen in the Cretaceous, as well as to the higher disparity seen among terrestrial forms (when compared to aquatic and semi-aquatic species). Although less disparate, crocodylians also display substantial cranial shape variability, mainly in snout lengths. Tighter morphological constraints seem to apply to marine/aquatic crocodylomorphs, as these forms are more restricted in terms of morphospace occupation.

Finally, perhaps most importantly, the results of this Chapter provide valuable evidence that disparity-through-time analyses are highly sensitive to methodological assumptions, since changes in the time sub-sampling method and in the phylogenetic hypothesis used in these analyses had significant impacts on the results. Although previous works have already acknowledged the importance of time sub-sampling, given the uneven nature of the fossil record, it is demonstrated here that the use of different time-scaled trees can also be a major cause of variability. Thus, future work quantifying disparity of long-lived clades, especially those with substantial phylogenetic and stratigraphic uncertainties (such as vertebrates), should ideally perform multiple analyses (with different time sub-sampling methods, numbers of time intervals, phylogenetic hypotheses, ancestral states estimation methods, and time-scaling methods), reporting shared patterns and treating incongruent results with caution.

Chapter 4: Heterochrony in the cranial evolution of notosuchians

This chapter is a modified version of a paper already published in the journal *Palaeontology*, with the following citation:

GODOY, P. L., FERREIRA, G. S., MONTEFELTRO, F. C., VILA NOVA, B. C., BUTLER, R. J. and LANGER, M. C. 2018*b*. Evidence for heterochrony in the cranial evolution of fossil crocodyliforms. *Palaeontology*, **61,** 543–558.

During the development of this project, my collaboration involved leading all parts of the research, including collecting the data, analysing it and interpreting the results, as well as writing the manuscript. My colleagues collaborated by co-designing the project, collecting part of the data, running some geometric morphometric analyses, providing feedback on interpretation of results, and giving important comments on earlier versions of the manuscript the manuscript.

4.1. Background

Heterochrony, the shifts in timing and rate of development, has been hypothesized to drive major phenotypic modifications in many groups (Gould 1977; McKinney 1988; McNamara and McKinney 2005; Bhullar *et al.* 2012; Koyabu *et al.* 2014). The identification of heterochronic processes requires information about the ancestral condition and the ontogenetic stage (age) of the studied organisms (Alberch *et al.* 1979; Shea 1983; Klingenberg 1998). However, as well-preserved ontogenetic series and precise information on absolute ages of individuals are rare for fossil vertebrates, palaeontologists have often used relative size as a proxy for ontogenetic stage (Erickson *et al.* 2004; Schoch 2010; Ezcurra and

Butler 2015; Foth *et al.* 2016*b*). In this context, the recent discovery of a beautifully preserved new specimen of the baurusuchid crocodylomorph *Pissarrachampsa sera* (Fig. 4.1), noticeably smaller than the other specimens previously reported (Montefeltro *et al.* 2011), provides the opportunity to investigate the role of ontogenetic changes in the evolution of one of the most remarkable crocodylomorph groups, the notosuchians.

Notosuchia is the most diverse crocodylomorph group in the Cretaceous of Gondwana (Turner and Sertich 2010; Godoy *et al.* 2014; Pol *et al.* 2014; Pol and Leardi 2015), showing an extraordinary taxonomical and ecological diversity (Stubbs *et al.* 2013; Bronzati *et al.* 2015; Mannion *et al.* 2015). Additionally, as indicated by the results in Chapters 2 and 3 of this thesis, notosuchians have a remarkable morphological disparity, which was likely driven by ecological diversification and might have been the result of modes of evolution distinct to that of most other crocodylomorphs.

Among the notosuchian subclades, baurusuchids are distinguished by their peculiar anatomy, including a high and laterally compressed skull and blade-like ziphodont teeth. These features have been used to infer an ecological role as land-dwelling hypercarnivores, acting as apex predators in specific Gondwanan ecosystems in which theropod dinosaurs, the dominant terrestrial predators throughout most of the Mesozoic, were scarce (Montefeltro *et al.* 2011; Riff and Kellner 2011; Godoy *et al.* 2014; 2016). Despite the long history of research on baurusuchids (Price 1945; Gasparini 1971), few studies have examined aspects of their ontogeny, as juvenile specimens have been rarely reported and their preserved fossils are mostly fragmentary (e.g., Carvalho *et al.* 2011). Likewise, although Crocodylomorpha is a highly diverse and fossil-rich clade, studies identifying the role of heterochronic processes in their evolutionary history are relatively rare and usually focused on extant crocodylians (e.g., Gignac and O'Brien 2016).

Figure 4.1. Photographs of the newly reported *Pissarrachampsa sera* juvenile specimen (LPRP/USP 0049) in dorsal (**A**), ventral (**B**) and lateral (**C**) views. Scale bar equals 5 cm.

When compared to adult baurusuchids, the juvenile individual reported here bears a general cranial morphology more typically seen in adults of non-baurusuchid notosuchians, such as *Mariliasuchus amarali*, *Comahuesuchus brachybuccalis*, and the various species of *Araripesuchus*. Based on these differences, peramorphic heterochronic processes are hypothesized to have modified the ancestral notosuchian cranial morphology, leading to the adult baurusuchid skull. Peramorphosis ("shape beyond") is identified when the descendant

development (size or shape) extends beyond that of the ancestor, producing exaggerated adult traits (Alberch *et al.* 1979; Klingenberg 1998). Ancestral adult characters are therefore seen in juveniles of the descendent. The opposite process is known as paedomorphosis, in which the descendant retains at adult size the shape (or the characteristics) of the ancestral juvenile (Alberch *et al.* 1979; Klingenberg 1998).

As previously documented (Erickson and Brochu 1999), large extant and extinct crocodylomorphs have achieved larger bodies by extending the growth period, suggesting the action of time hypermorphosis, a peramorphic process that leads to an increase in size. Accordingly, the evolution of larger body sizes in baurusuchids may have been the result of similar processes, but this hypothesis has not been previously examined. In this Chapter, the new specimen of *Pissarrachampsa sera* is used to document heterochronic changes and assess the action of peramorphic processes in the cranial evolution of Baurusuchidae.

4.1.1. Heterochrony terminology

It is important to clearly define the peramorphic processes used in the context of this Chapter, as distinct heterochronic processes have been defined using different formalisms (evolutionary *versus* developmental concepts, for example) in the past (Klingenberg 1998). The definitions of the peramorphic processes used herein (Fig. 4.2) follow mainly the works of Gould (1977), Alberch *et al*. (1979), Shea (1983), and Klingenberg (1998). Accordingly, it is acknowledged that the effects of heterochrony on the phenotype may be realized on three different and independent dimensions – shape of a given structure, body size, and age (Klingenberg 1998). The variation of three parameters – rate of change (either of a structure or the entire body), and times of onset and offset of growth (either of a structure or the entire body) – can be used to describe the processes (Alberch *et al*. 1979; Klingenberg 1998).

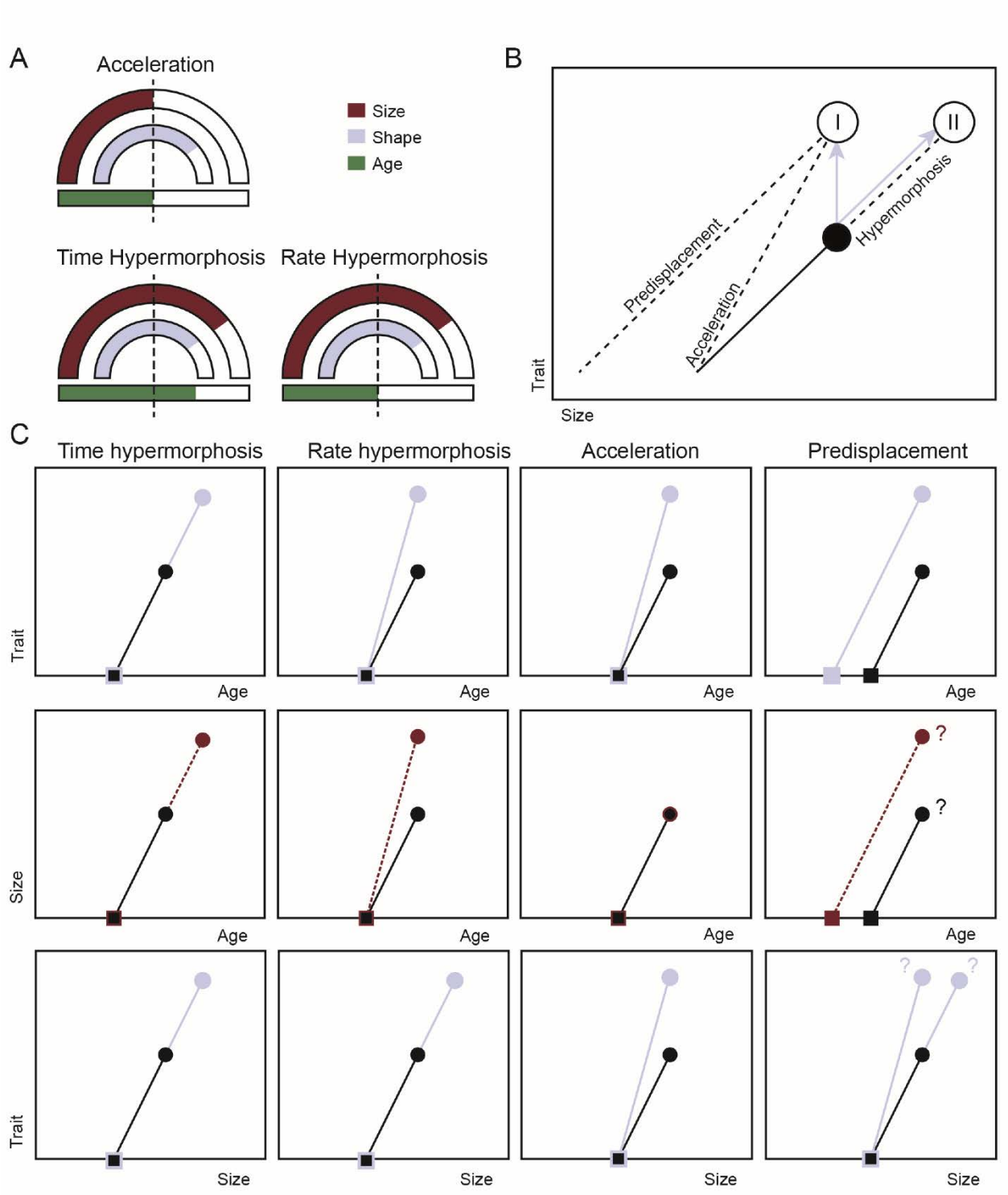

Figure 4.2. *Caption on next page.*

Figure 4.2. A, Comparison between effects of time hypermorphosis, rate hypermorphosis and acceleration on size (large arch), shape (small arch), and age (bottom bar) of ancestors (dotted midline) and descendants (filled bars), using the clock model devised by Gould (1977). **B,** Representation of morphological evolution and their relations to ontogenetic scaling (modified from Strelin *et al*. 2016). Full black circle and line represent the ancestor and ancestral ontogenetic trajectory, respectively. Dotted lines are descendant trajectories, and arrows are the deviations from the ancestral ontogenetic trajectory. Circles I and II represent modifications not predicted and modifications predicted by the ontogenetic scaling hypothesis, respectively. **C,** Pairwise comparison of the effects of time hypermorphosis, rate hypermorphosis, acceleration, and predisplacement on size, shape (trait) and ages, using hypothetical ontogenetic trajectories (lines), from the onset (square) to the offset of growth (circles) of ancestors (full lines) and descendants (dashed lines). The effects of predisplacement on size are not completely known and can potentially occur in two forms: size and shape (trait) growth are coupled and both are "predisplaced" in time (age); (i.e. the onset in descendant occurs earlier than in the ancestor), or size and trait growth are decoupled and predisplacement affects only descendant's shape, and size growth follows the same ancestral path.

Acceleration is identified when anatomical structures of the descendant develop faster (increased rate) than the rest of the body, when compared to the ancestor. There is a break of the ancestral allometry (size-shape relationship), so these changes are not ontogenetically scaled (i.e., heterochronic changes do not maintain the ancestral allometric relationship). There is no change of the times of onset and offset of growth. The outcome is a peramorphic structure, in an individual with the same body size and an equivalent period of development as the ancestor.

Hypermorphosis can be divided into two subtypes (Shea 1983). Time hypermorphosis, is when the entire body of the descendant (including the studied part) develops for a longer period than in the ancestor. The ancestral allometry is maintained, so the changes are ontogenetically scaled. There is no change in the time of growth onset, but the offset is delayed. The outcome is a peramorphic structure, in an individual with larger body size and a longer period of development than the ancestor. By contrast, in rate hypermorphosis the entire

body of the descendant (including the studied part) develops faster than in the ancestor. The ancestral allometry is maintained, so the changes are ontogenetically scaled. There is no change in the times of onset and offset of growth. The outcome is a peramorphic structure, in an individual with a larger body size and the same period of development as in the ancestor. The distinction between rate and time hypermorphosis, introduced by Shea (1983), was not part of the original classification of Alberch *et al*. (1979), and the use of the term rate hypermorphosis has been criticized by some authors (e.g., Gould 2000). In any case, the resulting morphology (i.e., the descendant's morphology) is ontogenetically scaled in both time and rate hypermorphosis.

Finally, predisplacement is when a structure of the descendant starts to develop earlier than in the ancestor. This often leads to a break of the ancestral allometry, but not if the entire body also starts developing earlier. The onset of growth is anticipated (at least that of the structure), but the offset is maintained. The outcome is a peramorphic structure, in an individual with the same body size and the same period of development as the ancestor or with a larger body size and a longer period of development than the ancestor if the earlier onset also affected the entire body.

4.2. Material and Methods

4.2.1. Systematic Palaeontology

CROCODYLIFORMES Benton and Clark 1988

MESOEUCROCODYLIA Whetstone and Whybrow 1983

BAURUSUCHIDAE Price 1945

PISSARRACHAMPSINAE Montefeltro *et al*. 2011

Pissarrachampsa sera Montefeltro *et al*. 2011

Holotype. LPRP/USP 0019; nearly complete skull and mandibles lacking the rostralmost portion of the rostrum, seven dorsal vertebrae, partial forelimb, pelvic girdle, and hindlimbs (Montefeltro *et al*. 2011; Godoy *et al.* 2016).

Newly referred specimen. LPRP/USP 0049; a juvenile individual comprised of a complete skull with lower jaws, articulated neck/trunk vertebrae and partial right scapula and forelimb (Fig. 4.1).

Locality. Inhaúmas-Arantes Farm, Gurinhatã, Minas Gerais state, Brazil (Martinelli and Teixeira 2105).

Age and horizon. Adamantina Formation, Bauru Group, Bauru Basin; Late Cretaceous, Campanian–Maastrichtian (Marsola *et al*. 2016; Batezelli 2017).

Diagnosis. The new specimen LPRP/USP 0049 was identified as *Pissarrachampsa sera* based on the presence of the following combination of features, unique to that taxon (Montefeltro *et al*. 2011; Godoy *et al.* 2016): a longitudinal depression on the rostral portion of frontal; frontal longitudinal ridge extending rostrally beyond the frontal midlength; supratemporal fenestra with equally developed medial and rostral rims; lacrimal duct positioned at the angular junction between the dorsal and lateral surfaces of the lacrimal; well-developed rounded foramen between the anterior and posterior palpebrals; quadratojugal and jugal do not form a continuous ventral border (a notch is present due to the ventral displacement of the quadratojugal); four subtympanic foramina (*sensu* Montefeltro *et al*. 2016) visible laterally; a

single ventral parachoanal fenestra and one ventral parachoanal fossa (divided into medial and lateral parachoanal subfossae); lateral Eustachian foramina larger than the medial one; a deep depression on the caudodorsal surface of the pterygoid wings; complete absence of postcranial osteoderms.

4.2.2. Sampling and data collection

To test if the cranial modifications seen in Baurusuchidae were generated by heterochronic processes, the cranial disparity of Notosuchia was assessed using 2D geometric morphometric analyses of general skull shape. The specimens/species sampling took into account the phylogenetic positions within Notosuchia of the species and the preservation of the specimens. Only fairly complete skulls, for which most of the landmarks could be readily identified and digitized, were sampled. Specimens too deformed or lacking important parts of the skull were not included. However, to maximise the sample size, specimens in which only a small portion of the skull was missing (e.g., the rostralmost tip of the snout) and specimens that were only slightly deformed were also included. In these cases, closely related taxa were used to project the landmark positions during the digitization.

As a result, 38 specimens were sampled, from a total of 27 taxa across Notosuchia, including four juvenile specimens: the baurusuchids *Pissarrachampsa sera* and *Campinasuchus dinizi*, as well as *Anatosuchus minor* and *Mariliasuchus amarali* (see Appendix E for further information on the sampled specimens). To obtain more detailed interpretations of skull shape variation, both lateral and dorsal views were used for the analyses (Openshaw *et al*. 2016), with 19 and 17 landmarks respectively (Fig. 4.3; see Appendix E for further information on the landmarks). Landmarks were digitized using the software tpsDig 2.22 (Rohlf 2015). Landmarks were digitised on both right and left sides of

the skulls, choosing the side that offered the best conditions for digitization (considering either preservation or quality of photographs). Then, the reflected shape of the specimens that were digitized on the right side was extracted while performing the Procrustes fit in MorphoJ. To minimize error, landmarks were collected twice for each specimen (by a single person), and the subsequent analyses employed the average coordinates from the two digitizations of each specimen.

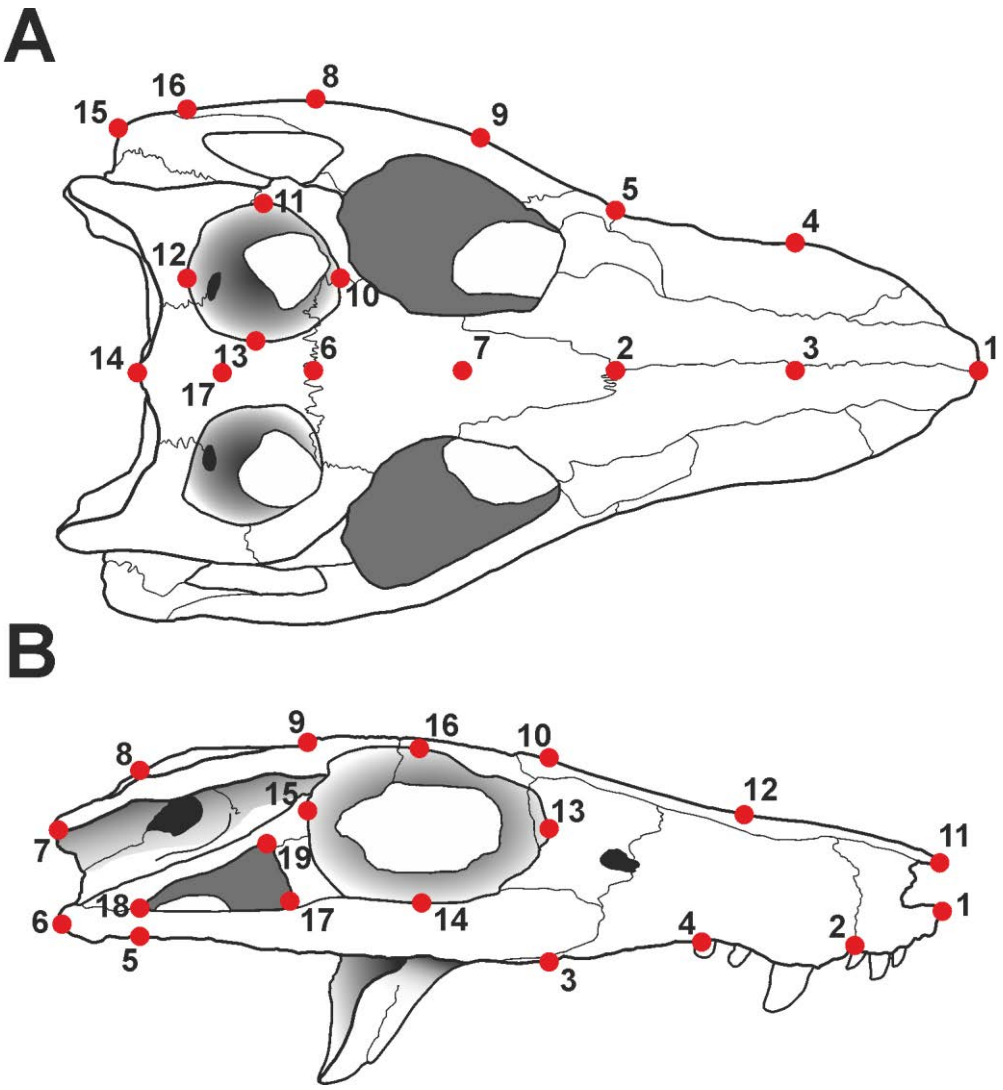

Figure 4.3. Example, using one specimen (*Araripesuchus wegeneri*, MNN GAD19), of the position of the landmarks for the geometric morphometrics analyses in this Chapter. **A,** dorsal view. **B,** lateral view.

4.2.3. Phylogenetic framework

Notosuchia is a group of mesoeucrocodylians that has been consistently supported as monophyletic, even though its exact taxonomic content may vary in different phylogenetic hypotheses (e.g., Turner and Sertich 2010; Andrade *et al*. 2011; Bronzati *et al.* 2012; Montefeltro *et al*. 2013; Pol *et al*. 2014; Sertich and O'Connor 2014; Turner 2015; Wilberg 2015). The placement of Baurusuchidae deeply nested within Notosuchia is supported even by studies that have highly distinct taxonomic and character samples (Montefeltro *et al*. 2013; Pol *et al.* 2014; Turner 2015; Martin and de Lapparent de Broin 2016; Meunier and Larsson 2017), but uncertainties remain regarding the nearest relatives of baurusuchids. The morphological similarities with Sebecidae, a group of Cenozoic terrestrial crocodylomorphs, have led many phylogenetic studies to cluster Baurusuchidae and Sebecidae into Sebecosuchia (Turner and Sertich 2010; Kellner *et al.* 2014; Pol *et al*. 2014). Alternative positions placed Baurusuchidae closer to other Cretaceous notosuchians, such as Sphagesauridae, with Sebecidae placed closer to other groups such as Peirosauridae and Mahajangasuchidae (Sereno and Larson 2009; Montefeltro *et al.* 2013; Wilberg 2015; Meunier and Larsson 2017). It is almost universally agreed, however, that baurusuchids are not very closely related to a set of mostly small-bodied notosuchians, such as *Mariliasuchus*, *Araripesuchus*, *Notosuchus*, and *Uruguaysuchus* (Kellner *et al.* 2014; Pol *et al*. 2014; Leardi *et al*. 2015*a*, *b*; Martin and de Lapparent de Broin 2016).

The phylogenetic hypothesis proposed by Montefeltro *et al.* (2013) was selected as the primary phylogenetic framework for the geometric morphometric analyses (Fig. 4.4A). Four additional taxa were added to the original topology of Montefeltro *et al.* (2013), for which morphometric data was available: *Aplestosuchus sordidus*, *Campinasuchus dinizi*, *Candidodon itapecuruensis*, and *Pakasuchus kapilimai*. The information from Godoy *et al.*

(2014) was employed to define the phylogenetic position of the first two taxa, and from Pol *et al.* (2014) for the latter two. Following this phylogenetic framework, the sampled specimens were divided into four different taxonomic groups, which was necessary to test the hypothesis of peramorphosis in baurusuchid evolution: "Baurusuchidae", "Sphagesauridae", "Peirosauridae + Sebecidae", and the remaining notosuchians falling outside of these groups (clustered here as "other notosuchians"). As *Sebecus icaeorhinus* was the only representative of Sebecidae included, it was combined with peirosaurids into a single group for the analyses.

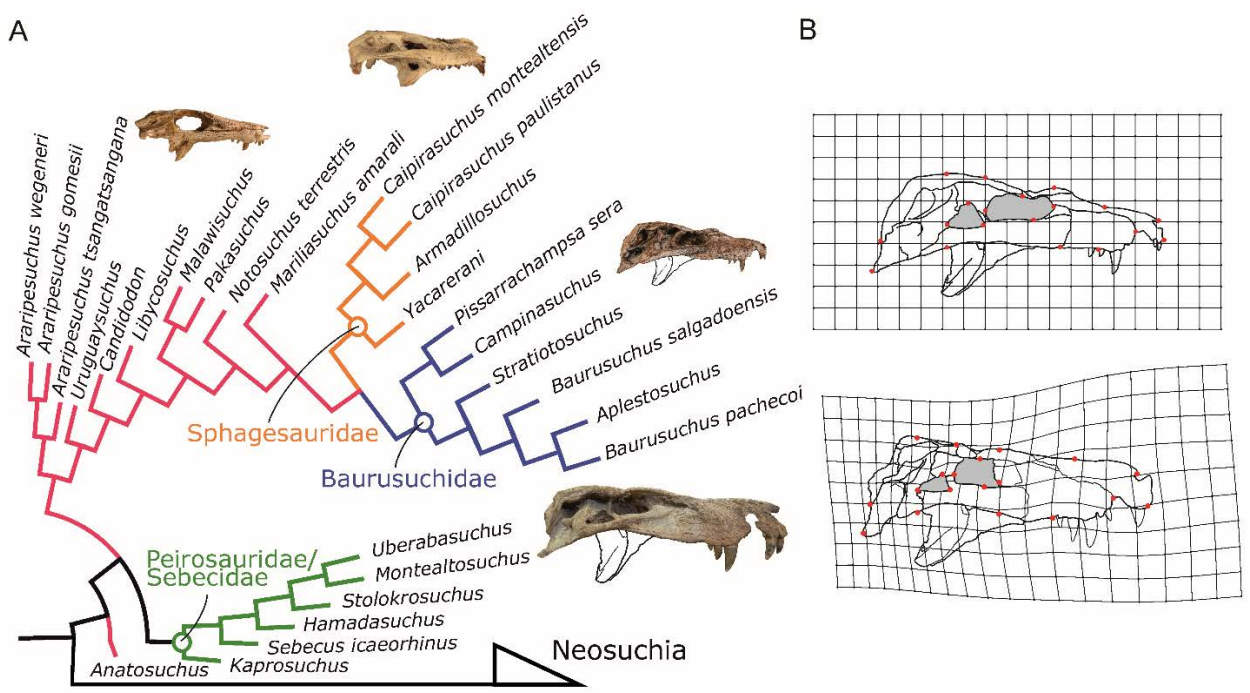

Figure 4.3. A, Phylogenetic hypothesis of the Notosuchia taxa included in our geometric morphometric analyses (based on Montefeltro *et al*. 2013), with clades Baurusuchidae, Sphagesauridae, and Peirosauridae/Sebecidae indicated, and other notosuchians distributed along the tree. The skulls of some notosuchians (not to scale) were selected to illustrate the cranial disparity of the group (clockwise, from the top left): adult *Araripesuchus wegeneri*, adult *Mariliasuchus amarali*, juvenile *Pissarrachampsa sera*¸ and an undescribed adult baurusuchid (LPRP/USP 0697). **B,** Morphological transformation during *Pissarrachampsa sera* ontogeny, shown by the results of the thin plate spline analysis with the juvenile (top) and adult (bottom) specimens, also illustrating the position of the landmarks (in lateral view).

In order to test the robustness of the results to changes in phylogenetic hypotheses, the sampled specimens were also divided to fit an alternative phylogenetic framework. For this, the topology of Pol *et al*. (2014) was selected, as the data matrix presented in this work has formed the basis of many subsequent phylogenetic analyses of notosuchians (e.g., Leardi *et al*. 2015*a*, *b*; Godoy *et al*. 2016). As a result, the specimens were reallocated within three alternative taxonomic groups: "Sebecosuchia" (baurusuchids + *Sebecus icaeorhinus*), "Uruguaysuchidae + Peirosauridae" (*Araripesuchus* species, *Uruguaysuchus* and *Anatosuchus* in Uruguaysuchidae + peirosaurids) and "other notosuchians" (all remaining species, including sphagesaurids).

4.2.4. Geometric morphometric analyses

To extract shape information from both lateral and dorsal view datasets, a Procrustes fit with reflection was applied using the software MorphoJ 1.06e (Klingenberg 2011), and also obtained centroid size, to be used in subsequent analyses as a proxy for size. Next, to visualize the skull shape transformations during the postnatal ontogeny of *Pissarrachampsa sera*, a thin plate spline was performed (Bookstein 1991), using the lateral view dataset of both the juvenile and adult specimens of this taxon. This procedure was conducted using *geomorph* package (Adams and Otárola-Castillo 2013) in R (R Core Team 2017), and shape variation (the position of the Procrustes coordinates) of the adult against the juvenile was plotted in a deformation grid. Then, a principal component analyses (PCA) was conducted in MorphoJ, to investigate the morphospace occupied by the sampled taxa. For these comparisons, the specimens were divided into taxonomic groups using both phylogenetic frameworks outlined above. The position of individual specimens within the morphospace will not change using

alternative phylogenetic frameworks (i.e., the only difference should be in the morphospace occupation by the different taxonomic groups). Furthermore, the topology of Montefeltro *et al*. (2013) was mapped onto centroid size (using only the lateral view dataset) to explore the size differences among the sampled taxa.

Subsequently, a set of analyses was performed to assess which specific heterochronic processes could be driving baurusuchid cranial evolution. Peramorphic changes in the shape of structures can be decoupled from (acceleration) or accompanied by (hypermorphosis and predisplacement) changes in size (Gould 1977; Alberch *et al*. 1979; Shea 1983; Klingenberg 1998). To explore this relationship, a size-correction was employed to both datasets to test whether the shape differences remained after removing the effect of allometric changes (Gould 1966; Revell 2009; Klingenberg 2016). Using MorphoJ, the residuals of a multivariate regression of the Procrustes coordinates against centroid size were obtained (Monteiro 1999; Klingenberg *et al*. 2012; Klingenberg 2016). For this, a subset restricted to adult specimens was used, as only interspecific size variation was being analysed. The residuals from this regression were then used as the input for a second PCA to explore the occupied morphospace after removing the effect of size on the observed variation. As for the first PCA, the specimens were also divided into taxonomic groups using both the primary and alternative phylogenetic frameworks. Non-parametric multivariate analysis of variance (npMANOVA) was used to test the significance of the differences in the distributions of groups in the morphospace. These tests were performed in PAST (Hammer *et al*. 2001), using the PC scores that represent at least 95 per cent of shape variation. These scores were then transformed into a Euclidean distance matrix (Euclidean similarity index), and permuted with 10,000 replications. Comparisons were made using Bonferroni correction for adjusted p-values. Additionally, the topology based on the hypothesis of Montefeltro *et al.* (2013) was

projected onto the PC scores (using both dorsal and lateral view datasets), creating a phylomorphospace to explore the evolutionary history of shape changes in the sampled taxa.

To evaluate the specific action of time hypermorphosis, the methodology described by Strelin *et al*. (2016) was applied, to test whether the shape modifications seen in the baurusuchid skull evolved by ontogenetic scaling. Time hypermorphosis corresponds to an extension of the ancestral ontogenetic trajectory, a pattern previously detected in other crocodylomorphs known to extend the growth period and attain larger body sizes (e.g., Erickson and Brochu 1999). As such, based on whether the differences among taxa remain or not after this procedure, hypermorphosis could be either rejected or confirmed as the sole peramorphic process acting on baurusuchid skull evolution, as this is the only process that extends the ontogenetic trajectory in time.

For this, skull size and shape variation from juvenile to adult baurusuchids was compared to those changes seen along the ontogenetic trajectory of a hypothetical ancestral notosuchian. The ancestral ontogenetic trajectory was inferred via a phylogenetic approach based on outgroup taxa to Baurusuchidae (i.e., using trajectories of other notosuchians as proxies for estimating this ancestral condition). Good proxies would, ideally, fulfil two requirements: (1) have at least one juvenile specimen, as well as at least one adult specimen, both with skulls sufficiently well-preserved to be sampled for the geometric morphometric analyses; (2) be unequivocally non-baurusuchid notosuchians (with their positions relative to baurusuchids supported by alternative phylogenetic hypotheses), as the aim was an ontogenetic trajectory of a hypothetical notosuchian ancestor that was at least outside Baurusuchidae. Preferably, this approach would incorporate information from as many species as possible. However, only two non-baurusuchid notosuchians satisfy the first requirement: *Mariliasuchus amarali* and *Anatosuchus minor*. Among the six *Mariliasuchus*

amarali specimens sampled for the geometric morphometric analyses, one (the holotype, UFRJ DG 50-R) is clearly a juvenile (Carvalho and Bertini 2009). The second species, *Anatosuchus minor*, has two specimens sampled, and its holotype (MNN GAD603) is a putative juvenile, due to its smaller size (Sereno and Larsson 2009). Although using only two taxa is not ideal, the phylogenetic positions of these two species relative to baurusuchids support their use as the best available proxies for the ancestral condition of baurusuchids (see Martinelli 2003; Sereno *et al*. 2003; Pol *et al*. 2009; Sereno and Larsson 2009; Turner and Sertich 2010; Andrade *et al*. 2011; Pol *et al*. 2012; Montefeltro *et al*. 2013; Kellner *et al*. 2014; Pol *et al*. 2014; Sertich and O'Connor 2014; Leardi *et al*. 2015*a*, *b*; Godoy *et al*. 2016; Meunier and Larsson 2017).

Accordingly, an ontogenetic regression model was created for both *Mariliasuchus amarali* and *Anatosuchus minor*, using all sampled specimens of these species (including juveniles), by regressing the Procrustes coordinates against the log-transformed centroid size in MorphoJ (Klingenberg 2011; Strelin *et al*. 2016). This ontogenetic regression model was used to perform an allometric size-correction (referred here as the "ancestral ontogenetic allometry correction") for all other taxa in the datasets (Strelin *et al*. 2016). Regression residuals were calculated in MorphoJ, by using the vector of regression coefficients for the ontogenetic allometry estimated for the two taxa and applying them to the shape data. This process removes the potential effect of ontogenetic scaling from the variation among taxa. These residuals were then used as the input data for a third PCA, again including only adults, to explore the morphospace occupied after removing the effect of the ancestral ontogenetic allometry trajectory from the landmark data. As for the first and second PCA, morphospace occupation was investigated using both primary and alternative phylogenetic frameworks. As also done following the size-correction, npMANOVA was used to test the significance of the

differences between groups and created phylomorphospaces, by projecting the topology of Montefeltro *et al*. (2013) onto the PC scores.

Finally, it is worth noting that the use of *Anatosuchus minor* as a proxy for the ancestral ontogenetic trajectory should be treated with caution. The holotype specimen of *Anatosuchus minor*, which has been interpreted as a juvenile, is not much smaller than the only other known specimen of this taxon, which has been interpreted as an adult. Moreover, this taxon also exhibits a cranial morphology notably distinct from those of other notosuchians (Sereno *et al*. 2003; Sereno and Larsson 2009). Accordingly, as a sensitivity test, the ancestral ontogenetic trajectory was also estimated without including *Anatosuchus minor*, instead performing the ancestral ontogenetic allometry correction using only the *Mariliasuchus amarali* specimens.

4.3. Results

The thin plate spline shows that the cranial changes observed during the ontogeny of *Pissarrachampsa sera* include an expansion of the rostrum (both rostrocaudally and dorsoventrally), a rostrocaudal shortening of the skull roof (orbitotemporal region), and the reduction of the relative size of the orbits and the lower temporal fenestrae (Fig. 4.4B). Furthermore, based on the primary phylogenetic framework (Montefeltro *et al.* 2013), the first PCA shows that juvenile and adult baurusuchids occupy different regions of the morphospace. In both the lateral (PC1 accounting for 60.6per cent of the variation, PC2 = 9.9 per cent) and dorsal views (PC1 = 57.9 per cent, PC2 = 11.3 per cent), juvenile baurusuchids fall outside the morphospace of adult baurusuchids, but within the morphospace occupied by non-baurusuchid notosuchians. By contrast, when compared to juveniles, adult baurusuchids occupy a distinct part of the morphospace, mainly displaced along the PC1 axis for the lateral

view dataset (Fig. 4.5A), and along both PC1 and PC2 axes for the dorsal view dataset (see Appendix E for information on additional results). A similar pattern of morphospace occupation was found when the alternative phylogenetic framework (Pol *et al*. 2014) was used, with the sampled taxa rearranged into different groups. In both lateral and dorsal views (Appendix E) juvenile sebecosuchians (the group that includes baurusuchids) are displaced in relation to the morphospace occupied by adults.

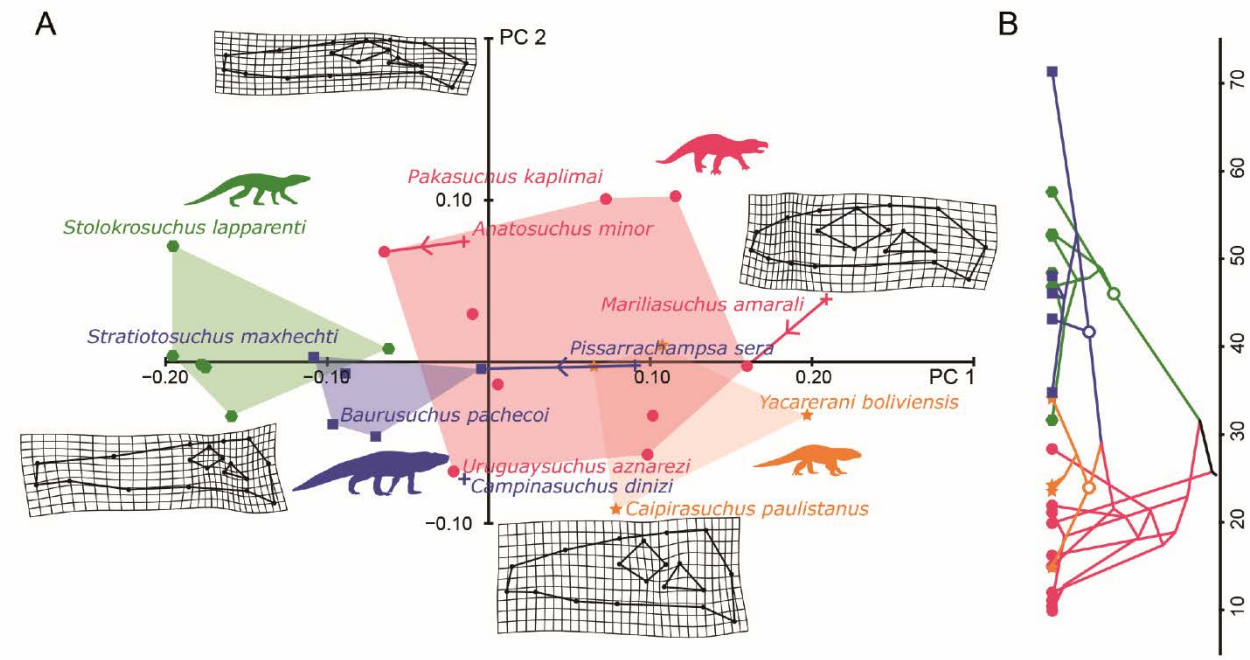

Figure 4.5. A, Two-dimensional morphospace (PCA results plot) of the first two PCs of the lateral view dataset, with deformation grids for hypothetical extremes along the two axes. The coloured polygons show the morphospace occupation by each of the four groups considered in this study. Crosses represent juvenile specimens, squares, stars, hexagons and circles represent adults of Baurusuchidae, Sphagesauridae, Peirosauridae/Sebecidae and other notosuchians, respectively (average values were used for taxa with more than one adult specimen sampled). The arrows represent an ontogenetic trajectory along this two-dimensional morphospace. **B,** Topology based on the phylogenetic hypothesis of Montefeltro *et al*. (2013) projected onto the log-transformed centroid size. The centroid size was obtained from the lateral view dataset using only adults. Silhouettes from Godoy *et al*. (2014).

The allometric regression of the Procrustes coordinates against log-transformed centroid size shows that changes related to size differences accounted for 36.4 and 40.5 per cent of the variation in the dorsal and lateral view datasets, respectively (see Appendix E for more information about this allometric regression, as well as additional results). The second PCA, with size-corrected data, shows that size variation strongly influences morphospace occupation of the different lineages, in both lateral and dorsal views (Fig. 4.6A and B). For the primary phylogenetic framework (Montefeltro *et al*. 2013), the confidence ellipses (90 per cent) for baurusuchids, sphagesaurids, and even peirosaurids/sebecids overlapped with the confidence ellipse of other notosuchians (see Appendix E for additional results). The absence of significant differences in the distribution of these groups was supported by the npMANOVA test (Table 4.1), showing that changes in size can explain the apparent separation of groups found in the previous analyses (first PC plots). Additionally, when the alternative phylogenetic framework (Pol *et al.* 2014) was taken into account through rearranging the specimens into different taxonomic groups (see above), very similar results were found. The npMANOVA results also indicate that the morphospaces of sebecosuchians (i.e., baurusuchids) and other notosuchians are not significantly different, in both dorsal and lateral views (see Appendix E for additional npMANOVA results).

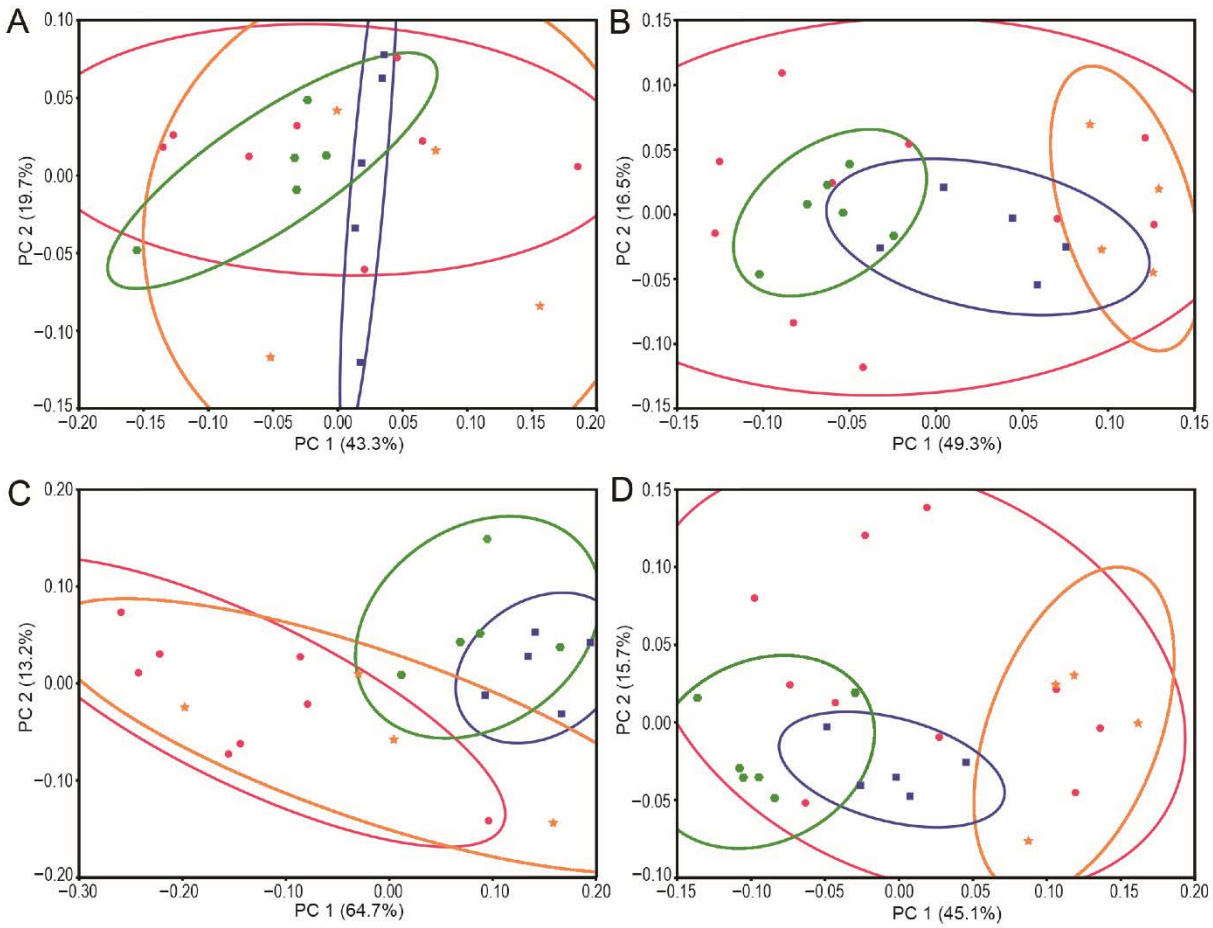

Figure 4.6. Two-dimensional morphospace (plot of PCA results) after the size-correction (**A,** dorsal view; **B,** lateral view) and after the ancestral ontogenetic allometry correction (**C,** dorsal view; **D,** lateral view). Average values were used for taxa with more than one adult specimen sampled. The 90 per cent confidence ellipses were added for each of the four groups considered in the other analyses: Peirosauridae/Sebecidae (hexagons), Baurusuchidae (circles), Sphagesauridae (stars), and other notosuchians (squares).

Finally, the ancestral ontogenetic trajectory was estimated by using the ontogenetic trajectories of *Mariliasuchus amarali* and *Anatosuchus minor* as proxies. First, to assure that the ontogenetic trajectories of these two species (representing the ancestral condition) differ from that of *Pissarrachampsa sera* (representing the baurusuchid trajectory), the reconstructed trajectories of these three taxa were compared with a regression analysis. As expected, the trajectories of these three species are clearly displaced in relation to one another

(Fig. 4.7). However, in dorsal view, whereas the trajectories of *Mariliasuchus amarali* and *Pissarrachampsa sera* exhibit a similar slope, that of *Anatosuchus minor* is clearly different. This might indicate that the use of *Anatosuchus minor* for reconstructing the ancestral ontogenetic trajectory should be treated with caution, given its unique cranial morphology among Notosuchia (see above).

Table 4.1. Pairwise comparison between morphospace occupation of different taxonomic groups. Bonferroni-corrected p-values obtained from npMANOVA, using PC scores of all specimens after both size and ancestral ontogenetic allometry corrections, with lateral and dorsal view datasets. Taxonomic groups based on the phylogenetic framework from Montefeltro *et al*. (2013). Significant differences are indicated by an asterisk.

Pairwise comparisons	**p-values**			
	Size correction		**"Ontogenetic" correction**	
	Dorsal view	**Lateral view**	**Dorsal view**	**Lateral view**
Baurusuchidae – other notosuchians	1	0.9923	0.0126*	0.064
Baurusuchidae – Peirosauridae/Sebecidae	0.1122	0.008*	0.267	0.019*
Baurusuchidae – Sphagesauridae	1	0.048*	0.1416	0.048*
Peirosauridae/Sebecidae – other notosuchians	1	1	0.0138*	0.0138*
Peirosauridae/Sebecidae – Sphagesauridae	0.3732	0.0402*	0.1836	0.0402*
Sphagesauridae – other notosuchians	1	0.1668	0.0126*	0.1944

The distinction between those ontogenetic trajectories (that of the hypothetical ancestor, represented by *Mariliasuchus* and *Anatosuchus*, and that of baurusuchids,

represented by *Pissarrachampsa*) allowed us to progress further with the ancestral ontogenetic allometry correction (i.e., removing the effect of ontogenetic scaling from the data). The results of the third PCA, after this correction, employing the primary phylogenetic framework (Montefeltro *et al.* 2013), are apparently conflicting. Using the lateral view dataset, the morphospaces occupied by adult baurusuchids and other notosuchians overlap and are not significantly separated (Fig. 4.6D; Table 4.1), suggesting that the shape variation observed in baurusuchids could be ontogenetically scaled. However, the dorsal dataset shows a different result, with baurusuchid and other notosuchian morphospaces significantly separated (Fig. 4.6C, Table 4.1). Furthermore, when using the alternative phylogenetic framework (Pol *et al*. 2014), the morphospaces of sebecosuchians (i.e., baurusuchids) and other notosuchians is significantly separated, in both dorsal and lateral views (Appendix E). Finally, to test the influence of the ontogenetic trajectory of *Anatosuchus minor* on these results (given its unique morphology, see above), an ancestral ontogenetic allometry correction was applied using only *Mariliasuchus amarali* for estimating the ancestral trajectory. The results, in both dorsal and lateral views, show the morphospaces of baurusuchids and other notosuchians to be significantly separated (Appendix E).

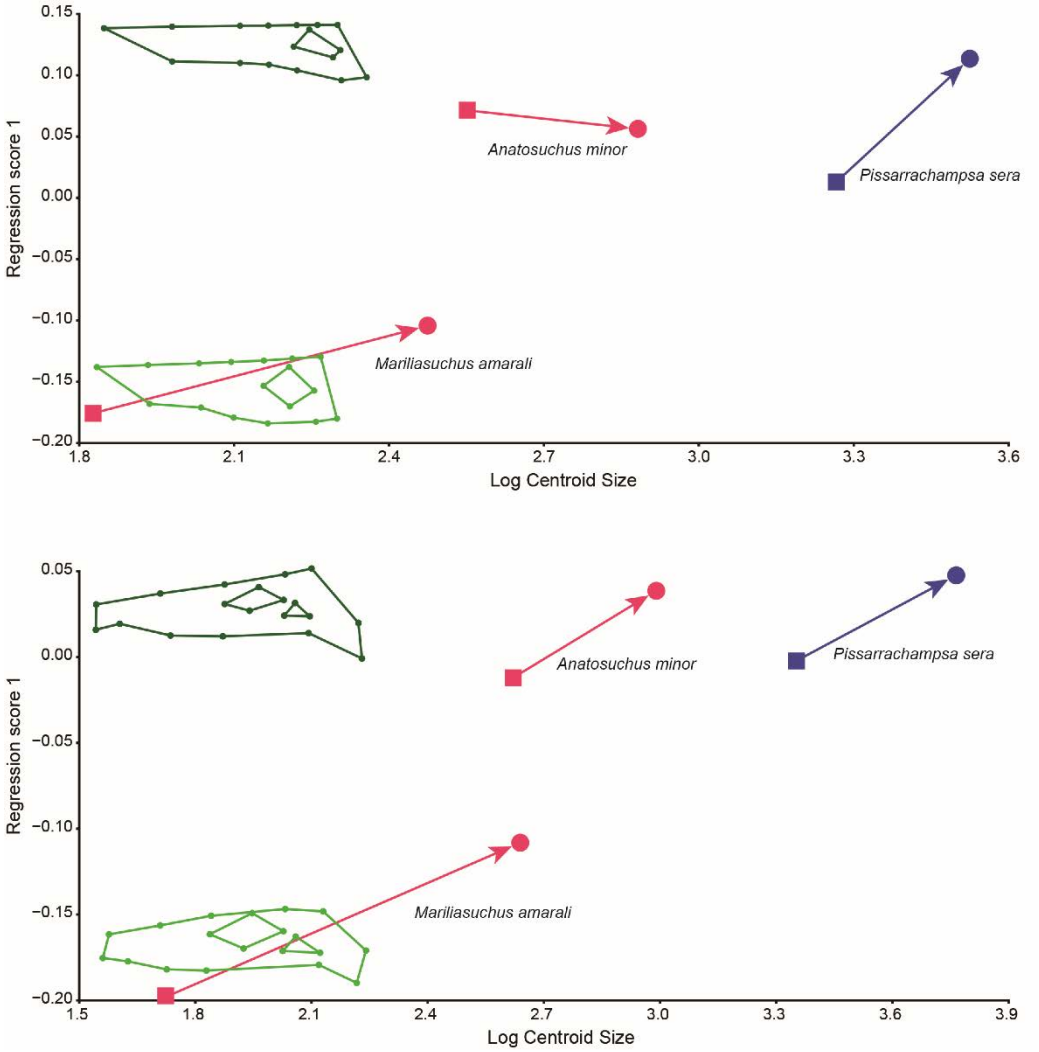

Figure 4.7. Comparisons between the ontogenetic trajectories of *Mariliasuchus amarali* and *Anatosuchus minor* (used as proxies for the ancestral ontogenetic trajectory) and that of *Pissarrachampsa sera* (representing the baurusuchid condition), based on regression analyses of Procrustes coordinates against log-transformed centroid size, in both dorsal (**A**) and lateral (**B**) views. Squares and circles represent juveniles and adults, respectively.

4.4. Discussion

4.4.1. Peramorphosis in Baurusuchidae

The results of the initial analyses (first PCA and thin plate spline) show that adult baurusuchids occupy distinct morphospaces in comparison to juveniles, even when using different phylogenetic frameworks (Appendix E). This could indicate that juvenile

baurusuchids bear a more generalized notosuchian morphotype (since they occupy the morphospace associated to other notosuchians), whereas adults diverge from this morphotype in later ontogenetic stages, supporting the hypothesis of peramorphic processes operating in the evolution of notosuchians. However, given that only one juvenile baurusuchid specimen was included in the lateral view dataset, while only two juvenile specimens were used in the dorsal view, these results should be taken with caution. Only new discoveries of juvenile specimens would provide us with information to clarify if other baurusuchids have similar ontogenetic trajectories.

Nevertheless, our results allow us to describe the cranial transformations during *Pissarrachampsa sera* ontogeny, which can serve as a reference for other baurusuchids. According to our results, during their ontogeny baurusuchids seem to expand their rostrum (both rostrocaudally and dorsoventrally), shorten their skull roof rostrocaudally, and reduce the relative sizes of the orbits and the lower temporal fenestrae, differences that can be observed on the deformation grid of the thin plate spline (Fig. 4.3B). The first PCA corroborates these ontogenetic transformations. In lateral view (Fig. 4.5A), the PC1 axis, from negative to positive values, represents relative rostrocaudal shortening of the rostrum as well as relative enlargement of the orbit, and the PC2 axis displays changes in skull height (higher skulls represented by more negative values). Adult baurusuchids are all located on the negative side of the PC1 axis, whereas the juvenile *Pissarrachampsa sera* is positioned in a positive region along this axis, illustrating the rostrocaudal expansion of the rostrum during the ontogeny of this taxon. Other modifications can be observed in the dorsal view morphospace (Appendix E), in which the PC1 axis also represents rostrocaudal shortening of the rostrum (as in lateral view). The PC2 axis accounts for the mediolateral compression of

the skull (from negative to positive values), and illustrates the mediolateral compression of the skull that occurs during the ontogeny of *Pissarrachampsa*.

Studies using geometric morphometric methods to investigate the ontogenetic trajectories of extant crocodylians (e.g., Piras *et al*. 2010; Watanabe and Slice 2014; Foth *et al*. 2017*a*) suggest similarities between the morphological modifications during the ontogeny of *Pissarrachampsa sera* and the ontogenies of living taxa. For example, the best documented transformation is the relative reduction of the orbits, also found in living representatives of the three main lineages of Crocodylia: Gavialoidea, Crocodyloidea and Alligatoroidea (e.g., Piras *et al*. 2010; Foth *et al*. 2015; 2017*a*). Other common modifications previously reported include the mediolateral compression of the rostrum, although in *Caiman latirostris* the opposite process is observed (i.e., snouts relatively broader later in ontogeny; Bona and Desojo 2011; Foth *et al*. 2017*a*). Nevertheless, quantitative investigations of possible heterochronic processes acting on the evolution of crocodylomorphs are rare (e.g., Gignac and O'Brien 2016), and the present work represents the first attempt to verify the action of heterochrony in fossil lineages of the group using geometric morphometric methods.

However, given the lack of juveniles of other baurusuchids with complete skulls, further assumptions cannot be quantitatively tested. For example, it is difficult to determine the phylogenetic distribution of cranial peramorphism within Baurusuchidae (i.e., asserting whether the action of peramorphic processes started at the base of Baurusuchidae or later within the lineage). The size and phylogenetic positions of *Cynodontosuchus rothi* and *Gondwanasuchus scabrosus* suggest that the peramorphic changes occurred just prior or within the clade composed of Pissarrachampsinae + Baurusuchinae (Godoy *et al*. 2014). These two early-diverging species, known from fragmentary remains, have been suggested to be adults, but are substantially smaller than other baurusuchids (estimated as approximately

50 per cent the size of an adult *Pissarrachampsa sera*; Montefeltro *et al.* 2011; Godoy *et al*. 2014).

4.4.2. Acceleration, predisplacement or hypermorphosis

Among the known peramorphic processes (i.e., acceleration, predisplacement, and hypermorphosis; Fig. 4.2; Gould 1977; Alberch *et al*. 1979; Shea 1983; Klingenberg 1998), acceleration is the only one that does not affect total body size (i.e., based on the definition used here, shape and size are not coupled; Fig. 4.2A) (Klingenberg 1998). The results show that the apparent separation between baurusuchids and other notosuchians seen in the first PCA disappears after applying the size-correction (Fig. 4.6A and B), suggesting a strong correlation between cranial shape and size (centroid size) variation in baurusuchids. Therefore, according to these results, acceleration cannot, as a sole process, explain the shape changes observed in the baurusuchid skull.

Further examination aimed to assess if hypermorphosis could explain the shape variation seen in baurusuchid cranial morphology, by testing the ontogenetic scaling hypothesis. The ontogenetic scaling hypothesis predicts that heterochronic changes can occur by maintaining the ancestral allometric relationships, generating a descendant morphology via proportional changes in size and shape that follow the same ancestral ontogenetic pathway (Fig. 4.2B) (Shea 1983; Klingenberg 1998; Strelin *et al*. 2016). Based on the definitions used here, hypermorphosis is the peramorphic process that incorporates the concept of ontogenetic scaling, either by increasing the duration of ontogeny (time hypermorphosis) or by increasing the rate of size and shape changes during the same period of growth (rate hypermorphosis) (Fig. 4.2A and C; Shea 1983). Accordingly, in both time and rate hypermorphosis the shape variation is ontogenetically scaled.

As such, if the data fit the predictions of the ontogenetic scaling model, after removing the effects of the ancestral ontogenetic allometry the confidence ellipses of baurusuchids should collapse to the same morphospace as other notosuchians. This should be true for all shape variation observed in the sampled specimens, in both lateral and dorsal views. Accordingly, the results do not corroborate the ontogenetic scaling hypothesis, since the apparently ontogenetically scaled shape variation seen in lateral view (Fig. 4.6D) is not congruent with the results for the dorsal view or for the other analyses performed. In dorsal view (Fig. 4.6C), the morphospaces of baurusuchids and other notosuchians remain separate after the ancestral ontogenetic allometry correction (significantly separated, as confirmed by the npMANOVA tests; Table 4.1), which indicates that the shape variation is not ontogenetically scaled. This also highlights the importance of using different views when studying skull shape and interpreting their evolutionary patterns (Openshaw *et al*. 2016). Furthermore, when a different phylogenetic framework was used, which essentially rearranged the sampled species into different taxonomic groups (see above), the morphospaces of sebecosuchians (which includes baurusuchids) and other notosuchians remain significantly separated (Appendix E). The same is observed when the *Anatosuchus minor* specimens were removed from the ancestral ontogenetic trajectory estimation (Appendix E). These complementary results corroborate the idea that the cranial shape variation observed in baurusuchids is not ontogenetically scaled.

Nevertheless, as highlighted before, the small number of juvenile specimens included in these analyses, particularly when estimating the ancestral trajectory, can be problematic. Only two species were used for inferring the ancestral state, with only one juvenile specimen each, making the analyses more susceptible to abnormalities derived from taphonomic

deformations, for example. As in the case of the transformations during baurusuchid ontogeny, only new specimens can corroborate or reject the results found here.

Even though the results should be interpreted carefully, the lack of support for the ontogenetic scaling hypothesis found here indicates that neither time nor rate hypermorphosis could be considered as the single, isolated driver of baurusuchid peramorphism (Shea 1983; Strelin *et al*. 2016). Accordingly, the only process that acting alone could possibly explain the peramorphism observed in baurusuchids is predisplacement, in which the onset age of growth of a structure occurs earlier than in the ancestor (Alberch *et al*. 1979; McNamara 1986) (Fig. 4.2C). However, changes in the time of onset can only be comprehensively assessed by comparing changes in traits (shape) as a function of ontogenetic stages (age) (Klingenberg 1998). As such, at present, it is not possible to confirm the role of predisplacement in the evolution of the baurusuchid skull. Indeed, information such as growth rates and time of onset and offset would be necessary to precisely identify the action of any specific heterochronic process, not only predisplacement. Histological studies comparing growth patterns among different notosuchians have the potential to test whether the onset of baurusuchid traits occurred earlier than in their close relatives (e.g., Cubo *et al*. 2017), which would allow further investigation on the action of peramorphic processes on the evolution of this group. Moreover, the action of a single evolutionary process on morphological structures is expected to be rare (Alberch *et al*. 1979; Klingenberg 1998) and one should expect a combination of two (or more) heterochronic processes acting in the evolution of such complex traits (Klingenberg 1998). Accordingly, as these results are derived from indirect investigation of the action of heterochrony, they only allow us to discard acceleration and hypermorphosis acting in isolation in the cranial evolution of baurusuchids.

4.4.3. Heterochrony explains hypercarnivory

Hypercarnivores, as defined by Van Valkenburgh (1991), are taxa that consume at least 70 per cent of vertebrate flesh. They frequently have a specialized dentition, such as the ziphodont teeth of baurusuchids (Riff and Kellner 2011), in which the primary function is slicing. The documentation presented here of peramorphosis in the evolution of the baurusuchid skull provides important palaeoecological insights, as it supports a strong relation between the reported cranial modifications and size, changes that might have occurred together with the shift to a hypercarnivorous habit. A link between size increase and the evolution of hypercarnivory has been previously documented in other vertebrate lineages, such as carnivoran and creodont mammals (Werdelin 1996; Van Valkenburgh 1999; Van Valkenburgh *et al*. 2004; Wesley-Hunt 2005). Furthermore, heterochrony is commonly associated with evolutionary trends leading to size increase (McNamara 1982; 1990), and one of the possible triggers of these trends is the positive pressure caused by competition (Van Valkenburgh *et al*. 2004; McKinney 1990*b*).

Theropod dinosaurs, the top predators of most terrestrial environments in the Mesozoic, are scarce in the Adamantina Formation, from which the greatest diversity of baurusuchids has been recovered (Méndez *et al*. 2012; Godoy *et al*. 2014). Thus, the large size of baurusuchids (Chapter 2), coupled with their cranial specializations, could have granted access to new feeding resources (Erickson *et al*. 2012), efficiently occupying the niches more commonly filled by theropods elsewhere. Baurusuchids coexisted and interacted with other crocodylomorph taxa in Gondwanan palaeoecosystems during the Late Cretaceous, including carnivorous forms such as peirosaurids (Carvalho *et al*. 2007; Barrios *et al*. 2016). Interestingly, the coeval notosuchians (including baurusuchids) are inferred to have filled a broad range of feeding habits (herbivorous, omnivorous, and carnivorous), with a high degree

of niche/resource partitioning (O'Connor *et al*. 2010; Stubbs *et al*. 2013; Ősi 2014). In this context, the peramorphic size increase of baurusuchids may have played a key role in this niche partitioning, and may also have influenced other aspects of their unique palaeobiology. The life history strategy hypothesized for baurusuchids, and notosuchians in general, includes a shift to the *K*-selected end of the *r*/*K* selection spectrum. The shift is suggested by the consistently smaller egg clutches present in notosuchians, including *Pissarrachampsa sera* (2–5 eggs per clutch; Marsola *et al*. 2016) when compared to fossil neosuchians, such as atoposaurids and dyrosaurids (approximately 12 eggs per clutch; Russo *et al*. 2014; Srivastava *et al*. 2015). The smaller egg clutches of notosuchians (and baurusuchids) is also dissimilar to those of extant crocodylians, in which the number of eggs varies from a lower limit of 10 and reaches up to 80 eggs (Brazaitis and Watanabe 2011; Marsola *et al*. 2016). The features of *K*-selected organisms are commonly associated with hypermorphosis, primarily because this process is classically related to size increase. Even though the results of the geometric morphometric analyses performed in this Chapter do not support the action of hypermorphosis as the single process in the cranial evolution of baurusuchids, predisplacement can also lead to size increase (Fig. 4.2C), and it may similarly be linked to the evolution of *K*-selection strategies.

4.5. Conclusions

In this Chapter, it is demonstrated that changes in the skull shape of baurusuchids, likely accompanied by highly specialized cranial modifications, were strongly linked to size increase in the lineage. As these shape changes occurred through their ontogeny, they provide evidence for the action of heterochronic processes (peramorphosis) in the shift to a hypercarnivorous diet during baurusuchid evolutionary history. These are interesting

advances in the knowledge of the underlying processes that drove notosuchian evolution, and provide important clues for understanding the exceptional diversity displayed by this peculiar group of crocodylomorphs.

Chapter 5: Summary and perspectives

5.1. General conclusions

This thesis employed a phylogenetic comparative approach to quantitatively and comprehensively investigate body size and cranial shape variation in Crocodylomorpha. Given the fundamental nature of these two aspects of animal morphology in evolutionary biology, the results presented here represent an important contribution to current knowledge of the groups' phenotypic evolution over the last ~220 million years.

In Chapter 2, model-fitting analyses used to investigate the modes of evolution that gave rise to the body size patterns during the group's evolutionary history provided overwhelmingly strong support for a multi-peak Ornstein-Uhlenbeck model (SURFACE). This indicates that the macroevolutionary dynamics of crocodylomorph body size evolution are better described within the concept of an adaptive landscape, with most body size variation emerging after shifts to new adaptive zones, which are represented by the macroevolutionary body size regimes. These results do not support, for example, the hypothesis of Cope's rule (i.e., a consistent evolutionary trend towards larger sizes based on Brownian motion dynamics) in crocodylomorphs.

Consistently, long-term crocodylomorph body size patterns (i.e., of maximum and mean body size values, as well as body size disparity) could not be fully explained by the abiotic factors tested here (i.e., palaeolatitude and palaeotemperature). Thus, on large phylogenetic scales, shifts between macroevolutionary regimes (representing lineage-specific innovations) are more important than isolated climatic factors. At more refined scales, however, body size variation may track changes in climate, as in the case of crocodylians, in which a global cooling event might explain the long-term increases in body size (as a result of

systematic reduction of available habits/niches, with differential extinction of smaller-bodied species).

In particular, the evolution of a more aquatic lifestyle (especially marine) correlates, in several clades, with increases in average body size, though not without exceptions. This is reflected in the shifts leading to larger body sizes that are more frequently detected at the base of predominantly aquatic or semi-aquatic groups, and suggests a link between ecological diversification and body size evolution in crocodylomorphs.

Indeed, ecology also seems to play an important role in determining cranial shape variation in crocodylomorphs, as indicated by the results of Chapters 3 and 4. Comprehensive investigation of cranial shape variation and disparity (Chapter 3) corroborates previous work in that most of it is related to changes in the dimensions of the crocodylomorph snout, in terms of both length and width. Given the tight relationship between snout morphology and feeding behaviour, strong ecological selective pressures are expected, suggesting that ecology may be driving most of the variability. This is supported by the relatively weak phylogenetic signal found in the shape data. Additionally, when subdivided into distinct lifestyle categories, crocodylomorphs occupy significantly different morphospaces, which further emphasises the association between crocodylomorph cranial shape variation and ecological specializations.

Among the crocodylomorph subgroups assessed, the highest cranial shape disparity was found among notosuchians, a group known for its species richness, but also for a remarkable variety of feeding strategies, including omnivorous, hypercarnivorous and even herbivorous diets. This higher disparity could be the result of more relaxed modes of evolution in the group, as suggested by the investigation of body size evolution performed exclusively within notosuchians (Chapter 2).

Finally, one of the processes that might have underpinned the cranial evolution of notosuchians is investigated in Chapter 4. The results demonstrated that the changes observed in the cranial shape of baurusuchids, a group of top-predator notosuchians, were linked to a size increase in the lineage, providing evidence for the action of heterochronic processes (peramorphosis). In this case, heterochrony would be related to the shift to a hypercarnivorous diet, possibly accompanied by highly specialized cranial modifications, reinforcing the importance of ecological selective pressures in determining phenotypic changes during crocodylomorph evolutionary history.

5.2. Prospects and future work

Chapter 2 of this thesis represents the first comprehensive investigation of the modes of evolution underlying crocodylomorph body size through the entire history of the group. Accordingly, the results presented here can pave the way for new studies, addressing more specific questions (e.g., association between larger sizes and aquatic lifestyle; correlation between body size and other biotic and abiotic factors) or testing the impact of different approaches (e.g., distinct proxies for body size or direct estimates of body mass; increases in taxon sample size; changes in the phylogenetic hypotheses).

Chapters 3 and 4 represent attempts to more deeply understand the patterns of cranial shape variation in crocodylomorphs. For instance, allometric changes can be assessed by testing the correlation between size and shape, and similar methodological approaches to that used in Chapter 4 can be used to investigate the presence of heterochrony in other crocodylomorph subgroups. Chapter 3 sheds light on the importance of methodological assumptions when estimating disparity through time, and future work will likely explore the impact of other differences (e.g., the use of distinct methods for time-scaling the trees), as

well as trying to clarify patterns that are currently ambiguous (e.g., evidence for either disparity increase or disparity decline from the Eocene onwards). Additionally, with the most comprehensive landmark dataset available for the group, other questions can be addressed. For example, the presence of integrated components in morphometric data can be tested by setting *a priori* defined modules (i.e., specific regions of the skull, such as the snout). Rates of morphological evolution can be also calculated, and a model fitting-approach could be used for investigating the modes of evolution underlying cranial shape variation in the group. Furthermore, patterns of cranial shape disparity through time can be compared to other evolutionary patterns (e.g., species diversity, body size disparity, and morphological disparity measured from discrete characters), as well as tested for correlations with abiotic environmental factors. Finally, unequal morphological diversification in different crocodylomorph groups can be investigated using the phylomorphospace approach proposed by Sidlauskas (2008), assessing, for example, if the unique morphological disparity seen in notosuchians significantly deviates from that expected for other crocodylomorphs.

Appendices

Appendix A: Supplementary information for Chapter 2

The supplementary material for Chapter 2 ("Crocodylomorph body size evolution") was uploaded to the online repository Zenodo (Godoy *et al*. 2018*c*) and can be found at: https://zenodo.org/record/1344593. The online content includes three documents (Additional files 1, 2, and 3) and four subfolders (Additional files 4, 5, 6, and 7), which are detailed below:

- Additional file 1: Supplementary methods and results, including information on (1) total length estimation from cranial measurements, (2) supertree construction, (3) time bins used for time series correlations and disparity calculation, and (4) regression results tables of all correlation analyses performed.
- Additional file 2: Datasets with information on crocodylomorph body size (cranial measurements), palaeolatitude, specimens and lifestyle.
- Additional file 3: AICc scores of all models fitted in our macroevolutionary analyses.
- Additional file 4: Folder containing all plots of SURFACE model fits.
- Additional file 5: Folder containing cross plotting of all SURFACE model fits, using distinct time-scaling methods.
- Additional file 6: Folder containing alternative crocodylomorph trees and FAD (First Appearance Datum) and LAD (Last Appearance Datum) of all species used in our analyses.
- Additional file 7: Folder containing R functions and data for running an example script of our model-fitting analyses.

Appendix B: List of specimens sampled for the geometric morphometric analyses of Chapter 3

Species	Specimen number	Source	Lifestyle (source)
Acynodon adriaticus	MCSNT 57248	Wilberg (2017)	semi-aquatic (PBDB)
Acynodon iberoccitanus	ACAP-FX1	Wilberg (2017)	semi-aquatic (PBDB)
Agaresuchus fontisensis	HUE-02502	Narváez *et al*. (2016)	semi-aquatic (PBDB)
Agaresuchus subjuniperus	MPZ 2012/288	Puértolas-Pascual *et al*. (2014)	semi-aquatic (PBDB)
Albertochampsa langstoni	SMM P67 15 3	Wilberg (2017)	semi-aquatic (PBDB)
Alligator mcgrewi	FMNH P 26242	Wilberg (2017)	semi-aquatic (PBDB)
Alligator mefferdi	AMNH 7016	Wilberg (2017)	semi-aquatic (PBDB)
Alligator mississippiensis	UF 10941	Wilberg (2017)	semi-aquatic (extant taxon)
Alligator olseni	reconstruction	White (1942)	semi-aquatic (PBDB)
Alligator prenasalis	YPM-PU 14063	Wilberg (2017)	semi-aquatic (PBDB)
Alligator sinensis	IVPP 1342	Wilberg (2017)	semi-aquatic (extant taxon)
Alligator thomsoni	AMNH 1736	Wilberg (2017)	semi-aquatic (PBDB)
Allodaposuchus precedens	reconstruction	Wilberg (2017)	semi-aquatic (PBDB)
Allognathosuchus haupti	HLMD-Me 1435	First-hand examination	semi-aquatic (PBDB)
Amphicotylus gilmorei	OMNH 2322	Wilberg (2017)	semi-aquatic (PBDB)
Amphicotylus lucasii	CM 1339	Wilberg (2017)	semi-aquatic (PBDB)
Anatosuchus minor	MNN GAD603	Wilberg (2017)	terrestrial (PBDB)
Anteophthalmosuchus hooleyi	IRSNB R47	Martin *et al*. (2016)	semi-aquatic (PBDB)

Anthracosuchus balrogus	UF/IGM 67	Hastings *et al*. (2015)	marine (Mannion *et al*. 2015)
Aplestosuchus sordidus	LPRP/USP 0229a	First-hand examination	terrestrial (PBDB)
Araripesuchus gomesii	reconstruction	Hecht (1991)	terrestrial (PBDB)
Araripesuchus patagonicus	reconstruction	Wilberg (2017)	terrestrial (PBDB)
Araripesuchus tsangatsangana	FMNH PR 2297	First-hand examination	terrestrial (PBDB)
Araripesuchus wegeneri	MNN GAD 19	Wilberg (2017)	terrestrial (PBDB)
Arenysuchus gascabadiolorum	MPZ ELI-1	Puértolas-Pascual *et al*. (2011)	semi-aquatic (PBDB)
Argochampsa krebsi	reconstruction	Wilberg (2017)	marine (Mannion *et al*. 2015)
Armadillosuchus arrudai	UFRJ DG 303-R	Marinho and Carvalho (2009)	terrestrial (PBDB)
Asiatosuchus germanicus	GM XIV 4757-a	Wilberg (2017)	semi-aquatic (PBDB)
Atlantosuchus coupatezi	reconstruction	Wilberg (2017)	marine (Mannion *et al*. 2015)
Australosuchus clarkae	reconstruction	Wilberg (2017)	semi-aquatic (PBDB)
Baurusuchus salgadoensis	MPMA 62-0001-02	First-hand examination	terrestrial (PBDB)
Bernissartia fagesii	IRSNB R46	Wilberg (2017)	semi-aquatic (PBDB)
Borealosuchus acutidentatus	NMC 8544	Wilberg (2017)	semi-aquatic (PBDB)
Borealosuchus formidabilis	SMM P75.22.29	Wilberg (2017)	semi-aquatic (PBDB)
Borealosuchus sternbergii	MOR 701	Wilberg (2017)	semi-aquatic (PBDB)
Borealosuchus wilsoni	FMNH PR 1647	Wilberg (2017)	semi-aquatic (PBDB)
Boverisuchus magnifrons	GM XVIII 3094	Brochu (2012)	semi-aquatic (PBDB)
Boverisuchus vorax	FMNH PR 399	Wilberg (2017)	semi-aquatic (PBDB)
Brachychampsa montana	UCMP 133901	Wilberg (2017)	semi-aquatic (PBDB)
Brachyuranochampsa eversolei	AMNH 4993	Wilberg (2017)	semi-aquatic (PBDB)
Caiman crocodilus apaporiensis	FMNH 69823	Wilberg (2017)	semi-aquatic (extant taxon)
Caiman crocodilus chiapasius	FMNH 73739	Wilberg (2017)	semi-aquatic (extant taxon)

Caiman crocodilus fuscus	FMNH 69852	Wilberg (2017)	semi-aquatic (extant taxon)
Caiman latirostris	MACN 1232 7.021	Wilberg (2017)	semi-aquatic (extant taxon)
Caiman yacare	MLP 9147	Wilberg (2017)	semi-aquatic (extant taxon)
Caipirasuchus montealtensis	MPMA 68-0003-12	First-hand examination	terrestrial (PBDB)
Caipirasuchus paulistanus	MPMA 67-0001-00	First-hand examination	terrestrial (PBDB)
Caipirasuchus stenognathus	MZSP-PV 139	Pol *et al*. (2014)	terrestrial (PBDB)
Candidodon itapecuruense	UFRJ DG 114-R	Photos from other researchers	terrestrial (PBDB)
Ceratosuchus burdoshi	FMNH P 15576	First-hand examination	semi-aquatic (PBDB)
Cerrejonisuchus improcerus	UF/IGM 29	Hastings *et al*. (2010)	marine (Mannion *et al*. 2015)
Chalawan thailandicus	CAS42-20	Martin *et al*. (2014)	semi-aquatic (PBDB)
Chenanisuchus lateroculi	reconstruction	Wilberg (2017)	marine (Mannion *et al*. 2015)
Comahuesuchus brachybuccalis	reconstruction	Wilberg (2017)	terrestrial (PBDB)
Cricosaurus araucanensis	MLP 72-IV-7-1	Parrilla-Bel *et al*. (2013)	marine (Mannion *et al*. 2015)
Cricosaurus lithographicus	MOZ-PV 5787	Herrera *et al*. (2013)	marine (Mannion *et al*. 2015)
Crocodylus acer	AMNH 1240	Wilberg (2017)	semi-aquatic (PBDB)
Crocodylus acutus	TMM m-6040	Wilberg (2017)	semi-aquatic (extant taxon)
Crocodylus affinis	YPM 1345	Wilberg (2017)	semi-aquatic (PBDB)
Crocodylus depressifrons	IRSNB R251	Wilberg (2017)	semi-aquatic (PBDB)
Crocodylus intermedius	FMNH 75659	Wilberg (2017)	semi-aquatic (extant taxon)
Crocodylus johnstoni	USNM 064091	Wilberg (2017)	semi-aquatic (extant taxon)
Crocodylus megarhinus	AMNH 5061	Wilberg (2017)	semi-aquatic (PBDB)
Crocodylus mindorensis	FMNH 19891	Wilberg (2017)	semi-aquatic (extant taxon)
Crocodylus moreletii	TMM m-4980	Wilberg (2017)	semi-aquatic (extant taxon)

Crocodylus niloticus	TMM m-1786	Wilberg (2017)	semi-aquatic (extant taxon)
Crocodylus novaeguinea	FMNH 2854	Wilberg (2017)	semi-aquatic (extant taxon)
Crocodylus palaeindicus	NHMUK 39795	First-hand examination	semi-aquatic (PBDB)
Crocodylus palustris	AMNH 96134	Wilberg (2017)	semi-aquatic (extant taxon)
Crocodylus porosus	AMNH 29949	Wilberg (2017)	semi-aquatic (extant taxon)
Crocodylus rhombifer	AMNH 6179	Wilberg (2017)	semi-aquatic (extant taxon)
Crocodylus siamensis	AMNH (unknown no.)	Wilberg (2017)	semi-aquatic (extant taxon)
Dakosaurus andiniensis	MOZ 6146P	Wilberg (2017)	marine (Mannion *et al*. 2015)
Dibothrosuchus elaphros	IVPP V7907	First-hand examination	terrestrial (PBDB)
Diplocynodon darwini	IRSNB R 0412	Wilberg (2017)	semi-aquatic (PBDB)
Diplocynodon deponiae	HLMD-Be 147	First-hand examination	semi-aquatic (PBDB)
Diplocynodon hantoniensis	AMNH 27632	Wilberg (2017)	semi-aquatic (PBDB)
Diplocynodon ratelii	MNHN.F SG 13728 a b	First-hand examination	semi-aquatic (PBDB)
Dollosuchoides densmorei	IRSNB 1748	Wilberg (2017)	semi-aquatic (PBDB)
Dromicosuchus grallator	UNC 15574	Sues *et al*. (2003)	terrestrial (PBDB)
Dyrosaurus maghribensis	reconstruction	Wilberg (2017)	marine (Mannion *et al*. 2015)
Dyrosaurus phosphaticus	OUMNH KX.15904	First-hand examination	marine (Mannion *et al*. 2015)
Elosuchus cherifiensis	MNHN.R MRS 340–25	First-hand examination	semi-aquatic (PBDB)
Eogavialis africanus	YPM 6263	Wilberg (2017)	marine (Mannion *et al*. 2015)
Eoneustes bathonicus	unnumbered specimen	Mercier (1933)	marine (Mannion *et al*. 2015)
Eosuchus lerichei	IRSNB R 48	Wilberg (2017)	marine (Mannion *et al*. 2015)
Eosuchus minor	USNM V 299730	First-hand examination	marine (Mannion *et al*. 2015)

Eothoracosaurus mississippiensis	MSU 3293	Wilberg (2017)	marine (Mannion *et al*. 2015)
Euthecodon arambourgi	MNHN ZEL 001	Wilberg (2017)	semi-aquatic (PBDB)
Euthecodon brumpti	KNM-ER 1773	Wilberg (2017)	semi-aquatic (PBDB)
Eutretauranosuchus delfsi	BYU 17628	Wilberg (2017)	semi-aquatic (PBDB)
Fruitachampsa callisoni	LACM 120455a	Clark (2011)	terrestrial (PBDB)
Gavialis gangeticus	NHMUK unnumbered	Wilberg (2017)	semi-aquatic (extant taxon)
Gavialosuchus americana	BHI 126440	Wilberg (2017)	marine (Mannion *et al*. 2015)
Gavialosuchus eggenburgensis	KM F/1358	Wilberg (2017)	marine (Mannion *et al*. 2015)
Geosaurus grandis	BSPG AS-VI-1	Young and Andrade (2009)	marine (Mannion *et al*. 2015)
Gobiosuchus kielanae	reconstruction	Wilberg (2017)	terrestrial (PBDB)
Goniopholis baryglyphaeus	reconstruction	Wilberg (2017)	semi-aquatic (PBDB)
Goniopholis kiplingi	DORCM 12154	Andrade *et al*. (2011)	semi-aquatic (PBDB)
Goniopholis simus	NHMUK R 41098	Wilberg (2017)	semi-aquatic (PBDB)
Gracilineustes leedsi	NHMUK PV R3015	Wilberg (2017)	marine (Mannion *et al*. 2015)
Gryposuchus pachakamue	reconstruction	Salas-Gismondi *et al*. (2016)	semi-aquatic (PBDB)
Guarinisuchus munizi	DG-CTG-UFPE 5723	Wilberg (2017)	marine (Mannion *et al*. 2015)
Hamadasuchus rebouli	ROM 52620	Photos from other researchers	terrestrial (PBDB)
Hemiprotosuchus leali	PVL 3829	First-hand examination	terrestrial (PBDB)
Hesperosuchus agilis	CM 29894	Clark *et al*. (2000)	terrestrial (PBDB)
Hsisosuchus chungkingensis	cast of CNM V 1090	First-hand examination	semi-aquatic (PBDB)
Hsisosuchus dashanpuensis	ZDM 3405	Gao (2001)	semi-aquatic (PBDB)
Hyposaurus rogersii	reconstruction	Wilberg (2017)	marine (Mannion *et al*. 2015)
Iharkutosuchus makadii	MTM 2006.52.1	Wilberg (2017)	semi-aquatic (PBDB)

Ikanogavialis gameroi	MCNC unnumbered	Photos from other researchers	marine (Mannion *et al*. 2015)
Isisfordia duncani	reconstruction	Salisbury *et al*. (2000)	semi-aquatic (PBDB)
Junggarsuchus sloani	IVPP V14010	First-hand examination	terrestrial (PBDB)
Kambara implexidens	QM F29662	Wilberg (2017)	semi-aquatic (PBDB)
Kaprosuchus saharicus	MNN IGU12	Wilberg (2017)	terrestrial (PBDB)
Knoetschkesuchus guimarotae	reconstruction	Wilberg (2017)	semi-aquatic (PBDB)
Knoetschkesuchus langenbergensis	DFMMh/FV 200	Schwarz *et al*. (2017)	semi-aquatic (PBDB)
Leidyosuchus canadensis	ROM 1903	Wilberg (2017)	semi-aquatic (PBDB)
Libycosuchus brevirostris	BSPG 1912 VIII 574	Wilberg (2017)	terrestrial (PBDB)
Litargosuchus leptorhynchus	BP/1/5237	Clark and Sues (2002)	terrestrial (PBDB)
Lomasuchus palpebrosus	MOZ 4084 PV	Gasparini *et al*. (1991)	terrestrial (PBDB)
Lorosuchus nodosus	PVL 6219	First-hand examination	semi-aquatic (Kellner *et al*. 2014)
Machimosaurus buffetauti	SMNS 91415	Martin and Vincent (2013)	marine (Mannion *et al*. 2015)
Machimosaurus hugii	reconstruction	Krebs (1967)	marine (Mannion *et al*. 2015)
Machimosaurus mosae	BHN2R 1100	Young *et al*. (2014)	marine (Mannion *et al*. 2015)
Malawisuchus mwakasyungutiensis	Mal-49	Gomani (1997)	terrestrial (PBDB)
Maledictosuchus riclaensis	MPZ 2001/130a	Parrilla-Bel *et al*. (2013)	marine (Mannion *et al*. 2015)
Maomingosuchus petrolica	DM-F0001	Shan *et al*. (2017)	semi-aquatic (PBDB)
Mariliasuchus amarali	UFRJ-106R	Wilberg (2017)	terrestrial (PBDB)
Maroccosuchus zennaroi	UF unnumbered	Wilberg (2017)	marine (Mannion *et al*. 2015)
Mecistops cataphractus	AMNH 10075	Wilberg (2017)	semi-aquatic (extant taxon)
Melanosuchus fisheri	MCNC 243	Medina (1976)	semi-aquatic (PBDB)
Melanosuchus niger	UF 53600	Wilberg (2017)	semi-aquatic (extant taxon)
metriorhynchus brachyrhynchus	NHMUK R3804	Wilberg (2017)	marine (Mannion *et al*. 2015)

metriorhynchus brachyrhynchus	NHMUK PV R3699	Wilberg (2017)	marine (Mannion *et al*. 2015)
metriorhynchus casamiquelai	MGHF 1-08573	Wilberg (2017)	marine (Mannion *et al*. 2015)
Metriorhynchus geoffroyii	OUMNH J.29823	Grange and Benton (1996)	marine (Mannion *et al*. 2015)
Metriorhynchus superciliosus	NHMUK PV R6860	Wilberg (2017)	marine (Mannion *et al*. 2015)
Metriorhynchus superciliosus	NHMUK PV R6859	Wilberg (2017)	marine (Mannion *et al*. 2015)
Montealtosuchus arrudacamposi	MPMA 16-0007-04	First-hand examination	terrestrial (PBDB)
Mourasuchus amazonensis	DGM 526-R	Wilberg (2017)	semi-aquatic (PBDB)
Nannosuchus gracilidens	NHMUK 48217	First-hand examination	semi-aquatic (PBDB)
Notosuchus terrestris	MACN-PV RN 1037	Wilberg (2017)	terrestrial (PBDB)
Oceanosuchus boecensis	MHNH 9036	Wilberg (2017)	marine (Mannion *et al*. 2015)
Orthogenysuchus olseni	AMNH 5178	Wilberg (2017)	semi-aquatic (PBDB)
Orthosuchus stormbergi	SAM-PK-K409	Wilberg (2017)	terrestrial (PBDB)
Osteolaemus osborni	AMNH 10082	Wilberg (2017)	semi-aquatic (extant taxon)
Osteolaemus tetraspis	FMNH 98936	Wilberg (2017)	semi-aquatic (extant taxon)
Pakasuchus kapilimai	RRBP 08631	O'Connor *et al*. (2010)	terrestrial (PBDB)
Paleosuchus palpebrosus	YPM R 11407	Wilberg (2017)	semi-aquatic (extant taxon)
Paleosuchus trigonatus	AMNH R-58136	Photos from other researchers	semi-aquatic (extant taxon)
Paralligator gradilifrons	PIN 554-1	Turner (2015)	semi-aquatic (PBDB)
Paralligator major	PIN 3726/501	Turner (2015)	semi-aquatic (PBDB)
Peipehsuchus teleorhinus	IVPP V10098	First-hand examination	marine (Mannion *et al*. 2015)
Pelagosaurus typus	BRLSI M 1413	Wilberg (2017)	marine (Mannion *et al*. 2015)
Pholidosaurus purbeckensis	reconstruction	Wilberg (2017)	semi-aquatic (PBDB)
Pietraroiasuchus ormezzanoi	Specimen PC-2	Buscalioni *et al*. (2011)	semi-aquatic (PBDB)

Piscogavialis jugaliperforatus	SMNK PAL 1282	First-hand examination	marine (Mannion *et al*. 2015)
Planocrania datangensis	IVPP V5016	First-hand examination	semi-aquatic (PBDB)
Platysuchus multicrobiculatus	SMNS 9930	First-hand examination	marine (Mannion *et al*. 2015)
Procaimanoidea kayi	CM 9600	Wilberg (2017)	semi-aquatic (PBDB)
Prodiplocynodon langi	AMNH 108	Wilberg (2017)	semi-aquatic (PBDB)
Protosuchus haughtoni	BP/1/4770	Gow (2000)	terrestrial (PBDB)
Protosuchus richardsoni	reconstruction	Wilberg (2017)	terrestrial (PBDB)
Pseudhesperosuchus jachaleri	PVL 3830	First-hand examination	terrestrial (PBDB)
Purranisaurus potens	MJCM PV 2060	Herrera *et al*. (2015)	marine (Mannion *et al*. 2015)
Purussaurus brasiliensis	UFAC 1403	Wilberg (2017)	semi-aquatic (PBDB)
Purussaurus mirandae	UNEFM-CIAAP-1369	Aguilera *et al*. (2006)	semi-aquatic (PBDB)
Purussaurus neivensis	reconstruction	Wilberg (2017)	semi-aquatic (PBDB)
Rhabdognathus keiniensis	reconstruction	Wilberg (2017)	marine (Mannion *et al*. 2015)
Rhacheosaurus gracilis	NHMUK PV R3948	Parrilla-Bel *et al*. (2013)	marine (Mannion *et al*. 2015)
Rimasuchus lloydi	NHMUK R 14145	Wilberg (2017)	semi-aquatic (PBDB)
Rugosuchus nonganensis	IGV 33	Wilberg (2017)	semi-aquatic (PBDB)
Sarcosuchus imperator	MNN 604	Wilberg (2017)	semi-aquatic (PBDB)
Sebecus icaeorhinus	reconstruction	Wilberg (2017)	terrestrial (PBDB)
Shantungosuchus brachycephalus	IVPP V4020	First-hand examination	terrestrial (PBDB)
Siamosuchus phuphokensis	reconstruction	Wilberg (2017)	semi-aquatic (PBDB)
Sichuanosuchus shuhanensis	IVPP V10594	First-hand examination	terrestrial (PBDB)
Simosuchus clarki	UA 8679	Wilberg (2017)	terrestrial (PBDB)
Siquisiquesuchus venezuelensis	MBLUZ-P-5050	Brochu and Rincón (2004)	marine (Mannion *et al*. 2015)
Sokotosuchus ianwilsoni	reconstruction	Wilberg (2017)	marine (Mannion *et al*. 2015)

Sphagesaurus huenei	cast of MACN-PV 19037	First-hand examination	terrestrial (PBDB)
Sphenosuchus acutus	reconstruction	Walker (1990)	terrestrial (PBDB)
Stangerochampsa mccabei	RTMP.86.61.1	Wilberg (2017)	semi-aquatic (PBDB)
Steneosaurus bollensis	MNHN.F 1885-28	Wilberg (2017)	marine (Mannion *et al*. 2015)
Steneosaurus edwardsi	NHMUK PV R2865	Wilberg (2017)	marine (Mannion *et al*. 2015)
Steneosaurus gracilirostris	NHMUK PV R15500	Wilberg (2017)	marine (Mannion *et al*. 2015)
Steneosaurus leedsi	NHMUK PV R3320	Wilberg (2017)	marine (Mannion *et al*. 2015)
Steneosaurus leedsi	NHMUK PV R3806	Wilberg (2017)	marine (Mannion *et al*. 2015)
Steneosaurus megistorhynchus	OUMNH J.29850	First-hand examination	marine (Mannion *et al*. 2015)
Stolokrosuchus lapparenti	MNN GDF 600	Wilberg (2017)	terrestrial (PBDB)
Stratiotosuchus maxhechti	DGM 1477-R	First-hand examination	terrestrial (PBDB)
Suchodus durobrivensis	NHMUK PV R2618	Wilberg (2017)	marine (Mannion *et al*. 2015)
Susisuchus anatoceps	SMNK PAL 3804	First-hand examination	semi-aquatic (PBDB)
Teleidosaurus calvadosii	cast of NHMUK PV R 2681	Wilberg (2017)	marine (Mannion *et al*. 2015)
Teleosaurus cadomensis	reconstruction	Wilberg (2017)	marine (Mannion *et al*. 2015)
Terminonaris browni	AMNH 5851	Wilberg (2017)	marine (Mannion *et al*. 2015)
Terminonaris robusta	AMNH 5850	Wilberg (2017)	marine (Mannion *et al*. 2015)
Terrestrisuchus gracilis	reconstruction	Crush (1984)	terrestrial (PBDB)
Thecachampsa antiqua	USNM 25243	Wilberg (2017)	marine (Mannion *et al*. 2015)
Thecachampsa carolinensis	ChM PV 4279	Erickson and Sawyer (1996)	marine (Mannion *et al*. 2015)
thoracosaurus macrorhynchus	LO 3076T	Wilberg (2017)	marine (Mannion *et al*. 2015)
Tomistoma schlegelii	RMBR unnumbered	Wilberg (2017)	semi-aquatic (extant taxon)
Torvoneustes carpenteri	reconstruction	Wilkinson *et al*. (2008)	marine (Mannion *et al*. 2015)

Toyotamaphimeia machikanensis	MOUF00001	Kobayashi *et al*. (2006)	semi-aquatic (PBDB)
Tsoabichi greenriverensis	SMNK PAL 2334 cast	First-hand examination	semi-aquatic (PBDB)
Tyrannoneustes lythrodectikos	PETMG:R176	Foffa and Young (2014)	marine (Mannion *et al*. 2015)
Uberabasuchus terrificus	CPP 0630*	Wilberg (2017)	terrestrial (PBDB)
Vectisuchus leptognathus	reconstruction	Wilberg (2017)	semi-aquatic (PBDB)
Voay robustus	NHMUK R 36685	Wilberg (2017)	semi-aquatic (PBDB)
Wannaganosuchus brachymans	SMM P76.28.247*	Wilberg (2017)	semi-aquatic (PBDB)
Yacarerani boliviensis	MNK-PAL 5063*	Novas *et al*. (2009)	terrestrial (PBDB)

Appendix C: Example R script of the geometric morphometric analyses performed in Chapter 3

```
#############################################################################
#Crocodylomorpha cranial shape variation and disparity
#Example script

#set work directory#
setwd("C:/R/9 - GM Crocs")


#load required packages
library(geomorph)
library(phytools)
library(paleotree)
library(dispRity)
library(RVAideMemoire)


#############################################################################
#loading landmark data for geometric morphometric analyses
#reads the .tps file with landmark data:
landmark_data <- readland.tps(file = "GM_Crocs.tps", specID="ID",
readcurves = TRUE)


#reads classifier (for groups):
classifiers <- read.table(file = "Classifiers.txt", header = T)


#sorting taxa for matching order of classifiers
taxa <- dimnames(landmark_data)
taxa <- taxa[[3]]
order_taxa <- match(classifiers$ID,taxa)
which(is.na(order_taxa)) #looking for NAs
landmark_data <- landmark_data[,,order_taxa]


#reads semi-landmark curve
semi_landmarks <- read.csv("curveslide.csv")
```

```
#performs GPA onto landmark data
landmarks_aligned <- gpagen(landmark_data, curves = semi_landmarks,
surfaces = NULL, PrinAxes = TRUE, max.iter = NULL, ProcD = F, Proj = TRUE,
print.progress = TRUE)

#performs PCA and plots morphospace (PC1 vs PC2) with tip labels
PCA_crocs <- plotTangentSpace(landmarks_aligned$coords, label =
names(landmarks_aligned$Csize))



################################################################################
#estimating interobserver error in shape data

#converting data to "geomorph data frame" format
#different groups represent different observer/operator during landmarks
digitisation
#information about observer/operator has to be in the classifiers file
gdf <- geomorph.data.frame(shape = landmarks_aligned$coords, groups =
classifiers$observer)

#performs Procrustes ANOVA
ANOVA_test <- procD.lm(shape ~ groups, data = gdf, iter=999)

#calculates the percentage of variation explained by interobserver error
interobserver_error <- (ANOVA_test$SS[1]/ANOVA_test$SS[3])*100
interobserver_error


################################################################################
#Burnaby's back-projection method (BBPM) or orthogonal projection method

#using PC2 as a proxy for measurement error
#calculating L (the orthogonal subspace)
f1 <- as.numeric(PCA_crocs$pc.scores[,2])
names(f1) <- names(landmarks_aligned$Csize)
I <- diag(1,209)
L <- I-f1 %*% ginv(t(f1) %*% f1) %*% t(f1)

#transforming landmark data into a two-dimensional array
landmark_data_2D <- two.d.array(landmark_data)
landmark_data_2D <- t(landmark_data_2D) #transpose
```

```
#projecting landmarks to orthogonal subspace
corrected_landmark_data <- landmark_data_2D %*% L
corrected_landmark_data <- t(corrected_landmark_data) #transpose

#back to three-dimensional array (64 landmarks and 2 dimensions)
corrected_landmark_data <- arrayspecs(corrected_landmark_data,64,2)


#performs GPA onto corrected landmark data
corrected_landmarks_aligned <- gpagen(corrected_landmark_data, curves =
semi_landmarks, surfaces = NULL, PrinAxes = TRUE, max.iter = NULL, ProcD =
F, Proj = TRUE, print.progress = TRUE)

#performs PCA
PCA_crocs_corrected <- plotTangentSpace(corrected_landmarks_aligned$coords,
label = names(corrected_landmarks_aligned$Csize))



################################################################################
#estimating ancestral states for phylomorphospace

#loads crocodylomorph tree
tree <- read.tree("croc_tree.tre")

#reads the age data (FADs and LADs)
ages <- read.table("croc_ages.txt", header=T)
#rownames as taxa names
rownames(ages) <- ages$taxa
ages <- ages[,-1]


#times-scaling the tree using the "mbl" method
#generates 20 randomly resolved time-scaled trees
ttrees <- timePaleoPhy(tree, ages, type="mbl", randres=T, vartime=1,
ntrees=20, dateTreatment="minMax")


#dropping taxa from trees for which I do not have landmark data
for (i in 1: length(ttrees)) {
ttrees[[i]] <- drop.tip (ttrees[[i]],
ttrees[[i]]$tip.label[!(ttrees[[i]]$tip.label %in%
unlist(dimnames(landmarks_aligned$coords)[3]))])}
```

```
#sorting taxa for matching order of trees' tip labels
taxa2 <- ttrees[[1]]$tip.label
order_taxa2 <- match(taxa2, classifiers$ID)
which(is.na(order_taxa2)) #looking for NAs
classifiers <- classifiers[order_taxa2,]
landmark_data <- landmark_data[,,order_taxa2]


#performs GPA onto landmark data
landmarks_aligned <- gpagen(landmark_data, curves = semi_landmarks,
surfaces = NULL, PrinAxes = TRUE, max.iter = NULL, ProcD = F, Proj = TRUE,
print.progress = TRUE)

#performs PCA and plots morphospace (PC1 vs PC2) with tip labels
PCA_crocs <- plotTangentSpace(landmarks_aligned$coords, label =
names(landmarks_aligned$Csize))

#estimates ancestral states and plots phylomorphospace using one time-
scaled tree
PhyloMorphoSpace <- plotGMPhyloMorphoSpace(ttrees[[1]],
landmarks_aligned$coords, tip.labels=F, node.labels=F)


#estimating phylogenetic signal (Kmult) of shape data
phylo_signal <- physignal(landmarks_aligned$coords, ttrees[[1]],iter=999)


#############################################################################
#disparity analyses

#gets Principal Components (PC) scores from landmark data previously
subjected to GPA
PC_scores <- geomorph.ordination(landmarks_aligned)


#gets PC scores for ancestors (from previous ancestral states estimation)
ancestral_states_array <- arrayspecs(PhyloMorphoSpace,64,2)
ancestral_states_aligned <- gpagen(ancestral_states_array, curves =
semi_landmarks, surfaces = NULL, PrinAxes = TRUE, max.iter = NULL, ProcD =
F, Proj = TRUE, print.progress = TRUE)
ancestral_PC_scores <- geomorph.ordination(ancestral_states_aligned)

#merges PC scores from tips and ancestors in a single object
PC_scores_all <- rbind(PC_scores, ancestral_PC_scores)
```

```
#disparity-through-time analysis using time-slicing method with 20 time
slices and gradual model
#creates time subsets
subsets <- chrono.subsets(data = PC_scores_all, tree = ttrees[[1]], method
= "continuous", model = "proximity", time = 20, FADLAD = ages)

#bootstrapping the time subsets
boot_subsets <- boot.matrix(subsets, bootstraps = 1000)

#calculates disparity (sum of variances)
disparity <- dispRity(boot_subsets, metric = c(sum, variances))
```

Appendix D: Supplementary results of the disparity-through-time analyses of Chapter 3

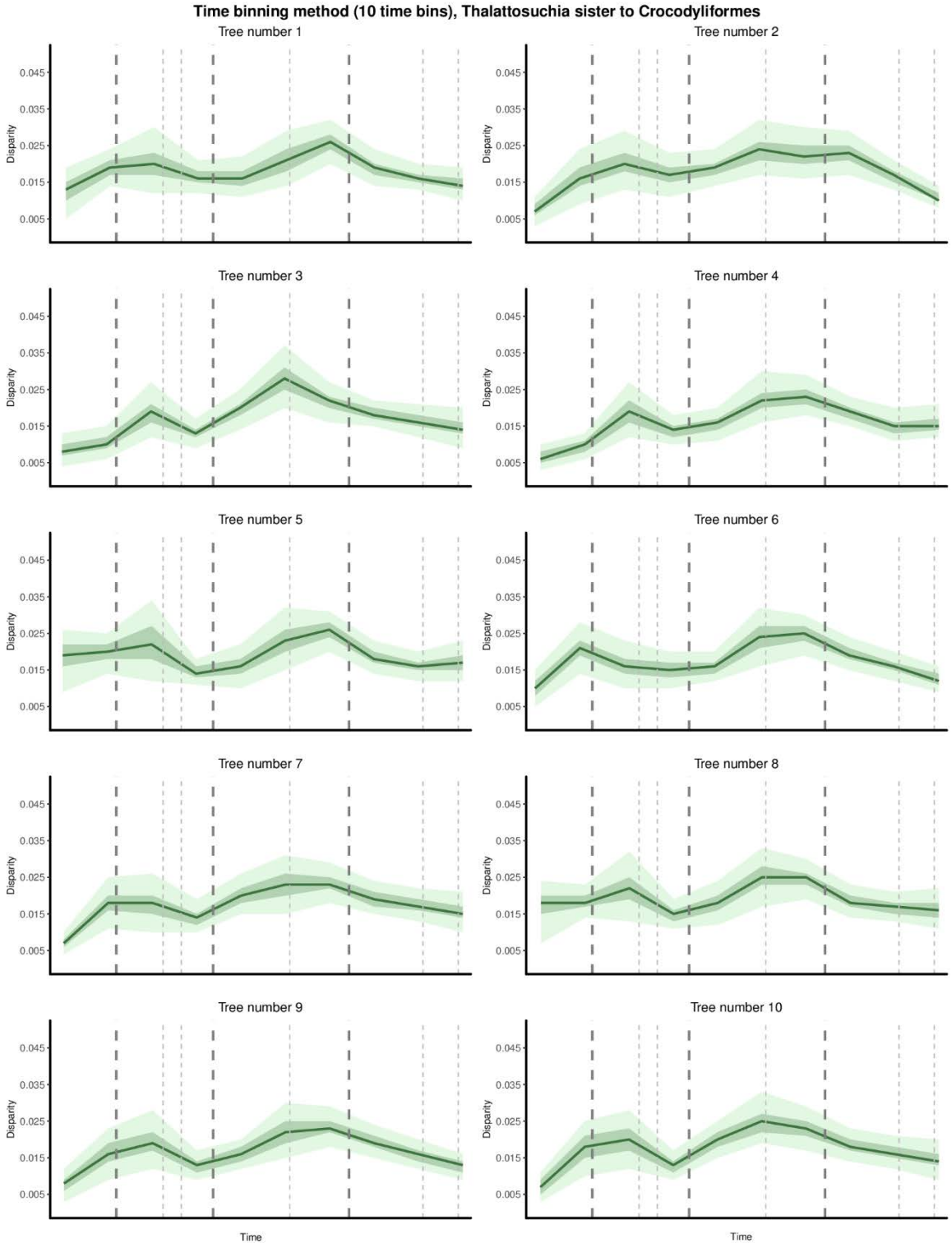

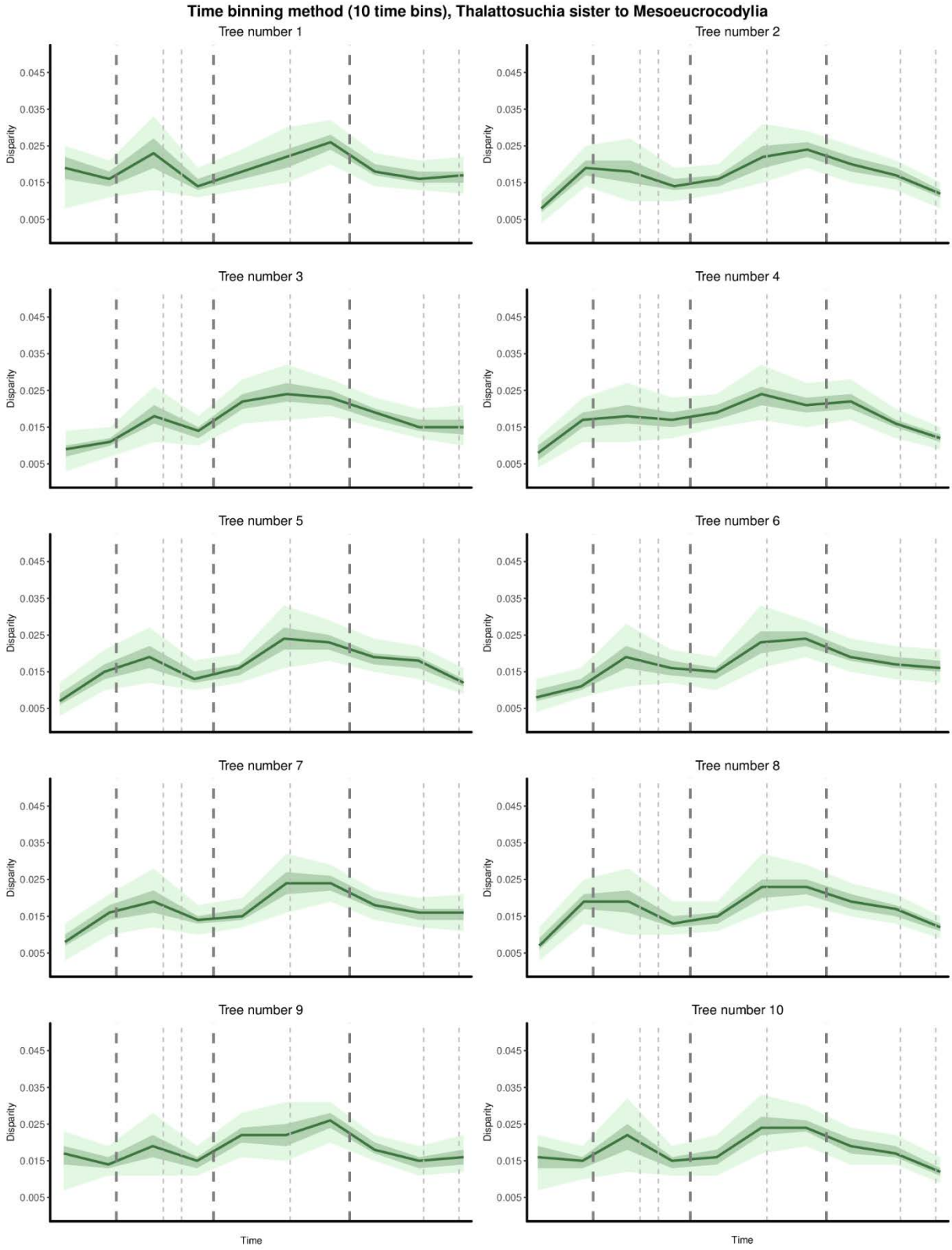
Time binning method (10 time bins), Thalattosuchia sister to Mesoeucrocodylia
Tree number 1
Tree number 2
Tree number 3
Tree number 4
Tree number 5
Tree number 6
Tree number 7
Tree number 8
Tree number 9
Tree number 10
Disparity
0.045
0.035
0.025
0.015
0.005
Time

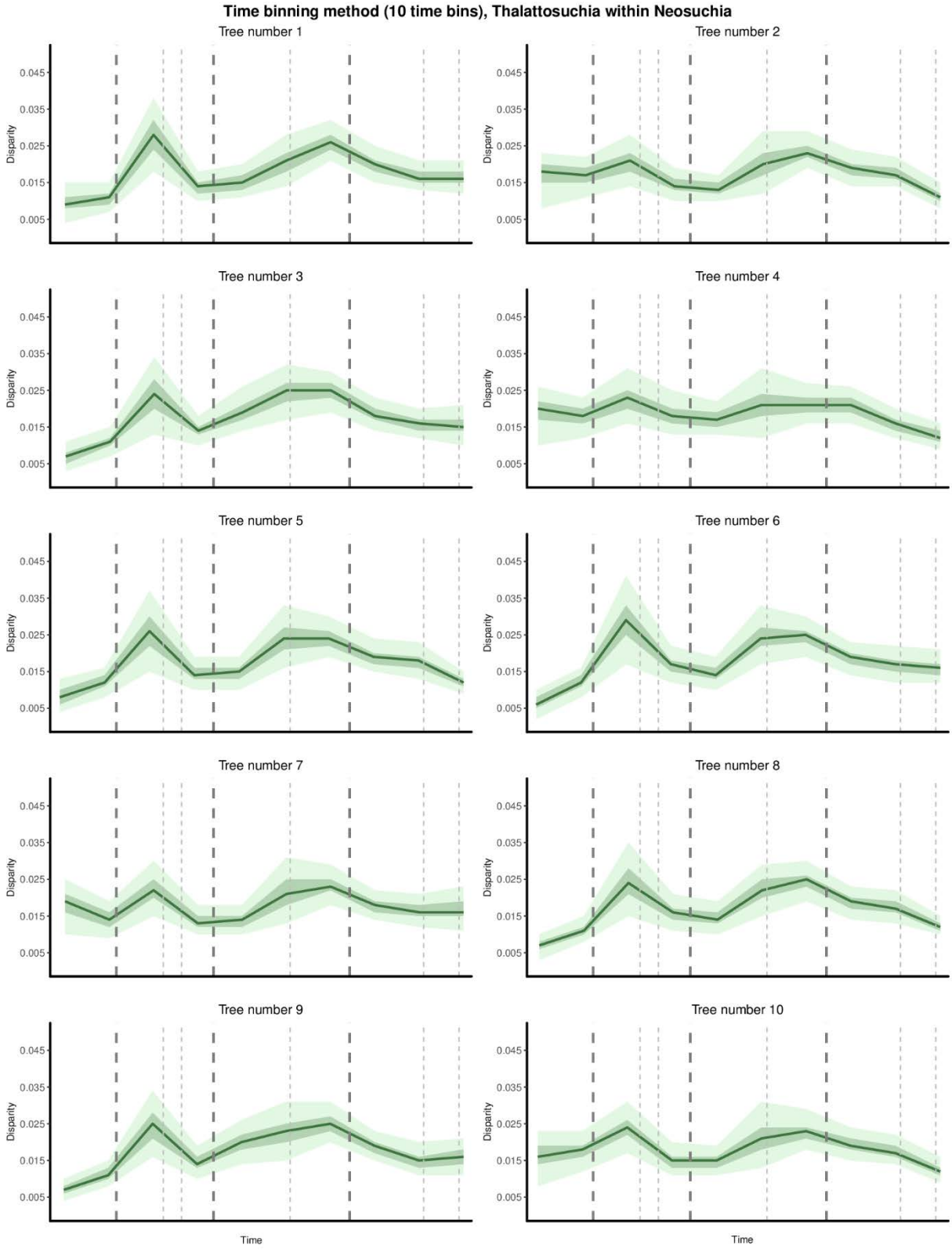
Time binning method (10 time bins), Thalattosuchia within Neosuchia
Tree number 1
Tree number 2
Tree number 3
Tree number 4
Tree number 5
Tree number 6
Tree number 7
Tree number 8
Tree number 9
Tree number 10
Disparity
0.045
0.035
0.025
0.015
0.005
Time

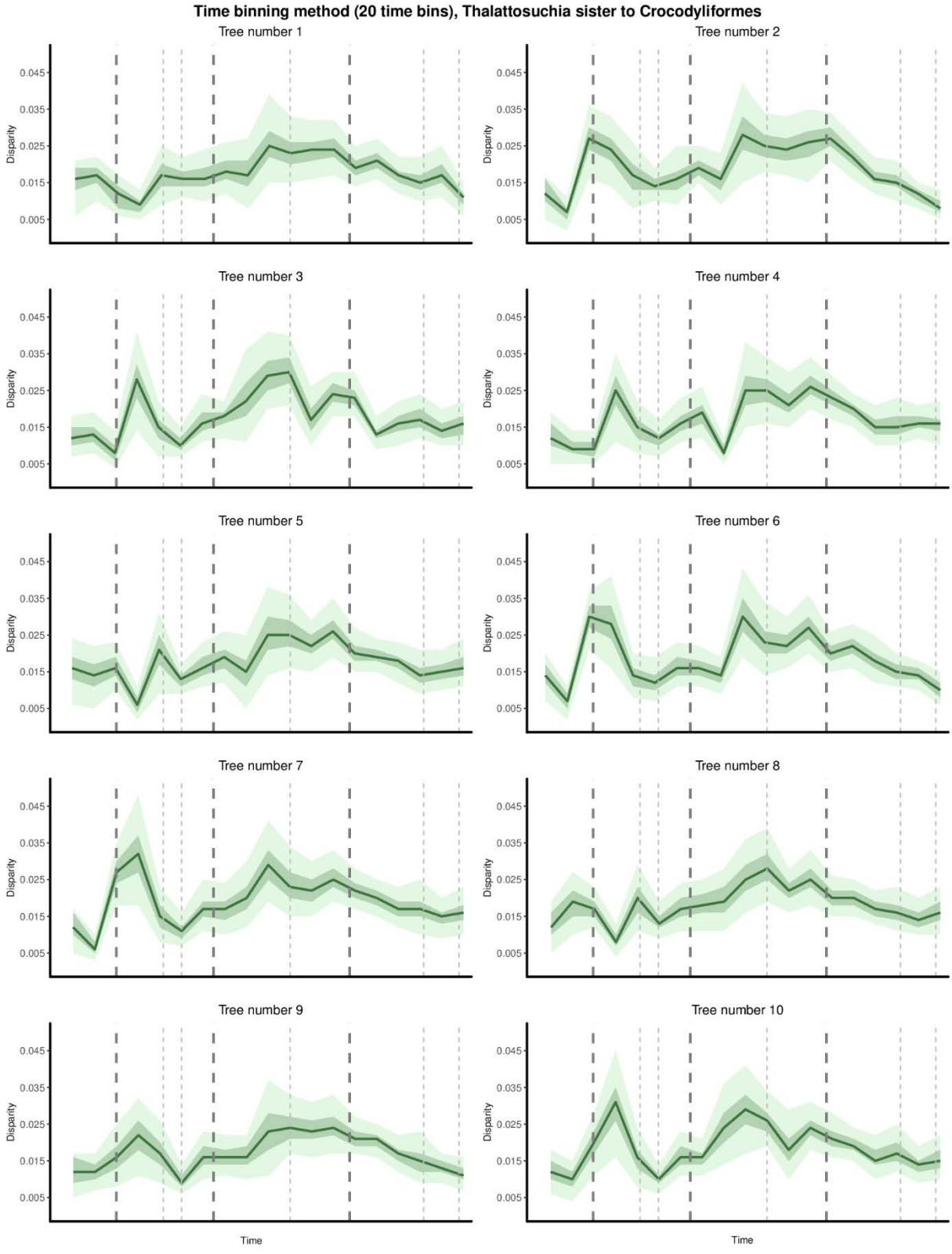
Time binning method (20 time bins), Thalattosuchia sister to Crocodyliformes
Tree number 1
Tree number 2
Tree number 3
Tree number 4
Tree number 5
Tree number 6
Tree number 7
Tree number 8
Tree number 9
Tree number 10
Disparity
0.045
0.035
0.025
0.015
0.005
Time

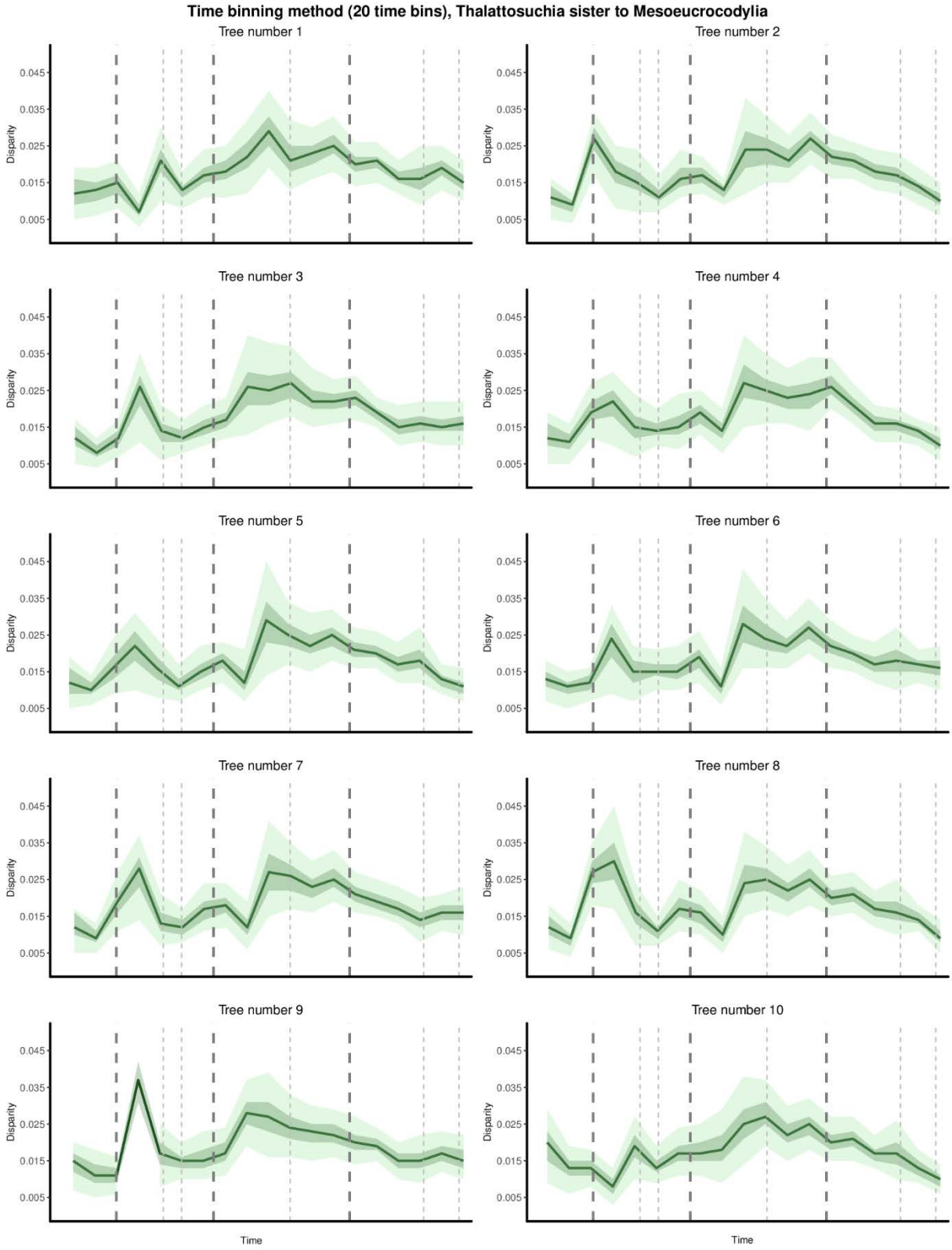
Time binning method (20 time bins), Thalattosuchia sister to Mesoeucrocodylia
Tree number 1
Tree number 2
Tree number 3
Tree number 4
Tree number 5
Tree number 6
Tree number 7
Tree number 8
Tree number 9
Tree number 10
Disparity
0.045
0.035
0.025
0.015
0.005
Time

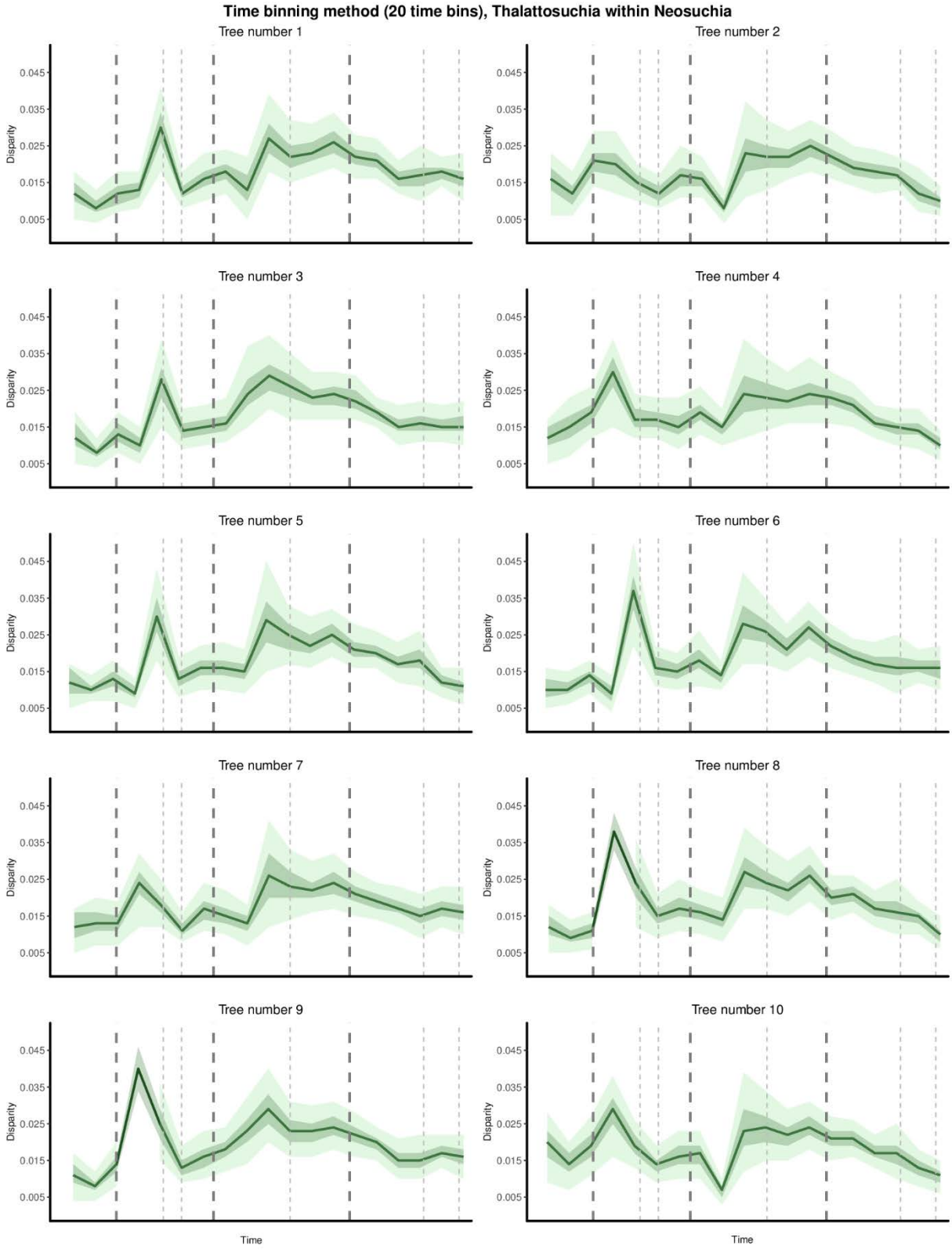
Time binning method (20 time bins), Thalattosuchia within Neosuchia
Tree number 1
Tree number 2
Tree number 3
Tree number 4
Tree number 5
Tree number 6
Tree number 7
Tree number 8
Tree number 9
Tree number 10
Disparity
0.045
0.035
0.025
0.015
0.005
Time

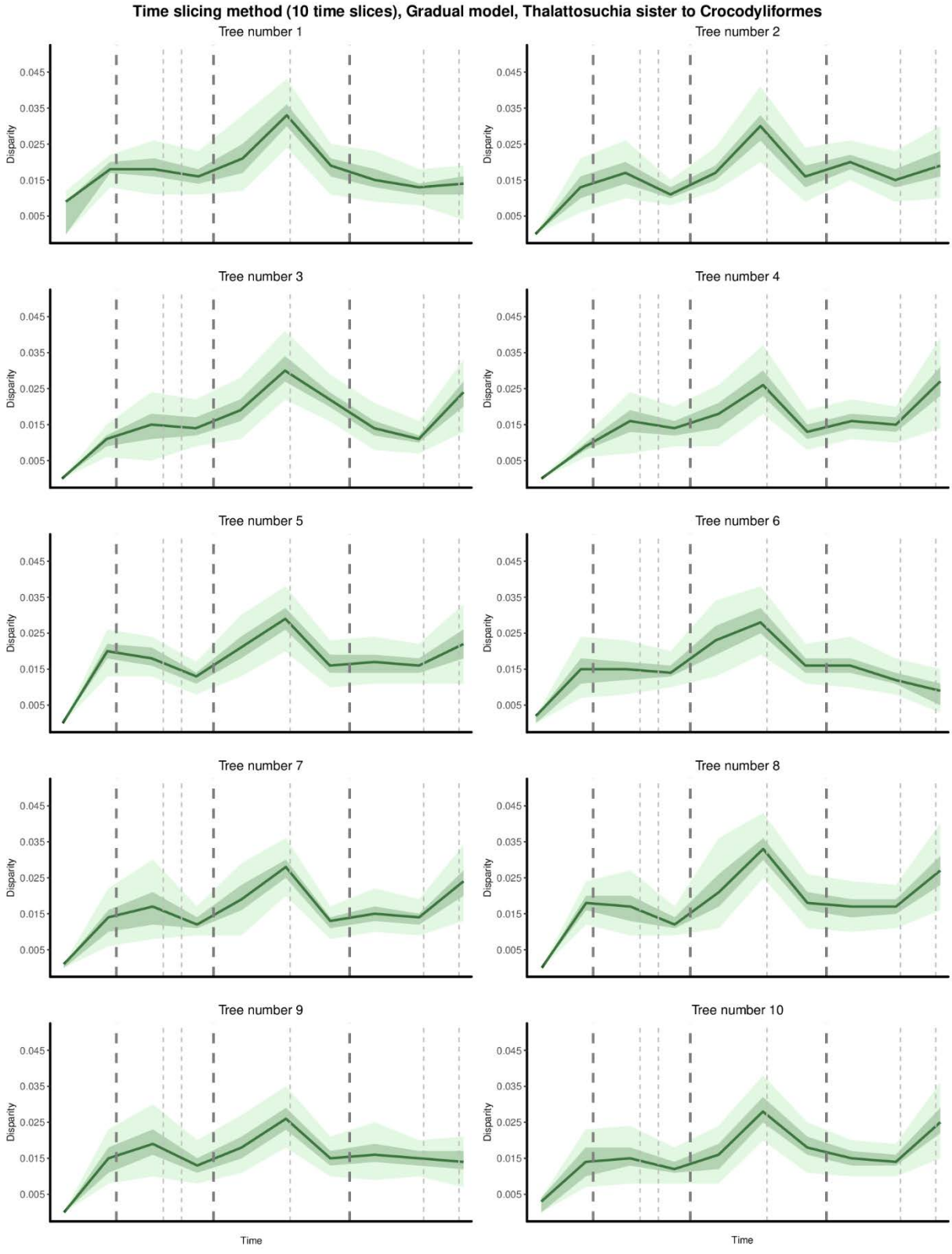
Time slicing method (10 time slices), Gradual model, Thalattosuchia sister to Crocodyliformes
Tree number 1
Tree number 2
Tree number 3
Tree number 4
Tree number 5
Tree number 6
Tree number 7
Tree number 8
Tree number 9
Tree number 10
Disparity
0.045
0.035
0.025
0.015
0.005
Time

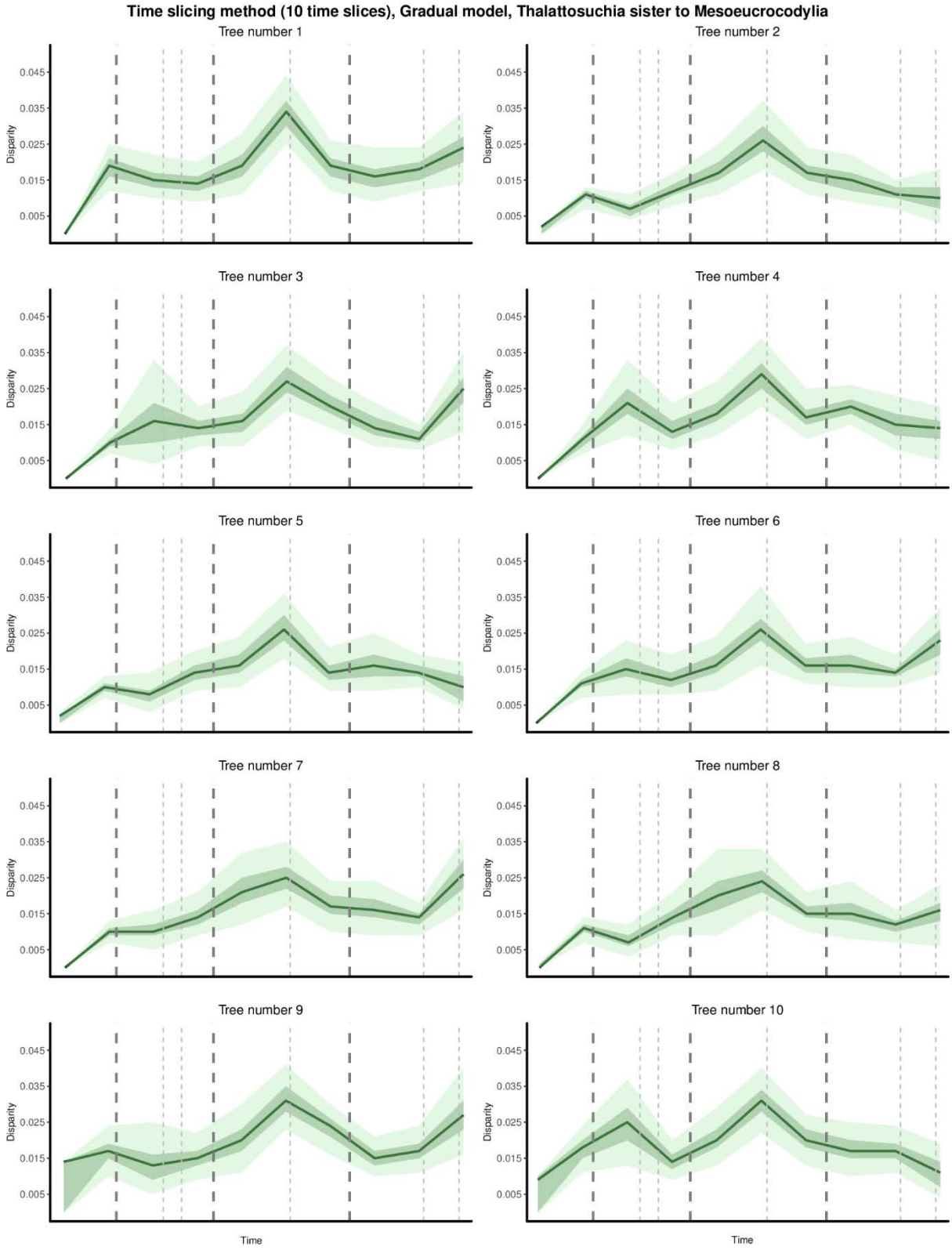
Time slicing method (10 time slices), Gradual model, Thalattosuchia sister to Mesoeucrocodylia
Tree number 1
Tree number 2
Tree number 3
Tree number 4
Tree number 5
Tree number 6
Tree number 7
Tree number 8
Tree number 9
Tree number 10
Disparity
0.045
0.035
0.025
0.015
0.005
Time

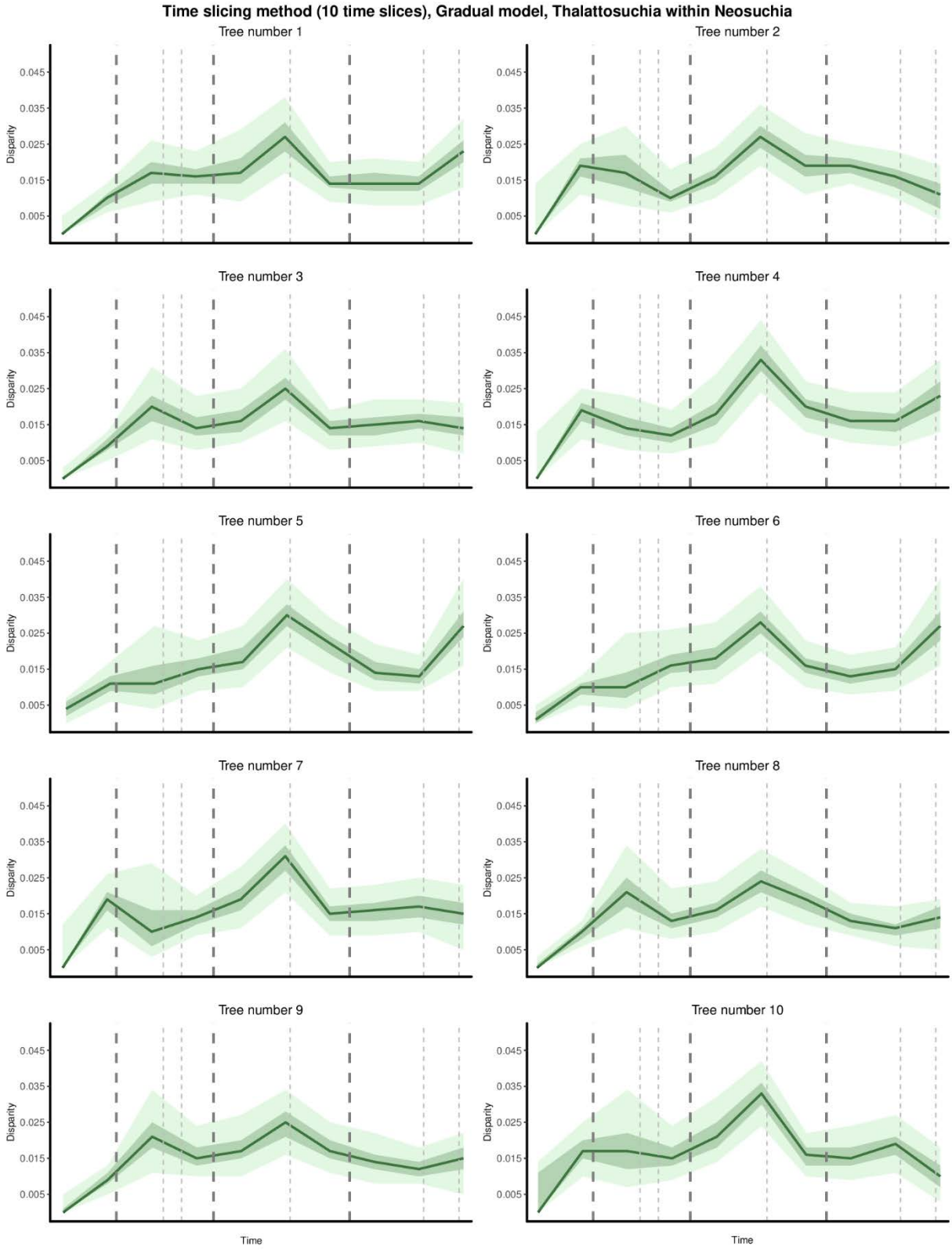
Time slicing method (10 time slices), Gradual model, Thalattosuchia within Neosuchia
Tree number 1
Tree number 2
Tree number 3
Tree number 4
Tree number 5
Tree number 6
Tree number 7
Tree number 8
Tree number 9
Tree number 10
Disparity
0.045
0.035
0.025
0.015
0.005
Time

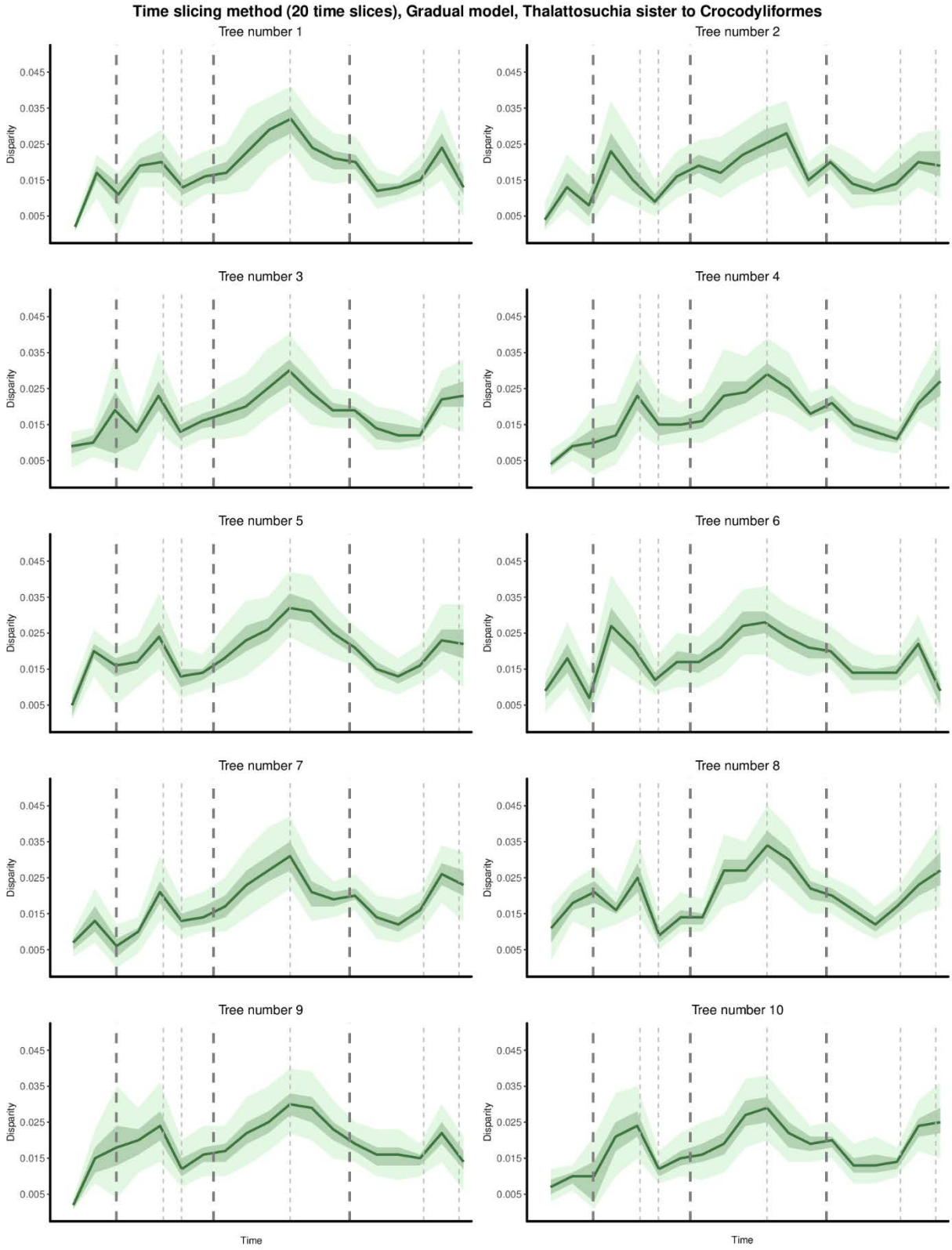
Time slicing method (20 time slices), Gradual model, Thalattosuchia sister to Crocodyliformes
Tree number 1
Tree number 2
Tree number 3
Tree number 4
Tree number 5
Tree number 6
Tree number 7
Tree number 8
Tree number 9
Tree number 10
Disparity
0.045
0.035
0.025
0.015
0.005
Time

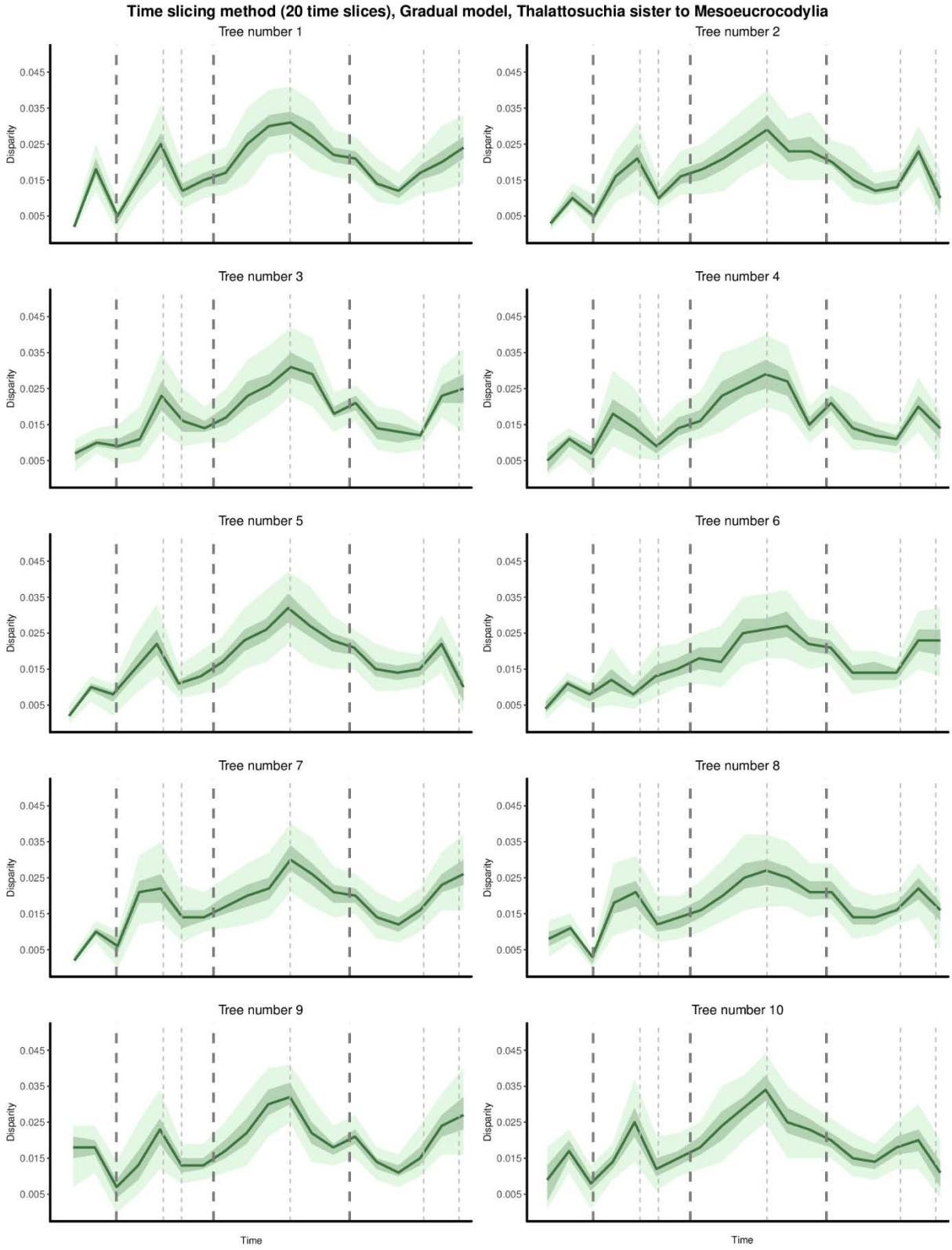
Time slicing method (20 time slices), Gradual model, Thalattosuchia sister to Mesoeucrocodylia
Tree number 1
Tree number 2
Tree number 3
Tree number 4
Tree number 5
Tree number 6
Tree number 7
Tree number 8
Tree number 9
Tree number 10
Disparity
0.045
0.035
0.025
0.015
0.005
Time

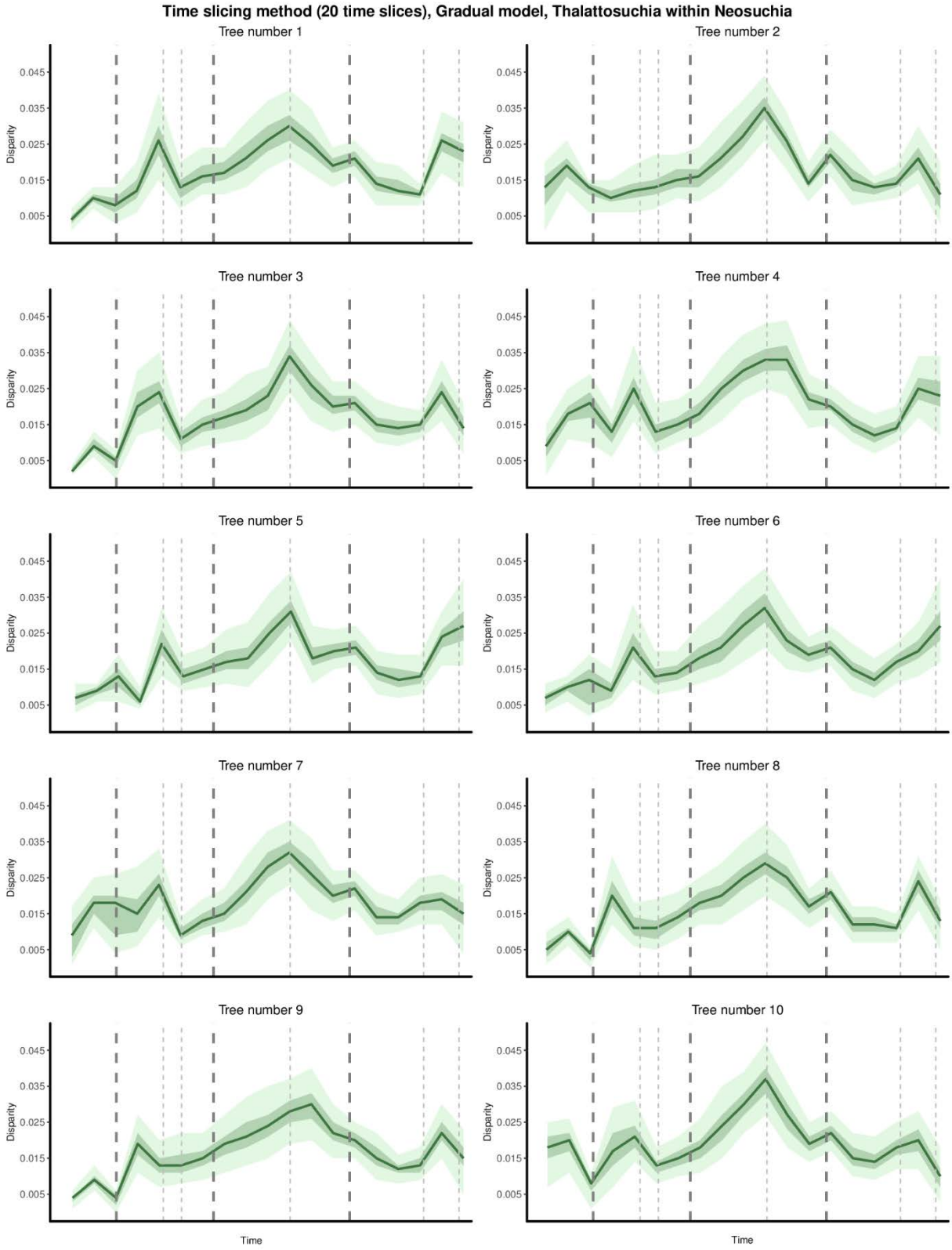
Time slicing method (20 time slices), Gradual model, Thalattosuchia within Neosuchia
Tree number 1
Tree number 2
Tree number 3
Tree number 4
Tree number 5
Tree number 6
Tree number 7
Tree number 8
Tree number 9
Tree number 10
Disparity
0.045
0.035
0.025
0.015
0.005
Time

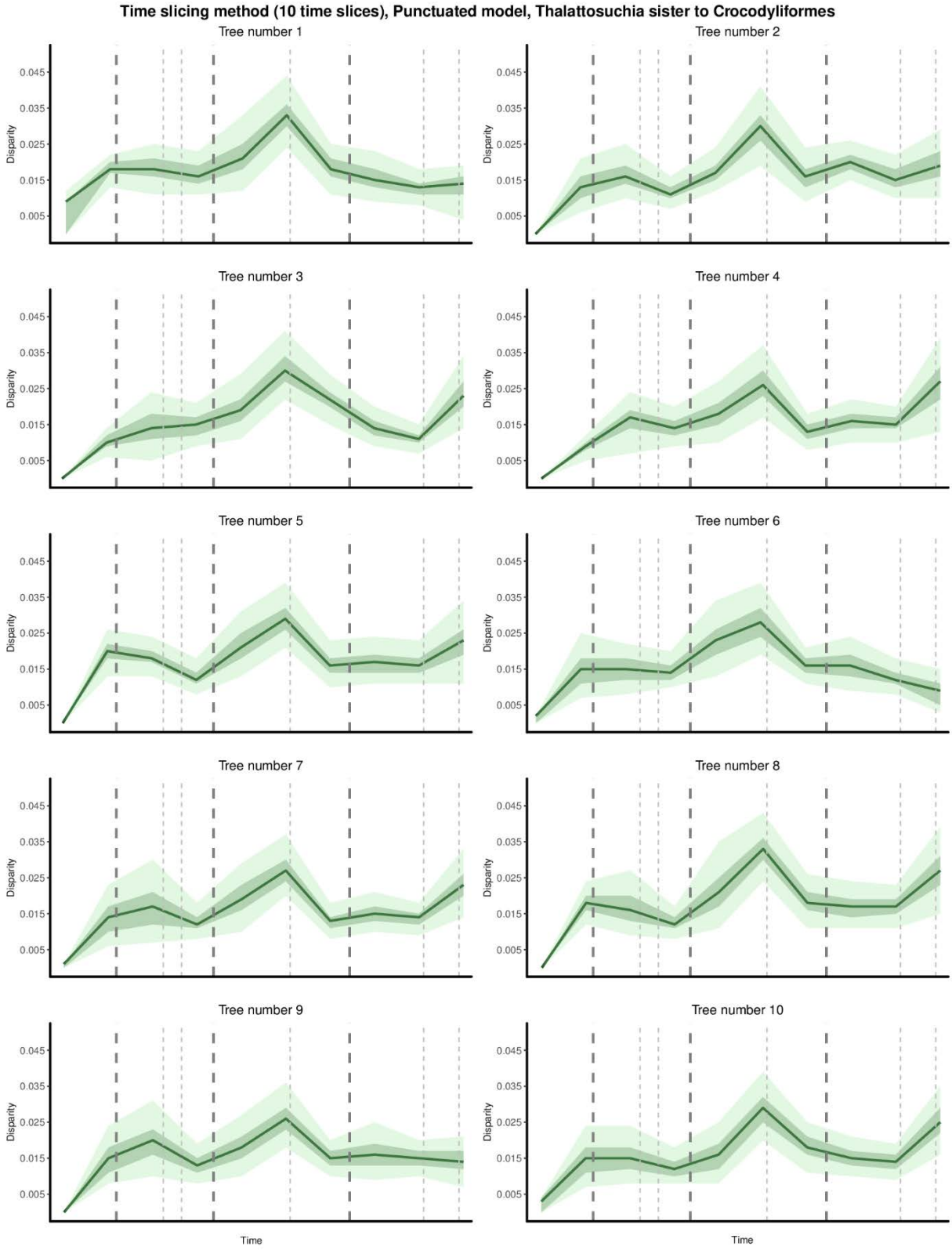
Time slicing method (10 time slices), Punctuated model, Thalattosuchia sister to Crocodyliformes
Tree number 1
Tree number 2
Tree number 3
Tree number 4
Tree number 5
Tree number 6
Tree number 7
Tree number 8
Tree number 9
Tree number 10
Disparity
0.045
0.035
0.025
0.015
0.005
Time

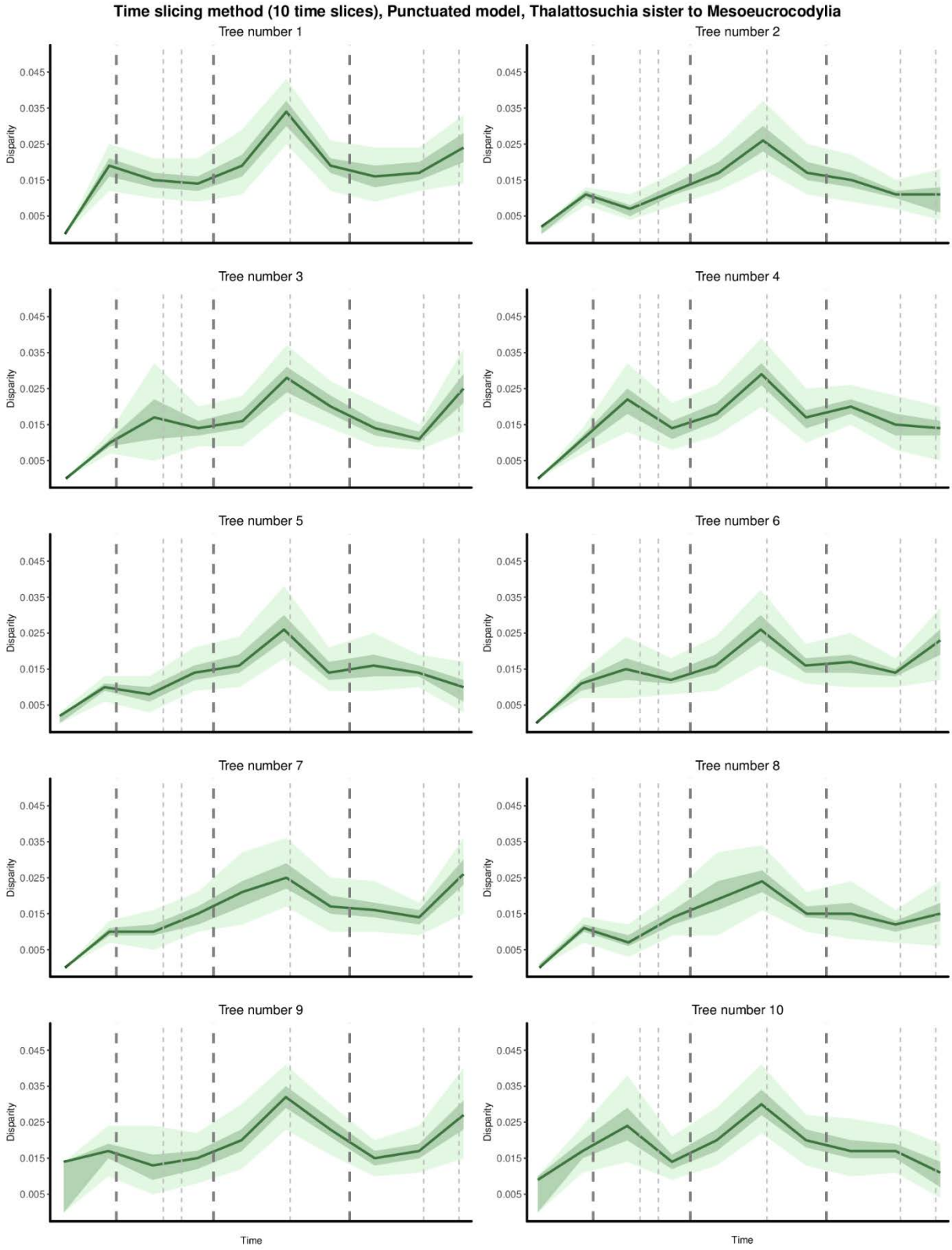
Time slicing method (10 time slices), Punctuated model, Thalattosuchia sister to Mesoeucrocodylia
Tree number 1
Tree number 2
Tree number 3
Tree number 4
Tree number 5
Tree number 6
Tree number 7
Tree number 8
Tree number 9
Tree number 10
Disparity
0.045
0.035
0.025
0.015
0.005
Time

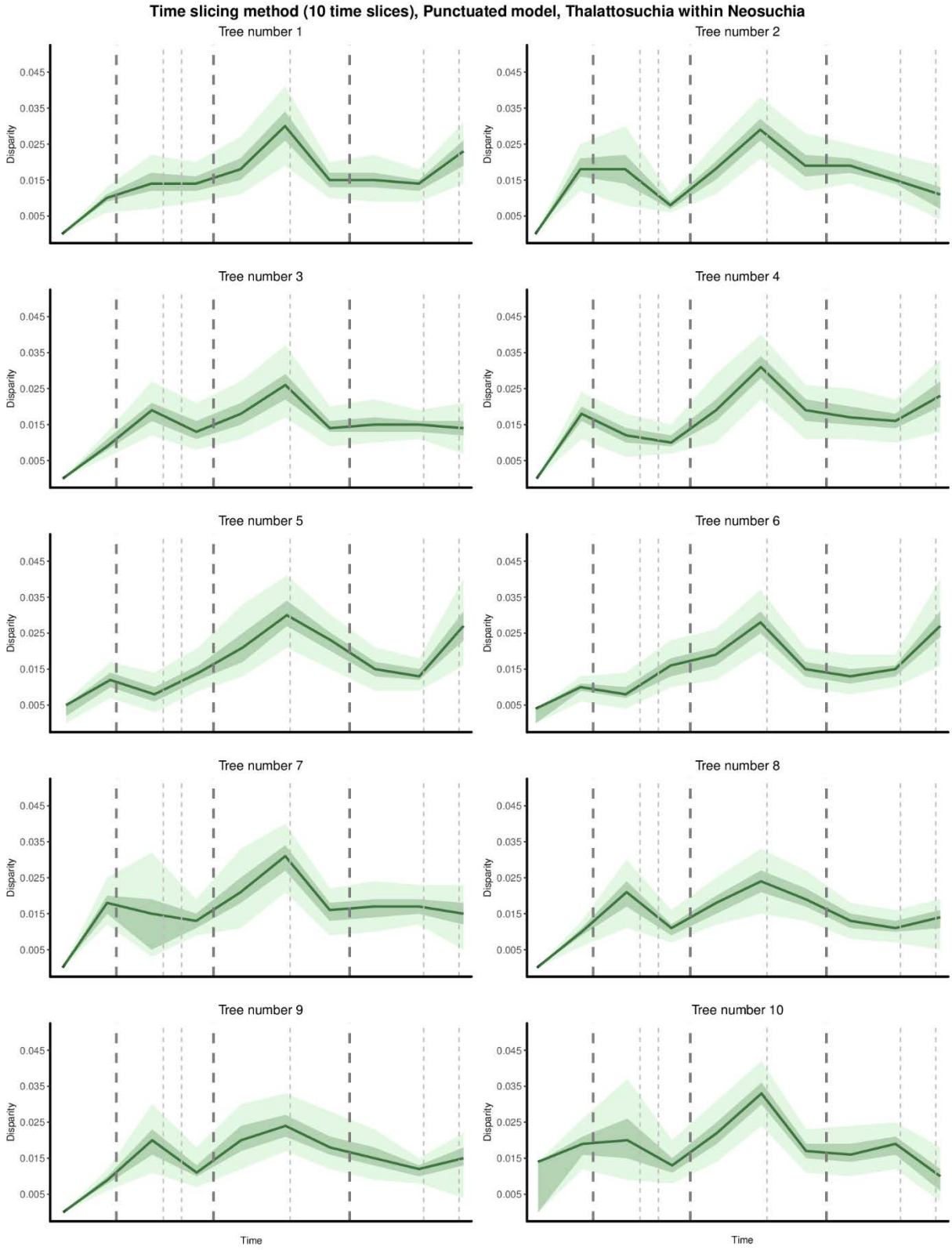
Time slicing method (10 time slices), Punctuated model, Thalattosuchia within Neosuchia
Tree number 1
Tree number 2
Tree number 3
Tree number 4
Tree number 5
Tree number 6
Tree number 7
Tree number 8
Tree number 9
Tree number 10
Disparity
0.045
0.035
0.025
0.015
0.005
Time

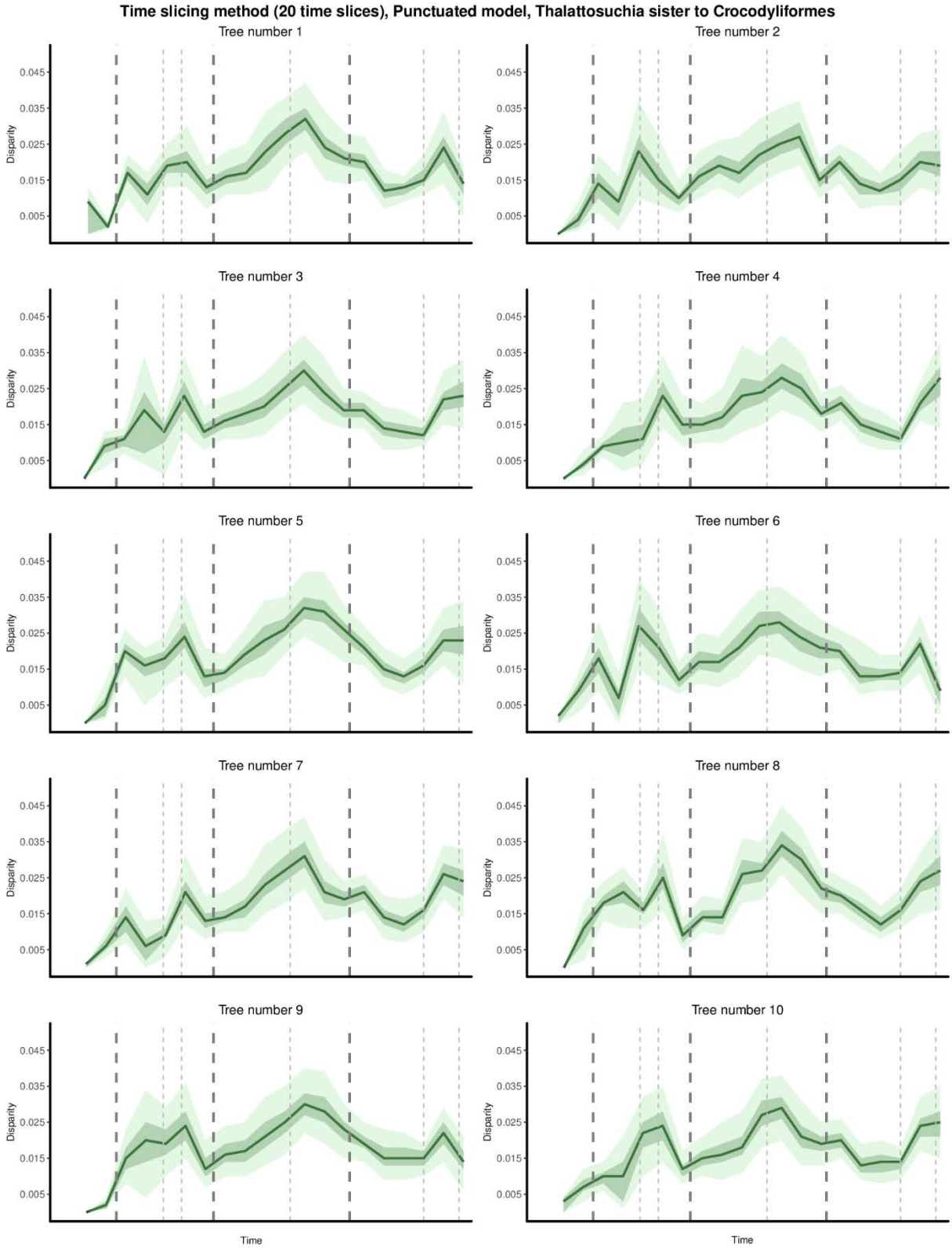
Time slicing method (20 time slices), Punctuated model, Thalattosuchia sister to Crocodyliformes
Tree number 1
Tree number 2
Tree number 3
Tree number 4
Tree number 5
Tree number 6
Tree number 7
Tree number 8
Tree number 9
Tree number 10
Disparity
0.045
0.035
0.025
0.015
0.005
Time

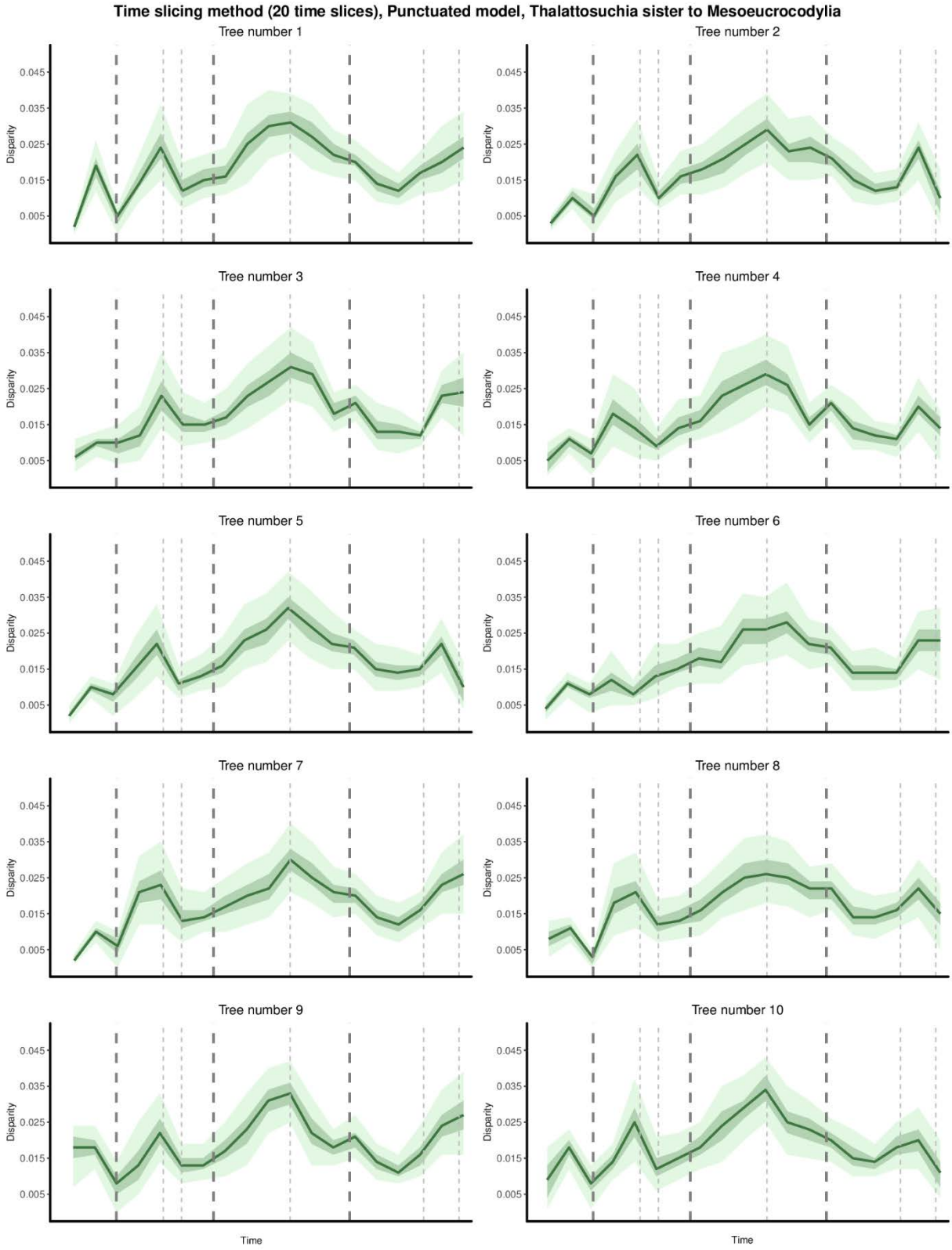
Time slicing method (20 time slices), Punctuated model, Thalattosuchia sister to Mesoeucrocodylia
Tree number 1
Tree number 2
Tree number 3
Tree number 4
Tree number 5
Tree number 6
Tree number 7
Tree number 8
Tree number 9
Tree number 10
Disparity
0.045
0.035
0.025
0.015
0.005
Time

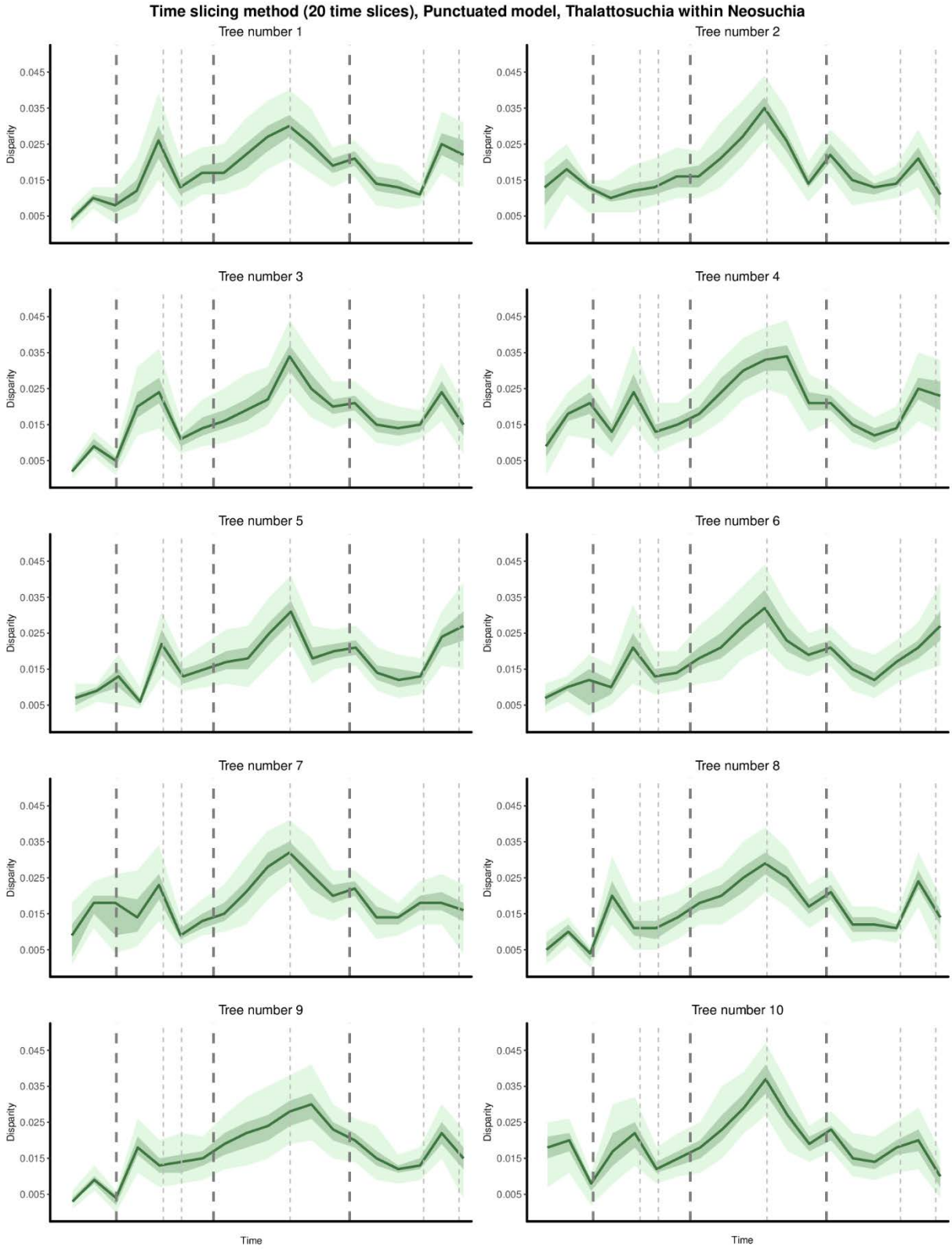
Time slicing method (20 time slices), Punctuated model, Thalattosuchia within Neosuchia
Tree number 1
Tree number 2
Tree number 3
Tree number 4
Tree number 5
Tree number 6
Tree number 7
Tree number 8
Tree number 9
Tree number 10
Disparity
0.045
0.035
0.025
0.015
0.005
Time

Appendix E: Supplementary information for Chapter 4

The supplementary material for Chapter 4 ("Heterochrony in the cranial evolution of notosuchians") was uploaded to the online repository Dryad (Godoy *et al*. 2018*d*) and can be found at: https://datadryad.org/resource/doi:10.5061/dryad.7m48r. The online content includes three documents and one compacted (ZIP file) file:

- Supporting information: file (.docx) containing supplementary text (with further explanation on the reconstruction of the ancestral ontogenetic trajectory), the complete list of sampled specimens, the description of the landmarks, as well as further tables and figures with supplementary results (including additional morphospaces, phylomorphospaces, regression scores and additional npMANOVA results).
- MorphoJ script (.morphoj): script used for all geometric morphometric analyses performed in Chapter 2.
- Thin plate spline: R script used for thin plate spline analyses.
- TPS files: compacted file containing .tps files with digitized landmarks of both lateral and dorsal view datasets.

References

ADAMS, D. C. 1999. Methods for shape analysis of landmark data from articulated structures. *Evolutionary Ecology Research*, **1,** 959–970.

ADAMS, D. C. 2014. A generalized K statistic for estimating phylogenetic signal from shape and other high-dimensional multivariate data. *Systematic Biology*, **63,** 685–697.

ADAMS, D. C. and OTÁROLA-CASTILLO, E. 2013. geomorph: an R package for the collection and analysis of geometric morphometric shape data. *Methods in Ecology and Evolution*, **4,** 393–399.

ADAMS, D. C., ROHLF, F. J. and SLICE, D. E. 2004. Geometric morphometrics: ten years of progress following the 'revolution'. *Italian Journal of Zoology*, **71,** 5–16.

AGUILERA, O. A., RIFF, D. and BOCQUENTIN-VILLANUEVA, J. 2006. A new giant *Purussaurus* (Crocodyliformes, Alligatoridae) from the upper Miocene Urumaco formation, Venezuela. *Journal of Systematic Palaeontology*, **4,** 221–232.

AHLBORN, B. K. and BLAKE, R. W. 1999. Lower size limit of aquatic mammals. *American Journal of Physics*, **67,** 920–922.

AKAIKE, H. 1974. A new look at the statistical model identification. *IEEE Transactions on Automatic Control*, **19,** 716–723.

ALBERCH, P., GOULD, S. J., OSTER, G. F. and WAKE, D. B. 1979. Size and shape in ontogeny and phylogeny. *Paleobiology*, **5,** 296–317.

ALBERDI, M. T., PRADO, J. L. and ORTIZ-JAUREGUIZAR, E. 1995. Patterns of body size changes in fossil and living Equini (Perissodactyla). *Biological Journal of the Linnean Society*, **54,** 349–370.

ALLSTEADT, J. and LANG, J. W. 1995. Incubation temperature affects body size and energy reserves of hatchling American alligators (*Alligator mississippiensis*). *Physiological Zoology*, **68,** 76–97.

ALROY, J. 1998. Cope's rule and the dynamics of body mass evolution in North American fossil mammals. *Science*, **280,** 731–734.

ALROY, J. 2001. A multispecies overkill simulation of the end-Pleistocene megafaunal mass extinction. *Science*, **292,** 1893–1896.

ALROY, J. 2010. Fair sampling of taxonomic richness and unbiased estimation of origination and extinction rates. 55–80. *In* ALROY, J. and HUNT, G. (eds.). *Quantitative Methods in Paleobiology*. The Paleontological Society Papers.

ANDERSON, M. J. 2001. A new method for non-parametric multivariate analysis of variance. *Austral Ecology*,. **26,** 32–46.

ANDRADE, M. B., YOUNG, M. T., DESOJO, J. B. and BRUSATTE, S. L. 2010. The evolution of extreme hypercarnivory in Metriorhynchidae (Mesoeucrocodylia: Thalattosuchia) based on evidence from microscopic denticle morphology. *Journal of Vertebrate Paleontology*, **30,** 1451–1465.

ANDRADE, M. B., EDMONDS, R., BENTON, M. J. and SCHOUTEN, R. 2011. A new Berriasian species of *Goniopholis* (Mesoeucrocodylia, Neosuchia) from England, and a review of the genus. *Zoological Journal of the Linnean Society*, **163**, 66–108.

ARNOLD, S. J. 2014. Phenotypic evolution: the ongoing synthesis. *The American Naturalist*. **1836,** 729–746.

ARNOLD, S. J., PFRENDER, M. E. and JONES, A. G. 2001. The adaptive landscape as a conceptual bridge between micro-and macroevolution. *Genetica*, **112,** 9–32.

AWRAMIK, S. M. 1992. The oldest records of photosynthesis. *Photosynthesis Research*, **33,** 75–89.

BANAVAR, J. R., COOKE, T. J., RINALDO, A. and MARITAN, A. 2014. Form, function, and evolution of living organisms. *Proceedings of the National Academy of Sciences*, **111,** 3332–3337.

BAPST, D. W. 2012. paleotree: an R package for paleontological and phylogenetic analyses of evolution. *Methods in Ecology and Evolution*, **3,** 803–807.

BAPST, D. W. 2013. A stochastic rate-calibrated method for time-scaling phylogenies of fossil taxa. *Methods in Ecology and Evolution*, **4,** 724–733.

BAPST, D. W. 2014*a*. Preparing paleontological datasets for phylogenetic comparative methods. 515–544. *In* GARAMSZEGI, L. Z. (ed.). *Modern Phylogenetic Comparative Methods and Their Application in Evolutionary Biology*. Springer Berlin Heidelberg.

BAPST, D. W. 2014*b*. Assessing the effect of time-scaling methods on phylogeny-based analyses in the fossil record. *Paleobiology*, **40,** 331–351.

BARBOSA, J. A., KELLNER, A. W. A. and VIANA, M. S. S. 2008. New dyrosaurid crocodylomorph and evidences for faunal turnover at the K–P transition in Brazil. *Proceedings of the Royal Society of London B*, **275,** 1385–1391.

BARRIOS, F., PAULINA-CARABAJAL, A. and BONA P. 2016. A new peirosaurid (Crocodyliformes, Mesoeucrocodylia) from the Upper Cretaceous of Patagonia, Argentina. *Ameghiniana*, **53,** 14–25.

BATES, K. T., MANNING, P. L., HODGETTS, D. and SELLERS, W. I. 2009. Estimating mass properties of dinosaurs using laser imaging and 3D computer modelling. *PLoS One*, **4,** e4532.

BATEZELLI, A. 2017. Continental systems tracts of the Brazilian Cretaceous Bauru Basin and their relationship with the tectonic and climatic evolution of South America. *Basin Research*, **29,** 1–25.

BEAULIEU, J. M. and O'MEARA, B. C. 2016. *OUwie: Analysis of Evolutionary Rates in an OU Framework. R package version 1.50*. https://CRAN.R-project.org/package=OUwie.

BEAULIEU, J. M., JHWUENG, D. C., BOETTIGER, C. and O'MEARA, B. C. 2012. Modeling stabilizing selection: expanding the Ornstein–Uhlenbeck model of adaptive evolution. *Evolution*, **66,** 2369–2383.

BELL, E. A., BOEHNKE, P., HARRISON, T. M. and MAO, W. L. 2015. Potentially biogenic carbon preserved in a 4.1 billion-year-old zircon. *Proceedings of the National Academy of Sciences*, **112,** 14518–14521.

BENJAMINI, Y. and HOCHBERG, Y. 1995. Controlling the false discovery rate: a practical and powerful approach to multiple testing. *Journal of the Royal Statistical Society Series B*, **57,** 289–300.

BENSON, R. B. and BUTLER, R. J. 2011. Uncovering the diversification history of marine tetrapods: ecology influences the effect of geological sampling biases. 191–208. *In* McGOWAN, A. J. and SMITH, A. B. (eds.). *Comparing the Geological and Fossil Records: Implications for Biodiversity Studies*. Geological Society, London, Special Publications, **358**.

BENSON, R. B., MANNION, P. D., BUTLER, R. J., UPCHURCH, P., GOSWAMI, A. and EVANS, S. E. 2013. Cretaceous tetrapod fossil record sampling and faunal turnover: implications for biogeography and the rise of modern clades. *Palaeogeography, Palaeoclimatology, Palaeoecology*, **372,** 88–107.

BENSON, R. B. J., FRIGOT, R. A., GOSWAMI, A., ANDRES, B. and BUTLER, R. J. 2014*a*. Competition and constraint drove Cope's rule in the evolution of giant flying reptiles. *Nature Communications*, **5,** 3567.

BENSON, R. B., CAMPIONE, N. E., CARRANO, M. T., MANNION, P. D., SULLIVAN, C., UPCHURCH, P. and EVANS, D. C. 2014*b*. Rates of dinosaur body mass evolution indicate 170 million years of sustained ecological innovation on the avian stem lineage. *PLoS Biology*, **12,** e1001853.

BENSON, R. B., HUNT, G., CARRANO, M. T. and CAMPIONE, N. 2018. Cope's rule and the adaptive landscape of dinosaur body size evolution. *Palaeontology*, **61,** 13–48.

BENTON, M. J. 2015. Exploring macroevolution using modern and fossil data. *Proceedings of the Royal Society of London B,* **282,** 20150569.

BENTON, M. and CLARK, J. M. 1988. Archosaur phylogeny and the relationships of the Crocodylia. 295–338. *In* BENTON, M. (ed.). *The phylogeny and Classification of the Tetrapods*. Clarendon Press.

BENTON, M. and HARPER, D. A. 2013. *Introduction to Paleobiology and the Fossil Record*. John Wiley & Sons.

BENTON, M. J., FORTH, J. and LANGER, M. C. 2014. Models for the rise of the dinosaurs. *Current Biology*, **24,** R87–R95.

BERNER, D. 2011. Size correction in biology: how reliable are approaches based on (common) principal component analysis? *Oecologia*, **166,** 961–971.

BHULLAR, B. A., MARUGÁN-LOBÓN, J., RACIMO, F., BEVER, G. S., ROWE, T. B., NORELL, M. A. and ABZHANOV, A. 2012. Birds have paedomorphic dinosaur skulls. *Nature*, **487,** 223–226.

BLOMBERG, S. P., GARLAND, T. and IVES, A. R. 2003. Testing for phylogenetic signal in comparative data: behavioral traits are more labile. *Evolution*, **57,** 717–745.

BONA, P. and DESOJO, J. B. 2011. Osteology and cranial musculature of *Caiman latirostris* (Crocodylia: Alligatoridae). *Journal of Morphology*, **272,** 780–795.

BONA, P., EZCURRA, M. D., BARRIOS, F. and BLANCO, M. V. F. 2018. A new Palaeocene crocodylian from southern Argentina sheds light on the early history of caimanines. *Proceedings of the Royal Society of London B*, **285,** 20180843.

BONNAN, M. F., FARLOW, J. O. and MASTERS, S. L. 2008. Using linear and geometric morphometrics to detect intraspecific variability and sexual dimorphism in femoral shape in *Alligator mississippiensis* and its implications for sexing fossil archosaurs. *Journal of Vertebrate Paleontology*, **28,** 422–431.

BOOKSTEIN, F. L. 1991. *Morphometric Tools for Landmark Data*. Cambridge University Press.

BOOKSTEIN, F. L. 1996. Applying landmark methods to biological outline data. 59–70. *In* MARDIA, K. V., GILL, C. A. and DRYDEN, I. L (eds.). *Image Fusion and Shape Variability*. Leeds University Press.

BOOKSTEIN, F. L. 1997. Landmark methods for forms without landmarks: morphometrics of group differences in outline shape. *Medical Image Analysis*, **1,** 225–243.

BOOKSTEIN, F. L. 1998. A hundred years of morphometrics. *Acta Zoologica Academiae Scientiarum Hungaricae*, **44,** 7–59.

BRAZAITIS, P. and WATANABE, M. E. 2011. Crocodilian behaviour: a window to dinosaur behaviour? *Historical Biology*, **23,** 73–90.

BROCHU, C. A. 1997. A review of "*Leidyosuchus*" (Crocodyliformes, Eusuchia) from the Cretaceous through Eocene of North America. *Journal of Vertebrate Paleontology*, **17,** 679–697.

BROCHU, C. A. 1999. Phylogenetics, taxonomy, and historical biogeography of Alligatoroidea. *Journal of Vertebrate Paleontology*, **19,** 9–100.

BROCHU, C. A. 2001. Crocodylian snouts in space and time: phylogenetic approaches toward adaptive radiation. *American Zoologist*, **41,** 564–585.

BROCHU, C. A. 2003. Phylogenetic approaches toward crocodylian history. *Annual Review of Earth and Planetary Sciences*, **31,** 357–397.

BROCHU, C. A. 2006. Osteology and phylogenetic significance of *Eosuchus minor* (Marsh, 1870) new combination, a longirostrine crocodylian from the late Paleocene of North America. *Journal of Paleontology*, **80,** 162–186.

BROCHU, C. A. 2010. A new alligatorid from the lower Eocene Green River Formation of Wyoming and the origin of caimans. *Journal of Vertebrate Paleontology*, **30,** 1109–1126.

BROCHU, C. A. 2011. Phylogenetic relationships of *Necrosuchus ionensis* Simpson, 1937 and the early history of caimanines. *Zoological Journal of the Linnean Society*, **163,** S228–S256.

BROCHU, C. A. 2012. Phylogenetic relationships of Palaeogene ziphodont eusuchians and the status of *Pristichampsus* Gervais, 1853. *Earth and Environmental Science Transactions of the Royal Society of Edinburgh*, **103,** 521–550.

BROCHU, C. A. and RINCÓN, A. D. 2004. A gavialoid crocodylian from the Lower Miocene of Venezuela. *Special Papers in Palaeontology*, **71,** 61–79.

BROCHU, C. A. and STORRS, G. W. 2012. A giant crocodile from the Plio-Pleistocene of Kenya, the phylogenetic relationships of Neogene African crocodylines, and the antiquity of *Crocodylus* in Africa. *Journal of Vertebrate Paleontology*, **32,** 587–602.

BROCHU, C. A., PARRIS, D. C., GRANDSTAFF, B. S., DENTON, R. K. and GALLAGHER, W. B. 2012. A new species of *Borealosuchus* (Crocodyliformes, Eusuchia) from the Late Cretaceous–early Paleogene of New Jersey. *Journal of Vertebrate Paleontology*, **32,** 105–116.

BROCKLEHURST, N. 2016. Rates and modes of body size evolution in early carnivores and herbivores: a case study from Captorhinidae. *PeerJ*, **4,** e1555.

BROCKLEHURST, N. 2017. Rates of morphological evolution in Captorhinidae: an adaptive radiation of Permian herbivores. *PeerJ*, **5,** e3200.

BRONZATI, M., MONTEFELTRO, F. C. and LANGER, M. C. 2012. A species-level supertree of Crocodyliformes. *Historical Biology*, **24,** 598–606.

BRONZATI, M., MONTEFELTRO, F. C. and LANGER, M. C. 2015. Diversification events and the effects of mass extinctions on Crocodyliformes evolutionary history. *Royal Society Open Science*, **2,** 140385.

BRUSATTE, S. L., BENTON, M. J., RUTA, M. and LLOYD, G. T. 2008. Superiority, competition, and opportunism in the evolutionary radiation of dinosaurs. *Science*, **321,** 1485–1488.

BRUSATTE, S. L., BENTON, M. J., RUTA, M. and LLOYD, G. T. 2008. The first 50 Myr of dinosaur evolution: macroevolutionary pattern and morphological disparity. *Biology Letters*, **4,** 733–736.

BRUSATTE, S. L., BUTLER, R. J., BARRETT, P. M., CARRANO, M. T., EVANS, D. C., LLOYD, G. T., MANNION, P. D., NORELL, M. A., PEPPE, D. J., UPCHURCH, P. and WILLIAMSON, T. E. 2015. The extinction of the dinosaurs. *Biological Reviews*, **90,** 628–642.

BUCKLEY, G. A. and BROCHU, C. A. 1999. An enigmatic new crocodile from the Upper Cretaceous of Madagascar. *Cretaceous Fossil Vertebrates*, **60,** 149–175.

BUCKLEY, G. A., BROCHU, C. A., KRAUSE, D. W. and POL, D. 2000. A pug-nosed crocodyliform from the Late Cretaceous of Madagascar. *Nature*, **405,** 941–944.

BURNABY, T. P. 1966. Growth-invariant discriminant functions and generalized distances. *Biometrics*, **22,** 96–110.

BURNESS, G. P., DIAMOND, J. and FLANNERY, T. 2001. Dinosaurs, dragons, and dwarfs: the evolution of maximal body size. *Proceedings of the National Academy of Sciences*, **98,** 14518–14523.

BURNHAM, K. P. and ANDERSON, D. R. 2003. *Model selection and multimodel inference: a practical information–theoretic approach*. Springer Science & Business Media.

BURNHAM, K. P., ANDERSON, D. R. and HUYVAERT, K. P. 2011. AIC model selection and multimodel inference in behavioral ecology: some background, observations, and comparisons. *Behavioral Ecology and Sociobiology*, **65,** 23–35.

BUSBEY, A. B. 1995. The structural consequences of skull flattening in crocodilians. 173–192. *In* THOMASON, J. J. (ed.). *Functional Morphology in Vertebrate Paleontology*. Cambridge University Press.

BUSCALIONI, Á. D. 2017. The Gobiosuchidae in the early evolution of Crocodyliformes. *Journal of Vertebrate Paleontology*, **37,** e1324459.

BUSCALIONI, Á. D., ORTEGA, F., WEISHAMPEL, D. B. and JIANU, C. M. 2001. A revision of the crocodyliform *Allodaposuchus precedens* from the Upper Cretaceous of the Hateg Basin, Romania. Its relevance in the phylogeny of Eusuchia. *Journal of Vertebrate Paleontology*, **21,** 74–86.

BUSCALIONI, Á. D., PIRAS, P., VULLO, R., SIGNORE, M. and BARBERA, C. 2011. Early Eusuchia Crocodylomorpha from the vertebrate-rich Plattenkalk of Pietraroia (Lower Albian, southern Apennines, Italy). *Zoological Journal of the Linnean Society*, **163,** S199–S227.

BUSTARD, H. R. and SINGH, L. A. K. 1977. Studies on the Indian Gharial *Gavialis gangeticus* (Gmelin) (Reptilia, Crocodilia) – I: Estimation of body length from scute length. *Indian Forester*, **103,** 140–149.

BUTLER, M. A. and KING, A. A. 2004. Phylogenetic comparative analysis: a modeling approach for adaptive evolution. *The American Naturalist*, **164,** 683–695.

BUTLER, R. J. and GOSWAMI, A. 2008. Body size evolution in Mesozoic birds: little evidence for Cope's rule. *Journal of Evolutionary Biology*, **21,** 1673–1682.

BUTLER, R. J., BRUSATTE, S. L., ANDRES, B. and BENSON, R. B. 2012. How do geological sampling biases affect studies of morphological evolution in deep time? A case study of pterosaur (Reptilia: Archosauria) disparity. *Evolution*, **66,** 147–162.

CALDER, W. A. 1984. *Size, Function, and Life History*. Harvard University Press.

CAMPIONE, N. E. and EVANS, D. C. 2012. A universal scaling relationship between body mass and proximal limb bone dimensions in quadrupedal terrestrial tetrapods. *BMC Biology*, **10,** 60.

CAMPIONE, N. E., EVANS, D. C., BROWN, C. M. and CARRANO, M. T. 2014. Body mass estimation in non-avian bipeds using a theoretical conversion to quadruped stylopodial proportions. *Methods in Ecology and Evolution*, **5,** 913–923.

CARBALLIDO, J. L., POL, D., OTERO, A., CERDA, I. A., SALGADO, L., GARRIDO, A. C., RAMEZANI, J., CÚNEO, N. R. and KRAUSE, J. M. 2017. A new giant titanosaur sheds light on body mass evolution among sauropod dinosaurs. *Proceedings of the Royal Society of London B*, **284,** 20171219.

CARDILLO, M., MACE, G. M., JONES, K. E., BIELBY, J., BININDA-EMONDS, O. R., SECHREST, W., ORME, C. D. L. and PURVIS, A. 2005. Multiple causes of high extinction risk in large mammal species. *Science*, **309,** 1239–1241.

CARRANO, M. T. 2006. Body-size evolution in the Dinosauria. 225–268. *In* CARRANO, M. T., BLOB, R. W., GAUDIN, T. and WIBBLE, J. R. (eds.). *Amniote Paleobiology: Perspectives on the Evolution of Mammals, Birds, and Reptiles*. University of Chicago Press.

CARVALHO, I. S. and BERTINI, R. J. 1999. *Mariliasuchus*: um novo Crocodylomorpha (Notosuchia) do Cretáceo da Bacia Bauru, Brasil. *Geologia Colombiana*, **24,** 83–105.

CARVALHO, I. S., RIBEIRO, L. C. B. and AVILLA, L. S. 2004. *Uberabasuchus terrificus* sp. nov., a new crocodylomorpha from the Bauru Basin, (Upper Cretaceous), Brazil. *Gondwana Research*, **7,** 975–1004.

CARVALHO, I. S., VASCONCELLOS, F. M. and TAVARES, S. A. S. 2007. *Montealtosuchus arrudacamposi*, a new peirosaurid crocodile (Mesoeucrocodylia) from the Late Cretaceous Adamantina Formation of Brazil. Zootaxa, **1607,** 35–46.

CARVALHO, I. S., GASPARINI, Z. B., SALGADO, L., VASCONCELLOS, F. M. and MARINHO, T. S. 2010. Climate's role in the distribution of the Cretaceous terrestrial Crocodyliformes throughout Gondwana. *Palaeogeography, Palaeoclimatology, Palaeoecology*, **297,** 252–262.

CARVALHO, I. S., TEIXEIRA, V. P. A., FERRAZ, M. L. F., RIBEIRO, L. C. B., MARTINELLI, A. G., NETO, F. M., SERTICH, J. J. W., CUNHA, G. C., CUNHA, I. C. and FERRAZ, P. F. 2011. *Campinasuchus dinizi* gen. et sp. nov., a new Late Cretaceous baurusuchid (Crocodyliformes) from the Bauru Basin, Brazil. *Zootaxa*, **2871,** 19–42.

CHAMERO, B., BUSCALIONI, Á. D. and MARUGÁN-LOBÓN, J. 2013. Pectoral girdle and forelimb variation in extant Crocodylia: the coracoid–humerus pair as an evolutionary module. *Biological Journal of the Linnean Society*, **108,** 600–618.

CHURCHILL, M., CLEMENTZ, M. T. and KOHNO N. 2015. Cope's rule and the evolution of body size in Pinnipedimorpha (Mammalia: Carnivora). *Evolution*, **69,** 201–215.

CLARAC, F., SOUTER, T., CUBO, J., DE BUFFRENIL, V., BROCHU, C. and CORNETTE, R. 2016. Does skull morphology constrain bone ornamentation? A morphometric analysis in the Crocodylia. *Journal of Anatomy*, **229,** 292–301.

CLARK, J. M. 1994. Patterns of evolution in Mesozoic Crocodyliformes. 84–97. *In* FRASER, N. C. and SUES, H. D. (eds.). *In the Shadow of the Dinosaurs. Early Mesozoic Tetrapods*. Cambridge University Press.

CLARK, J. M. 2011. A new shartegosuchid crocodyliform from the Upper Jurassic Morrison Formation of western Colorado. *Zoological Journal of the Linnean Society*, **163,** S152–S172.

CLARK, J. M. and SUES, H. D. 2002. Two new basal crocodylomorph archosaurs from the Lower Jurassic and the monophyly of the Sphenosuchia. *Zoological Journal of the Linnean Society*, **136,** 77–95.

CLARK, J. M., SUES, H. D. and BERMAN, D. S. 2000. A new specimen of *Hesperosuchus agilis* from the Upper Triassic of New Mexico and the interrelationships of basal crocodylomorph archosaurs. *Journal of Vertebrate Paleontology*, **20,** 683–704.

CLARK, J. M., XU, X., FORSTER, C. A. and WANG, Y. 2004. A Middle Jurassic 'sphenosuchian'from China and the origin of the crocodylian skull. *Nature*, **430,** 1021–1024.

CLAUDE, J. 2008. *Morphometrics with R*. Springer-Verlag.

CLAUSET, A. and ERWIN, D. H. 2008. The evolution and distribution of species body size. *Science*, **321,** 399–401.

CLELAND, C. E. 2001. Historical science, experimental science, and the scientific method. *Geology*, **29,** 987–990.

CLELAND, C. E. 2002. Methodological and epistemic differences between historical science and experimental science. *Philosophy of Science*, **69,** 474–496.

COLBERT, E. H. 1962. The weights of dinosaurs. *American Museum Novitates*, **2076,** 1–16.

COLLYER, M. L., SEKORA, D. J. and ADAMS, D. C. 2015. A method for analysis of phenotypic change for phenotypes described by high-dimensional data. *Heredity*, **115,** 357–365.

COOKE, S. B. and TERHUNE, C. E. 2015. Form, function, and geometric morphometrics. *The Anatomical Record*, **298,** 5–28.

COOPER, N. and PURVIS, A. 2010. Body size evolution in mammals: complexity in tempo and mode. *The American Naturalist*, **175,** 727–738.

COOPER, N., THOMAS, G. H., VENDITTI, C., MEADE, A. and FRECKLETON, R. P. 2016. A cautionary note on the use of Ornstein Uhlenbeck models in macroevolutionary studies. *Biological Journal of the Linnean Society*, **118,** 64–77.

COPE, E. D. 1887. *The Origin of the Fittest: Essays on Evolution*. D. Appleton and Company.

COPE, E. D. 1896. *The Primary Factors of Organic Evolution*. Open Court Press.

CORNWELL, W. K., SCHWILK, D. W. and Ackerly, D. D. 2006. A traitbased test for habitat filtering: Convex hull volume. *Ecology*, **87,** 1465–1471.

COWEN, R. 2013. *History of life*. John Wiley & Sons.

CRUSH, P. J. 1984. A late Upper Triassic sphenosuchid crocodilian from Wales. *Palaeontology*, **27,** 131–157.

CUBO, J., KÖHLER, M. and BUFFRENIL, V. 2017. Bone histology of *Iberosuchus macrodon* (Sebecosuchia, Crocodylomorpha). *Lethaia*, **50,** 495–503.

CURRIE, P. J. 1978. The orthometric linear unit. *Journal of Paleontology*, **5,** 964–971.

CUVIER, G. 1817. *Le Règne Animal Distribué d'après son Organisation, pour Servir de Base à l'Histoire Naturelle des Animaux et d'Introduction à l'Anatomie Comparée*. Fortin, Masson et cie, Libraires.

DABOUL, A., IVANOVSKA, T., BÜLOW, R., BIFFAR, R. and CARDINI, A. 2018. Procrustes-based geometric morphometrics on MRI images: An example of inter-operator bias in 3D landmarks and its impact on big datasets. *PLoS One*, **13,** e0197675.

DARWIN, C. 1859. *On the Origin of Species by Means of Natural Selection, or, the Preservation of Favoured Races in the Struggle for Life*. John Murray.

DAVIS, A. M., UNMACK, P. J., PUSEY, B. J., PEARSON, R. G. and MORGAN, D. L. 2014. Evidence for a multi-peak adaptive landscape in the evolution of trophic morphology in terapontid fishes. *Biological journal of the Linnean Society*, **113,** 623–634.

DELFINO, M. and DE VOS, J. 2014. A giant crocodile in the Dubois Collection from the Pleistocene of Kali Gedeh (Java). *Integrative Zoology*, **9,** 141–147.

DELFINO, M., PIRAS, P. and SMITH, T. 2005. Anatomy and phylogeny of the gavialoid crocodylian *Eusuchus lerichei* from the Paleogene of Europe. *Acta Palaeontologica Polonica*, **50,** 565–580.

DELFINO, M., CODREA, V., FOLIE, A., DICA, P., GODEFROIT, P. and SMITH, T. 2008*a*. A complete skull of *Allodaposuchus precedens* Nopcsa, 1928 (Eusuchia) and a reassessment of the morphology of the taxon based on the Romanian remains. *Journal of Vertebrate Paleontology*, **28,** 111–122.

DELFINO, M., MARTIN, J. E. and BUFFETAUT, E. 2008*b*. A new species of *Acynodon* (Crocodylia) from the upper cretaceous (Santonian–Campanian) of Villaggio del Pescatore, Italy. *Palaeontology*, **51,** 1091–1106.

DEPÉRET, C. J. J. 1909. *The Transformations of the Animal World*. D. Appleton and Company.

DODD, M. S., PAPINEAU, D., GRENNE, T., SLACK, J. F., RITTNER, M., PIRAJNO, F., O'NEIL, J. and LITTLE, C. T. 2017. Evidence for early life in Earth's oldest hydrothermal vent precipitates. *Nature*, **543,** 60–64.

DOLLMAN, K. N., CLARK, J. M., NORELL, M. A., XING, X. and CHOINIERE, J. N. 2018. Convergent evolution of a eusuchian-type secondary palate within Shartegosuchidae. *American Museum Novitates*, **3901,** 1–23.

DOWNHOWER, J. F. and BLUMER, L. S. 1988. Calculating just how small a whale can be. *Nature*, **335,** 675.

EKMAN, S., ANDERSEN, H. L. and WEDIN, M. 2008. The limitations of ancestral state reconstruction and the evolution of the ascus in the Lecanorales (lichenized Ascomycota). *Systematic Biology*, **57,** 141–156.

ERICKSON, B. R. and SAWYER, G. T. 1996. The estuarine crocodile *Gavialosuchus carolinensis* n. sp. (Crocodylia: Eusuchia) from the late Oligocene of South Carolina, North America. *The Science Museum of Minnesota Monograph Paleontology*, **3,** 1–49.

ERICKSON, G. M. and BROCHU, C. A. 1999. How the 'terror crocodile'grew so big. *Nature*, **398**, 205–206.

ERICKSON, G. M., MAKOVICKY, P. J., CURRIE, P. J., NORELL, M. A., YERBY, S. A. and BROCHU, C. A. 2004. Gigantism and comparative life-history parameters of tyrannosaurid dinosaurs. *Nature*, **430,** 772–775.

ERICKSON, G. M., GIGNAC, P. M., STEPPAN, S. J., LAPPIN, A. K., VLIET, K. A., BRUEGGEN, J. D., INOUYE, B. D., KLEDZIK, D. and WEBB, G. J. 2012. Insights into the ecology and evolutionary success of crocodilians revealed through bite-force and tooth-pressure experimentation. *PLoS One*, **7,** e31781.

EZCURRA, M. D. and BUTLER, R. J. 2015. Post-hatchling cranial ontogeny in the Early Triassic diapsid reptile *Proterosuchus fergusi*. *Journal of Anatomy*, **226,** 387–402.

FANTI, F., MIYASHITA, T., CANTELLI, L., MNASRI, F., DRIDI, J., CONTESSI, M. and CAU, A. 2016. The largest thalattosuchian (Crocodylomorpha) supports teleosaurid survival across the Jurassic-Cretaceous boundary. *Cretaceous Research*, **61,** 263–274.

FARLOW, J. O., HURLBURT, G. R., ELSEY, R. M., BRITTON, A. R. and LANGSTON, W. 2005. Femoral dimensions and body size of *Alligator mississippiensis*: estimating the size of extinct mesoeucrocodylians. *Journal of Vertebrate Paleontology*, **25,** 354–369.

FELSENSTEIN, J. 1985. Phylogenies and the comparative method. *The American Naturalist*, **125,** 1–15.

FELSENSTEIN, J. 1988. Phylogenies and quantitative characters. *Annual Review of Ecology and Systematics*, **19,** 445–471.

FIORELLI, L. E. and CALVO, J. O. 2007. The first "protosuchian"(Archosauria: Crocodyliformes) from the Cretaceous (Santonian) of Gondwana. *Arquivos do Museu Nacional*, **65,** 417–459.

FIORELLI, L. E. and CALVO, J. O 2008. New remains of *Notosuchus terrestris* Woodward, 1896 (Crocodyliformes: Mesoeucrocodylia) from Late Cretaceous of Neuquén, Patagonia, Argentina. *Arquivos do Museu Nacional*, **66,** 83–124.

FIORELLI, L. E., LEARDI, J. M., HECHENLEITNER, E. M., POL, D., BASILICI, G. and GRELLET-TINNER, G. 2016. A new Late Cretaceous crocodyliform from the western margin of Gondwana (La Rioja Province, Argentina). *Cretaceous Research*, **60,** 194–209.

FISHER, D. O. and OWENS, I. P. 2004. The comparative method in conservation biology. *Trends in Ecology & Eevolution*, **19,** 391–398.

FOFFA, D. and YOUNG, M. T. 2014. The cranial osteology of *Tyrannoneustes lythrodectikos* (Crocodylomorpha: Metriorhynchidae) from the Middle Jurassic of Europe. *PeerJ*, **2,** e608.

FOFFA, D., YOUNG, M. T., BRUSATTE, S. L., GRAHAM, M. R. and STEEL, L. 2018. A new metriorhynchid crocodylomorph from the Oxford Clay Formation (Middle Jurassic) of England, with implications for the origin and diversification of Geosaurini. *Journal of Systematic Palaeontology*, **16,** 1123–1143.

FOOTE, M. 1993. Discordance and concordance between morphological and taxonomic diversity. *Paleobiology*, **19,** 185–204.

FOOTE, M. 1997. The evolution of morphological diversity. *Annual Reviews of Ecology and Systematics*, **28,** 129–152.

FORTIER, D. C. and SCHULTZ, C. L. 2009. A new neosuchian crocodylomorph (Crocodyliformes, Mesoeucrocodylia) from the Early Cretaceous of north-east Brazil. *Palaeontology*, **52,** 991–1007.

FORTIER, D., PEREA, D. and SCHULTZ, C. 2011. Redescription and phylogenetic relationships of *Meridiosaurus vallisparadisi*, a pholidosaurid from the Late Jurassic of Uruguay. *Zoological Journal of the Linnean Society*, **163,** S257–S272.

FORTIER, D. C., SOUZA-FILHO, J. P., GUILHERME, E., MACIENTE, A. A. and SCHULTZ, C. L. 2014. A new specimen of *Caiman brevirostris* (Crocodylia, Alligatoridae) from the Late Miocene of Brazil. *Journal of Vertebrate Paleontology*, **34,** 820–834.

FOTH, C. and JOYCE, W. G. 2016. Slow and steady: the evolution of cranial disparity in fossil and recent turtles. *Proceedings of the Royal Society of London B*, **283,** 20161881.

FOTH, C., BRUSATTE, S. L. and BUTLER, R. J. 2012. Do different disparity proxies converge on a common signal? Insights from the cranial morphometrics and evolutionary history of Pterosauria (Diapsida: Archosauria). *Journal of Evolutionary Biology*, **25,** 904–915.

FOTH, C., BONA, P. and DESOJO, J. B. 2015. Intraspecific variation in the skull morphology of the black caiman *Melanosuchus niger* (Alligatoridae, Caimaninae). *Acta Zoologica*, **96,** 1–13.

FOTH, C., EZCURRA, M. D., SOOKIAS, R. B., BRUSATTE, S. L. and BUTLER R. J. 2016*a*. Unappreciated diversification of stem archosaurs during the Middle Triassic predated the dominance of dinosaurs. *BMC Evolutionary Biology*, **16,** 188.

FOTH, C., HEDRICK, B. P. and EZCURRA M. D. 2016*b.* Cranial ontogenetic variation in early saurischians and the role of heterochrony in the diversification of predatory dinosaurs. *PeerJ*, **4,** e1589.

FOTH, C., FERNANDEZ BLANCO, M. V., BONA, P. and SCHEYER, T. M. 2017*a*. Cranial shape variation in jacarean caimanines (Crocodylia, Alligatoroidea) and its implications in the taxonomic status of extinct species: The case of *Melanosuchus fisheri*. *Journal of Morphology*. *Journal of Morphology*, **279,** 259–273.

FOTH, C., ASCARRUNZ, E. and JOYCE, W. G. 2017*b*. Still slow, but even steadier: an update on the evolution of turtle cranial disparity interpolating shapes along branches. *Royal Society Open Science*, **4,** 170899.

FRANCHINI, P., FRUCIANO, C., SPREITZER, M. L., JONES, J. C., ELMER, K. R., HENNING, F. and MEYER, A. 2014. Genomic architecture of ecologically divergent

body shape in a pair of sympatric crater lake cichlid fishes. *Molecular Ecology*, **23,** 1828–1845.

FRUCIANO, C. 2016. Measurement error in geometric morphometrics. *Development Genes and Evolution*, **226,** 139–158.

FRUCIANO, C., TIGANO, C. and FERRITO, V. 2011. Geographical and morphological variation within and between colour phases in *Coris julis* (L. 1758), a protogynous marine fish. *Biological Journal of the Linnean Society*, **104,** 148–162.

FRUCIANO, C., TIGANO, C. and FERRITO, V. 2012. Body shape variation and colour change during growth in a protogynous fish. *Environmental Biology of Fishes*, **94,** 615–622.

FRUCIANO, C., FRANCHINI, P., KOVACOVA, V., ELMER, K. R., HENNING, F. and MEYER, A. 2016. Genetic linkage of distinct adaptive traits in sympatrically speciating crater lake cichlid fish. *Nature Communications*, **7,** 12736.

FRUCIANO, C., CELIK, M. A., BUTLER, K., DOOLEY, T., WEISBECKER, V. and PHILLIPS, M. J. 2017. Sharing is caring? Measurement error and the issues arising from combining 3D morphometric datasets. *Ecology and Evolution*, **7,** 7034–7046.

GAO, Y. H. 2001. A new species of *Hsisosuchus* from Dashanpu, Zigong, Sichuan. *Vertebrata PalAsiatica*, **39,** 177–184.

GARLAND, T. and IVES, A. R. 2000. Using the past to predict the present: confidence intervals for regression equations in phylogenetic comparative methods. *The American Naturalist*, **155,** 346–364.

GARLAND JR, T., DICKERMAN, A. W., JANIS, C. M. and JONES, J. A. 1993. Phylogenetic analysis of covariance by computer simulation. *Systematic Biology*, **42,** 265–292.

GASPARINI, Z. B. 1971. Los Notosuchia del Cretácico de América del Sur como un nuevo Infraorden de los Mesosuchia (Crocodilia). *Ameghiniana*, **8,** 83–103.

GASPARINI, Z., POL, D. and SPALLETTI, L. A. 2006. An unusual marine crocodyliform from the Jurassic-Cretaceous boundary of Patagonia. *Science*, **311,** 70–73.

GASPARINI, Z., CHIAPPE, L. M. and FERNANDEZ, M. 1991. A new Senonian peirosaurid (Crocodylomorpha) from Argentina and a synopsis of the South American Cretaceous crocodilians. *Journal of Vertebrate Paleontology*, **11,** 316–333.

GEARTY, W., M$_C$CLAIN, C. R. and PAYNE, J. L. 2018. Energetic tradeoffs control the size distribution of aquatic mammals. *Proceedings of the National Academy of Sciences*, **115,** 4194–4199.

GHARAIBEH, W. 2005. Correcting for the effect of orientation in geometric morphometric studies of side-view images of human heads. 117–143. *In* SLICE, D. (ed.). *Modern morphometrics in physical anthropology*. Springer.

GIGNAC, P. and O'BRIEN, H. 2016. Suchian feeding success at the interface of ontogeny and macroevolution. *Integrative and Comparative Biology*, **56,** 449–458.

GODOY, P. L., MONTEFELTRO, F. C., NORELL, M. A. and LANGER, M. C. 2014. An additional baurusuchid from the Cretaceous of Brazil with evidence of interspecific predation among Crocodyliformes. *PLoS One*, **9,** e97138.

GODOY, P. L., BRONZATI, M., ELTINK, E., MARSOLA, J. C. A., CIDADE, G. M., LANGER, M. C. and MONTEFELTRO, F. C. 2016. Postcranial anatomy of

Pissarrachampsa sera (Crocodyliformes, Baurusuchidae) from the Late Cretaceous of Brazil: insights on lifestyle and phylogenetic significance. *PeerJ*, **4,** e2075.

GODOY, P. L., BENSON, R. B. J., BRONZATI, M. and BUTLER, R. J. 2018*a*. The multi-peak adaptive landscape of crocodylomorph body size evolution. *bioRxiv*, 405621, https://doi.org/10.1101/405621.

GODOY, P. L., FERREIRA, G. S., MONTEFELTRO, F. C., VILA NOVA, B. C., BUTLER, R. J. and LANGER, M. C. 2018*b*. Evidence for heterochrony in the cranial evolution of fossil crocodyliforms. *Palaeontology*, **61,** 543–558.

GODOY, P. L., BENSON, R. B. J., BRONZATI, M. and BUTLER, R. J. 2018*c*. Supporting data for: The multi-peak adaptive landscape of crocodylomorph body size evolution. *Zenodo*. http://doi.org/10.5281/zenodo.1344593.

GODOY, P. L., FERREIRA, G. S., MONTEFELTRO, F. C., VILA NOVA, B. C., BUTLER, R. J. and LANGER, M. C. 2018*d*. Data from: Evidence for heterochrony in the cranial evolution of fossil crocodyliforms. *Dryad Digital Repository*. https://doi.org/10.5061/dryad.7m48r.

GOLD, M. E. L., BROCHU, C. A. and NORELL, M. A. 2014. An expanded combined evidence approach to the *Gavialis* problem using geometric morphometric data from crocodylian braincases and Eustachian systems. *PLoS One*, **9,** e105793.

GOMANI, E. M. 1997. A crocodyliform from the Early Cretaceous dinosaur beds, northern Malawi. *Journal of Vertebrate Paleontology*, **17,** 280–294.

GOODALL, C. 1991. Procrustes methods in the statistical analysis of shape. *Journal of the Royal Statistical Society. Series B (Methodological)*, **53,** 285–339.

GOULD, S. J. 1966. Allometry and size in ontogeny and phylogeny. *Biological Reviews of the Cambridge Philosophical Society*, **41,** 587–640.

GOULD, S. J. 1977. *Ontogeny and Phylogeny*. Harvard University Press.

GOULD, S. J. 1991. The disparity of the Burgess Shale arthropod fauna and the limits of cladistic analysis: why we must strive to quantify morphospace. *Paleobiology*, **17,** 411–423.

GOULD, S. J. 2000. Of coiled oysters and big brains: how to rescue the terminology of heterochrony, now gone astray. *Evolution & Development*, **2,** 241–248.

GOULD, S. J. and ELDREDGE, N. 1977. Punctuated equilibria: the tempo and mode of evolution reconsidered. *Paleobiology*, **3,** 115–151.

GOW, C. E. 2000. The skull of *Protosuchus haughtoni*, an Early Jurassic crocodyliform from southern Africa. *Journal of Vertebrate Paleontology*, **20,** 49–56.

GOWER, J. C. 1975. Generalized procrustes analysis. *Psychometrika*, **40,** 33–51.

GRANGE, D. R. and BENTON, M. J. 1996. Kimmeridgian metriorhynchid crocodiles from England. *Palaeontology*, **39,** 497–514.

GRIGG, G. C., SEEBACHER, F. and FRANKLIN, C. E. 2001. *Crocodilian Biology and Evolution*. Surrey Beatty & Sons.

GUILLERME, T. 2018. dispRity: A modular R package for measuring disparity. *Methods in Ecology and Evolution*, **9,** 1755–1763.

GUILLERME, T. and COOPER, N. 2018. Time for a rethink: time sub-sampling methods in disparity-through-time analyses. *Palaeontology*, **61,** 481–493.

HAINES, A. J. and CRAMPTON, J. S. 2000. Improvements to the method of Fourier shape analysis as applied in morphometric studies. *Palaeontology*, **43,** 765–783.

HALL, P. M. and PORTIER, K. M. 1994. Cranial morphometry of New Guinea crocodiles (*Crocodylus novaeguineae*): ontogenetic variation in relative growth of the skull and an assessment of its utility as a predictor of the sex and size of individuals. *Herpetological Monographs*, **8,** 203–225.

HAMMER, Ø., HARPER, D. A. T. and RYAN, P. D. 2001. PAST: Paleontological statistics software package for education and data analysis. *Paleontologia Electronica*, **4,** 1–9.

HANSEN, T. F. 1997. Stabilizing selection and the comparative analysis of adaptation. *Evolution*, **51,** 1341–1351.

HANSEN, T. F. 2012. Adaptive landscapes and macroevolutionary dynamics. 205–226. *In* SVENSSON, E. and CALSBEEK, R. (eds.). *The Adaptive Landscape in Evolutionary Biology*. Oxford University Press.

HANSEN, T. F. and MARTINS, E. P. 1996. Translating between microevolutionary process and macroevolutionary patterns: the correlation structure of interspecific data. *Evolution*, **50,** 1404–1417.

HARMON, L. J., WEIR, J. T., BROCK, C. D., GLOR, R. E. and CHALLENGER, W. 2007. GEIGER: investigating evolutionary radiations. *Bioinformatics*, **24,** 129–131.

HARMON, L. J., LOSOS, J. B., DAVIES, T. J., GILLESPIE, R. G., GITTLEMAN, J. L., JENNINGS, B. W., KOZAK, K. H., MCPEEK, M. A., MORENO-ROARK, F., NEAR, T. J., PURVIS, A., RICKLEFS, R. E., SCHLUTER, D., SCHULTE II, J. A., SEEHAUSEN, O., SIDLAUSKAS, B. L., TORRES-CARVAJAL, O., WEIR, J. T. and

MOOERS, A. Ø., 2010. Early bursts of body size and shape evolution are rare in comparative data. *Evolution*, **64,** 2385–2396.

HARVEY, P. H. and PAGEL, M. D. 1991. *The Comparative Method in Evolutionary Biology.* Oxford University Press.

HASTINGS, A. K., BLOCH, J. I., CADENA, E. A. and JARAMILLO, C. A. 2010. A new small short-snouted dyrosaurid (Crocodylomorpha, Mesoeucrocodylia) from the Paleocene of Northeastern Colombia. *Journal of Vertebrate Paleontology*, **30,** 139–162.

HASTINGS, A. K., BLOCH, J. I. and JARAMILLO, C. A. 2011. A new longirostrine dyrosaurid (Crocodylomorpha, Mesoeucrocodylia) from the Paleocene of north-eastern Colombia: biogeographic and behavioural implications for New-World Dyrosauridae. *Palaeontology*, **54,** 1095–1116.

HASTINGS, A. K., BLOCH, J. I., JARAMILLO, C. A., RINCON, A. F. and MACFADDEN, B. J. 2013. Systematics and biogeography of crocodylians from the Miocene of Panama. *Journal of Vertebrate Paleontology*, **33,** 239–263.

HASTINGS, A. K., BLOCH, J. I. and JARAMILLO, C. A. 2015. A new blunt-snouted dyrosaurid, *Anthracosuchus balrogus* gen. et sp. nov.(Crocodylomorpha, Mesoeucrocodylia), from the Palaeocene of Colombia. *Historical Biology*, **27,** 998–1020.

HECHT, M. K. 1991. *Araripesuchus* Price, 1959. 342–347. *In* MAISEY, J. G. (ed.). *Santana Fossils: an Illustrated Guide*. T.F.H. Publications.

HEDMAN, M. M. 2010. Constraints on clade ages from fossil outgroups. *Paleobiology,* **36,** 16–31.

HEIM, N. A., KNOPE, M. L., SCHAAL, E. K., WANG, S. C. and PAYNE, J. L. 2015. Cope's rule in the evolution of marine animals. *Science*, **347,** 867–870.

HERRERA, Y., GASPARINI, Z. and FERNANDEZ, M. S. 2013. A new Patagonian species of *Cricosaurus* (Crocodyliformes, Thalattosuchia): first evidence of *Cricosaurus* in Middle–Upper Tithonian lithographic limestone from Gondwana. *Palaeontology*, **56,** 663–678.

HERRERA, Y., GASPARINI, Z. and FERNÁNDEZ, M. S. 2015. *Purranisaurus potens* Rusconi, an enigmatic metriorhynchid from the Late Jurassic–Early Cretaceous of the Neuquén Basin. *Journal of Vertebrate Paleontology*, **35,** e904790.

HERRERA, Y., FERNANDEZ, M. S., LAMAS, S. G., CAMPOS, L., TALEVI, M. and GASPARINI, Z. 2017. Morphology of the sacral region and reproductive strategies of Metriorhynchidae: a counter-inductive approach. *Earth and Environmental Science Transactions of the Royal Society of Edinburgh*, **106,** 247–255.

HERVÉ, M. 2018. *RVAideMemoire: Testing and Plotting Procedures for Biostatistics. R package version 0.9-69-3*. https://CRAN.R-project.org/package=RVAideMemoire.

HO, L. S. T. and ANÉ, C. 2014. Intrinsic inference difficulties for trait evolution with Ornstein-Uhlenbeck models. *Methods in Ecology and Evolution*, **5,** 1133–1146.

HOLM, S. 1979. A simple sequentially rejective multiple test procedure. *Scandinavian Journal of Statistics*, **6,** 65–70.

HONE, D. W. E., DYKE, G. J., HADEN, M. and BENTON, M. J. 2008. Body size evolution in Mesozoic birds. *Journal of Evolutionary Biology*, **21,** 618–624.

HOPKINS, M. J. and GERBER, S. 2017. Morphological disparity. 1–12. *In* NUÑO DE LA ROSA, L. and MÜLLER G. B. (eds.). *Evolutionary Developmental Biology*. Springer.

HOTELLING, H. 1933. Analysis of a complex of statistical variables into principal components. *Journal of Educational Psychology*, **24,** 417–441.

HUA, S. and JOUVE, S. 2004. A primitive marine gavialoid from the Paleocene of Morocco. *Journal of Vertebrate Paleontology*, **24,** 341–350.

HUA, S., BUFFETAUT, E., LEGALL, C. and ROGRON, P. 2007. *Oceanosuchus boecensis* n. gen, n. sp., a marine pholidosaurid (Crocodylia, Mesosuchia) from the Lower Cenomanian of Normandy (western France). *Bulletin de la Société Géologique de France*, **178,** 503–513.

HUGHES, M., GERBER, S. and WILLS, M. A. 2013. Clades reach highest morphological disparity early in their evolution. *Proceedings of the National Academy of Sciences*, **110,** 13875–13879.

HUNT, G. 2008*a*. Evolutionary patterns within fossil lineages: model-based assessment of modes, rates, punctuations and process. 117–131. *In* BAMBACH, R. K. and KELLEY, P. H. (eds.). *From Evolution to Geobiology: Research Questions Driving Paleontology at the Start of a New Century*. The Paleontological Society Papers.

HUNT, G. 2008*b*. Gradual or pulsed evolution: when should punctuational explanations be preferred?. *Paleobiology*, **34,** 360–377.

HUNT, G. 2012. Measuring rates of phenotypic evolution and the inseparability of tempo and mode. *Paleobiology*, **38,** 351–373.

HUNT, G. and CARRANO, M. T. 2010. Models and methods for analyzing phenotypic evolution in lineages and clades. 245–269. *In* ALROY, J. and HUNT, G. (eds.). *Quantitative Methods in Paleobiology*. The Paleontological Society Papers.

HUNT, G., CRONIN, T. M. and ROY, K. 2005. Species–energy relationship in the deep sea: a test using the Quaternary fossil record. *Ecology Letters*, **8,** 739–747.

HUNT, G., HOPKINS, M. J. and LIDGARD, S. 2015. Simple versus complex models of trait evolution and stasis as a response to environmental change. *Proceedings of the National Academy of Sciences*, **112,** 4885–4890.

HURLBURT, G. 1999. Comparison of body mass estimation techniques, using recent reptiles and the pelycosaur *Edaphosaurus boanerges*. *Journal of Vertebrate Paleontology*, **19,** 338–350.

HURLBURT, G. R., HECKERT, A. B. and FARLOW, J. O. 2003. Body mass estimates of phytosaurs (Archosauria: Parasuchidae) from the Petrified Forest Formation (Chinle Group: Revueltian) based on skull and limb bone measurements. *New Mexico Museum of Natural History and Science Bulletin*, **24,** 105–113.

HUTCHINSON, G. E. and M$_{AC}$ARTHUR, R. H. 1959. A theoretical ecological model of size distributions among species of animals. *The American Naturalist*, **93,** 117–125.

HUTTENLOCKER, A. K. 2014. Body size reductions in nonmammalian eutheriodont therapsids (Synapsida) during the end-Permian mass extinction. *PLoS One*, **9,** e87553.

HUXLEY, J. S. 1932. *Problems of relative growth*. Johns Hopkins University Press.

IIJIMA, M. 2017. Assessment of trophic ecomorphology in non-alligatoroid crocodylians and its adaptive and taxonomic implications. *Journal of Anatomy*, **231,** 192–211.

IORDANSKY, N. N. 1973. The skull of the Crocodilia. 201–260. *In* GANS, C. and PARSONS, T. (eds.). *Biology of the Reptilia, Vol. 4.* Academic Press.

INGRAM, T. 2015. Diversification of body shape in *Sebastes* rockfishes of the north-east Pacific. *Biological Journal of the Linnean Society*, **116,** 805–818.

INGRAM, T. and MAHLER, D. L. 2013. SURFACE: detecting convergent evolution from comparative data by fitting Ornstein-Uhlenbeck models with stepwise Akaike Information Criterion. *Methods in Ecology and Evolution*, **4,** 416–425.

IRMIS, R. B., NESBITT, S. J. and SUES, H. D. 2013. Early Crocodylomorpha. 275–302. *In*. NESBITT, S. J., DESOJO, J. B. and IRMIS, R. B. (eds.). *Anatomy, phylogeny and palaeobiology of early archosaurs and their kin*. Geological Society of London, Special Publications, **379**.

JOHNSON, C. N. 2002. Determinants of loss of mammal species during the Late Quaternary 'megafauna' extinctions: life history and ecology, but not body size. *Proceedings of the Royal Society of London B,* **269,** 2221–2227.

JOUVE, S. 2005. A new description of the skull of *Dyrosaurus phosphaticus* (Thomas, 1893) (Mesoeucrocodylia: Dyrosauridae) from the Lower Eocene of North Africa. *Canadian Journal of Earth Sciences*, **42,** 323–337.

JOUVE, S. 2009. The skull of *Teleosaurus cadomensis* (Crocodylomorpha; Thalattosuchia), and phylogenetic analysis of Thalattosuchia. *Journal of Vertebrate Paleontology*, **29,** 88–102.

JOUVE, S. 2016. A new basal tomistomine (Crocodylia, Crocodyloidea) from Issel (Middle Eocene; France): palaeobiogeography of basal tomistomines and palaeogeographic consequences. *Zoological Journal of the Linnean Society*, **177,** 165–182.

JOUVE, S., BOUYA, B. and AMAGHZAZ, M. 2005. A short-snouted dyrosaurid (Crocodyliformes, Mesoeucrocodylia) from the Palaeocene of Morocco. *Palaeontology*, **48,** 359–369.

JOUVE, S., IAROCHENE, M., BOUYA, B. and AMAGHZAZ, M. 2006. A new species of *Dyrosaurus* (Crocodylomorpha, Dyrosauridae) from the early Eocene of Morocco: phylogenetic implications. *Zoological Journal of the Linnean Society*, **148,** 603–656.

JOUVE, S., BARDET, N., JALIL, N. E., SUBERBIOLA, X. P., BOUYA, B. and AMAGHZAZ, M. 2008. The oldest African crocodylian: phylogeny, paleobiogeography, and differential survivorship of marine reptiles through the Cretaceous-Tertiary boundary. *Journal of Vertebrate Paleontology*, **28,** 409–421.

JOUVE, S., BOUYA, B., AMAGHZAZ, M. and MESLOUH, S. 2015. *Maroccosuchus zennaroi* (Crocodylia: Tomistominae) from the Eocene of Morocco: phylogenetic and palaeobiogeographical implications of the basalmost tomistomine. *Journal of Systematic Palaeontology*, **13,** 421–445.

JUNGERS, W. L., FALSETTI, A. B. and WALL, C. E. 1995. Shape, relative size, and size-adjustments in morphometrics. *American Journal of Physical Anthropology*, **38,** 137–161.

KELLNER, A. W., PINHEIRO, A. E. and CAMPOS, D. A. 2014. A new sebecid from the paleogene of Brazil and the crocodyliform radiation after the K-Pg boundary. *PLoS One* **9,** e81386.

KHABBAZIAN, M., KRIEBEL, R., ROHE, K. and ANÉ, C. 2016. Fast and accurate detection of evolutionary shifts in Ornstein–Uhlenbeck models. *Methods in Ecology and Evolution*, **7,** 811–824.

KLEY, N. J., SERTICH, J. J., TURNER, A. H., KRAUSE, D. W., O'CONNOR, P. M. and GEORGI, J. A. 2010. Craniofacial morphology of *Simosuchus clarki* (Crocodyliformes:

Notosuchia) from the Late Cretaceous of Madagascar. *Journal of Vertebrate Paleontology*, **30(sup1),** 13–98.

KLINGENBERG, C. P. 1996. Multivariate allometry. 23–49. *In* MARCUS, L. F., CORTI, M., LOY, A., NAYLOR, G. J. P. and SLICE, D. E. (eds.). *Advances in Morphometrics*. Springer.

KLINGENBERG, C. P. 1998. Heterochrony and allometry: the analysis of evolutionary change in ontogeny. *Biological Reviews of the Cambridge Philosophical Society*, **73,** 79–123.

KLINGENBERG, C. P. 2011. MorphoJ: an integrated software package for geometric morphometrics. *Molecular Ecology Resouces*, **11,** 353–357.

KLINGENBERG, C. P. 2016. Size, shape, and form: concepts of allometry in geometric morphometrics. *Development Genes and Evolution*, **226**, 113–137.

KLINGENBERG, C. P. and M$_C$INTYRE, G. S. 1998. Geometric morphometrics of developmental instability: analyzing patterns of fluctuating asymmetry with Procrustes methods. *Evolution*, **52,** 1363–1375.

KLINGENBERG, C. P., DUTTKE, S., WHELAN, S. and KIM, M. 2012. Developmental plasticity, morphological variation and evolvability: a multilevel analysis of morphometric integration in the shape of compound leaves. *Journal of Evolutionary Biology*, **25,** 115–129.

KOBAYASHI, Y., TOMIDA, Y., KAMEI, T. and EGUCHI, T. 2006. Anatomy of a Japanese tomistomine crocodylian, *Toyotamaphimeia machikanensis* (Kamei et Matsumoto, 1965), from the middle Pleistocene of Osaka Prefecture: the reassessment of its phylogenetic status within Crocodylia. *National Science Museum Monographs*, **35,** 1-121.

KOYABU, D., WERNEBURG, I., MORIMOTO, N., ZOLLIKOFER, C. P., FORASIEPI, A. M., ENDO, H., KIMURA, J., OHDACHI, S. D., SON, N. T. and SANCHEZ-VILLAGRA, M. R. 2014. Mammalian skull heterochrony reveals modular evolution and a link between cranial development and brain size. *Nature Communications*, **5,** 3625.

KREBS, B. 1967. Der Jura-Krokodilier *Machimosaurus* H. v. Meyer. *Paläontologische Zeitschrift*, **41,** 46–59.

LANGSTON W. 1973. The crocodilian skull in historical perspective. 263–284. *In* GANS, C. and PARSONS, T. S. (eds.). *Biology of the Reptilia*. Academic Press.

LARSSON, H. C. and SUES, H. D. 2007. Cranial osteology and phylogenetic relationships of *Hamadasuchus rebouli* (Crocodyliformes: Mesoeucrocodylia) from the Cretaceous of Morocco. *Zoological Journal of the Linnean Society*, **149,** 533–567.

LAUDER, G. V. 1981. Form and function: structural analysis in evolutionary morphology. *Paleobiology*, **7,** 430–442.

LAUPRASERT, K., CUNY, G., BUFFETAUT, E., SUTEETHORN, V. and THIRAKHUPT, K. 2007. *Siamosuchus phuphokensis*, a new goniopholidid from the Early Cretaceous (ante-Aptian) of northeastern Thailand. *Bulletin de la Société Géologique de France*, **178,** 201–216.

LAURIN, M. 2004. The evolution of body size, Cope's rule and the origin of amniotes. *Systematic Biology*, **53,** 594–622.

LEARDI, J. M., FIORELLI, L. E. and GASPARINI, Z. 2015*a*. Redescription and reevaluation of the taxonomical status of *Microsuchus schilleri* (Crocodyliformes: Mesoeucrocodylia) from the Upper Cretaceous of Neuquén, Argentina. *Cretaceous Research*, **52,** 153–166.

LEARDI, J. M., POL, D., NOVAS, F. E. and SUÁREZ RIGLOS, M. 2015*b*. The postcranial anatomy of *Yacarerani boliviensis* and the phylogenetic significance of the notosuchian postcranial skeleton. *Journal of Vertebrate Paleontology*, **35,** e995187.

LEARDI, J. M., POL, D. and CLARK, J. M. 2017. Detailed anatomy of the braincase of *Macelognathus vagans* Marsh, 1884 (Archosauria, Crocodylomorpha) using high resolution tomography and new insights on basal crocodylomorph phylogeny. *PeerJ*, **5,** e2801.

LECUONA, A., EZCURRA, M. D. and IRMIS, R. B. 2016. Revision of the early crocodylomorph *Trialestes romeri* (Archosauria, Suchia) from the lower Upper Triassic Ischigualasto Formation of Argentina: one of the oldest-known crocodylomorphs. *Papers in Palaeontology*, **2,** 585–622.

LEE, M. S., CAU, A., NAISH, D. and DYKE, G. J. 2014. Sustained miniaturization and anatomical innovation in the dinosaurian ancestors of birds. *Science*, **345,** 562–566.

LEE, M. S. and YATES, A. M. 2018. Tip-dating and homoplasy: reconciling the shallow molecular divergences of modern gharials with their long fossil record. *Proceedings of the Royal Society of London B*, **285,** 20181071.

LELE, S. and RICHTSMEIER, J. T. 1991. Euclidean distance matrix analysis: A coordinate-free approach for comparing biological shapes using landmark data. *American Journal of Physical Anthropology*, **86,** 415–427.

LELE, S. R. and RICHTSMEIER, J. T. 2001. *An Invariant Approach to Statistical Analysis of Shapes*. Chapman and Hall/CRC.

LESTREL, P. E. 1982. A Fourier analytic procedure to describe complex morphological shapes. 393–409. *In* Dixon, A. and Sarnat B. (eds.). *Factors and mechanisms influencing bone growth*. Alan R. Liss.

LINNERT, C., ROBINSON, S. A., LEES, J. A., BOWN, P. R., PÉREZ-RODRÍGUEZ, I., PETRIZZO, M. R., FALZONI, F., LITTLER, K., ARZ, J. A. and RUSSELL, E. E. 2014. Evidence for global cooling in the Late Cretaceous. *Nature Communications*, **5,** 4194.

LLOYD, G. T., BAPST, D. W., FRIEDMAN, M. and DAVIS, K. E. 2016. Probabilistic divergence time estimation without branch lengths: dating the origins of dinosaurs, avian flight and crown birds. *Biology Letters*, **12,** 20160609.

LONGRICH, N. R., BHULLAR, B. A. S. and GAUTHIER, J. A. 2012. Mass extinction of lizards and snakes at the Cretaceous–Paleogene boundary. *Proceedings of the National Academy of Sciences*, **109,** 21396–21401.

LYDEKKER, R. 1888. *Catalogue of the Fossil Reptilia and Amphibia in the British Museum (Natural History), Part 1. Containing the orders Ornithosauria, Crocodilia, Dinosauria, Squamata, Rhynchocephalia, and Proterosauria*. Trustees of the British Museum of Natural History, London.

MACFADDEN, B. J. 1986. Fossil horses from "Eohippus"(*Hyracotherium*) to *Equus*: scaling, Cope's Law, and the evolution of body size. *Paleobiology*, **12,** 355–369.

MADDISON, W. P. and MADDISON, D. R. 2018. *Mesquite: a Modular System for Evolutionary Analysis. Version 3.51*. Available at: http://www.mesquiteproject.org.

MAHLER, D. L. and INGRAM, T. 2014. Phylogenetic comparative methods for studying clade-wide convergence. 425–450. *In* GARAMSZEGI, L. Z. (ed.). *Modern Phylogenetic Comparative Methods and their Application in Evolutionary Biology*. Springer.

MAHLER, D. L., INGRAM, T., REVELL, L. J. and LOSOS, J. B. 2013. Exceptional convergence on the macroevolutionary landscape in island lizard radiations. *Science*, **341,** 292–295.

MANNION, P. D., BENSON, R. B., CARRANO, M. T., TENNANT, J. P., JUDD, J. and BUTLER, R. J. 2015. Climate constrains the evolutionary history and biodiversity of crocodylians. *Nature Communications*, **6,** 8438.

MARCUS, L. F. 1990. Traditional morphometrics. 77–122. *In* ROHLF, F. J. and BOOKSTEIN, F. L. (eds.). *Proceedings of the Michigan Morphometrics Workshop*. University of Michigan Museum of Zoology Special Publication, **1990**.

MARINHO, T. S. and CARVALHO, I. S. 2009. An armadillo-like sphagesaurid crocodyliform from the Late Cretaceous of Brazil. *Journal of South American Earth Sciences*, **27,** 36–41.

MARKWICK, P. J. 1998*a*. Crocodilian diversity in space and time: the role of climate in paleoecology and its implication for understanding K/T extinctions. *Paleobiology*, **24,** 470–497.

MARKWICK, P. J. 1998*b*. Fossil crocodilians as indicators of Late Cretaceous and Cenozoic climates: implications for using palaeontological data in reconstructing palaeoclimate. *Palaeogeography, Palaeoclimatology, Palaeoecology*, **137,** 205–271.

MARSOLA, J. C. A., BATEZELLI, A., MONTEFELTRO, F. C., GRELLET-TINNER, G. and LANGER, M. C. 2016. Palaeoenvironmental characterization of a crocodilian nesting site from the Late Cretaceous of Brazil and the evolution of crocodyliform nesting strategies. *Palaeogeography, Palaeoclimatology, Palaeoecology*, **457,** 221–232.

MARTIN, J. E. 2007. New material of the Late Cretaceous globidontan *Acynodon iberoccitanus* (Crocodylia) from southern France. *Journal of Vertebrate Paleontology*, **27,** 362–372.

MARTIN, J. E 2010. A new species of *Diplocynodon* (Crocodylia, Alligatoroidea) from the Late Eocene of the Massif Central, France, and the evolution of the genus in the climatic context of the Late Palaeogene. *Geological Magazine*, **147,** 596–610.

MARTIN, J. E. and VINCENT, P. 2013. New remains of *Machimosaurus hugii* von Meyer, 1837 (Crocodilia, Thalattosuchia) from the Kimmeridgian of Germany. *Fossil Record*, **16,** 179–196.

MARTIN, J. E. and DE LAPPARENT DE BROIN, F. A. 2016. A miniature notosuchian with multicuspid teeth from the Cretaceous of Morocco. *Journal of Vertebrate Paleontology*, **36,** e1211534.

MARTIN, J. E., LAUPRASERT, K., BUFFETAUT, E., LIARD, R. and SUTEETHORN, V. 2014. A large pholidosaurid in the Phu Kradung Formation of north-eastern Thailand. *Palaeontology*, **57,** 757–769.

MARTIN, J. E., DELFINO, M. and SMITH, T. 2016. Osteology and affinities of Dollo's goniopholidid (Mesoeucrocodylia) from the Early Cretaceous of Bernissart, Belgium. *Journal of Vertebrate Paleontology*, **36,** e1222534.

MARTINELLI, A. G. 2013. *Comahuesuchus brachybuccalis* (Archosauria, Crocodyliformes) from the Late Cretaceous of Río Negro Province (Argentina). *Ameghiniana*, **40,** 559–572.

MARTINELLI , A. G. and TEIXEIRA, V. P. 2015. The late Cretaceous vertebrate record from the Bauru group in the Triângulo Mineiro, southeastern Brazil. *Boletín Geológico y Minero*, **126,** 129–158.

MARTINS, E. P. and HANSEN, T. F. 1997. Phylogenies and the comparative method: a general approach to incorporating phylogenetic information into the analysis of interspecific data. *The American Naturalist*, **149,** 646–667.

MARX, F. G. and UHEN, M. D. 2010. Climate, critters, and cetaceans: Cenozoic drivers of the evolution of modern whales. *Science*, **327,** 993–996.

MAYR, E. 1982. *The growth of Biological Thought: Diversity, Evolution, and Inheritance*. Harvard University Press.

M$_C$CLAIN, C. R. and BOYER, A. G. 2009. Biodiversity and body size are linked across metazoans. *Proceedings of the Royal Society of London B*, **276,** 2209–2215.

M$_C$COY, M. W., BOLKER, B. M., OSENBERG, C. W., MINER, B. G. and VONESH, J. R. 2006. Size correction: comparing morphological traits among populations and environments. *Oecologia*, **148,** 547–554.

M$_C$CURRY, M. R., EVANS, A. R., FITZGERALD, E. M., ADAMS, J. W., CLAUSEN, P. D. and M$_C$HENRY, C. R. 2017*a*. The remarkable convergence of skull shape in crocodilians and toothed whales. *Proceedings of the Royal Society of London B*, **284,** 20162348.

M$_C$CURRY, M. R., WALMSLEY, C. W., FITZGERALD, E. M. G. and M$_C$HENRY, C. R. 2017*b*. The biomechanical consequences of longirostry in crocodilians and odontocetes. *Journal of Biomechanics*, **56,** 61–70.

M$_C$HENRY, C. R., CLAUSEN, P. D., DANIEL, W. J., MEERS, M. B. and PENDHARKAR, A. 2006. Biomechanics of the rostrum in crocodilians: a comparative analysis using finite-element modeling. *The Anatomical Record Part A*, **288A,** 827–849.

M$_C$KINNEY, M. L. 1988. Classifying heterochrony: allometry, size, and time. 17–34. *In* M$_C$KINNEY, M. L. (ed.). *Heterochrony in Evolution. A Multidisciplinary Approach.* Plenum Press.

M$_C$KINNEY, M. L. 1990*a*. Trends in body size evolution. 75–118. *In* M$_C$NAMARA, K. J. (ed.). *Evolutionary Trends*. The University of Arizona Press.

M$_C$KINNEY, M. L. 1990*b*. Classifying and analyzing evolutionary trends. 28–58. *In* M$_C$NAMARA, K. J. (ed.). *Evolutionary Trends*. The University of Arizona Press.

M$_C$NAMARA, K. J. 1982. Heterochrony and phylogenetic trends. *Paleobiology*, **8,** 130–142.

M$_C$NAMARA, K. J. 1986. A guide to the nomenclature of heterochrony. *Journal of Paleontology*, **60,** 4–13.

M$_C$NAMARA, K. J. 1990. The role of heterochrony in evolutionary trends. 59–74. *In* M$_C$NAMARA, K. J. (ed.). *Evolutionary Trends*. The University of Arizona Press.

M$_C$NAMARA, K. J. and M$_C$KINNEY, M. L. 2005. Heterochrony, disparity, and macroevolution. *Paleobiology*, **31,** 17–26.

M$_C$SHEA, D. W. 1994. Mechanisms of large-scale evolutionary trends. *Evolution*, **48,** 1747–1763.

MEDINA, C. J. 1976. Crocodilians from the Late Tertiary of northwestern Venezuela: *Melanosuchus fisheri* sp. nov. *Breviora*, **438,** 1–14.

MÉNDEZ, A. H., NOVAS, F. E. and IORI FV. 2012. First record of Megaraptora (Theropoda, Neovenatoridae) from Brazil. *Comptes Rendus Palevol*, **11,** 251–256.

MERCIER, J. 1933. Contribution à l'étude des Métriorhynchidés (crocodiliens). *Annales de Paléontologie*, **22,** 99–119.

MEUNIER, L. and LARSSON, H. C. 2017. Revision and phylogenetic affinities of *Elosuchus* (Crocodyliformes). *Zoological Journal of the Linnean Society*, **179,** 169–200.

MITTEROECKER, P. and GUNZ, P. 2009. Advances in geometric morphometrics. *Evolutionary Biology*, **36,** 235–247.

MONTEFELTRO, F. C., LARSSON, H. C. and LANGER, M. C. 2011. A new baurusuchid (Crocodyliformes, Mesoeucrocodylia) from the Late Cretaceous of Brazil and the phylogeny of Baurusuchidae. *PLoS One* **6,** e21916.

MONTEFELTRO, F. C., LARSSON, H. C. FRANCA, M. A. and LANGER, M. C. 2013. A new neosuchian with Asian affinities from the Jurassic of northeastern Brazil. *Naturwissenschaften*, **100,** 835–841.

MONTEFELTRO, F. C., ANDRADE, D. V. and LARSSON, H. C. 2016. The evolution of the meatal chamber in crocodyliforms. *Journal of Anatomy*, **228,** 838–863.

MONTEIRO, L. R. 1999. Multivariate regression models and geometric morphometrics: the search for causal factors in the analysis of shape. *Systematic Biology*, **48,** 192–199.

MONTEIRO, L. R. 2013. Morphometrics and the comparative method: studying the evolution of biological shape. *Hystrix, the Italian Journal of Mammalogy*, **24,** 25–32.

MONTEIRO, L. R., CAVALCANTI, M. J. and SOMMER III, H. J. S. 1997. Comparative ontogenetic shape changes in the skull of *Caiman* species (Crocodylia, Alligatoridae). *Journal of Morphology*, **231,** 53–62.

MOTANI, R. 2001. Estimating body mass from silhouettes: testing the assumption of elliptical body cross-sections. *Paleobiology*, **27,** 735–750.

NARVÁEZ, I., BROCHU, C. A., ESCASO, F., PÉREZ-GARCÍA, A. and ORTEGA, F. 2015. New crocodyliforms from southwestern Europe and definition of a diverse clade of European Late Cretaceous basal eusuchians. *PLoS One*, **10,** e0140679.

NARVÁEZ, I., BROCHU, C. A., ESCASO, F., PÉREZ-GARCÍA, A. and ORTEGA, F. 2016. New Spanish Late Cretaceous eusuchian reveals the synchronic and sympatric presence of two allodaposuchids. *Cretaceous Research*, **65,** 112–125.

NESBITT, S. J. 2011. The early evolution of archosaurs: relationships and the origin of major clades. *Bulletin of the American Museum of Natural History*, **352,** 1–292.

NEWELL, N. D. 1949. Phyletic size increase, an important trend illustrated by fossil invertebrates. *Evolution*, **3,** 103–124.

NOVAS, F. E., PAIS, D. F., POL, D., CARVALHO, I. D. S., SCANFERLA, A., MONES, A. and RIGLOS, M. S. 2009. Bizarre notosuchian crocodyliform with associated eggs from the Upper Cretaceous of Bolivia. *Journal of Vertebrate Paleontology*, **29,** 1316–1320.

O'CONNOR, P. M., SERTICH, J. J. W., STEVENS, N. J., ROBERTS, E. M., GOTTFRIED, M. D., HIERONYMUS, T. L., JINNAH, Z. A., RIDGELY, R., NGASALA, S. E. and TEMBA, J. 2010. The evolution of mammal-like crocodyliforms in the Cretaceous Period of Gondwana. *Nature*, **466,** 748–751.

OPENSHAW, G. H., D'AMORE, D. C., VIDAL-GARCÍA, M. and KEOGH, .J. S. 2016. Combining geometric morphometric analyses of multiple 2D observation views improves interpretation of evolutionary allometry and shape diversification in monitor lizard (*Varanus*) crania. *Biological Journal of the Linnean Society*, **120,** 539–552.

ORME, C. D. L., FRECKLETON, R., THOMAS, G., PETZOLDT, T., FRITZ, S., ISAAC, N. and PEARSE, W. 2018. *CAPER: comparative analyses of phylogenetics and evolution in R. R package version 1.0.1.* https://CRAN.R-project.org/package=caper.

ORTEGA, F., GASPARINI, Z., BUSCALIONI, A. D. and CALVO, J. O. 2000. A new species of *Araripesuchus* (Crocodylomorpha, Mesoeucrocodylia) from the lower Cretaceous of Patagonia (Argentina). *Journal of Vertebrate Paleontology*, **20,** 57–76.

ŐSI, A. 2014. The evolution of jaw mechanism and dental function in heterodont crocodyliforms. *Historical Biology*, **26,** 279–414.

ŐSI, A., CLARK, J. M. and WEISHAMPEL, D. B. 2007. First report on a new basal eusuchian crocodyliform with multicusped teeth from the Upper Cretaceous (Santonian) of Hungary. *Neues Jahrbuch für Geologie und Paläontologie-Abhandlungen*, **243,** 169–177.

ŐSI, A., YOUNG, M. T., GALÁCZ, A. and RABI, M. 2018. A new large-bodied thalattosuchian crocodyliform from the Lower Jurassic (Toarcian) of Hungary, with further evidence of the mosaic acquisition of marine adaptations in Metriorhynchoidea. *PeerJ*, **6,** e4668.

PAGEL, M. 1999. Inferring the historical patterns of biological evolution. *Nature*, **401,** 877–884.

PAGEL, M. 2002. Modelling the evolution of continuously varying characters on phylogenetic trees. 269–286. *In* MACLEOD, N. and FOREY, P. L. (eds.). *Morphology, Shape and Phylogeny*. Taylor & Francis.

PARRILLA-BEL, J., YOUNG, M. T., MORENO-AZANZA, M. and CANUDO, J. I. 2013. The first metriorhynchid crocodylomorph from the Middle Jurassic of Spain, with implications for evolution of the subclade Rhacheosaurini. *PLoS One*, **8,** e54275.

PENNELL, M. W. and HARMON, L. J. 2013. An integrative view of phylogenetic comparative methods: connections to population genetics, community ecology, and paleobiology. *Annals of the New York Academy of Sciences*, **1289,** 90–105.

PETERS, R. H. 1986. *The Ecological Implications of Body Size*. Cambridge University Press.

PIERCE, S. E., ANGIELCZYK, K. D. and RAYFIELD, E. J. 2008. Patterns of morphospace occupation and mechanical performance in extant crocodilian skulls: a combined geometric morphometric and finite element modeling approach. *Journal of Morphology*, **269,** 840–864.

PIERCE, S. E., ANGIELCZYK, K. D. and RAYFIELD, E. J. 2009*a*. Morphospace occupation in thalattosuchian crocodylomorphs: skull shape variation, species delineation and temporal patterns. *Palaeontology*, **52,** 1057–1097.

PIERCE, S. E., ANGIELCZYK, K. D. and RAYFIELD, E. J. 2009*b*. Shape and mechanics in thalattosuchian (Crocodylomorpha) skulls: implications for feeding behaviour and niche partitioning. *Journal of Anatomy*, **215,** 555–576.

PINHEIRO, J., BATES, D., DEBROY, S., SARKAR, D. and R CORE TEAM. 2017. *nlme: linear and nonlinear mixed effects models. R package version 3.1–131*. https://CRAN.R-project.org/package=nlme.

PIRAS, P., DELFINO, M., DEL FAVERO, L. and KOTSAKIS, T. 2007. Phylogenetic position of the crocodylian *Megadontosuchus arduini* and tomistomine palaeobiogeography. *Acta Palaeontologica Polonica*, **52,** 315–328.

PIRAS, P., TERESI, L., BUSCALIONI, Á. D. and CUBO, J. 2009. The shadow of forgotten ancestors differently constrains the fate of Alligatoroidea and Crocodyloidea. *Global Ecology and Biogeography*, **18,** 30–40.

PIRAS, P., COLANGELO, P., ADAMS, D. C., BUSCALIONI, Á. D., CUBO, J., KOTSAKIS, T., MELORO, C. and RAIA, P. 2010. The *Gavialis–Tomistoma* debate: the contribution of skull ontogenetic allometry and growth trajectories to the study of crocodylian relationships. *Evolution & Development*, **12,** 568–579.

PIRAS, P., BUSCALIONI, A. D., TERESI, L., RAIA, P., SANSALONE, G., KOTSAKIS, T. and CUBO, J. 2014. Morphological integration and functional modularity in the crocodilian skull. *Integrative Zoology*, **9,** 498–516.

PLATT, S. G., RAINWATER, T. R., THORBJARNARSON, J. B., FINGER, A. G., ANDERSON, T. A. and McMURRY, S. T. 2009. Size estimation, morphometrics, sex ratio, sexual size dimorphism, and biomass of Morelet's crocodile in northern Belize. *Caribbean Journal of Science*, **45,** 80–93.

PLATT, S. G., RAINWATER, T. R., THORBJARNARSON, J. B. and MARTIN, D. 2011. Size estimation, morphometrics, sex ratio, sexual size dimorphism, and biomass of *Crocodylus acutus* in the coastal zone of Belize. *Salamandra*, **47,** 179–192.

POL, D. 2003. New remains of *Sphagesaurus huenei* (Crocodylomorpha: Mesoeucrocodylia) from the Late Cretaceous of Brazil. *Journal of Vertebrate Paleontology*, **23,** 817–831.

POL, D. 2005. Postcranial remains of *Notosuchus terrestris* Woodward (Archosauria: Crocodyliformes) from the Upper Cretaceous of Patagonia, Argentina. *Ameghiniana*, **42,** 21–38.

POL, D. and NORELL, M. A. 2004. A new gobiosuchid crocodyliform taxon from the Cretaceous of Mongolia. *American Museum Novitates*, **3458,** 1–31.

POL, D. and GASPARINI, Z. 2009. Skull anatomy of *Dakosaurus andiniensis* (Thalattosuchia: Crocodylomorpha) and the phylogenetic position of Thalattosuchia. *Journal of Systematic Palaeontology*, **7,** 163–197.

POL, D. and LEARDI, J. M. 2015. Diversity patterns of Notosuchia (Crocodyliformes, Mesoeucrocodylia) during the Cretaceous of Gondwana. 172–186. *In* FERNÁNDEZ, M. and HERRERA, Y. (eds.). *Reptiles Extintos – Volumen en Homenaje a Zulma Gasparini*. Publicación Electrónica de la Asociación Paleontológica Argentina, Buenos Aires, Argentina.

POL, D., JI, S. A., CLARK, J. M. and CHIAPPE, L. M. 2004. Basal crocodyliforms from the Lower Cretaceous Tugulu Group (Xinjiang, China), and the phylogenetic position of *Edentosuchus*. *Cretaceous Research*, **25,** 603–622.

POL, D., TURNER, A. H. and NORELL, M. A. 2009. Morphology of the Late Cretaceous crocodylomorph *Shamosuchus djadochtaensis* and a discussion of neosuchian phylogeny as related to the origin of Eusuchia. *Bulletin of the American Museum of Natural History*, **324,** 1–103.

POL, D., LEARDI, J. M., LECUONA, A. and KRAUSE, M. 2012. Postcranial anatomy of *Sebecus icaeorhinus* (Crocodyliformes, Sebecidae) from the Eocene of Patagonia. *Journal of Vertebrate Paleontology*, **32,** 328–354.

POL, D., RAUHUT, O. W., LECUONA, A., LEARDI, J. M., XU, X. and CLARK, J. M. 2013. A new fossil from the Jurassic of Patagonia reveals the early basicranial evolution and the origins of Crocodyliformes. *Biological Reviews*, **88,** 862–872.

POL, D., NASCIMENTO, P. M., CARVALHO, A. B., RICCOMINI, C., PIRES-DOMINGUES, R. A. and ZAHER, H. 2014. A new notosuchian from the Late Cretaceous of Brazil and the phylogeny of advanced notosuchians. *PLoS One*, **9,** e93105.

PRENTICE, K. C., RUTA, M. and BENTON, M. J. 2011. Evolution of morphological disparity in pterosaurs. *Journal of Systematic Palaeontology*, **9,** 337–353.

PRICE, L. I. 1945. A new reptil from the Cretaceous of Brazil. *Divisão de Geologia e Mineralogia, Notas Preliminares e Estudos*, **25,** 1–8.

PRICE, S. A. and HOPKINS, S. S. B. 2015. The macroevolutionary relationship between diet and body mass across mammals. *Biological Journal of the Linnean Society*, **115,** 173–184.

PROKOPH, A., SHIELDS, G. A. and VEIZER, J. 2008. Compilation and time-series analysis of a marine carbonate $\delta^{18}O$, $\delta^{13}C$, $^{87}Sr/^{86}Sr$ and $\delta^{34}S$ database through Earth history. *Earth-Science Reviews*, **87,** 113–133.

PUÉRTOLAS-PASCUAL, E., CANUDO, J. I. and CRUZADO-CABALLERO, P. 2011. A new crocodylian from the Late Maastrichtian of Spain: implications for the initial radiation of crocodyloids. *PLoS One*, **6,** e20011.

PUÉRTOLAS-PASCUAL, E., CANUDO, J. I. and MORENO-AZANZA, M. 2014. The eusuchian crocodylomorph *Allodaposuchus subjuniperus* sp. nov., a new species from the latest Cretaceous (upper Maastrichtian) of Spain. *Historical Biology*, **26,** 91–109.

PURVIS, A., GITTLEMAN, J. L., COWLISHAW, G. ans MACE, G. M. 2000. Predicting extinction risk in declining species. *Proceedings of the Royal Society of London B*, **267,** 1947–1952.

R CORE TEAM. 2017. *R: A language and environment for statistical computing. v. 3.4.1*. R Foundation for Statistical Computing, Vienna, Austria. https://www.R-project.org/.

R CORE TEAM. 2018. *R: A language and environment for statistical computing. v. 3.5.1*. R Foundation for Statistical Computing, Vienna, Austria. URL https://www.R-project.org/.

RAUP, D. M. 1972. Taxonomic diversity during the Phanerozoic. *Science*, **177,** 1065–1071.

RAUP, D. M. 1988. Testing the fossil record for evolutionary progress. 293–317. *In* Nitecki, M. H. (ed.). *Evolutionary Progress*. University of Chicago Press.

RAUP, D. M. and SEPKOSKI, J. J. 1982. Mass extinctions in the marine fossil record. *Science*, **215,** 1501–1503.

REVELL, L. J. 2009. Size-correction and principal components for interspecific comparative studies. *Evolution*, **63,** 3258–3268.

REVELL, L. J. 2012. phytools: an R package for phylogenetic comparative biology (and other things). *Methods in Ecology and Evolution*, **3,** 217–223.

RICE, W. R. 1989. Analyzing tables of statistical tests. *Evolution*, **43,** 223–225.

RIFF. D. and KELLNER AWA. 2011. Baurusuchid crocodyliforms as theropod mimics: clues from the skull and appendicular morphology of *Stratiotosuchus maxhechti* (Upper Cretaceous of Brazil). *Zoological Journal of the Linnean Society*, **163,** 37–56.

RISTEVSKI, J., YOUNG, M. T., ANDRADE, M. B. and HASTINGS, A. K. 2018. A new species of *Anteophthalmosuchus* (Crocodylomorpha, Goniopholididae) from the Lower Cretaceous of the Isle of Wight, United Kingdom, and a review of the genus. *Cretaceous Research*, **84,** 340–383.

ROBINSON, C. and TERHUNE, C. E. 2017. Error in geometric morphometric data collection: Combining data from multiple sources. *American Journal of Physical Anthropology*, **164,** 62–75.

ROHLF, F. J. 2001. Comparative methods for the analysis of continuous variables: geometric interpretations. *Evolution*, **55,** 2143–2160.

ROHLF, F. J. 2015. The tps series of software. *Hystrix, the Italian Journal of Mammalogy*, **26,** 9–12

ROHLF, F. J. and BOOKSTEIN, F. L. 1987. A comment on shearing as a method for "size correction". *Systematic Zoology*, **36,** 356–367.

ROHLF, F. J. and SLICE, D. E. 1990. Extensions of the Procrustes method for the optimal superimposition of landmarks. *Systematic Biology*, **39,** 40–59.

ROHLF, F. J. and MARCUS, L. F. 1993. A revolution in morphometrics. *Trends in Ecology & Evolution*, **8,** 129–129.

ROMER, A. S. and PRICE, L. W. 1940. Review of the Pelycosauria. *Geological Society of America, Special Papers*, **28,** 1–534.

ROSS, J. P. 1998. *Crocodiles: Status Survey and Conservation Action Plan*. IUCN/SSC Crocodile Specialist Group.

RUSSELL, E. S. 1916. *Form and function: A Contribution to the History of Animal Morphology*. John Murray.

RUSSELL, A. P. and WU, X. 1997. The Crocodylomorpha at and between geological boundaries. *Zoology*, **100,** 164–182.

RUSSO, J., MATEUS, O., BALBINO, A. and MARZOLA, M. 2014. Crocodylomorph eggs and eggshells from the Lourinhã Fm. (Upper Jurassic), Portugal. *Comunicações Geológicas*, **101,** 563–566.

SAARINEN, J. J, BOYER, A. G., BROWN, J. H., COSTA, D. P., ERNEST, S. M., EVANS, A. R., FORTELIUS, M., GITTLEMAN, J. L., HAMILTON, M. J., HARDING, L. E., LINTULAAKSO, K., LYONS, S. K., OKIE, J. G., SIBLY, R. M., STEPHENS, P. R., THEODOR, J., UHEN, M. D. and SMITH, F. A. 2014. Patterns of maximum body size evolution in Cenozoic land mammals: eco-evolutionary processes and abiotic forcing. *Proceedings of the Royal Society of London B*, **281,** 20132049.

SADLEIR, R. W. and MAKOVICKY, P. J. 2008. Cranial shape and correlated characters in crocodilian evolution. *Journal of Evolutionary Biology*, **21,** 1578–1596.

SALAS-GISMONDI, R., FLYNN, J. J., BABY, P., TEJADA-LARA, J. V., WESSELINGH, F. P. and ANTOINE, P. O. 2015. A Miocene hyperdiverse crocodylian community reveals peculiar trophic dynamics in proto-Amazonian mega-wetlands. *Proceedings of the Royal Society of London B*, **282,** 20142490.

SALAS-GISMONDI, R., FLYNN, J. J., BABY, P., TEJADA-LARA, J. V., CLAUDE, J. and ANTOINE, P. O. 2016. A new 13 million year old gavialoid crocodylian from proto-Amazonian mega-wetlands reveals parallel evolutionary trends in skull shape linked to longirostry. *PLoS One*, **11,** e0152453.

SALISBURY, S. W., MOLNAR, R. E., FREY, E. and WILLIS, P. M. 2006. The origin of modern crocodyliforms: new evidence from the Cretaceous of Australia. *Proceedings of the Royal Society of London B*, **273,** 2439–2448.

SCHEYER, T. M., AGUILERA, O. A., DELFINO, M., FORTIER, D. C., CARLINI, A. A., SÁNCHEZ, R., CARRILLO-BRICEÑO, J. D., QUIROZ, L. and SÁNCHEZ-VILLAGRA, M. R. 2013. Crocodylian diversity peak and extinction in the late Cenozoic of the northern Neotropics. *Nature Communications*, **4,** 1907.

SCHMIDT-NIELSEN, K. 1984. *Scaling: Why is Animal Size so Important?*. Cambridge University Press.

SCHOCH, R. R. 2010. Heterochrony: the interplay between development and ecology exemplified by a Paleozoic amphibian clade. *Paleobiology*, **36,** 318–334.

SCHWARZ, D., RADDATZ, M. and WINGS, O. 2017. *Knoetschkesuchus langenbergensis* gen. nov. sp. nov., a new atoposaurid crocodyliform from the Upper Jurassic Langenberg Quarry (Lower Saxony, northwestern Germany), and its relationships to Theriosuchus. *PLoS One*, **12,** e0160617.

SELLERS, W. I., HEPWORTH-BELL, J., FALKINGHAM, P. L., BATES, K. T., BRASSEY, C. A., EGERTON, V. M. and MANNING, P. L. 2012. Minimum convex hull mass estimations of complete mounted skeletons. *Biology Letters*, **8,** 842–845.

SEPKOSKI, J. J. 1978. A kinetic model of Phanerozoic taxonomic diversity I. Early Phanerozoic families and multiple equilibria. *Paleobiology*, **4,** 223–251.

SEPKOSKI, J. J. 1979. A kinetic model of Phanerozoic taxonomic diversity II. Early Phanerozoic families and multiple equilibria. *Paleobiology*, **5,** 222–251.

SEPKOSKI, J. J. 1981. A factor analytic description of the Phanerozoic marine fossil record. *Paleobiology*, **7,** 36–53.

SEPKOSKI, J. J. 1984. A kinetic model of Phanerozoic taxonomic diversity II. Early Phanerozoic families and multiple equilibria. *Paleobiology*, **10,** 246–267.

SEPKOSKI, D. 2012. *Rereading the Fossil Record: the Growth of Paleobiology as an Eevolutionary Discipline*. University of Chicago Press.

SEPKOSKI JR, J. J., BAMBACH, R. K., RAUP, D. M. and VALENTINE, J. W. 1981. Phanerozoic marine diversity and the fossil record. *Nature*, **293,** 435–437.

SERENO, P. C. 2005. The logical basis of phylogenetic taxonomy. *Systematic Biology*, **54,** 595–619.

SERENO, P. and LARSSON. H. 2009. Cretaceous crocodyliforms from the Sahara. *ZooKeys*, **28,** 1–143.

SERENO, P. C., LARSSON, H. C., SIDOR, C. A. and GADO, B. 2001. The giant crocodyliform *Sarcosuchus* from the Cretaceous of Africa. *Science*, **294,** 1516–1519.

SERENO, P., SIDOR, C. A., LARSSON, H. C. E. and GADO, B. 2003. A new notosuchian from the Early Cretaceous of Niger. *Journal of Vertebrate Paleontology*, **23,** 477–482.

SERTICH, J. J. W. and O'CONNOR, P. M. 2014. A new crocodyliform from the middle Cretaceous Galula Formation, southwestern Tanzania. *Journal of Vertebrate Paleontology*, **34,** 576–596.

SHAN, H. Y., WU, X. C., CHENG, Y. N. and SATO, T. 2017. *Maomingosuchus petrolica*, a restudy of "*Tomistoma*" *petrolica* Yeh, 1958. *Palaeoworld*, **26,** 672–690.

SHEA, B. T. 1983. Allometry and heterochrony in the African apes. *American Journal of Physical Anthropology*, **62,** 275–289.

SHEARER, B. M., COOKE, S. B., HALENAR, L. B., REBER, S. L., PLUMMER, J. E., DELSON, E. and TALLMAN, M. 2017. Evaluating causes of error in landmark-based data collection using scanners. *PLoS One*, **12,** e0187452.

SIDLAUSKAS, B. 2008. Continuous and arrested morphological diversification in sister clades of characiform fishes: a phylomorphospace approach. *Evolution*, **62,** 3135–3156.

SIMPSON, G. G. 1944. *Tempo and Mode in Evolution*. Columbia University Press.

SIMPSON, G. G. 1953. *Major Features of Evolution*. Columbia University Press.

SLATER, G. J. 2013. Phylogenetic evidence for a shift in the mode of mammalian body size evolution at the Cretaceous-Palaeogene boundary. *Methods in Ecology and Evolution*, **4,** 734–744.

SLATER, G. J. 2015. Iterative adaptive radiations of fossil canids show no evidence for diversity-dependent trait evolution. *Proceedings of the National Academy of Sciences*, **112,** 4897–4902.

SLATER, G. J., HARMON, L. J. and ALFARO, M. E. 2012. Integrating fossils with molecular phylogenies improves inference of trait evolution. *Evolution*, **66,** 3931–3944.

SMITH, E. N. 1976. Heating and cooling rates of the American alligator, *Alligator mississippiensis*. *Physiological Zoology*, **49,** 37–48.

SMITH, F. A. and LYONS, S. K. 2011. How big should a mammal be? A macroecological look at mammalian body size over space and time. *Philosophical Transactions of the Royal Society of London B*, **366,** 2364–2378.

SMITH, F. A., BOYER, A. G., BROWN, J. H., COSTA, D. P., DAYAN, T., ERNEST, S. M., EVANS, A. R., FORTELIUS, M., GITTLEMAN, J. L., HAMILTON, M. J., HARDING, L. E., LINTULAAKSO, K., LYONS, S. K., McCAIN, C., OKIE, J. G., SAARINEN, J. J., SIBLY, R. M., STEPHENS, P. R., THEODOR, J. and UHEN, M. D. 2010. The evolution of maximum body size of terrestrial mammals. *Science*, **330,** 1216–1219.

SOOKIAS, R. B., BUTLER, R. J. and BENSON, R. B. 2012*a*. Rise of dinosaurs reveals major body-size transitions are driven by passive processes of trait evolution. *Proceedings of the Royal Society of London B,* **279,** 2180–2187.

SOOKIAS, R. B., BUTLER, R. J. and BENSON, R. B. 2012*b*. Biology, not environment, drives major patterns in maximum tetrapod body size through time. *Biology Letters*, **8,** 674–677.

SRIVASTAVA, R., PATNAIK, R., SHUKLA, U. K. and SAHNI, A. 2015. Crocodilian nest in a Late Cretaceous sauropod hatchery from the type Lameta Ghat locality, Jabalpur, India. *PLoS One,* **10,** e0144369.

STANLEY, S. M. 1973. An explanation for Cope's rule. *Evolution,* **27,** 1–26.

STRELIN, M. M., BENITEZ-VIEYRA, S., FORNONI, J., KLINGENBERG, C. P. and COCUCCI, A. A. 2016. Exploring the ontogenetic scaling hypothesis during the diversification of pollination syndromes in *Caiophora* (Loasaceae, subfam. Loasoideae). *Annals of Botany*, **117,** 937–947.

STUBBS, T. L., PIERCE, S. E., RAYFIELD, E. J. and ANDERSON, P. S. 2013. Morphological and biomechanical disparity of crocodile-line archosaurs following the end-Triassic extinction. *Proceedings of the Royal Society of London B,* **280,** 20131940.

SUES, H. D., OLSEN, P. E., CARTER, J. G. and SCOTT, D. M. 2003. A new crocodylomorph archosaur from the Upper Triassic of North Carolina. *Journal of Vertebrate Paleontology*, **23,** 329–343.

SUGIURA, N. 1978. Further analysts of the data by Akaike's information criterion and the finite corrections. *Communications in Statistics–Theory and Methods*, **7,** 13–26.

TAYLOR, M. A. 1987. How tetrapods feed in water: a functional analysis by paradigm. *Zoological Journal of the Linnean Society*, **91,** 171–195.

TENNANT, J. P., MANNION, P. D. and UPCHURCH, P. 2016*a*. Evolutionary relationships and systematics of Atoposauridae (Crocodylomorpha: Neosuchia): implications for the rise of Eusuchia. *Zoological Journal of the Linnean Society*, **177,** 854–936.

TENNANT, J. P., MANNION, P. D. and UPCHURCH, P. 2016*b*. Environmental drivers of crocodyliform extinction across the Jurassic/Cretaceous transition. *Proceedings of the Royal Society of London B*, **283,** 20152840.

TENNANT, J. P., MANNION, P. D. and UPCHURCH, P. 2016*c*. Sea level regulated tetrapod diversity dynamics through the Jurassic/Cretaceous interval. *Nature Communications*, **7,** 12737.

TENNANT, J. P., MANNION, P. D., UPCHURCH, P., SUTTON, M. D. and PRICE, G. D. 2017. Biotic and environmental dynamics through the Late Jurassic–Early Cretaceous transition: evidence for protracted faunal and ecological turnover. *Biological Reviews*, **92,** 776–814.

THOMPSON, D. W. 1917. *On growth and form*. Cambridge University Press.

THORBJARNARSON, J. B. 1990. Notes on the feeding behavior of the gharial (*Gavialis gangeticus*) under semi-natural conditions. *Journal of Herpetology*, 24, 99–100.

TOLJAGIĆ, O. and BUTLER, R. J. 2013. Triassic–Jurassic mass extinction as trigger for the Mesozoic radiation of crocodylomorphs. *Biology Letters*, **9,** 20130095.

TURNER, A. H. 2006. Osteology and phylogeny of a new species of *Araripesuchus* (Crocodyliformes: Mesoeucrocodylia) from the Late Cretaceous of Madagascar. *Historical Biology*, **18,** 255–369.

TURNER, A. H. 2015. A review of *Shamosuchus* and *Paralligator* (Crocodyliformes, Neosuchia) from the Cretaceous of Asia. *PLoS One*, **10,** e0118116.

TURNER, A. H. and BUCKLEY, G. A. 2008. *Mahajangasuchus insignis* (Crocodyliformes: Mesoeucrocodylia) cranial anatomy and new data on the origin of the eusuchian-style palate. *Journal of Vertebrate Paleontology*, **28,** 382–408.

TURNER, A. and SERTICH, J. J. W. 2010. Phylogenetic history of *Simosuchus clarki* (Crocodyliformes: Notosuchia) from the Late Cretaceous of Madagascar. *Journal of Vertebrate Paleontology*, **30,** 177–236.

TURNER, A. H. and NESBITT, S. J. 2013. Body size evolution during the Triassic archosauriform radiation. 573–597. *In*. NESBITT, S. J., DESOJO, J. B. and IRMIS, R. B. (eds.). *Anatomy, phylogeny and palaeobiology of early archosaurs and their kin*. Geological Society of London, Special Publications, **379**.

TURNER, A. H. and PRITCHARD, A. C. 2015. The monophyly of Susisuchidae (Crocodyliformes) and its phylogenetic placement in Neosuchia. *PeerJ*, **3,** e759.

TURNER, A. H., POL, D., CLARKE, J. A., ERICKSON, G. M. and NORELL, M. A. 2007. A basal dromaeosaurid and size evolution preceding avian flight. *Science*, **317,** 1378–1381.

TYKOSKI, R. S., ROWE, T. B., KETCHAM, R. A. and COLBERT, M. W. 2002. *Calsoyasuchus valliceps*, a new crocodyliform from the Early Jurassic Kayenta Formation of Arizona. *Journal of Vertebrate Paleontology*, **22,** 593–611.

UYEDA, J. C. and HARMON, L. J. 2014. A novel Bayesian method for inferring and interpreting the dynamics of adaptive landscapes from phylogenetic comparative data. *Systematic Biology*, **63,** 902–918.

VALENTIN, A. E., PENIN, X., CHANUT, J. P., SÉVIGNY, J. M. and ROHLF, F. J. 2008. Arching effect on fish body shape in geometric morphometric studies. *Journal of Fish Biology*, **73,** 623–638.

VAN VALEN, L. 1971. Adaptive zones and the orders of mammals. *Evolution*, **25,** 420–428.

VAN VALKENBURGH, B. 1991. Iterative evolution of hypercarnivory in canids (Mammalia: Carnivora): evolutionary interactions among sympatric predators. *Paleobiology*, **17,** 340–361.

VAN VALKENBURGH, B. 1999. Major patterns in the history of carnivorous mammals. *Annual Review of Earth and Planetary Sciences*, **27,** 463–493.

VAN VALKENBURGH, B., WANG, X. and DAMUTH, J. 2004. Cope's rule, hypercarnivory, and extinction in North American canids. *Science*, **306,** 101–104.

VENDITTI, C., MEADE, A. and PAGEL, M. 2011. Multiple routes to mammalian diversity. *Nature*, **479,** 393–396.

VERMEIJ, G. J. 2016. Gigantism and its implications for the history of life. *PLoS One*, **11,** e0146092.

WALKER, A. D. 1990. A revision of *Sphenosuchus acutus* Haughton, a crocodylomorph reptile from the Elliot Formation (late Triassic or early Jurassic) of South Africa. *Philosophical Transactions of the Royal Society of London B*, **330,** 1–120.

WALMSLEY, C. W., SMITS, P. D., QUAYLE, M. R., M$_C$CURRY, M. R., RICHARDS, H. S., OLDFIELD, C. C., WROE, S., CLAUSEN, P. D. and M$_C$HENRY, C. R. 2013. Why the long face? The mechanics of mandibular symphysis proportions in crocodiles. *PLoS One*, **8,** e53873.

WATANABE, A. and SLICE, D. E. 2014. The utility of cranial ontogeny for phylogenetic inference: a case study in crocodylians using geometric morphometrics. *Journal of Evolutionary Biology*, **27,** 1078–1092.

WEBB, G. J. W. and MESSEL, H. 1978. Morphometric analysis of *Crocodylus porosus* from the north coast of Arnhem Land, northern Australia. *Australian Journal of Zoology*, **26,** 1–27.

WERDELIN, L. 1996. Carnivoran ecomorphology: a phylogenetic perspective. 582–624. *In* GITTLEMAN, J. (ed.). *Carnivore Behavior, Ecology and Evolution.* Cornell University Press.

WESLEY-HUNT, G. D. 2005. The morphological diversification of carnivores in North America. *Paleobiology*, **31,** 35–55.

WHETSTONE, K. N. and WHYBROW, P. J. 1983. A "cursorial" crocodilian from the Triassic of Lesotho (Basutoland), southern Africa. *Occasional Papers of the Museum of Natural History of University of Kansas*, **106,** 1–37.

WHITE, T. E. 1942. A new alligator from the Miocene of Florida. *Copeia*, **1942,** 3–7.

WILBERG, E. W. 2015. What's in an outgroup? The impact of outgroup choice on the phylogenetic position of Thalattosuchia (Crocodylomorpha) and the origin of Crocodyliformes. *Systematic Biology*, **64,** 621–637.

WILBERG, E. W. 2017. Investigating patterns of crocodyliform cranial disparity through the Mesozoic and Cenozoic. *Zoological Journal of the Linnean Society*, **181,** 189–208.

WILKINSON, L. E., YOUNG, M. T. and BENTON, M. J. 2008. A new metriorhynchid crocodilian (Mesoeucrocodylia: Thalattosuchia) from the Kimmeridgian (Upper Jurassic) of Wiltshire, UK. *Palaeontology*, **51,** 1307–1333.

WILLIAMS, T. M. 1999. The evolution of cost efficient swimming in marine mammals: limits to energetic optimization. *Philosophical Transactions of the Royal Society of London B,* **354,** 193–201.

WILLS, M. A. 2001. Morphological disparity: a primer. 55–145. *In*: ADRAIN, J. M., EDGECOMBE, G. D. and LIEBERMAN, B. S. (eds.). *Fossils, Phylogeny, and Form: An Analytical Approach*. Springer.

WILLS, M. A., BRIGGS, D. E. G. and FORTEY, R. A. 1994. Disparity as an evolutionary index: a comparison of Cambrian and Recent arthropods. *Paleobiology,* **20,** 93–130.

WILSON, G. P. 2013. Mammals across the K/Pg boundary in northeastern Montana, USA: dental morphology and body-size patterns reveal extinction selectivity and immigrant-fueled ecospace filling. *Paleobiology,* **39,** 429–469.

YANG, Z., KUMAR, S. and NEI, M. 1996. A new method of inference of ancestral nucleotide and amino acid sequences. *Genetics,* **141,** 1641–1650.

YOUNG, M. T. 2014. Filling the 'Corallian Gap': re-description of a metriorhynchid crocodylomorph from the Oxfordian (Late Jurassic) of Headington, England. *Historical Biology,* **26,** 80–90.

YOUNG, M. T. and ANDRADE, M. B. 2009. What is *Geosaurus*? Redescription of *Geosaurus giganteus* (Thalattosuchia: Metriorhynchidae) from the Upper Jurassic of Bayern, Germany. *Zoological Journal of the Linnean Society,* **157,** 551–585.

YOUNG, M. T., BRUSATTE, S. L., RUTA, M. and ANDRADE, M. B. 2010. The evolution of Metriorhynchoidea (Mesoeucrocodylia, Thalattosuchia): an integrated approach using geometric morphometrics, analysis of disparity, and biomechanics. *Zoological Journal of the Linnean Society,* **158,** 801–859.

YOUNG, M. T., BELL, M. A., ANDRADE, M. B. and BRUSATTE, S. L. 2011. Body size estimation and evolution in metriorhynchid crocodylomorphs: implications for species diversification and niche partitioning. *Zoological Journal of the Linnean Society*, **163,** 1199–1216.

YOUNG, M. T., BRUSATTE, S. L., ANDRADE, M. B., DESOJO, J. B., BEATTY, B. L., STEEL, L., FERNÁNDEZ, M. S., SAKAMOTO, M., RUIZ-OMEÑACA, J. I. and SCHOCH, R. R. 2012. The cranial osteology and feeding ecology of the metriorhynchid crocodylomorph genera *Dakosaurus* and *Plesiosuchus* from the Late Jurassic of Europe. *PLoS One*, **7,** e44985.

YOUNG, M. T., ANDRADE, M. B., ETCHES, S. and BEATTY, B. L. 2013. A new metriorhynchid crocodylomorph from the Lower Kimmeridge Clay Formation (Late Jurassic) of England, with implications for the evolution of dermatocranium ornamentation in Geosaurini. *Zoological Journal of the Linnean Society*, **169,** 820–848.

YOUNG, M. T., HUA, S., STEEL, L., FOFFA, D., BRUSATTE, S. L., THÜRING, S., MATEUS, O., RUIZ-OMEÑACA, J. I., HAVLIK, P., LEPAGE, Y. and ANDRADE, M. B. 2014. Revision of the Late Jurassic teleosaurid genus *Machimosaurus* (Crocodylomorpha, Thalattosuchia). *Royal Society Open Science*, **1,** 140222.

YOUNG, M. T., RABI, M., BELL, M. A., FOFFA, D., STEEL, L., SACHS, S. and PEYER, K. 2016*a*. Big-headed marine crocodyliforms and why we must be cautious when using extant species as body length proxies for long-extinct relatives. *Palaeontologia Electronica*, **19,** 1–14.

YOUNG, M. T., TENNANT, J. P., BRUSATTE, S. L., CHALLANDS, T. J., FRASER, N. C., CLARK, N. D. and ROSS, D. A. 2016*b*. The first definitive Middle Jurassic

atoposaurid (Crocodylomorpha, Neosuchia), and a discussion on the genus *Theriosuchus*. *Zoological Journal of the Linnean Society*, **176,** 443–462.

YOUNG, M. T., HASTINGS, A. K., ALLAIN, R. and SMITH, T. J. 2017. Revision of the enigmatic crocodyliform *Elosuchus felixi* de Lapparent de Broin, 2002 from the Lower–Upper Cretaceous boundary of Niger: potential evidence for an early origin of the clade Dyrosauridae. *Zoological Journal of the Linnean Society*, **179,** 377–403.

ZACHOS, J. C., DICKENS, G. R. and ZEEBE, R. E. 2008. An early Cenozoic perspective on greenhouse warming and carbon-cycle dynamics. *Nature*, **451,** 279–283.

ZANNO, L. E., DRYMALA, S., NESBITT, S. J. and SCHNEIDER, V. P. 2015. Early crocodylomorph increases top tier predator diversity during rise of dinosaurs. *Scientific Reports*, **5,** 9276.

ZELDITCH, M. L., SWIDERSKI, D. L. and SHEETS. H. D. 2012. *Geometric Morphometrics for Biologists: A Primer*. Elsevier/Academic Press.

ZHANG, N. R. and SIEGMUND, D. O. 2007. A modified Bayes information criterion with applications to the analysis of comparative genomic hybridization data. *Biometrics*, **63,** 22–32.